

TECHNISCHE UNIVERSITÄT MÜNCHEN

Lehrstuhl für organische Chemie II

Synthesis of gamma-lactones for activity based protein profiling: Investigation of their protein reactivity and inhibition of bacterial virulence

Martin Herbert Kunzmann

Vollständiger Abdruck der von der Fakultät für Chemie der Technischen Universität München zur Erlangung des akademischen Grades eines Doktors der Naturwissenschaften genehmigten Dissertation.

Vorsitzender:

Univ.-Prof. Dr. Michael Groll

Prüfer der Dissertation:

1. Univ.-Prof. Dr. Stephan A. Sieber
2. TUM Junior Fellow Dr. Sabine Schneider

Die Dissertation wurde am 26.11.2013 bei der Technischen Universität München eingereicht und durch die Fakultät für Chemie am 13.01.2014 angenommen.

Für meine Familie

Diese Arbeit wurde im Fachbereich Chemie
der Technischen Universität München unter Leitung von
Herrn Prof. Dr. Stephan A. Sieber
in der Zeit von Oktober 2010 bis November 2013 durchgeführt.

Danksagung

Ich danke Prof. Dr. Stephan Sieber für die interessante Themenstellung, die exzellenten Arbeitsbedingungen und die hervorragende Betreuung dieser Arbeit. Seine Begeisterungsfähigkeit für mein Forschungsthema sowie seine Unterstützung haben einen großen Beitrag zum Erfolg dieser Dissertation geleistet. Des Weiteren möchte ich mich für die Möglichkeit der Teilnahme an einer Vielzahl von Konferenzen und Kursen bedanken, wodurch ich meinen wissenschaftlichen Horizont stets erweitern konnte.

Mein Dank gilt auch dem Prüfungsvorsitzenden Prof. Dr. Michael Groll sowie der Zweitprüferin Dr. Sabine Schneider für die Begutachtung meiner Dissertation und die Kooperation bei der Proteinkristallographie. Ich bedanke mich auch bei Dr. Tobias Aumüller für die Unterstützung bei spektroskopischen Messungen sowie bei Dr. Jeanette Winter und Dr. Martin Haslbeck für die Unterstützung bei biologischen Fragestellungen.

Mein Dank gilt besonders Mona Wolff und Katja Bäuml für ihre exzellente Unterstützung bei Experimenten und dem Laboralltag. Für zahlreiche wissenschaftliche Diskussionen sowie ihre große Hilfsbereitschaft und Unterstützung möchte ich mich besonders bei meinen Laborkollegen Dr. Nina Bach, Dr. Bianca Bauer, Dr. Thomas Böttcher, Dr. Ronald Frohnapfel, Dr. Malte Gersch, Dr. Vadim Korotkov, Dr. Joanna Krysiak, Dr. Matthew Nodwell, Dr. Katrin Lorenz-Baath, Dr. Maximilian Pitscheider, Dr. Isabell Staub, Dr. Franziska Weinandy, Dr. Evelyn Zeiler, Maria Dahmen, Jürgen Eirich, Christian Fetzer, Mathias Hackl, Wolfgang Heydenreuter, Philipp Kleiner, Max Koch, Roman Kolb, Johannes Kreuzer, Elena Kunold, Johannes Lehmann, Franziska Mandl, Georg Rudolf, Matthias Stahl, Franziska Traube, Jan Vomacka, Tanja Wirth und Weining Zhao bedanken.

Mein größter Dank gilt meiner Familie und meinen Freunden für ihre große Unterstützung während der gesamten Studien- und Promotionszeit.

Parts of this work have already been published:

Publications in international Journals

M. H. Kunzmann, N. C. Bach, B. Bauer, S. A. Sieber. α -Methylene- γ -butyrolactones attenuate *Staphylococcus aureus* virulence by inhibition of transcriptional regulation. *Chem. Sci.* **2014**, Accepted Manuscript. DOI: 10.1039/C3SC52228H

M. H. Kunzmann, S. A. Sieber. Target analysis of α -alkylidene- γ -butyrolactones in uropathogenic *E. coli*. *Mol. BioSyst.* **2012**, *8*, 3061-3067. DOI: 10.1039/C2MB25313E

M. H. Kunzmann*, I. Staub*, T. Böttcher, S. A. Sieber. Protein Reactivity of Natural Product-Derived γ -Butyrolactones. *Biochemistry* **2011**, *50*, 910-916. DOI: 10.1021/BI101858G

Poster presentations

M. H. Kunzmann, S. A. Sieber. Potent inhibition of hemolysis in *Staphylococcus aureus* by α -methylene- γ -butyrolactones. Bayer HealthCare-Workshop, Center for integrated Protein Science Munich (CiPSM), 6th December 2012, Munich.

M. H. Kunzmann, N. C. Bach, B. Bauer, S. A. Sieber. An α -methylene- γ -butyrolactone attenuates *S. aureus* virulence by covalent binding to the transcriptional regulators SarA, SarR and MgrA. Challenges in Chemical Biology (ISACS11), Royal Society of Chemistry (RSC), 23th–26th July 2013, Boston, USA.

*these authors contributed equally to this work

TABLE OF CONTENTS

Introduction	1
Pathogenic bacteria and resistance development.....	1
Proteomics.....	4
Activity-based protein profiling	5
Introduction	5
Probe design	5
Tag-free ABPP	6
Analytical ABPP	9
Competitive ABPP	10
Preparative ABPP	11
Protein-reactive natural products for ABPP	12
Michael acceptor systems	13
3-Membered ring-strained scaffolds	15
4/5-Membered ring-strained scaffolds.....	16
Photocrosslinking.....	18
Aim of this work.....	20
Summary.....	21
Protein Reactivity of Natural Product-Derived γ-Butyrolactones.....	21
Target analysis of α-alkylidene-γ-butyrolactones in uropathogenic <i>E. coli</i>	22
α-Methylene-γ-butyrolactones attenuate <i>Staphylococcus aureus</i> virulence by inhibition of transcriptional regulation	23
Zusammenfassung	25
Protein-Reaktivität von Naturstoff-abgeleiteten γ-Butyrolactonen	25
Analyse der Protein-Angriffsziele von α-Alkyliden-γ-Butyrolactonen in uropathogenen <i>E. coli</i>-Stämmen	26

α-Methylen-γ-Butyrolactone vermindern die Virulenz von <i>Staphylococcus aureus</i> durch Inhibition der transkriptionellen Regulation	27
Results and discussion.....	29
Protein Reactivity of Natural Product-Derived γ-Butyrolactones	29
Abstract.....	29
Introduction	30
Results and Discussion	32
Conclusion.....	38
Experimental.....	39
Appendix.....	53
Target analysis of α-alkylidene-γ-butyrolactones in uropathogenic <i>E. coli</i>	69
Abstract.....	69
Introduction	69
Results and Discussion	72
Conclusion.....	76
Experimental.....	77
Appendix.....	91
α-Methylene-γ-butyrolactones attenuate <i>Staphylococcus aureus</i> virulence by inhibition of transcriptional regulation	109
Abstract.....	109
Introduction	110
Results and Discussion	112
Conclusion.....	121
Experimental.....	122
Appendix.....	138
Abbreviations.....	162
Bibliography.....	164
Curriculum Vitae	172

INTRODUCTION

Pathogenic bacteria and resistance development

A bacterial infection consists of colonization of a host organism's body by pathogenic bacteria, their multiplication and the subsequent reaction of the host tissue to foreign pattern recognition factors. Hosts can fight bacterial infections by using their immune system.¹ Although the majority of bacteria are harmless or even beneficial, some are pathogenic and can cause serious diseases like tuberculosis, which kills about two million people a year.²

Some non-pathogenic bacteria are part of the human microbiota and exist on the skin and in the respiratory tract as commensals without causing disease; in case of *Staphylococcus aureus* it is estimated that about 25-30% of the human population are long-term carriers.³ These bacteria are only pathogenic under certain circumstances, which are strongly associated with the expression of selective virulence factors or colonization of immunosuppressed patients. Under such conditions, *S. aureus* can cause serious diseases like bacteraemia, endocarditis, metastatic infections, sepsis and toxic shock syndrome.⁴ With about 500,000 patients contracting a staphylococcal infection each year in American hospitals, *S. aureus* is one of the main causes for nosocomial infections.⁵⁻⁸ Infections can spread through the contact of superficial wounds with *S. aureus* carriers or via contaminated objects such as clothes or surgical instruments.⁹

Bacterial infections can be treated with antibiotics, which are small molecules and either kill bacteria (bactericidal) or prevent their growth (bacteriostatic) by selective inhibition of essential bacterial enzymes, while their human homologs remain unaffected.^{10, 11} Most commonly used antibiotics derive from compounds which were originally isolated from natural sources like bacteria or fungi.^{12, 13} In these organisms, they serve as defensive weapons which are life-threatening to other organisms, like competitive bacteria, and therefore aid to maintain their existence.¹² Since the application of the first antibiotics in 1935 (sulfonamide prontosil) and 1940 (penicillin G), bacterial infections could be successfully treated and even more antibiotics were developed and introduced (Figure 1).¹² Unfortunately, bacteria can combat antimicrobial effects by developing resistance, and despite increasing resistance development, there were only two new classes of antibiotics established from 1970 until now (Figure 1)¹⁴, Daptomycin and Linezolid.

Antibiotic deployment

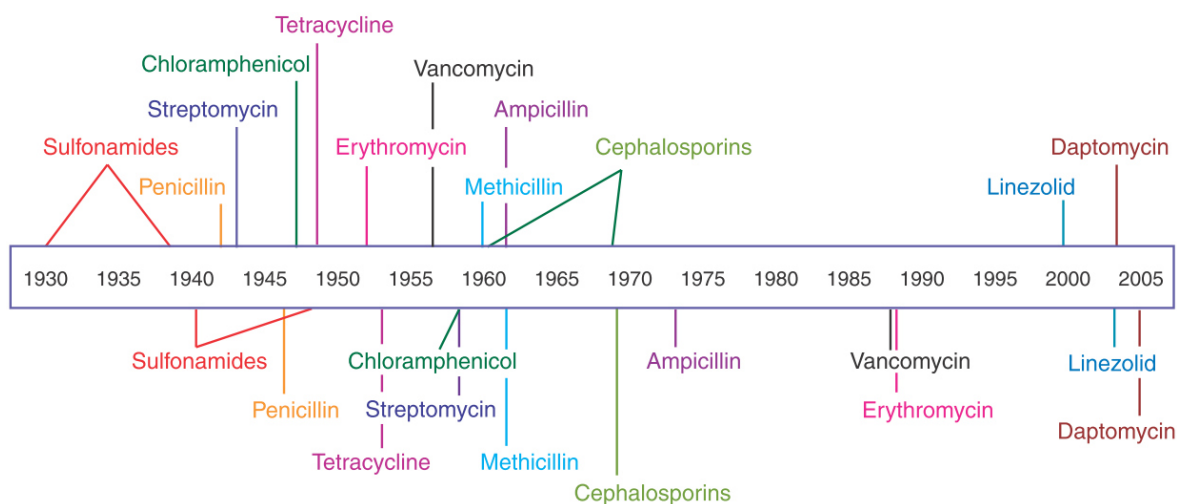


Figure 1: Introduction of new antibiotics (top) and resistance development (bottom). Adapted by permission from Macmillan Publishers Ltd: Nature Chemical Biology¹⁴, copyright 2007.

The major causes of rapid resistance development are discontinued antibiotic treatments, prescriptions of antibiotics for non-bacterial infections, hygiene deficits in hospitals and the liberal use of antibiotics in intensive mass animal farming.¹⁵⁻¹⁸ The irresponsible broad-range application of antibiotics puts selective pressure on bacteria leading to the development of different resistance mechanisms. Furthermore, most antibiotics target only a limited number of crucial bacterial cellular functions such as cell wall synthesis, DNA replication, transcription or translation (Figure 2).^{19, 20} Therefore, establishing only a few antibiotic resistance mechanisms can lead to resistance against a broad range of antibiotic compound-classes. During a bacterial infection and a respective antibiotic treatment, these resistant or even multiresistant (resistant against at least two different antibiotics) bacteria are not affected by the antibiotic, have fewer competitive bacteria and can therefore proliferate in the host.¹²

There are four main antibiotic-resistance mechanisms such as target modification, production of efflux pumps, and development of antibiotic inactivating enzymes occurring in bacteria (Figure 2).²¹ The antibiotic target can be modified by point mutations in the corresponding gene, resulting in still functional but antibiotic resistant enzymes.²² In some cases, even a single point mutation is sufficient to render enzymes highly resistant to antibiotics. For example, mutation of Ser83 to Leu, Trp, or Ile as well as mutation of Asp87 to Asn, Tyr or Gly leads to the fluoroquinolone resistant type IIA topoisomerase GyrA, an enzyme that is required for relaxing supercoiled DNA at the bacterial replication fork.²³ Target modification by enzymes is also

possible. One example is the methylation of the 23S rRNA of the large ribosomal subunit at position A2058 by ribosome methyltransferases, which confer resistance to three distinct classes of antibiotics (macrolides, lincosamides and type B streptogramins).²³ A quite simple strategy is the production of efflux pumps, which actively transport the antibiotic compound out of the cell.²⁴ Finally, the antibiotic can be inactivated by degrading enzymes. In case of β -lactam antibiotics like penicillin, the β -lactam ring is cleaved by Ser- β -lactamases or metallo- β -lactamases, leading to the corresponding inactive acids.^{22, 25} These established resistance mechanisms can then be shared between other bacteria through gene transfer leading to an increasing percentage of resistant or even multiresistant bacteria.²⁶

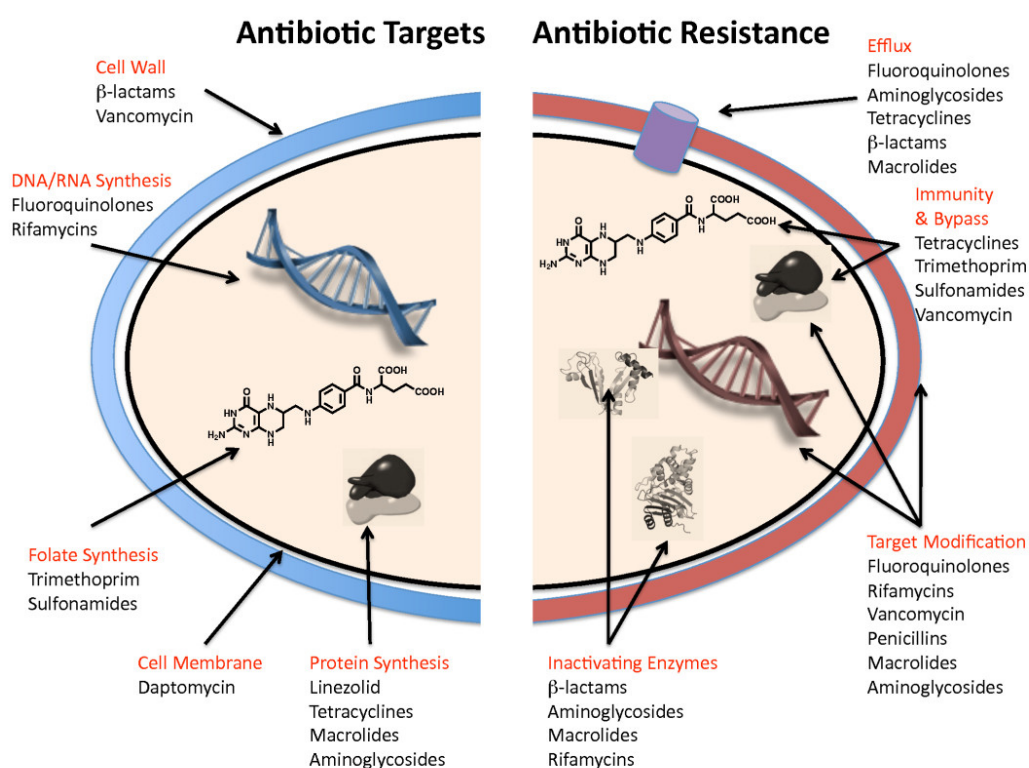


Figure 2: Antibiotic targets (left) and resistance mechanism (right) in bacteria. Adapted by permission from G. D. Wright: BMC Biology¹⁹, copyright 2010.

The increasing number of multiresistant bacterial strains, the rapid resistance development against new antibiotics and the lack of novel drug targets demand new approaches to treat bacterial infections.²⁷ The major problem in resistance development is the selective pressure which is put on bacteria during antibiotic treatment. A new approach to treat these infections is to disarm bacteria instead of killing them. This can be done by inhibition of virulence-associated proteins, which are responsible for the infection but not for bacterial viability. Inhibition of virulence may reduce the selective pressure, expands the amount of drug targets and preserves

the host microbiome during treatment.¹⁴ It was recently shown that β -lactones attenuate the expression of virulence factors in *S. aureus* by inhibition of the bacterial protease ClpP and decrease the intracellular virulence of *Listeria monocytogenes* in macrophages.²⁸⁻³⁰ To find new inhibitors of bacterial virulence and their corresponding protein targets, proteomic techniques such as activity based protein profiling (ABPP) can be applied.

Proteomics

The International Human Genome Sequencing Consortium finally succeeded in sequencing the whole human genome in 2001.³¹ This raised the hope to understand the chemistry of life by only decoding the DNA sequence of different organisms but it became soon clear that the regulation of protein expression is much more complex than expected.

It is common knowledge that DNA is transcribed into messenger RNA (mRNA) and their translation leads to the corresponding protein. However, not all genes are transcribed and the mRNA level does not always correlate with the corresponding protein level or protein activity.³² In prokaryotic cells, DNA is transcribed in the cytosol by RNA polymerases into mRNA, which is then translated into the polypeptide by ribosomes. Ribosome-associated proteins catalyse folding of the polypeptide chain to functional proteins. In eukaryotic cells, DNA is transcribed in the nucleus to pre-mRNA, which is first processed (alternative splicing). Splicing processes can lead to different mRNA products, which are exported into the cytosol and translated by ribosomes.³³ Folding to the native protein occurs co-translational and proteins are often post-translationally modified. The polypeptide chain can then be proteolytically cleaved (pre-, pro- or prepro-proteins) by protein splicing.³⁴ Furthermore, proteins can be modified by glycosylation, lipidation, hydroxylation or carboxylation of side chains or the N- or C-terminus. The protein activity is also often regulated by posttranslational modifications such as phosphorylation, methylation and acetylation.³⁵⁻³⁷ All these modifications lead to a multiplicity of possible proteins, which cannot be determined by genome analysis.

Since the proteome also depends on cell cycle and environmental conditions, proteomics focuses on the analysis of a global set of proteins measured at a determined time point and under specific conditions. Next to characterisation and quantification of proteins, proteomics also analyses protein structure, function, activity and protein-protein interactions to understand biochemical processes.³⁸ A powerful chemical proteomic approach to study the function of proteins and their

inhibition by small molecules is activity-based protein profiling (ABPP), which was introduced by Cravatt and Bogoy about ten years ago.³⁹⁻⁴²

Activity-based protein profiling

Introduction

Activity based protein profiling (ABPP) is a powerful technique to analyse interactions of small molecule probes with individual proteins in a whole proteome.⁴³ Probes usually comprise a protein-reactive group – based on protein-reactive natural products or other electrophilic motifs – to bind to the active site of functional proteins and a reporter group, which allows the visualization and/or enrichment of the protein targets. The visualisation can be achieved via SDS-PAGE followed by fluorescent scanning, which enables the detection of labelled proteins, even if they are of low abundance (Figure 3). ABPP can be applied to prokaryotes or eukaryotes *in vitro* as well as *in situ* and can for example be used to identify new drug targets.

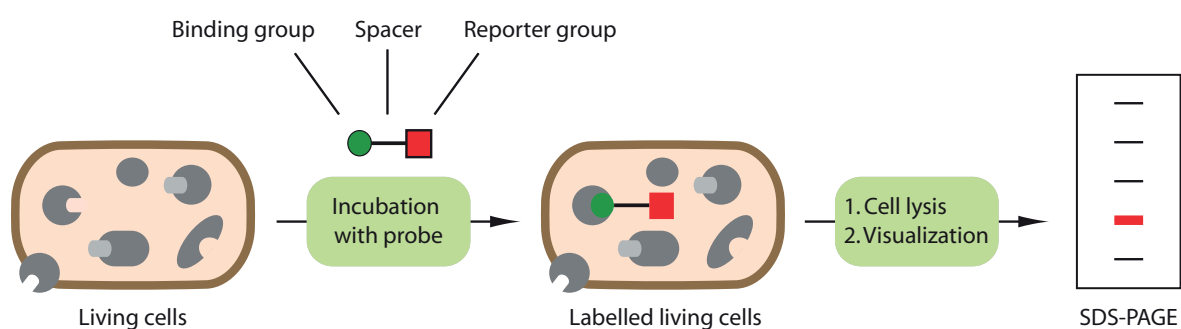


Figure 3: Scheme of an ABPP experiment. Living cells are incubated with ABPP probe. Labelled cells are lysed by sonication or bead beating and clicked proteome is separated via SDS-PAGE. Bands are then visualized on the gel by e.g. fluorescence.

Probe design

Probes for ABPP are small molecules consisting of at least three essential elements. The binding group binds to the active site of protein targets, the reporter group (e.g. rhodamine dye or biotin) is used for visualization or enrichment and the spacer links the elements together (Figure 4A).

Binding groups are responsible for affinity-mediated binding to complementary protein structures. Natural products are a unique class of small molecules with diverse biological effects. In contrast to synthetic molecules, they show a fine-tuned selectivity and reactivity for the interaction with biological macromolecules such as proteins and are thus ideal sources for binding groups.

The ABPP workflow requires several denaturation steps, which lead to disruption of non-covalent probe-protein interactions. A covalent bond between the probe and the protein target is therefore essential for this approach. In case of non-covalent binding groups, a covalent binding can be accomplished by introduction of an additional photo-reactive group (e.g. benzophenones, aryl azides or aryl diazirines). The spacer serves as a connecting scaffold and can be part of the natural product (Figure 4B).

Reporter groups are necessary for visualization by fluorescence (e.g. rhodamine dye) or target enrichment (e.g. biotin for enrichment on immobilized avidin). If the probe contains the corresponding functional group (e.g. terminal alkyne or azide, Figure 4B), the reporter group can also be introduced after protein labelling via bioorthogonal chemistry such as Staudinger ligation or Huisgen 1,3-dipolar cycloaddition.⁴⁰

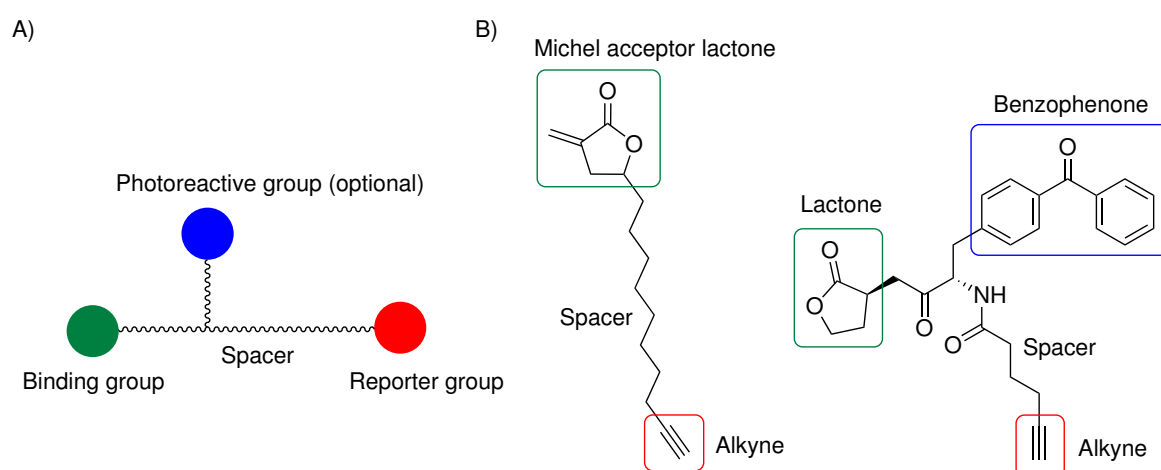


Figure 4: A) Schematic structure of an ABPP probe. B) Examples of ABPP probes containing a terminal alkyne, which allows introduction of a reporter group via bioorthogonal chemistry.

Tag-free ABPP

Since introduction of large reporter groups may alter the biological profile, cell permeability and solubility of natural products, the use of small functional groups (e. g. terminal alkynes or azides)

for introduction of reporter groups (e.g. rhodamine dye or biotin) after protein labelling is a major improvement.

Probes containing an azide can be coupled with the desired reporter group by the Staudinger ligation.⁴⁴ Therefore, a phosphane is first acylated with the desired reporter group (R^1) and reaction with an azide (N_3-R^2) forms the corresponding phosphazide (a). Under expulsion of nitrogen (b, c), an iminophosphorane is formed (d), the corresponding aza-ylide rearranges (e) and its hydrolysis leads to the final amine (Figure 5A). Figure 5B shows commonly used phosphanes in the traceless Staudinger ligation.

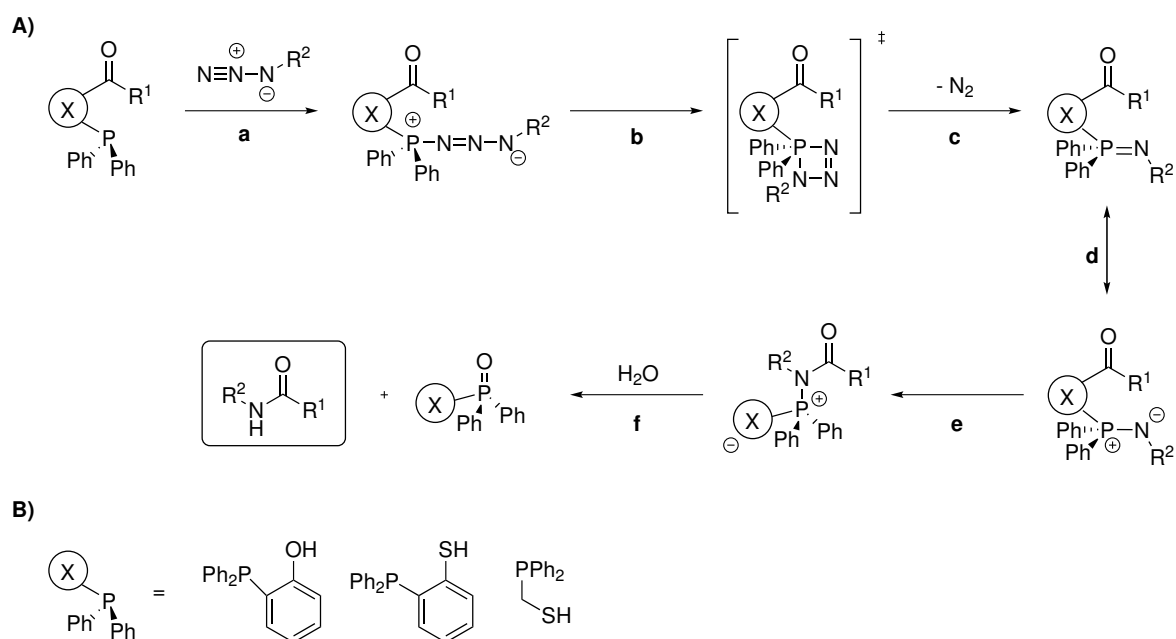


Figure 5: A) Proposed mechanism of the traceless Staudinger ligation. An acylated phosphane carrying the reporter group (R^1) react with an azide (N_3-R^2) to the corresponding phosphazide (a) and under expulsion of nitrogen (b, c), an iminophosphorane is formed (d). Rearrangement (e) and hydrolysis of the iminophosphorane (f) leads to the final amine (framed). B) Compounds used for the traceless Staudinger ligation.⁴⁴

In case of probes containing a terminal alkyne, reporter groups can be introduced by click chemistry. The Cu^I -catalysed Huisgen 1,3-dipolar cycloaddition of azides and terminal alkynes (click chemistry) is regioselective and leads only to the formation of 1,4-substituted 1,2,3-triazoles (Figure 6A).^{45, 46} The first step is the π -coordination of an alkyne (part of the probe) to the copper complex (not shown), which leads to acidification of the terminal alkyne hydrogen, allowing its deprotonation to form a Cu-acetylide (a). The azide (carrying the reporter group) is then activated by coordination to the copper complex (b) and a strained metallacycle is formed (c). The next step

leads to a Cu-triazolide (d), which is energetically favourable and its protonation forms the final triazole (e).^{47, 48} There is also further evidence that dinuclear Cu^I-acetylides are involved in this reaction, which leads to a further drop of in the activation barriers.⁴⁸⁻⁵⁰ Commonly used ligands for click chemistry are shown in Figure 6B.

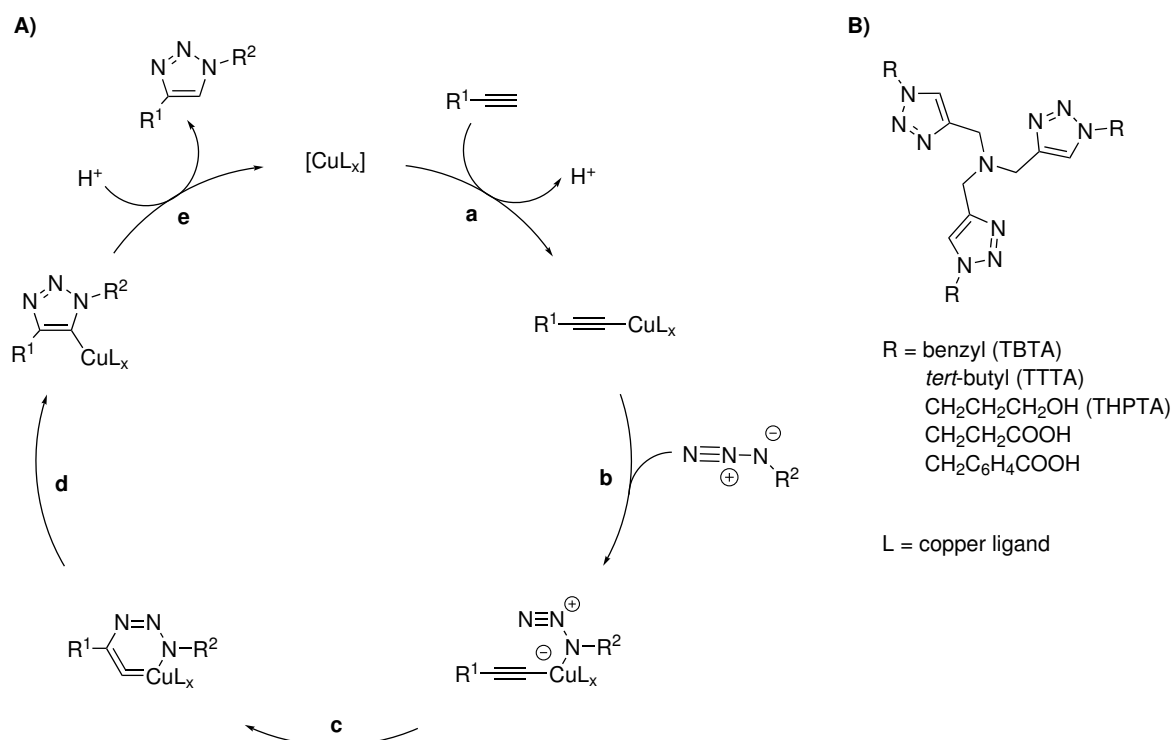


Figure 6: A) Proposed mechanism of Cu^I-catalysed Huisgen 1,3-dipolar cycloaddition of azides and terminal alkynes. a) Deprotonation of the terminal alkyne (part of the probe) and formation of a Cu-acetylide complex (former π -complex not shown). b) Activation of the azide (carrying the reporter group) by coordination to the copper complex. c) Formation of a strained metallacycle. d) Formation of copper triazolide. e) Protonation of copper triazolide leads to the final triazole. B) Commonly used copper ligands for click chemistry.⁴⁷

The click reaction can be performed over a wide range of temperatures (0-160 °C) and pH values (5-12). Furthermore, the catalysed reaction is 10^7 times faster than the uncatalysed version and the reaction is nearly unaffected by steric factors. Azides and alkynes are stable under physiological conditions and the reaction tolerates oxygen, water, common organic solvents, biological molecules, a reducing environment and can be applied in cell lysates.⁴⁸ Therefore it is a model example of a cycloaddition, which is ideal for ABPP. There have also been major improvements in the last years leading to copper-free strain-promoted azide-alkyne cycloadditions and Pd-mediated protein cross couplings in living systems.⁵¹⁻⁵⁴

Analytical ABPP

Analytical ABPP is used to visualize probe-bound proteins on a polyacrylamide gel via fluorescence imaging (Figure 7). Therefore living cells (prokaryotes or eukaryotes) are incubated with the desired probe for approximately two hours and are subsequently washed to remove the excess of probe. The cells are then lysed by sonication or bead beating and the labelled proteome (supernatant, cytosol fraction) is subjected to click chemistry with rhodamine azide (Rh-N₃). The proteins are separated according to their protein size via one dimensional sodium dodecyl sulfate polyacrylamide gel electrophoresis (SDS-PAGE) and visualized by rhodamine fluorescence (absorption at 543 nm, emission at 572 nm).⁵⁵

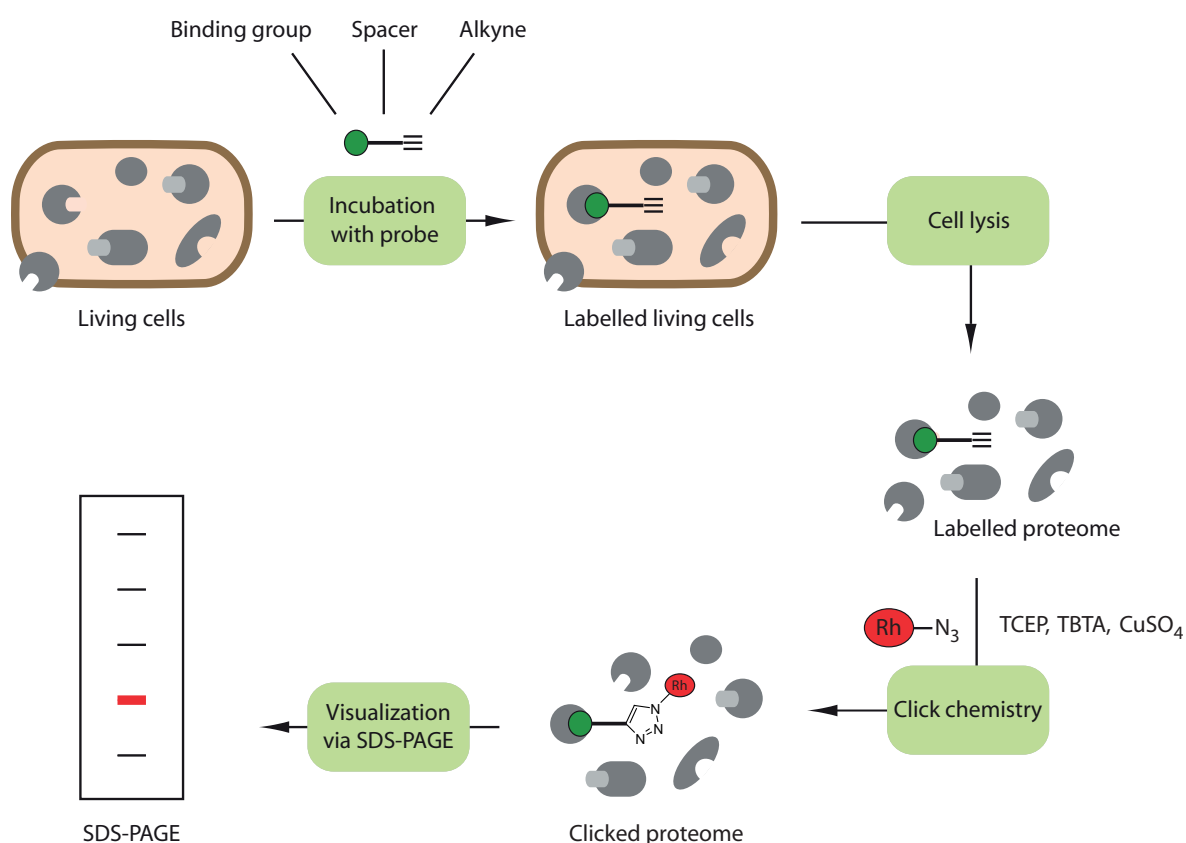


Figure 7: Analytical *in situ* ABPP experiment. Living cells are incubated with ABPP probes. Labelled cells are lysed by sonication or bead beating and labelled proteome is subjected to click chemistry. The clicked proteome is separated via SDS-PAGE and bands are visualized by rhodamine fluorescence. In case of probes which cannot cross the cell membrane or cell wall, unlabelled cells are first lysed by ultrasound or bead beating and are then subsequently labelled with the desired probe.

The analytical ABPP experiment provides results such as labelling pattern, fluorescence band intensity and number of protein targets. Furthermore the probe concentration can be optimized

and proteomes of different bacterial strains (e.g. pathogenic and non-pathogenic bacterial strains) can be compared to identify proteins, which may be virulence associated. Protein identification can then be achieved by preparative ABPP.

Competitive ABPP

To allow bioorthogonal introduction of reporter groups (e.g. rhodamine or biotin), natural products have to be modified with a small functional group (e.g. terminal alkyne or azide), which may alter its protein target specificity. To investigate this effect, competitive ABPP experiments can be performed *in situ* (Figure 8) as well as *in vitro* in case of probes, which cannot penetrate the cell membrane or cell wall.

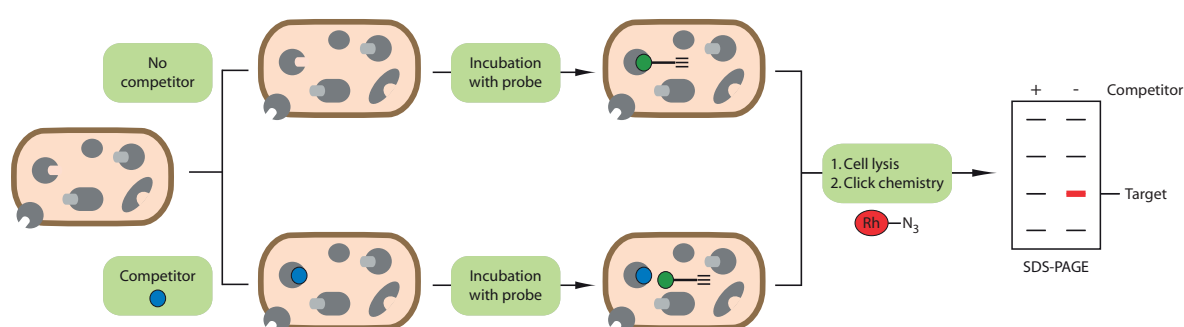


Figure 8: Analytical competitive *in situ* ABPP experiment. Living cells are pre-treated with the desired competitor or DMSO (control). Pre-treated cells are incubated with the corresponding probe and after cell lysis by sonication or bead beating and click chemistry (with e.g. rhodamine azide), proteins are separated via SDS-PAGE and bands are visualized by fluorescence. In case of probes which cannot cross the cell membrane or cell wall, unlabelled cells are first lysed by ultrasound or bead beating and are then pre-treated with the desired inhibitor and subsequently incubated with the desired probe.

The cells are therefore pre-treated with the desired competitor (e.g. natural product or probe without the alkyne group) or DMSO (as control). Then the corresponding probe is added and, after incubation and cell lysis, the labelled proteome is subjected to click chemistry with rhodamine azide and the proteins are separated by SDS-PAGE. If the competitor has the same protein target and binding site, the binding sites of the protein target are occupied after pre-treatment by the competitor and the probe cannot bind anymore. Therefore the fluorescent band on the gel will diminish with an increasing ratio of competitor to probe.⁵⁶

Preparative ABPP

As stated previously, the analytical ABPP experiment reveals labelling patterns, fluorescence band intensities and a number of protein targets. After optimizing the labelling conditions for probe concentration and labelling time by analytical ABPP experiments, the protein targets can be identified by preparative ABPP experiments (Figure 9).

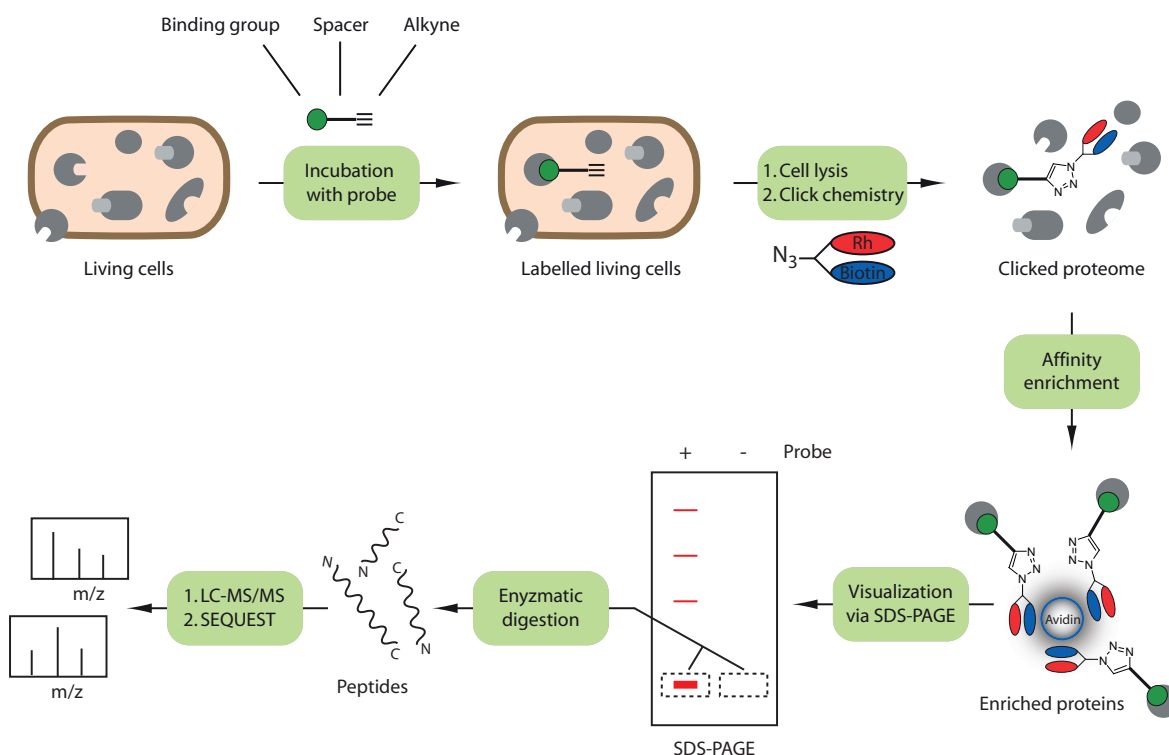


Figure 9: Preparative *in situ* ABPP experiment. Living cells are incubated with the desired probe or DMSO (negative control to subtract unspecific binding proteins). Labelled cells are lysed by sonication or bead beating and labelled proteome is subjected to click chemistry with a trifunctional linker containing an azide tag, a rhodamine dye and biotin. Proteins are enriched on avidin immobilized on beads. The beads are washed; enriched proteins are cleaved from the beads and separated via SDS-PAGE. Bands are cut out and corresponding proteins are enzymatically digested. Peptides are then subjected to LC-MS/MS analysis to identify the enriched proteins. In case of probes that cannot cross the cell membrane or cell wall, unlabelled cells are first lysed by ultrasound or bead beating and are then subsequently labelled with the desired probe.

Therefore, cells are incubated with the desired probe or DMSO (negative control to exclude unspecific binding proteins) for approximately two hours and are subsequently washed to remove the excess of probe. The cells are then lysed by sonication or bead beating and the labelled proteome (supernatant, cytosol fraction) is subjected to click chemistry with a trifunctional linker

containing an azide tag for click chemistry, a rhodamine dye for visualization and biotin for enrichment on immobilized avidin. Proteins are then enriched on avidin, which is immobilized on beads and additional washing steps are done to remove background proteins. Proteins are cleaved from the beads by their denaturation and separated by SDS-PAGE. Fluorescent bands are cut out and the corresponding proteins are enzymatically digested.

The resulting peptides are applied to a liquid chromatography-tandem mass spectrometry system (LC-MS/MS) to yield their fragmentation pattern and the corresponding mass/charge-ratios.⁵⁷ The observed data is then compared to databases containing proteomes, which are based on translation of the corresponding sequenced genome. Algorithms such as SEQUEST⁵⁸ or MASCOT⁵⁹ virtually digest the desired proteome resulting in predicted peptide masses. Comparison of the measured peptides with the predicted ones, allow the identification of enriched peptides.

Protein-reactive natural products for ABPP

Natural products have been optimized by nature over millions of years to bind specifically and selectively to their target molecules such as proteins or nucleic acids. Their fine-tuned reactivity leads to only a few off-targets and therefore, making them predestined candidates for pharmaceutical research. It is therefore not surprising, that natural products represent almost two thirds of all pharmacologically active compounds but unfortunately most modes of action still remain unknown until now.⁶⁰⁻⁶²

ABPP is the ideal technology to broaden our knowledge about protein-reactive natural products, by representing a powerful method to unravel their targets and the complex interaction of biological macromolecules inside the cell. Natural products display high affinities to biological macromolecules and the interactions reach from weak complexes to stable covalent bonds.

The ABPP protocol includes several denaturation steps and thereby restricts the analysis to natural products with a covalent target-binding mode. In particular, electrophilic natural products fulfil the requirements for this technology. They are bound to biological macromolecules such as proteins by a covalent attack of nucleophilic protein side chains (e.g. lysine, threonine, serine or cysteine) on the electrophilic core of the natural product.

Michael acceptors and ring-strained scaffolds (Figure 10) represent potent natural products, which display a broad range of biological activities (e.g. antibacterial, antifungal, antitumor) and are therefore introduced in this chapter.⁶³

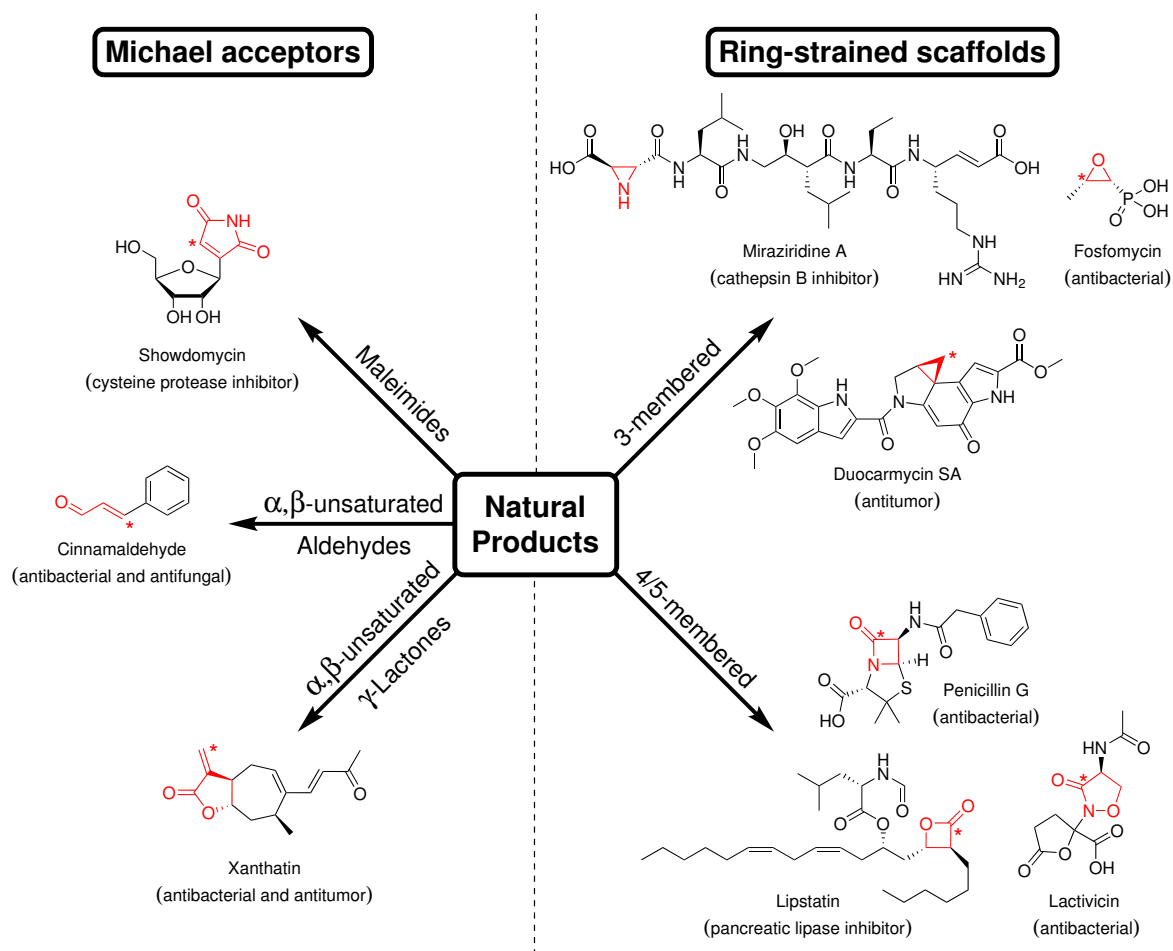


Figure 10: Michael acceptors and ring-strained scaffolds as protein-reactive electrophilic natural products. Biological activities are given in brackets, reactive groups are coloured in red and sites of attack by nucleophiles are marked by asterisks.

Michael acceptor systems

Natural products containing a Michael acceptor system can exhibit a broad range of biological activities (Figure 11). The molecular mechanism is generally based on the attack of nucleophilic amino acid side chains on the Michael acceptor scaffold. A representative selection of three compounds was chosen to describe their protein-reactivity and the corresponding biological effect.

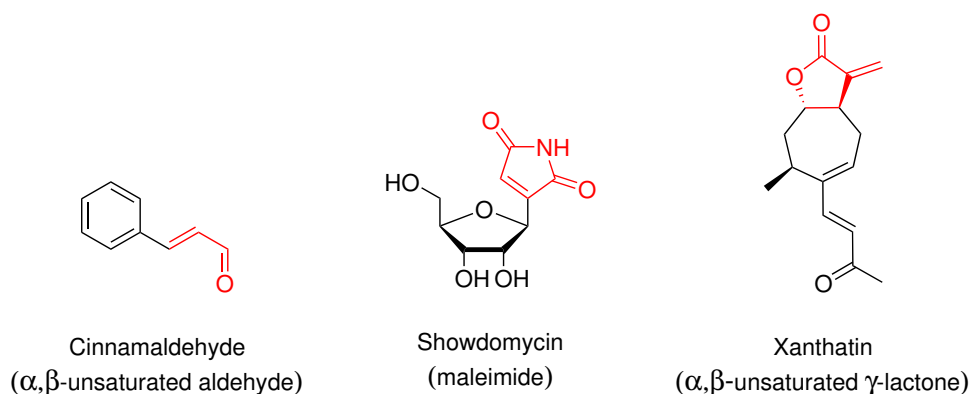


Figure 11: Representative selection of natural products containing a Michael acceptor scaffold (coloured in red) as electrophilic moieties.

1) Cinnamaldehyde

Cinnamaldehyde is an α,β -unsaturated aldehyde that was isolated from the cinnamon tree. In human cancer cells it interferes with the oxidative stress response and NF κ B signalling.⁶⁴ In bacteria it weakly inhibits the thioredoxin reductase, an enzyme involved in protein-disulfide reduction and other redox reactions inside the cell. Interestingly, the reduced compound (cinnamaldehyde lacking the double bond) is biologically inactive.⁶⁵ Cinnamaldehyde reacts preferentially with activated cysteine residues but can undergo two types of reactions. Cysteine can attack at the double bond or amines can form an imine with the aldehyde moiety.⁶⁶⁻⁶⁸

2) Showdomycin

Maleimides are potent alkylating agents and are frequently used in bioorganic chemistry to specifically label protein cysteine residues. In contrast to that, showdomycin, a maleimide isolated from *Streptomyces showdoensis*, shows structural similarity to uridine and therefore inhibits enzymes involved in uridine metabolism. ABPP experiments with showdomycin-derived probes show labelling of 13 enzymes including MurA1 and MurA2, which are involved in cell wall biosynthesis. A maleimide-free probe showed a completely unspecific labelling pattern.⁶⁹⁻⁷¹

3) Xanthatin

About 3% of all known compounds of natural origin contain the α -methylene- γ -butyrolactone motif⁷² and one member of this class is xanthatin, which was isolated from *Xanthium pennsylvanicum*. It exhibits potent antibiotic activities against *S. aureus* strains, including MRSA.⁷³ Recent reports show also activity of xanthatin against human breast cancer cells by inducing caspase-independent cell death.⁷⁴ In case of the natural products andrographolide and parthenolide (both anti-inflammatory α,β -unsaturated γ -lactones), the biological activity is

mediated via covalent attachment to an activated cysteine residue.^{75, 76} Reduced andrographolide lacking the exocyclic double bond was shown to be biologically inactive implicating its fine-tuned reactivity towards nucleophilic active site cysteine residues.

3-Membered ring-strained scaffolds

Ring-strained scaffolds can be classified by their ring size (3-, 4- and 5-membered) and the contained heteroatoms. As a result of their ring strain, they show an intrinsic reactivity towards suitable nucleophiles (e.g. serine, threonine and cysteine protein side chains) leading to the acyclic reaction product. Representative 3-membered compounds are shown in Figure 12 and two of them, duocarmycin and fosfomicin are utilized to describe the fine-tuned reactivity of this natural product class towards biomolecules.

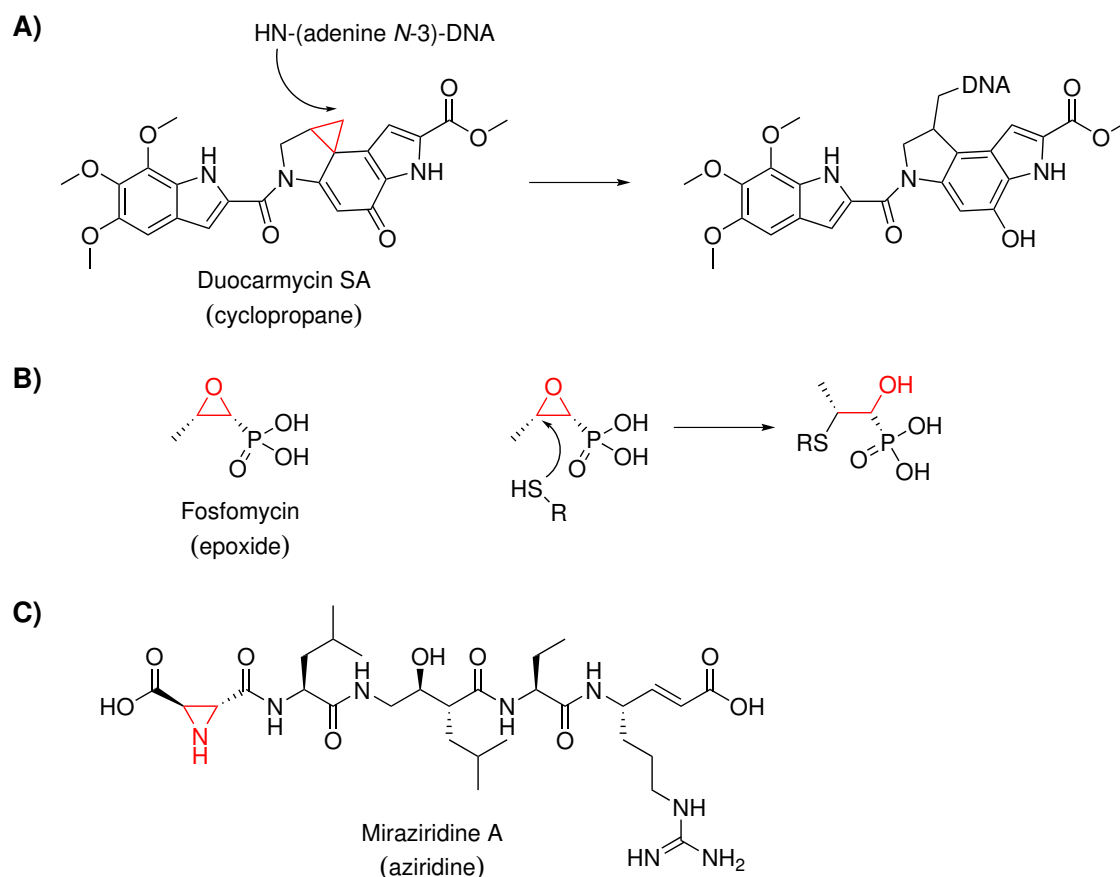


Figure 12: Natural products containing 3-membered ring-strained scaffolds as electrophilic moieties. A) Duocarmycin exhibits its antitumor activity by alkylating adenine *N*-3 of double stranded DNA. B) Fosfomicin inhibits the bacterial cell wall synthesis by binding to an essential cysteine residue of the MurA protein. C) Structure of miraziridine A, an inhibitor of a human cysteine protease cathepsin A.

1) Duocarmycin

Duocarmycin SA, a cyclopropane was isolated from *Streptomyces* DO-113⁷⁷ and exhibits its antitumor activity via DNA binding. Noncovalent binding to the minor groove of double-stranded DNA is followed by alkylation of adenine N-3, which leads to rearomatization of the cyclohexadienone ring to form a stable covalent bond (Figure 13A).⁷⁸ Further ABPP studies showed that a duocarmycin-derived *seco*-drug lacking the DNA-targeting indole still displays antitumor activity⁷⁹ and the target identified by ABPP in cancer cell lines, was shown to be aldehyde dehydrogenase 1 (inhibited by duocarmycin via covalent modification of two cysteine residues), a protein that is upregulated in a number of cancer cell lines.⁸⁰

2) Fosfomicin

Fosfomicin is an epoxide with a relatively simple structure. It was isolated from various *Streptomyces* strains and mediates its antibiotic activity⁸¹ via inhibition of the bacterial cell wall biosynthesis.⁸² UDP-*N*-acetyl-glucosamine-3-enolpyruvyltransferase (MurA) is an enzyme involved in the peptidoglycan synthesis and catalyses the ligation of phosphoenolpyruvate to UDP-*N*-acetylglucosamine. The inhibition is caused by binding of the active-site cysteine to the epoxide resulting in a covalent linkage (Figure 12B).^{83, 84} Fosfomicin is active against a broad spectrum of gram-positive as well as gram-negative bacteria and is used e.g. in the treatment of sepsis and urinary tract infections.⁸⁵

4/5-Membered ring-strained scaffolds

Since the ring-strain of 5-membered scaffolds is very low compared to their 3- and 4-membered relatives, the reactivity of 4-membered but only some 5-membered scaffolds towards biomolecules is similar to that described for 3-membered scaffolds in the last chapter. Three members of these compound classes, some of them are currently used drugs, are shown in Figure 13. Their chemistry is illustrated by introduction of two representative compounds, lipstatin and lactivicin.

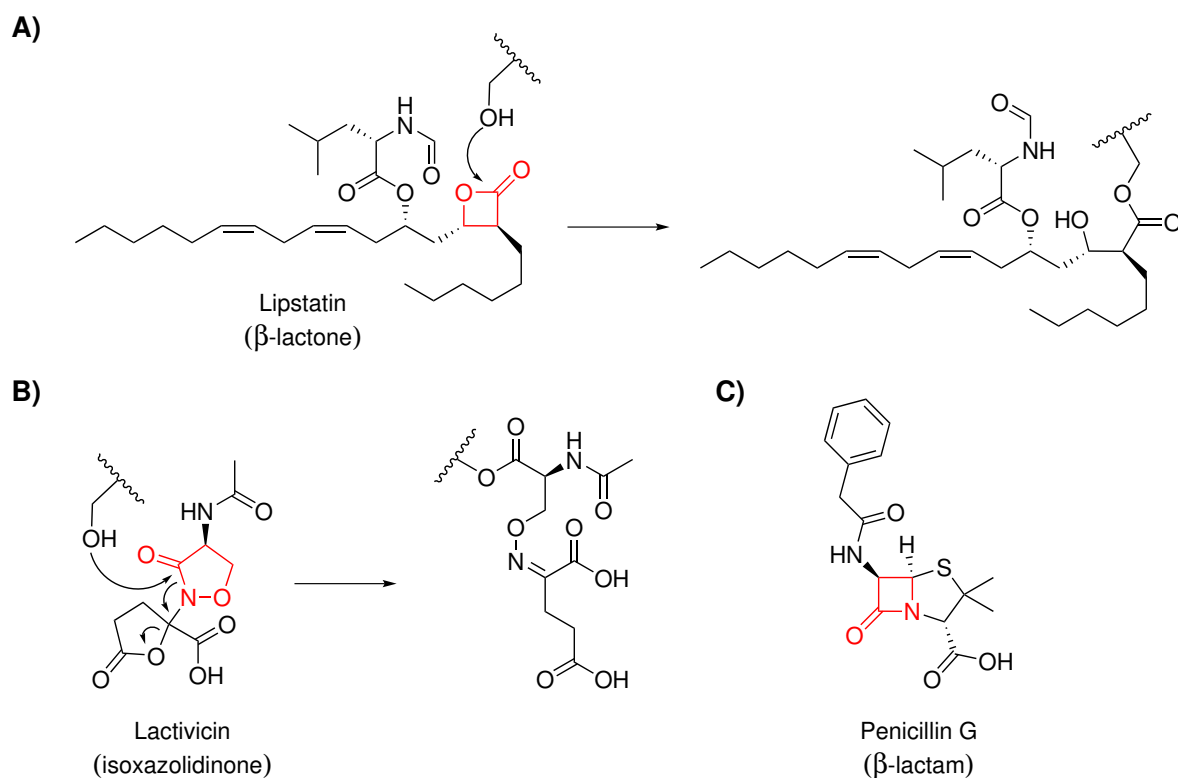


Figure 13: Natural products containing 4- and 5-membered ring-strained scaffolds as electrophilic moieties. A) Lipstatin inhibits the pancreatic lipase by covalent binding to the essential serine residue of its catalytic triad. B) Nucleophilic attack of lactivicin by an activated serine residue mediates ring opening of the cycloserine and γ -lactone. C) Structure of the β -lactam antibiotic penicillin G.

1) Lipstatin

The β -lactone lipstatin was isolated from *Streptomyces toxytricini* and is an irreversible inhibitor of the pancreatic lipase, an enzyme involved in lipid metabolism.⁸⁶ It catalyses hydrolysis of triacylglycerol to fatty acids and monoacylglycerols and inhibition leads to a reduced fat absorption. This is thereby mediated via binding to the activated serine residue of the catalytic triad leading to a β -hydroxy serine ester that blocks the active site.^{87, 88}

2) Lactivicin

Lactivicin is an isoxazolidinone and inhibits the bacterial cell wall synthesis of β -lactam hypersensitive mutants.⁸⁹ It shows antibiotic activities against gram-positive penicillin-resistant bacteria and protein targets are penicillin binding proteins and β -lactamases.⁹⁰⁻⁹² Inhibition is mediated by an attack of the nucleophilic active-site serine, which mediates cycloserine ring opening coupled by opening of the γ -lactone. The resulting intermediate is more stable towards hydrolysis than other β -lactams such as penicillin.^{92, 93}

Photocrosslinking

A huge amount of natural products mediate their biological effects by reversible binding to their protein targets. To apply the ABPP technology to this class of natural products, a photoreactive group has to be included into the corresponding ABPP probe to allow covalent attachment to their protein targets. Furthermore, one additional step has to be integrated into the ABPP workflow. After incubation of the photoreactive probe with the desired cells (*in situ*) or proteome (*in vitro*), the formation of a covalent bond is initiated by irradiation with UV light. This leads to the formation of reactive species that react with amino acids near the probe binding site.^{94, 95}

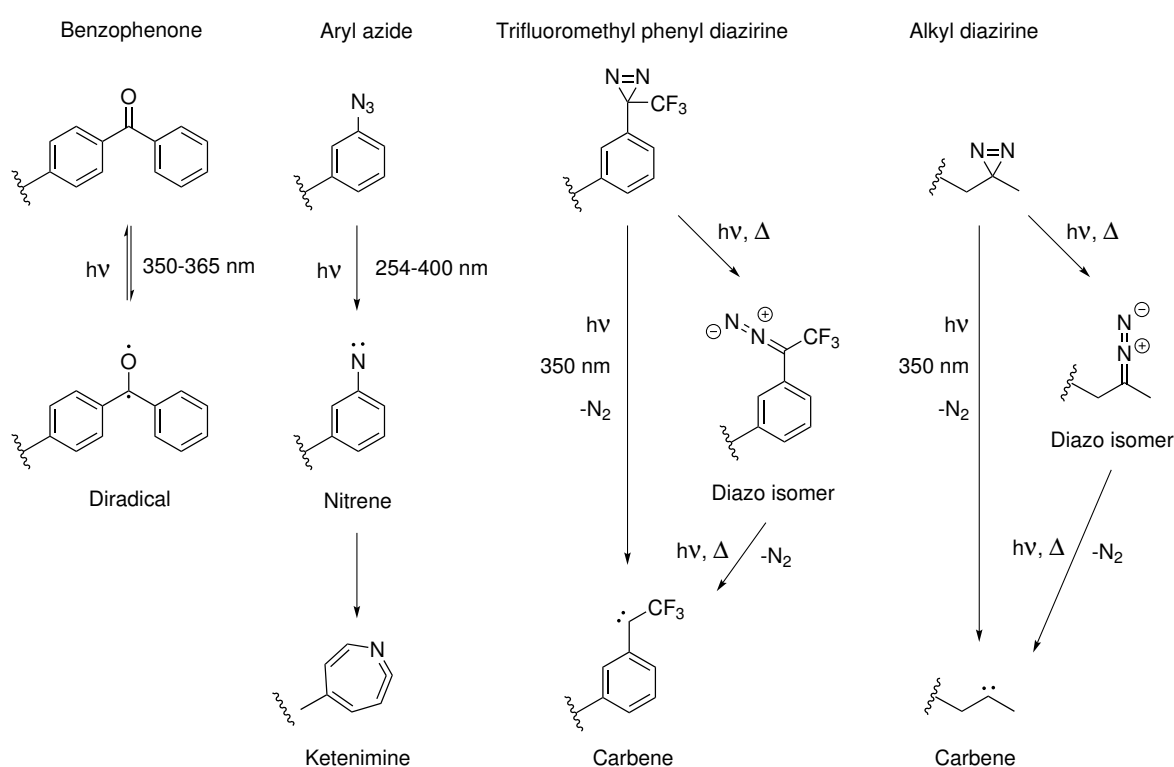


Figure 14: Chemistry of four common photoreactive groups used in ABPP experiments. The structures on top show the stable photoreactive groups, which form under irradiation highly reactive species (diradical, nitrene or carbene). These can then react with C-H or heteroatom-H bonds of biological samples. Nitrenes can undergo further rearrangement to ketenimines, which are reactive towards nucleophiles. Isomerization of diazirines yields the corresponding nucleophilic diazo-isomers, which can further react to the corresponding carbenes.⁹⁴

A major drawback of this concept is that the photoreactive group alters the chemical structure of the natural product and may influence target-binding specificity. Therefore, it is crucial to avoid bulky groups. Furthermore the reactive species formed by irradiation should be highly reactive

but have only a short lifetime. This favours crosslinking to the protein target before dissociation of the probe-enzyme complex can occur. At last, the photoreactive group has to be stable in biological samples and no light independent background reactivity should be observed.^{96, 97} Commonly used photoreactive groups for ABPP (e.g. benzophenones, aryl azides and diazirines) are shown in Figure 14.⁹⁸ Photoreactive probes lacking the binding group can thereby be used as minimal probes to visualise unspecific labelling events.

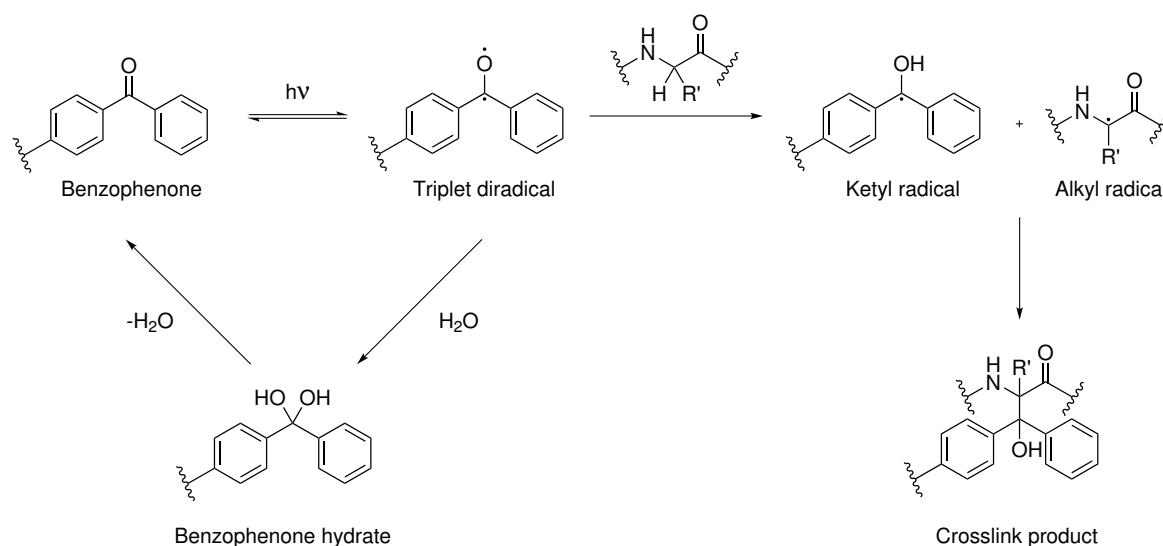


Figure 15: Benzophenone as photocrosslinker. Irradiation of benzophenone with UV light in the range of 350-365 nm leads to the formation of a triplet diradical, which can abstract hydrogen atoms of C-H bonds from proteins. This leads to a ketyl and an alkyl radical and recombination of both forms the crosslink product. The triplet diradical can also react with water to form a hydrate, which reacts, under elimination of water, to the educt benzophenone.⁹⁴

The formation of the corresponding reactive species, which can then react with C-H or heteroatom-H bonds, of common photoreactive groups is shown in Figure 14. ABPP probes used in this work contain benzophenone as a photoreactive group and therefore the detailed overview of benzophenone reactivity is shown in Figure 15.

Excitation of benzophenones with UV light of wavelengths between 350 and 365 nm leads to reversible formation of a triplet diradical, which can react with biological compounds. The reaction is reversible and relaxation to the ground state occurs within 120 μ s. As the reaction of the diradical with water forms the corresponding benzophenone hydrate, which eliminates water under reforming the initial benzophenone, unspecific labelling by unbound probe is reduced. The diradical reacts preferentially with C-H bonds and the first step is abstraction of a hydrogen atom, which leads to a ketyl and an alkyl radical. Favoured positions for hydrogen abstraction are α -

positions of amino acids, tertiary carbon atoms and heteroatom stabilized positions, which is due to their stabilization of the generated carbon radical. Both radicals combine, which results in formation of the desired crosslink product.^{97,99}

AIM OF THIS WORK

β -Lactams and other natural products have been successfully applied to treat bacterial infections¹² but due to the increasing antibiotic resistance development, new compounds exhibiting potent antibacterial or antivirulent activities are urgently needed.¹⁴ Former members of our research group successfully applied the ABPP approach to diverse natural product classes and showed that mono- and bicyclic β -lactones display potent antivirulent effects in *Listeria monocytogenes* and *S. aureus* strains including MRSA.^{28-30, 71, 100, 101}

Inspired by these results, a former group member synthesized a diverse set of γ -butyrolactone ABPP probes to investigate their protein-reactivity and binding-specificity in diverse bacterial strains. This project is continued in this work and can be divided into two parts:

1. Application of the ABPP technology to the natural product class of γ -butyrolactones and investigation of their protein-reactivity and binding-specificity in diverse bacterial strains.
2. Design, synthesis and application of monocyclic and xanthatin inspired bicyclic α -methylene- γ -butyrolactone ABPP probes to investigate their protein targets in pathogenic bacteria.

SUMMARY

Protein Reactivity of Natural Product-Derived γ -Butyrolactones

Although β -lactams and other natural products have been successfully used in the treatment of bacterial infections, the increasing development of antibiotic resistance provokes an urgent need for the discovery of novel target-drug pairs in chemical and pharmaceutical science. Recent studies have successfully applied ABPP to diverse natural product classes, and found that mono- and bicyclic β -lactones exhibit potent antivirulent effects in *Listeria monocytogenes* and *Staphylococcus aureus* strains.

Inspired by these results and the huge structural diversity of naturally occurring γ -butyrolactones, the ABPP approach was extended to this natural product class to unravel targets for antivirulent drugs. Hence, a diverse set of γ -butyrolactone (and thiolactone) probes, including compounds containing an endo- or exocyclic Michael system, was synthesized.

Proteome-profiling in *Staphylococcus aureus*, *Pseudomonas aeruginosa* and *Escherichia coli* revealed that γ -butyrolactone probes lacking the exocyclic Michael system show almost no labelling in the investigated strains, which may be due to a reversible and non-covalent binding mode. This result is in line with the relatively low ring strain of 5-membered scaffolds compared to their 4-membered relatives, which leads to a decreased intrinsic reactivity towards nucleophiles.

Therefore, proteome-profiling and identification of the protein targets of γ -butyrolactones was achieved by introduction of a photoreactive group, which led to a covalent target-binding and revealed an enzyme involved in protein folding as major protein target in *Pseudomonas* and *Burkholderia* strains. Competitive ABPP showed that γ -butyrolactones can compete with the photoreactive probe in labelling of this protein, which supports the reversible and noncovalent target-binding mode.

In comparison to γ -butyrolactones, the α -methylene- γ -butyrolactone probe showed a distinct labelling pattern in gram-positive and -negative bacterial strains. Identified proteins are involved in diverse cellular functions and mostly contain active site cysteines.

These results demonstrate that α -butyrolactones can be successfully applied in ABPP independent if they contain a photoreactive group or an exocyclic Michael system. In particular, α -methylene- γ -butyrolactones seem to exhibit a fine-tuned reactivity towards cysteines of elevated nucleophilicity. To further explore their protein-reactivities and binding specificities, a set of structurally diverse α -methylene- γ -butyrolactone ABPP probes has to be synthesized.

Target analysis of α -alkylidene- γ -butyrolactones in uropathogenic *E. coli*

It was previously shown that α -methylene- γ -butyrolactones have been successfully applied to the activity-based protein profiling (ABPP) technology and exhibit diverse biological activities (e.g. antibiotic and cytotoxic). To further explore their protein-reactivities and binding specificities, a small library of xanthatin (natural product with potent antibiotic activity) inspired bicyclic α -alkylidene-, α -benzylidene- and α -methylene- γ -butyrolactone probes was synthesized.

Interestingly, α -alkylidene- and α -benzylidene- γ -butyrolactones showed almost no labelling in the investigated strains. This may be due to the heptyl- and phenyl-substituent, which causes steric hindrance and leads to an electron donating effect resulting in a decreased reactivity of the Michael system towards nucleophiles. In contrast to that, proteome-profiling as well as the comparison of pathogenic and non-pathogenic *E. coli* strains by ABPP with α -methylene- γ -butyrolactones revealed protein targets that are involved in several cellular redox processes. ThiI (tRNA sulfurtransferase) catalyses the transfer of sulphur to cytidine of tRNAs to produce 4-thiouridine. The catalytic mechanism involves two cysteines, which are both essential for the catalytic activity. Unfortunately, it was not possible to identify the probe binding site. KatG (catalase-peroxidase) and AhpC (alkyl hydroperoxide reductase) are members of reactive oxygen species defensive proteins. AhpC catalyses the reduction of alkyl hydroperoxides and contains two important cysteine residues. Mass spectrometric analysis revealed one of these two cysteine residues as probe binding sites, emphasizing a potent enzyme inhibition by probe treatment.

The gene of one protein, C2450, which was only identified in pathogenic *E. coli*, belongs to a genomic island that encodes for a hybrid polyketide/non-ribosomal peptide synthetase (PKS/NRPS). This system is responsible for the synthesis of colibactin, a natural product which causes DNA double strand breaks in eukaryotic cells leading to the activation of the DNA damage checkpoint pathway and subsequent cell cycle arrest. While the role of several proteins that are involved in colibactin synthesis is already known, the function of C2450 remains unclear.

Investigation of the binding site was achieved by mass spectrometric analysis and revealed probe modification of the single cysteine residue. To characterize the function of C2450, the enzymatic turnover of peptidase-, protease- and esterase-substrates was investigated, but no hydrolytic activity was detected. Therefore, further substrate screens will be required in order to understand its biological role.

The results demonstrate a successful application of α -methylene- γ -butyrolactone probes in ABPP by identifying covalent bound target proteins involved in diverse cellular processes. Here, probe binding was mediated via active site cysteine residues of elevated nucleophilicity.

α -Methylene- γ -butyrolactones attenuate *Staphylococcus aureus* virulence by inhibition of transcriptional regulation

The increase in antibiotic resistance development leads to a lack of novel and effective antibiotic drugs and raises the interest for compounds targeting bacterial virulence instead of killing them. The existing probe library was expanded by the synthesis of structural diverse monocyclic α -methylene- γ -butyrolactone probes and all compounds were screened for inhibition of α -hemolysin expression, which represents a major *Staphylococcus aureus* virulence factor. Interestingly, only monocyclic probes containing a Michael system showed inhibitory effects, with hemolysis IC₅₀ values of 2-26 μ M. The corresponding minimal inhibitory concentrations were above 100 μ M and no influence on bacterial growth was detected for the two most active compounds with concentrations in the range of their hemolysis IC₅₀ values. These two probes were used for further studies.

Target deconvolution by ABPP revealed five major protein targets (MurA, TrxA, SarA, SarR and MgrA). MurA1 and MurA2 are involved in bacterial cell wall biogenesis and the concentration depended inhibition of both proteins, which was shown via *in vitro* monitoring the MurA1/2-catalysed enolpyruvyl transfer reaction of phosphoenolpyruvate and UDP-*N*-acetylglucosamine, may account for the observed MIC values. TrxA maintains the intracellular thiol-disulfide balance via forming or breaking disulfide bonds by inter-protein exchange reactions. Probe treatment leads to an inhibition of TrxA, which was determined by monitoring the *in vitro* reduction of disulfide bonds within insulin.

Probe binding to the transcriptional virulence regulators SarA, SarR and MgrA was investigated by tryptic digestion of the purified proteins followed by mass spectrometric analysis and occurred exclusively on the conserved redox sensing cysteine residues. A derivate lacking the exocyclic double bond has shown no effect on *S. aureus* hemolysis, rendering the Michael system essential for biological activity. EMSA (electrophoretic mobility shift assay) studies revealed that probe binding induces target protein-DNA dissociation, which alters the target gene expression. The comparison of probe-treated strains with knockout strains showed that the inhibition of hemolysis is due to the inhibition of the transcriptional regulators SarA, SarR and MgrA.

These results demonstrate that the probe binds covalently to all three transcriptional regulators and causes dissociation from their corresponding promoter regions, which results in a reduced α -hemolysin expression. This emphasizes the drugability of these virulence regulators for medical applications by α -methylene- γ -butyrolactones.

ZUSAMMENFASSUNG

Protein-Reaktivität von Naturstoff-abgeleiteten γ -Butyrolactonen

β -Lactame und andere Naturstoffe werden erfolgreich zur Behandlung bakterieller Infektionen verwendet. Aufgrund der Zunahme von antibiotikaresistenten Bakterienstämmen, ist die Erforschung neuer Wirkstoffe und ihrer Angriffsziele ein wichtiges Ziel der chemischen und pharmazeutischen Forschung. Kürzlich veröffentlichte Studien untersuchten verschiedene Naturstoffklassen mittels aktivitätsbasierendes Protein-Profilings (ABPP) und beobachteten antivirulente Eigenschaften von mono- und bicyklischen β -Lactonen in *Listeria monocytogenes* und *Staphylococcus aureus*.

Inspiziert durch diese Ergebnisse sowie die große strukturelle Vielfalt an natürlich vorkommenden γ -Butyrolactonen, wurde ABPP auf diese Naturstoffklasse angewendet um neue Angriffsziele für antivirulente Medikamente aufzudecken. Dazu wurden verschiedene γ -Butyrolacton-Sonden, ihre Thiolacton-Derivate sowie γ -Butyrolacton-Sonden mit endo- oder exozyklischem Michael-System synthetisiert.

ABPP in *Staphylococcus aureus*, *Pseudomonas aeruginosa* und *Escherichia coli* zeigte, dass γ -Butyrolactone ohne exozyklischem Michael-System nur schwache Markierungen in den untersuchten Bakterienstämmen lieferten, was zu der Annahme eines reversiblen und nichtkovalenten Bindungsmodus führt. Dieser kann durch die vergleichsweise geringe Ringspannung von 5-gliedrigen Ringen im Vergleich zu 4-gliedrigen Ringen erklärt werden, wodurch ihre intrinsische Reaktivität gegenüber Nucleophilen geschwächt wird. Um eine kovalente Sondenbindung zu ermöglichen, wurde eine photoreaktive Gruppe eingeführt und ABPP lieferte ein in die Proteinfaltung involviertes Protein als Hauptziel in verschiedenen *Pseudomonas* und *Burkholderia* Stämmen. Kompetitives ABPP zeigte, dass γ -Butyrolactone bei der Markierung dieses Proteins mit der photoreaktiven Sonde konkurrieren konnten, was die Annahme eines nichtkovalenten Bindungsmodus unterstützt.

Im Gegensatz zu γ -Butyrolactonen lieferten α -Methylen- γ -Butyrolactone ein ausgeprägtes Markierungsmuster in gram-positiven und -negativen Bakterienstämmen. Die identifizierten Proteine sind in verschiedene Zellfunktionen involviert und enthalten meist Cysteine im aktiven

Zentrum des Proteins. Diese Ergebnisse zeigen, dass γ -Butyrolactone erfolgreich in ABPP eingesetzt werden können, wenn sie eine photoreaktive Gruppe oder ein exozyklisches Michael-System besitzen. Besonders α -Methylen- γ -Butyrolactone besitzen eine feinabgestimmte Reaktivität gegenüber Cysteinen mit erhöhter Nucleophilie. Durch die Synthese von weiteren strukturell unterschiedlichen α -Methylen- γ -Butyrolactonen könnten detaillierte Erkenntnisse bezüglich ihrer Proteinreaktivität und Bindungsspezifität erlangt werden.

Analyse der Protein-Angriffsziele von α -Alkyliden- γ -Butyrolactonen in uropathogenen *E. coli*-Stämmen

Es wurde bereits gezeigt, dass α -Methylen- γ -Butyrolactone erfolgreich in ABPP verwendet wurden und eine Vielzahl an biologischen Aktivitäten (z.B. antibiotische und zytotoxische) besitzen. Um ihre Proteinreaktivität und Bindungsspezifität näher zu untersuchen, wurden verschiedene, von Xanthatin (antibiotisch aktiver Naturstoff) abgeleitete, bicyklische α -Alkyliden-, α -Benzyliden- und α -Methylen- γ -Butyrolacton-Sonden synthetisiert.

Interessanterweise zeigten α -Alkyliden- und α -Benzyliden- γ -Butyrolactone nahezu keine Markierung in den untersuchten Bakterienstämmen. Dies liegt wahrscheinlich an den sterisch anspruchsvollen Heptyl- und Phenyl-Substituenten, welche darüber hinaus die Reaktivität des Michael Systems gegenüber Nucleophilen durch ihren elektronenschiebenden Effekt vermindern. Im Gegensatz dazu lieferte der Vergleich von pathogenen und nichtpathogenen *Escherichia coli* Stämmen durch ABPP mit α -Methylen- γ -Butyrolactonen Zielproteine, welche in zelluläre Redox-Prozesse involviert sind. ThiI (tRNA Sulfurtransferase) katalysiert den Transfer von Schwefel auf tRNA-gebundenes Cytidin, um 4-Thiouridin zu produzieren. Der Mechanismus benötigt zwei Cysteine, welche für die katalytische Aktivität essentiell sind. KatG (Catalase-Peroxidase) und AhpC (Alkyl Hydroperoxid Reductase) dienen dem Abbau von reaktiven Sauerstoffspezies. Dabei katalysiert AhpC die Reduktion von Alkyl-Hydroperoxiden und enthält zwei katalytisch wichtige Cysteine. Massenspektrometrische Analyse identifizierte eines der beiden Cysteine als Bindungsstelle, was eine Enzyminhibition durch Sondenbindung nahelegt.

Das Gen eines Proteins, C2450, wurde nur in pathogenen *E. coli* identifiziert und gehört zu einer genomischen Insel, welche für eine Polyketid/nichtribosomale-Peptidsynthetase (PKS/NRPS) kodiert. Dieses System ist für die Synthese von Colibactin verantwortlich. Colibactin induziert DNA Doppelstrangbrüche in eukaryotischen Zellen, wodurch der „DNA-Checkpoint Pathway“ aktiviert wird, was zu einem Arrest des Zellzyklus führt. Während die Funktion der meisten Proteine der

Colibactin Biosynthese aufgeklärt wurde, ist die Funktion von C2450 unbekannt. Massenspektrometrische Untersuchungen zeigten eine kovalente Sondenbindung an dem einzigen Cystein-Rest. Um die Funktion von C2450 aufzuklären, wurde der enzymatische Umsatz von Peptidase-, Protease- und Esterase-Substraten untersucht; es konnte allerdings keine hydrolytische Aktivität beobachtet werden. Weitere Substrat-Screenings sind daher notwendig um die biologische Rolle von C2450 aufzuklären.

Die Ergebnisse zeigen die erfolgreiche Anwendung von α -Methylen- γ -Butyrolactonen in ABPP. Die identifizierten Proteine sind in verschiedene zelluläre Prozesse involviert und die kovalente Sondenbindung erfolgt durch Cysteine mit erhöhter Nukleophilie im aktiven Zentrum von Proteinen.

α -Methylen- γ -Butyrolactone vermindern die Virulenz von *Staphylococcus aureus* durch Inhibition der transkriptionellen Regulation

Die zunehmende Entwicklung von Antibiotikaresistenzen führt zu einem Mangel an neuen und effektiven Medikamenten und erhöht damit das Interesse an neuen Verbindungen, welche lediglich die bakterielle Virulenz inhibieren anstatt die Bakterien zu töten. Die existierende Sondenbibliothek wurde durch die Synthese von monocyclischen α -Methylen- γ -Butyrolactonen erweitert. Alle Sonden wurden dann auf Inhibition der α -Hämolsin-Produktion, einer der bedeutendsten Virulenzfaktoren von *Staphylococcus aureus*, getestet. Interessanterweise zeigten nur die monozyklischen Sonden mit Michael System eine Inhibition mit IC_{50} -Werten von 2-26 μ M. Dabei lagen die minimalen Hemmkonzentrationen (MICs) jeweils über 100 μ M. Die zwei aktivsten Hämolyse-Inhibitoren zeigten keinen Einfluss auf das Wachstum von *S. aureus* in Konzentrationen im Bereich ihrer IC_{50} -Werte und wurden deshalb für die weiteren Versuche verwendet.

Durch ABPP wurden fünf Proteine identifiziert (MurA, TrxA, SarA, SarR und MgrA). MurA1 und MurA2 sind essentielle Enzyme zur Biogenese der bakteriellen Zellwand. Die Konzentrationsabhängige Inhibition der MurA1/2-katalysierten Enolpyruvyl-Transferreaktion von Phosphoenolpyruvat und UDP-*N*-Acetylglucosamin, trägt wahrscheinlich zu den beobachteten MICs bei. TrxA hält das intrazelluläre Thiol-Disulfid-Gleichgewicht durch Bindung und Spaltung von Disulfidbindungen mittels Protein-Protein Austauschreaktionen konstant. Die Sondeninkubation

fürte dabei zu einer konzentrationsabhängigen Inhibition von TrxA, welche *in vitro* durch Messung der Reduktion der Disulfidbrücken von Insulin bestimmt wurde.

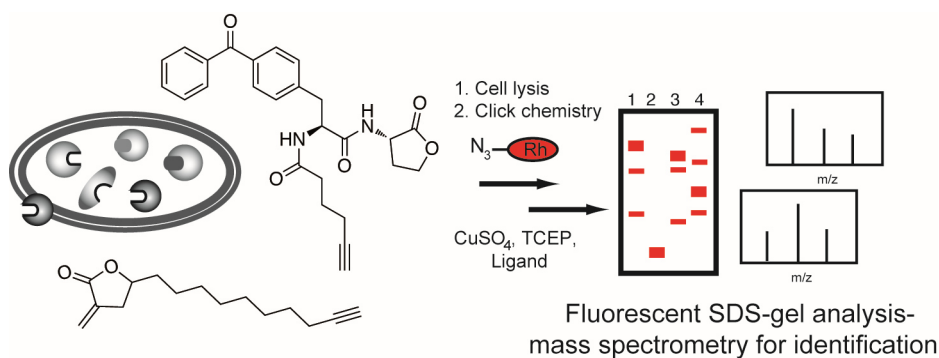
Die Sondenbindung zu den transkriptionellen Regulatoren SarA, SarR und MgrA wurde durch tryptischen Verdau der gereinigten Proteine und anschließender massenspektrometrischer Analyse untersucht und erfolgte ausschließlich durch das, für die regulatorische Funktion essentielle, reaktive Cystein. Ein Derivat ohne exozyklische Doppelbindung hat keinen Einfluss auf die Hämolyse, wonach das Michael System der Sonden essentiell für ihre biologische Aktivität ist. EMSA-Studien zeigten, dass die kovalente Modifikation dieses Cysteins zur Protein-DNA Dissoziation führt, wodurch sich die Expression der Zielgene ändert. Aus einem Vergleich von sondenbehandelten *S. aureus* Kulturen mit den entsprechenden Knockout-Stämmen folgt, dass die verminderte Hämolyse durch die Inhibition von SarA, SarR und MgrA verursacht wird.

Die Ergebnisse implizieren, dass die Sonden kovalent an alle drei transkriptionellen Regulatoren binden, diese daraufhin von ihren Promoter-Regionen dissoziieren, was zu einer reduzierten Expression von α -Hämolyisin führt. Dies zeigt eine Möglichkeit auf, bakterielle Virulenzregulatoren durch α -Methylen- γ -Butyrolactone zu medizinischen Zwecken zu inhibieren.

RESULTS AND DISCUSSION

Protein Reactivity of Natural Product-Derived γ -Butyrolactones

Reproduced with permission from M. H. Kunzmann, I. Staub, T. Böttcher, S. A. Sieber, *Biochemistry* **2011**, *50*, 910-916. DOI: 10.1021/BI101858G. Copyright 2011 American Chemical Society.



Abstract

The discovery of novel and unique target-drug pairs for the treatment of human diseases such as cancer and bacterial infections is an urgent goal of chemical and pharmaceutical sciences. Natural products represent an inspiring source of compounds for designing chemical biology methods for target identification and characterization. Inspired by the huge structural diversity of γ -butyrolactones, that constitute up to 10% of all known compounds of natural origin, we extended the “activity-based protein profiling” (ABPP) target identification technology to this promising and so far unexplored natural compound class. We designed and synthesized a comprehensive set of natural product derived γ -lactones and thiolactones that varied in their protein reactivity. We obtained several important bacterial enzymes that are involved in diverse cellular functions such as metabolism (dihydrolipoyl dehydrogenase and 6-phosphofructokinase), cell wall biosynthesis (MurA1 and MurA2) as well as protein folding (trigger factors). Especially protein folding in bacteria could represent a novel strategy for antibiotic intervention and

requires chemical tools for characterization and inhibition. Future studies that extend on structural modifications on protein reactive α -methylene- γ -butyrolactone as well as on reversible binding γ -lactones and thiolactones will reveal if this premise holds true.

Introduction

Electrophilic entities such as epoxides, β -lactams, β -lactones and Michael acceptor systems constitute a large fraction of natural products with a huge diversity of biological activities. In many cases the biological potency is directly linked to the intrinsic electrophilic reactivity that leads to covalent modifications of nucleophilic active site residues such as serine, cysteine and lysine of many important enzyme classes including dehydrogenases, hydrolases and transferases.^{87, 102} These enzymes play crucial roles in diseases such as cancer, diabetes as well as bacterial infections and are of major interest as novel drug targets. However, especially in case of bacterial infections new potent and selective drugs and their corresponding novel and resistance-free targets are lacking which has led to a renaissance of untreatable infectious diseases caused by multiresistant bacteria. In order to identify these urgently needed unique target-drug pairs, natural products represent an inspiring source of compounds for designing chemical biology methods for target identification (tools) and characterization.^{55, 57, 71, 103} Initial studies with β -lactones already demonstrated the power of this approach by the identification of a central regulator of virulence as a novel concept to combat pathogenic bacteria.^{28, 57} Inspired by this approach we extended the “activity-based protein profiling” (ABPP)^{40, 102, 104} target identification technology to the γ -butyrolactones, a structural motif found in up to 10% of all known compounds of natural origin.⁷² The high abundance and structurally diverse decoration of this motif already suggests that evolution has selected γ -butyrolactones for a variety of important biological applications which could give rise to novel lead structures for potent drugs.¹⁰⁵ Structurally closely related γ -butyrothiolactones also exhibit interesting biological activities like the natural product antibiotic thiolactomycin.¹⁰⁶

In order to explore the full reactivity profile of 5-membered cyclic lactones and thiolactones we synthesized a diverse set of γ -butyrolactones and thiolactones as well as their Michael acceptor activated derivatives α -methylene- γ -butyrolactones and α -butenolides. All core scaffolds were equipped with an alkyne handle that serves as a benign tag for the modification with rhodamine azide or rhodamine-biotin-azide for visualization (fluorescence scanning) and identification (mass spectrometry) of labelled proteins, respectively, via the Huisgen, Sharpless, Meldal click chemistry (CC) reaction (Figure 1).^{46, 107-109}

γ -Butyrolactone probes:

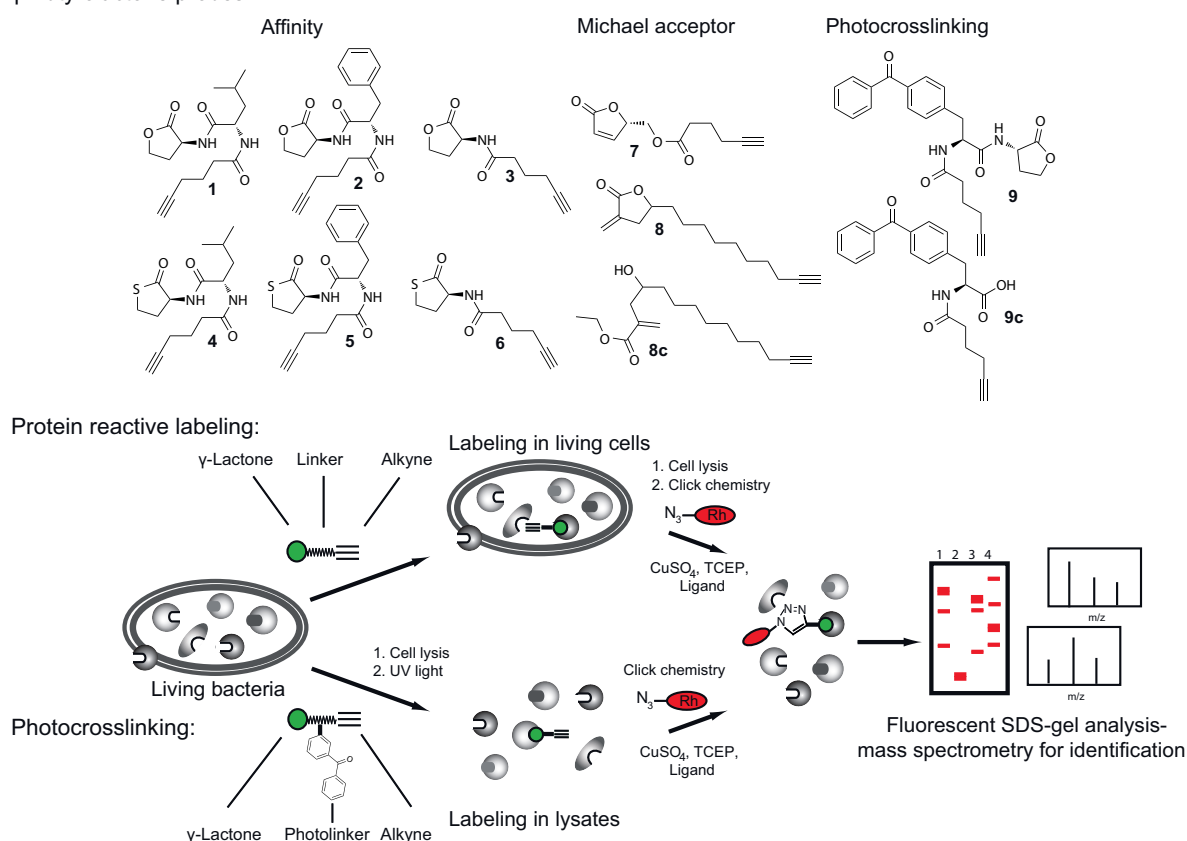


Figure 1: Design of γ -butyrolactone and thiolactone probes and their application in bacterial proteome-profiling. Probes are directly incubated with living bacteria to penetrate the cells and label dedicated protein targets *in situ*. The cells are subsequently lysed and the labelled proteins are “clicked” to a fluorescent rhodamine-azide dye for visualization by SDS gel electrophoresis and identification by MS. In case of photocrosslinking, the lactone binds its target in cellular extracts and gets covalently attached by UV irradiation at 366 nm.

The advantage of this approach is the small size and less perturbed structure of the original lactone motif which is particularly suitable to label proteins in living cells (*in situ*). We here show that this approach with several 5-membered lactones reveals important insights into the reactivity and binding preferences of these natural product inspired probes. While regular γ -butyrolactones and thiolactones displayed only little reactivity with proteomic samples, the Michael acceptor based α -methylene- γ -butyrolactones exhibited a high tendency to covalently label a series of important bacterial enzymes. To compensate the lack of labelling for the majority of γ -butyrolactones, we synthesized an affinity binding probe with a photocrosslinking moiety¹¹⁰⁻¹¹³ (benzophenone) that revealed a remarkable selectivity for the binding of bacterial cis-trans prolyl isomerases (Figure 1).

Results and Discussion

For our initial reactivity studies with cyclic 5-membered ring systems we designed several probes that were either based on a lactone or thiolactone ring equipped with hexynoyl, leucyl-hexynoyl or phenylalanyl-hexynoyl peptidic side chains in the 3-position (probes **1-6**). Synthesis of these probes was achieved by the modification of L-homoserine lactone and L-homocysteine thiolactone, respectively (Scheme S1, Appendix). In addition, the initial probe selection was complemented by the synthesis of a butenolide probe **7**. We rationalized that this compound could be of elevated electrophilicity due to the presence of an internal Michael acceptor system. The probe was prepared by hexynoic acid coupling to commercially available (S)-(-)-5-(hydroxymethyl)-2(5H)-furanone (Scheme S1, Appendix).

In order to test these probes towards their protein reactivities we incubated them with intact bacterial cells as well as bacterial lysates derived from non-pathogenic strains such as *B. thailandensis*, *E. coli* and *P. putida* as well as pathogenic strains such as *B. cenocepacia*, *P. aeruginosa* and *S. aureus* for 1 h at room temperature. Upon incubation, cells were lysed and a fluorescent rhodamine-azide tag attached via CC. In all cases, almost no or only weak labelling intensities were observed indicating that the unactivated γ -lactones and thiolactones, including the internal Michael acceptor system, are not reactive enough to be attacked by nucleophilic enzyme active site residues (Figure S1, Appendix). This result clearly indicates that these motifs are not suitable for direct proteome-profiling and suggests that most likely many natural products that contain these structural motifs such as homoserine lactones which are involved in bacterial quorum sensing, most likely exhibit their biological activities via a reversible binding mode of their dedicated targets.¹¹⁴ We therefore adjusted our initial strategy and designed two additional γ -lactone based probes that either contained a benzophenone photocrosslinker (**9**) in the side chain to monitor reversible binding interactions or an α -methylene- γ -butyrolactone probe (**8**) with elevated electrophilicity due to an external Michael acceptor system. In the following we will first discuss the profiling results of the α -methylene- γ -butyrolactone probe and then compare these studies with the photocrosslinking probe.

The α -methylene- γ -butyrolactone group is present in many bioactive compounds of natural as well as synthetic origin. Remarkably, about 3% of all known natural products contain this functional group which emphasizes its potential role in its parent compounds which display a diverse range of bioactivities such as anticancer, antimalarial, antiviral and antibacterial.⁷² To test the proteome reactivity and dedicated target preferences of this structural motif we designed and

synthesized an alkyne substituted α -methylene- γ -butyrolactone probe for global proteome analysis. The synthesis started with oxidation of undecynol by Dess-Martin periodinane leading to the corresponding aldehyde undecynal. The aldehyde was subsequently coupled to ethyl-2-(bromomethyl)-acrylate via a Reformatsky reaction, which lead to 4-hydroxy-2-methylene-tetradec-13-ynoic acid ethyl ester (**8c**). The cyclization of **8c** was initiated by addition of a catalytic amount of 4-toluene sulfonic acid leading to 5-dec-9-ynyl-3-methylene-dihydro-furan-2-one (**8**). (Scheme S2, Appendix). The precursor molecule (**8c**) of the cyclized α -methylene- γ -butyrolactone probe (**8**) contains a linear Michael acceptor system which was used as a control to investigate the influence of the intact cyclic γ -lactone motif for reactivity and selectivity compared to the open form.

Proteome-profiling experiments were initiated by incubation of probes **8** and **8c** with several pathogenic bacterial organisms such as *P. aeruginosa* and *S. aureus* under *in situ* conditions with intact cells. Subsequent CC, SDS-gel analysis and fluorescent scanning revealed a distinct set of specific protein bands in all proteomes investigated, emphasizing that the probe displays suitable properties for *in situ* studies. A concentration of 200 μ M for gram negative *P. aeruginosa* and 40 μ M for gram positive *S. aureus* as well as an incubation time of 1 h turned out to be optimal for saturated labelling (Figure 2 and Figure S2, Appendix). Some targets could be even labelled at significantly lower concentrations down to 5 μ M indicating an increased sensitivity and specificity. In addition, the control probe **8c** with the open Michael acceptor displays significantly less labelling indicating that the cyclic γ -lactone motif is required for the obtained target preferences.

Subsequent target identification was carried out by mass spectrometry using a quantitative enrichment strategy for labelled enzymes.⁵⁷ In brief, labelled proteomes were incubated with a trifunctional rhodamine-biotin azide tag under CC conditions, enriched and purified on avidin beads, separated by SDS gel electrophoresis, fluorescent bands isolated, digested and subjected to mass spectrometric (MS) analysis with an orbitrap MS. Fragmentation data was analysed with the SEQUEST algorithm and several protein hits were obtained that correlated in their molecular weight with the sizes of the corresponding gel bands (Table S1, Appendix). Several proteins were identified that play important roles in the primary metabolism of bacteria such as 6-phosphofructokinase (PFK) in *S. aureus* which is a key enzyme in glycolysis as well as dihydrolipoamide dehydrogenase (DLDH) in both *S. aureus* and *P. aeruginosa* which is also important for glycolysis and the citrate cycle. Moreover, MurA1 and MurA2, two essential enzymes for cell wall biosynthesis in *S. aureus*, were identified in multiresistant *S. aureus* cells (MRSA). Interestingly, these enzymes have been previously labelled by a showdomycin probe

which also represents a Michael acceptor natural product emphasizing a similar reactivity and affinity profile.⁷¹

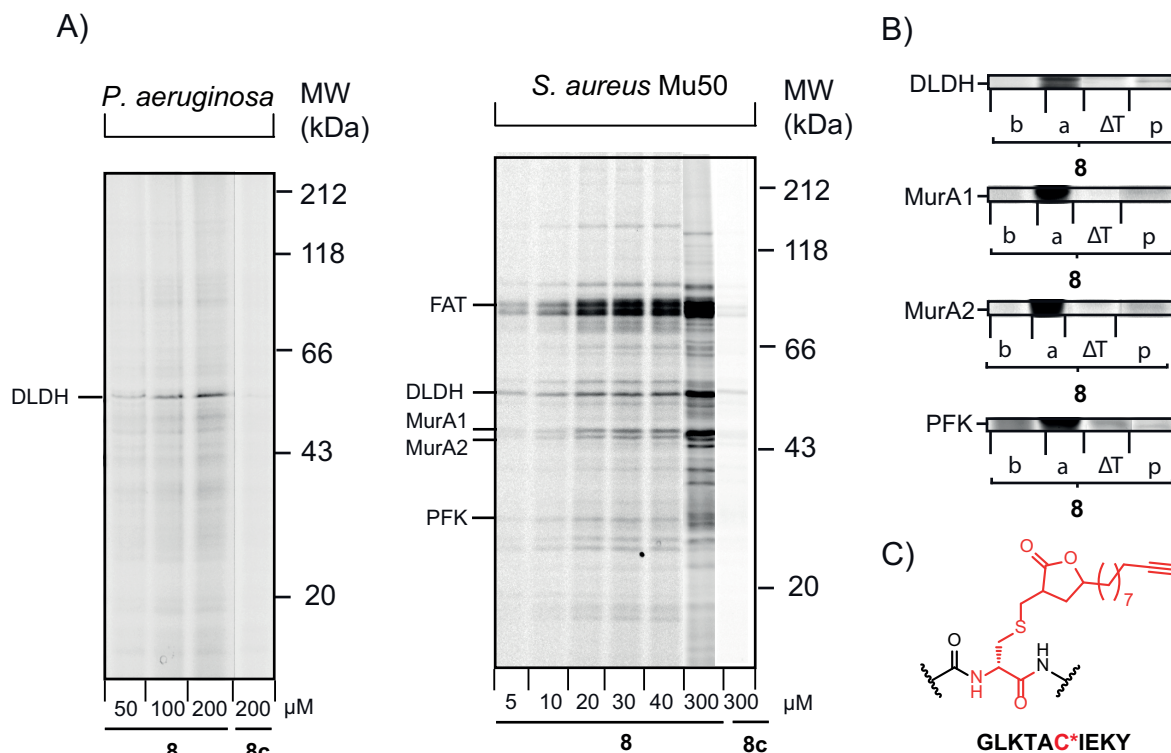


Figure 2: *In situ* labelling of bacterial proteomes with the α -methylene- γ -butyrolactone probe (**8**). A) Fluorescent SDS gels with labelled proteins. The protein identity is abbreviated next to the gels: DLDH = Dihydrolipoamide dehydrogenase, FAT = Formate acyltransferase, MurA1,2 = UDP-*N*-acetylglucosamine 1-carboxyvinyltransferase, PFK = 6-Phosphofructokinase, MW = molecular weight marker. B) Recombinant expression and labelling of target proteins (b = before induction, a = after induction, ΔT = heat control of induced recombinant protein, p = native protein band in the corresponding proteome). C) Site of modification of *P. aeruginosa* DLDH.

To confirm the results of mass spectrometry by additional independent experiments, we recombinantly expressed several of our observed targets and labelled them subsequently with the corresponding probes. In fact, in all cases the probes labelled their targets in an activity dependent manner as confirmed by heat denaturation controls (Figure 2B). As an example for the binding mode of the α -methylene- γ -butyrolactone probes to their targets we investigated the site of modification of *P. aeruginosa* DLDH with probe **8** by MS. One cysteine residue was found to be modified by the probe while no other cysteine and none of the 19 serine residues reacted with the Michael acceptor (Figure 2 and Figure S6, Appendix).

These results emphasize the fine-tuned reactivity of the α -methylene- γ -butyrolactone probe and demonstrate the value of this reactive motif for proteome profiling experiments and further suggest that the full potential of this motif can be explored by an increasing number of structural diverse molecules that bind a vast array of enzymes based on dedicated and customized affinity features.

To broaden our knowledge about the binding preferences of γ -lactones that are not activated by an electrophilic Michael acceptor system, we designed and synthesized a photocrosslinker functionalized lactone probe with a benzophenone moiety and the alkyne handle embodied in a peptidic side chain (probe **9**, Figure 1). Since benzophenone represents a large structural element it could influence and direct the binding of the probe to additional, γ -lactone unrelated, targets. In order to identify only those targets that specifically bind the γ -lactone motif, we synthesized a control probe **9c**, in which only the benzophenone and alkyne containing peptidic side chain without the γ -lactone moiety are present. All targets that are labelled by both probes are presumably bound predominantly by the benzophenone peptide whereas targets that are only labelled by the γ -lactone probe represent proteins with specific recognition elements for this motif. Since we are interested in the biological targets of reversible binding γ -lactones we will only focus on the identification of their corresponding protein bands.

The synthesis of probes **9** and **9c** followed standard peptide coupling procedures and is described in more detail in the experimental section (Scheme S3, Appendix). Labelling experiments were carried out in bacterial lysates of several pathogenic and non-pathogenic organisms such as *P. aeruginosa*, *P. putida*, *B. cenocepacia*, *B. thailandensis* and *E. coli*. 20 μ M of probe **9** and control probe **9c** were incubated with each bacterial proteome on ice and irradiated at 366 nm for 1 h. Proteomes were then subject to CC and separated and visualized by SDS gel electrophoresis and fluorescent scanning as described above. Several fluorescent bands were observed on the gels but only one strong band that was present in all proteomes correlated uniquely to the γ -lactone containing probe **9** (Figure 3A and Figure S3, Appendix).

The band was investigated by mass spectrometry and identified as a trigger factor (TF). Trigger factors are essential bacterial enzymes for the cis-trans isomerization of peptidyl-prolyl bonds and represent a molecular switch for the regulation of enzyme activity.¹¹⁵ The trigger factors such as found in *E. coli* K12 belong to the FK506 binding protein family of peptidyl prolyl cis-trans isomerases and assist the initial folding steps during bacterial protein synthesis.¹¹⁶⁻¹¹⁸ They consist of the *N*-domain, which mediates binding to the ribosomal tunnel exit protein, the PPIase

(peptidyl prolyl isomerase) domain and the C-domain with chaperone activity. The folding is downstream assisted by the ATP-dependent DnaK/J and GroEL/ES.

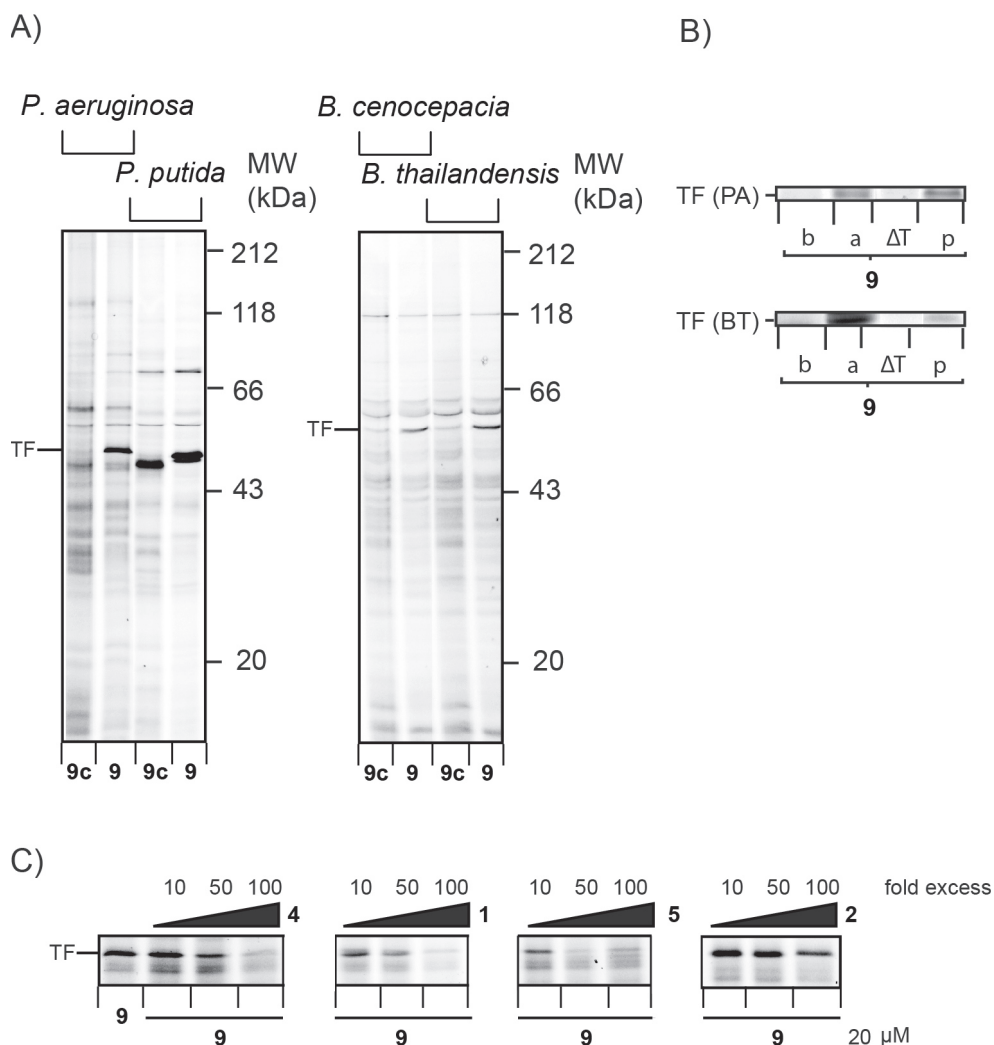


Figure 3: Labelling of bacterial lysates with a γ -lactone photocrosslinking probe. A) Fluorescent SDS gels (TF = trigger factor, MW = molecular weight marker). B) Recombinant expression of trigger factor and labelling (b = before induction, a = after induction, ΔT = heat control of induced recombinant protein, p = native protein band in the corresponding proteome). C) Competitive profiling with reversible binding γ -lactones 4, 1, 5, 2. Lactones were pre-incubated in 10, 50 and 100 fold excess with the *P. aeruginosa* proteome and subsequently labelled with photocrosslinking probe 9.

The results from mass spectrometric identification were again independently verified by recombinant expression of several trigger factor enzymes from *B. thailandensis*, *B. cenocepacia*, *P. aeruginosa* and *E. coli* (Figure 3B and Figure S3, Appendix). All recombinant enzymes were specifically labelled by the corresponding lactone probe 9 whereas heat denatured enzymes did not reveal any labelling indicating that only the native and folded protein can interact with the probe. Moreover, we were able to demonstrate trigger factor binding of probe 9 in living cells of

P. putida emphasizing the relevance and great utility of this probe as a tool in proteomics (Figure S5, Appendix).

Since the labelling of the trigger factors by probe **9** is UV dependent, a reversible binding mode of the γ -lactone is most likely. We therefore tested all our other reversible binding γ -lactones and thiolactones that we used for initial screens (see above, compounds **1-7**) in competitive assays to investigate whether they could compete for the same binding site which would further confirm that the γ -lactone moiety, as a close mimic of proline, is the central recognition element of trigger factors. Interestingly, several γ -lactones and thiolactones were able to compete for binding in various degrees. Probe **5** for instance revealed strong competition at 50 and 100 fold excess while all other compounds such as structurally closely related probes **1**, **2** and **4** exhibited much weaker competition for the binding site indicating that a phenyl substituted thiolactone is the most promising motif out of our initial library to bind and inhibit trigger factors (Figure 3 and Figure S4, Appendix). To evaluate its potency for the inhibition of PPIase (peptidyl prolyl isomerase) activity, we used an assay that is based on the solvent dependent cis/trans re-equilibration of the tetrapeptide *N*-succinyl-Ala-Ala-Pro-Phe-*p*-nitroanilide.¹¹⁹ The peptide was dissolved in 0.5 M LiCl in trifluoroethanol, which lead to a cis-content of the Pro-Phe bond of about 50%. After dilution into aqueous buffer (50 mM Hepes, pH 7.8) the cis-content decreased to about 10%. Because the cis-peptide has a higher absorption coefficient, the decrease during dilution into aqueous buffer can be measured by monitoring the absorption at 330 nm at 10 °C for 10 min.

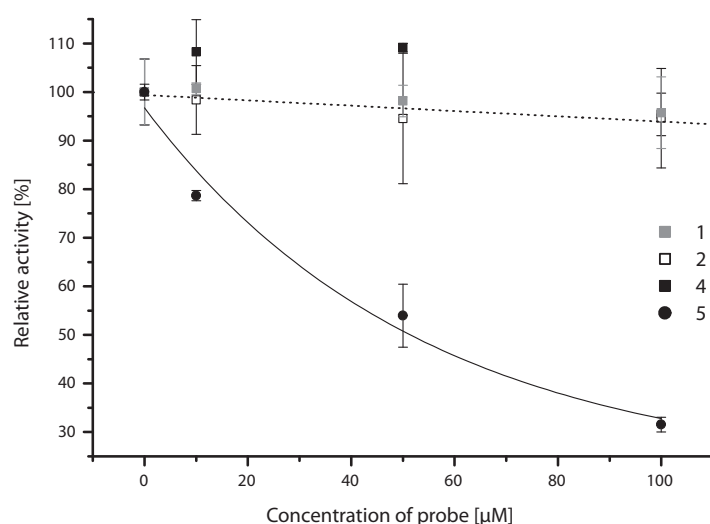


Figure 4: IC₅₀ determination of the *E. coli* TF by the lactones **1**, **2**, **4** and **5**.

The mean average kinetic constant (each out of three independent experiments) versus lactone concentration was plotted and the concentration of 50% inhibition (IC₅₀) was determined. Figure 4

shows the IC_{50} determination of the *E. coli* trigger factor by the lactones **1**, **2**, **4** and **5**. Interestingly, an IC_{50} value of 50 μ M emphasizes that the compound directly targets the PPIase domain of trigger factors and leads to a potent inhibition. Vice versa, compounds **1**, **2** and **4** exhibited weaker binding in the competition assay and showed almost no inhibition in the assay. Although compounds **1-7** were initially designed as reactive probes, their conserved structural lactone motifs can be utilized in combination with crosslinking groups to identify reversible binding inhibitors for dedicated targets.

Conclusion

In summary we designed and synthesized an initial set of γ -lactones and thiolactones that varied in their protein reactivity. Our initial selection of non-activated compounds did not reveal significant protein reactivities but one individual member turned out to be a reversible inhibitor of the trigger factor. This result emphasizes the potency of our chemical proteomic strategy that utilizes protein reactive probes in combination with photoreactive affinity probes to identify the biological targets of γ -lactones. We obtained several important bacterial enzymes that are involved in diverse cellular functions such as metabolism, cell wall biosynthesis as well as protein folding. Protein folding in bacteria could particularly represent a novel strategy for antibiotic intervention and requires chemical tools for characterization and inhibition. In fact, it could be already demonstrated that a dual knockout of trigger factor and complimentary chaperone folding machinery, DnaK and DnaJ, is lethal.^{120, 121} We here introduce novel tools to study trigger factors and present novel lead structures based on the γ -lactone structural moiety for inhibition and potential therapeutic application. Future studies that extend structural modifications on protein reactive α -methylene- γ -butyrolactone as well as on reversible binding γ -lactones and thiolactones will reveal if this premise holds true.

Acknowledgements

We thank Matthew Nodwell for valuable comments on the manuscript and Mona Wolff for excellent technical assistance.

Experimental

Materials. All chemicals were of reagent grade or better and used without further purification. Chemicals and solvents were purchased from Sigma Aldrich or Acros Organics. For all reactions, only commercially available solvents of purissimum grade, dried over molecular sieve and stored under argon atmosphere were used. Solvents for chromatography and workup purposes were generally of reagent grade and purified before use by distillation. In all reactions, temperatures were measured externally. All experiments were carried out under argon. Column chromatography was performed on Merck silica gel (Acros Organics 0.035-0.070 mm, mesh 60 Å). ^1H NMR spectra were recorded on a Varian Mercury 200 (200 MHz), a Varian NMR-System 600 (600 MHz) or a Varian NMR-System 300 (300 MHz) and ^{13}C NMR spectra were measured with a Varian NMR-System 600 (600 MHz) and a Varian NMR-System 300 (300 MHz) and referenced to the residual proton and carbon signal of the deuterated solvent, respectively. Mass spectra were obtained by GC-MS with a Varian 3400 gas chromatograph via a 25 m CS Supreme-5 capillary column (0.25 mm, layer 0.25 μm) with a gradient of 50 °C (1 min isotherm) to 300 °C (4 min isotherm), 25 °C min^{-1} coupled with a Finnigan MAT 95 mass spectrometer in EI mode (70 eV, 250 °C source). For DEI measurements, samples were directly desorbed from platinum wire (20-1600 °C, 120 °C min^{-1}). ESI spectra were recorded with a Thermo Finnigan LTQ FT. HPLC analysis was accomplished with a Waters 2695 separations module, a X-Bridge™ BEH130 C18 column (4.6 x 100 mm) and a Waters 2996 PDA detector.

Probe Synthesis (Probes 1-9c were synthesized by Dr. Isabell Staub).

Hex-5-ynoyl chloride (3a). A 10-mL one-necked, round-bottomed flask was charged with hex-5-ynoic acid (1.1 mL, 10 mmol, 1.0 eq) and thionyl chloride (1.1 mL, 12 mmol, 1.2 eq) and the mixture refluxed under argon for 1 h (90 °C, oil bath). Subsequently, the product was distilled off ($T_b = 32$ °C, 100 mbar) yielding 1.25 g (96 %) of **3a** as colourless liquid. ^1H NMR (360 MHz, CDCl_3): $\delta = 3.07$ (t, $J = 7.2$ Hz, 2 H, C(O)- $\underline{\text{CH}_2}$), 2.30 (dt, $J = 6.8, 2.7$ Hz, 2 H, $\text{HC}\equiv\text{C}-\underline{\text{CH}_2}$), 2.02 (t, $J = 2.7$ Hz, 1 H, $\underline{\text{H}}\text{C}\equiv\text{C}$), 1.92 (ps. quint., $J = 7.0$ Hz, 2 H, C(O)- CH_2 - $\underline{\text{CH}_2}$). ^{13}C NMR (90 MHz, CDCl_3): $\delta = 173.5, 82.1, 70.0, 45.6, 23.6, 17.2$.

2,5-Dioxopyrrolidin-1-yl hex-5-ynoate (1a). *N*-Hydroxysuccinimide (1.08 g, 9.35 mmol, 1.05 eq) and 1-ethyl-3-(3-dimethyl-aminopropyl)carbodiimide hydrochloride EDAC (1.79 g, 9.36 mmol, 1.05 eq) were added to a solution of hex-5-ynoic acid (984 μL , 8.92 mmol, 1.00 eq) in dichloromethane (40 mL) and stirred for 7 h at r.t. The reaction mixture was washed three times with water (30 mL, each) and once with brine (30 mL). The aqueous phases were re-extracted

with dichloromethane (30 mL) and the combined organic layers were dried over MgSO_4 , filtered and evaporated in vacuo to yield 1.83 g (93 %) of **1a** as pale yellow oil. ^1H NMR (400 MHz, CDCl_3): δ = 2.83 (s, 4 H, $\text{C(O)-CH}_2\text{-CH}_2\text{-C(O)}$), 2.77 (t, J = 7.4 Hz, 2 H, C(O)-CH_2), 2.34 (dt, J = 6.9, 2.7 Hz, 2 H, $\text{HC}\equiv\text{C-CH}_2$), 2.01 (t, J = 2.7 Hz, 1 H, $\text{HC}\equiv\text{C}$), 1.92 (ps. quint., J = 7.1 Hz, 2 H, $\text{C(O)-CH}_2\text{-CH}_2$). ^{13}C NMR (101 MHz, CDCl_3): δ = 168.9, 168.0, 82.2, 69.6, 29.5, 25.4, 23.2, 17.4.

N-Hex-5-ynoyl-L-leucine (1c). 2,5-Dioxopyrrolidin-1-yl hex-5-ynoate (418 mg, 2.00 mmol, 1.00 eq) was added to a solution of L-leucine (262 mg, 2.00 mmol, 1.00 eq) in a mixture of MeCN (3 mL) and water (3.5 mL) with triethylamine (1.7 mL, 12 mmol) and stirred at r.t. over night. The solvent was evaporated under reduced pressure and the product purified by flash column chromatography on silica gel with the TLC optimized solvent mixture $\text{CH}_2\text{Cl}_2/\text{EtOH}$ 10:1, R_f = 0.35. Evaporation of the solvent afforded 341 mg (75 %) of **1c** as pale yellow oil. ^1H NMR (400 MHz, CDCl_3): δ = 6.20 (d, J = 8.3 Hz, 1 H, NH), 4.57 (ddd, J = 9.2, 8.5, 4.7 Hz, 1 H, NH-CH-C(O)OH), 2.39 (t, J = 7.4 Hz, 2 H, C(O)-CH_2), 2.26 (dt, J = 6.7, 2.6 Hz, 2 H, $\text{HC}\equiv\text{C-CH}_2$), 1.98 (t, J = 2.5 Hz, 1 H, $\text{HC}\equiv\text{C}$), 1.86 (ps. quint., J = 7.1 Hz, 2 H, $\text{C(O)-CH}_2\text{-CH}_2$), 0.95 (d, J = 6.0 Hz, 3 H, CH_3), 0.94 (d, J = 5.9 Hz, 3 H, CH_3). ^{13}C NMR (101 MHz, CDCl_3): δ = 176.3, 173.3, 83.4, 69.3, 50.9, 41.0, 34.8, 24.9, 24.0, 22.8, 21.8, 17.7. HRMS ESI positive mode (m/z): 226.1434 [$\text{M}+\text{H}$] $^+$ (calc.: 226.1438), 451.2792 [$2\text{M}+\text{H}$] $^+$ (calc.: 451.2803), 468.3057 [$2\text{M}+\text{NH}_4$] $^+$ (calc.: 468.3068), 676.4155 [$3\text{M}+\text{H}$] $^+$ (calc.: 676.4168), 693.4422 [$3\text{M}+\text{NH}_4$] $^+$ (calc.: 693.4433), 698.3974 [$3\text{M}+\text{Na}$] $^+$ (calc.: 698.3987). HRMS ESI negative mode (m/z): 224.1297 [$\text{M}-\text{H}$] $^-$ (calc.: 224.1292), 449.2660 [$2\text{M}-\text{H}$] $^-$ (calc.: 449.2657).

N-Hex-5-ynoyl-L-phenylalanine (2a). 2,5-Dioxopyrrolidin-1-yl hex-5-ynoate (418 mg, 2.00 mmol, 1.00 eq) was added to a solution of L-phenylalanine (330 mg, 2.00 mmol, 1.00 eq) in a mixture of MeCN (2 mL) and water (3 mL) with triethylamine (1.7 mL, 12 mmol) and stirred at r.t. over night. The solvent was evaporated under reduced pressure and the product purified by flash column chromatography on silica gel with the TLC optimized solvent mixture $\text{CH}_2\text{Cl}_2/\text{EtOH}$ 10:1, R_f = 0.69. Evaporation of the solvent afforded 440 mg (58 %) of **2a** as pale yellow solid. ^1H NMR (600 MHz, CDCl_3): δ = 7.31-7.24 (m, 3 H, H_{arom}), 7.17-7.16 (m, 2 H, H_{arom}), 6.13 (br d, J = 5.5 Hz, 1 H, NH), 4.85 (ps. dt, J = 6.8, 5.6 Hz, 1 H, NH-CH-C(O)OH), 3.23 (dd, J = 14.1, 5.4 Hz, 1 H, $\text{CH-CH}_a\text{H}_b$), 3.10 (dd, J = 14.1, 6.6 Hz, 1 H, $\text{CH-CH}_a\text{H}_b$), 2.32 (t, J = 7.3 Hz, 2 H, C(O)-CH_2), 2.22-2.12 (m, 2 H, $\text{HC}\equiv\text{C-CH}_2$), 1.95 (t, J = 2.6 Hz, 1 H, $\text{HC}\equiv\text{C}$), 1.79 (ps. quint., J = 7.1 Hz, 2 H, $\text{C(O)-CH}_2\text{-CH}_2$), ^{13}C NMR (151 MHz, CDCl_3): δ = 174.5, 173.0, 135.7, 129.3, 128.7, 127.2, 83.3, 69.3, 50.8, 37.3, 34.7, 25.3, 17.7. HRMS ESI positive mode (m/z): 260.1277 [$\text{M}+\text{H}$] $^+$ (calc.: 260.1287), 282.1096 [$\text{M}+\text{Na}$] $^+$ (calc.: 282.1106), 519.2477 [$2\text{M}+\text{H}$] $^+$ (calc.: 519.2495), 536.2746 [$2\text{M}+\text{NH}_4$] $^+$ (calc.: 536.2755), 541.2299 [$2\text{M}+\text{Na}$] $^+$

(calc.: 541.2309), 557.1950 [2M+K]⁺ (calc.: 557.2048), 800.3380 [3M+Na]⁺ (calc.: 800.3517). HRMS ESI negative mode (m/z): 258.1136 [M-H]⁻ (calc.: 258.1136), 517.2333 [2M-H]⁻ (calc.: 517.2344).

L-Homoserine lactone hydrochloride (1b). The synthetic strategy was adopted from Boyle et al.¹²² L-Homoserine (200.0 mg, 1.679 mmol, 1.0 eq) was dissolved in HCl_{aq} (2.4 M, 3.3 mL) and stirred for 7 h at 140 °C under reflux. After cooling to room temperature, ice cold EtOH (20 mL) was added and the solvents were evaporated under reduced pressure until the total volume of the residue was 3 mL. The resulting colourless precipitate was filtered and washed with ice cold EtOH resulting in 158 mg (68 %) of **1b** as colourless solid. ¹H NMR (600 MHz, D₂O): δ = 4.49 (ps. t, *J* = 9.3 Hz, 1 H, NH₃⁺-CH), 4.29–4.35 (m, 2 H, COO-CH₂), 2.65–2.70 (m, 1 H, CH-CH_aH_b), 2.31 (ps. quint, 1 H, *J* = 10.9 Hz, CH-CH_aH_b). ¹³C NMR (101 MHz, D₂O): δ = 174.4, 67.3, 48.4, 26.7.

N-Hex-5-ynoyl-L-homoserine lactone (3). To a solution of L-homoserine lactone hydrochloride (34.8 mg, 0.25 mmol, 1.00 eq) in dimethylformamide DMF (2 mL) with *N,N*-diisopropylethylamine DIPEA (418 μL, 2.40 mmol, 9.60 eq) was added hex-5-ynoyl chloride (32.6 mg, 0.250 mmol, 1.00 eq). The reaction mixture was stirred for 6 h and another portion of DIPEA (418 μL, 2.40 mmol, 9.60 eq) and hex-5-ynoyl chloride (3.3 mg, 0.030 mmol, 0.10 eq) added. The solvent was removed in vacuo and the residue stirred with diethyl ether (10 mL) and 1 M HCl_{aq} (5 mL) The organic layer was separated and the aqueous phase extracted two times with dichloromethane (15 mL, each). The organic layers were collected, dried over MgSO₄, filtered, and the solvent evaporated in vacuo. The product was purified by flash column chromatography on silica gel with the TLC optimized solvent mixture ethyl acetate/iso-hexane 4:1, *R*_f = 0.28. Evaporation of the solvent afforded 23.2 mg (48 %) of **3** as colourless solid. ¹H NMR (600 MHz, CDCl₃): δ = 6.35 (br d, *J* = 5.0 Hz, 1 H, NH), 4.58 (ddd, *J* = 11.6, 8.7, 6.3 Hz, 1 H, OC(O)-CH-NH), 4.45 (ps. dt, *J* = 9.1, 1.2 Hz, 1 H, C(O)O-CH_aH_b), 4.27 (ddd, *J* = 11.2, 9.3, 6.0 Hz, 1 H, C(O)O-CH_aH_b), 2.79 (dddd, *J* = 12.5, 8.7, 6.0, 1.2, 1 H, C(O)O-CH₂-CH_aH_b), 2.39 (ps. dt, *J* = 7.6, 1.7 Hz, 2 H, C(O)-CH₂), 2.26 (dt, *J* = 6.8, 2.7, 2 H, HC≡C-CH₂), 2.16 (ps. dtd, *J* = 12.5, 11.4, 8.9 Hz, 1 H, C(O)O-CH₂-CH_aH_b), 1.98 (t, *J* = 2.6 Hz, 1 H, HC≡C), 1.86 (ps. quint, *J* = 7.3 Hz, HC≡C-CH₂-CH₂). ¹³C NMR (151 MHz, CDCl₃): δ = 175.5, 172.9, 83.3, 69.3, 66.0, 49.1, 34.4, 30.2, 23.8, 17.7. GC retention time: 8.8 min. HRMS EI positive mode (m/z): 195.0877 [M]⁺ (calc.: 195.0895), 143.0568 [M-C₃H₅]⁺ (calc.: 143.0582).

N-Hex-5-ynoyl-L-homocysteine thiolactone (6). To a solution of L-homocysteine thiolactone hydrochloride (15.4 mg, 0.100 mmol, 1.00 eq) in dimethylformamide DMF (2 mL) with *N,N*-diisopropylethylamine DIPEA (209 μL, 1.20 mmol, 12.0 eq) was added hex-5-ynoyl chloride (22.0 mg, 0.170 mmol, 1.70 eq). The reaction mixture was stirred for 12 h, the solvent was removed in

vacuo and the residue stirred with dichloromethane (8 mL) and 1 M HCl_{aq} (5 mL). The organic layer was separated and the aqueous phase extracted two times with dichloromethane (8 mL, each). The organic layers were collected, dried over MgSO₄, filtered, and the solvent evaporated in vacuo. The product was purified by flash column chromatography on silica gel with the TLC optimized solvent mixture ethyl acetate/iso-hexane 3:2, *R*_f = 0.20. Evaporation of the solvent afforded 12.6 mg (60 %) of **6** as colourless solid. ¹H NMR (300 MHz, CDCl₃): δ = 5.99 (br, 1 H, NH), 4.52 (ddd, *J* = 12.8, 6.9, 6.0 Hz, 1 H, SC(O)-CH-NH), 3.36 (ddd, *J* = 12.1, 11.5, 5.1 Hz, 1 H, C(O)S-CH_aH_b), 3.25 (ddd, *J* = 11.4, 7.0, 1.2 Hz, 1 H, C(O)S-CH_aH_b), 2.94 (dddd, *J* = 12.3, 6.6, 5.1, 1.3, 1 H, C(O)S-CH₂-CH_aH_b), 2.39 (t, *J* = 7.6 Hz, 2 H, C(O)-CH₂), 2.27 (dt, *J* = 7.1, 2.6, 2 H, HC≡C-CH₂), 1.98 (t, *J* = 2.7 Hz, 1 H, HC≡C), 1.99-1.93 (m, 1 H, C(O)S-CH₂-CH_aH_b), 1.87 (ps. quint., *J* = 7.2 Hz, HC≡C-CH₂-CH₂). ¹³C NMR (75 MHz, CDCl₃): δ = 205.5, 172.8, 83.3, 69.4, 59.5, 34.7, 32.0, 27.6, 23.9, 17.8. HRMS DEI positive mode (*m/z*): 211.0658 [M]⁺ (calc.: 211.0667).

***N*-Hex-5-ynoyl-L-leucyl-L-homoserine lactone (1).** DIPEA (68 μL, 0.40 mmol, 4.0 eq) was added to *N*-hex-5-ynoyl-L-leucine (38.3 mg 0.170 mmol, 1.70 eq) in dry DMF (1.0 mL). The mixture was stirred at room temperature for 10 min, treated with *N,N'*-diisopropyl carbodiimide, DIC (50 μL, 0.32 mmol, 3.2 eq) and stirred for another 10 min before L-homoserine lactone hydrochloride (13.8 mg, 0.100 mmol, 1.00 eq) was added. The solution was stirred at room temperature overnight. After evaporation under reduced pressure the residue was purified by HPLC to afford 25.9 mg (84 %) of **1** as colourless solid. ¹H NMR (400 MHz, CD₃CN): δ = 7.13 (d, *J* = 7.5 Hz, 1 H, NH-C(O)-CH-NH), 6.66 (d, *J* = 7.6 Hz, 1 H, NH-C(O)-CH-NH), 4.48 (ddd, *J* = 11.0, 9.2, 8.0, 1 H, OC(O)-CH-NH), 4.39 – 4.30 (m, 2 H, NH-C(O)-CH-NH, C(O)O-CH_aH_b), 4.21 (ddd, *J* = 10.5, 9.0, 6.6 Hz, 1 H, C(O)O-CH_aH_b), 2.46 (dddd, *J* = 12.3, 9.1, 6.5, 1.9 Hz, 1 H, C(O)O-CH₂-CH_aH_b), 2.29 (t, *J* = 7.1 Hz, 2 H, C(O)-CH₂), 2.24 – 2.18 (m, 4 H, C(O)O-CH₂-CH_aH_b, HC≡C, HC≡C-CH₂), 1.76 (ps. quint, *J* = 7.1 Hz, 2 H, HC≡C-CH₂-CH₂), 1.69 – 1.47 (m, 3 H, CH_aH_b-CH(CH₃)₂, CH_aH_b-CH(CH₃)₂, CH(CH₃)₂), 0.93 (d, *J* = 6.6 Hz, 1 H, CH₃), 0.89 (d, *J* = 6.5 Hz, 1 H, CH₃). ¹³C NMR (101 MHz, CD₃CN): δ = 175.9, 173.5, 173.3, 84.7, 70.1, 66.5, 52.4, 49.2, 41.5, 35.2, 29.1, 25.4, 25.2, 23.2, 21.8, 18.3. HRMS ESI positive mode (*m/z*): 309.1800 [M+H]⁺ (calc.: 309.1809), 326.2065 [M+NH₄]⁺ (calc.: 326.2074), 331.1619 [M+Na]⁺ (calc.: 331.1628), 617.3525 [2M+H]⁺ (calc.: 617.3545), 639.3342 [2M+Na]⁺ (calc.: 639.3364). HRMS ESI negative mode (*m/z*): 307.1677 [M-H]⁻ (calc.: 307.1663).

***N*-Hex-5-ynoyl-L-leucyl-L-homocysteine thiolactone (4).** *N*-Hex-5-ynoyl-L-leucine (76.6 mg, 0.340 mmol, 1.70 eq) was added to a solution of DIPEA (136 μL, 0.800 mmol, 4.00 eq) in dry DMF (2.0 mL). The mixture was stirred at room temperature for 10 min, treated with *N,N'*-diisopropyl carbodiimide, DIC (52.7 μL, 0.340 mmol, 1.70 eq) and stirred for another 5 min before L-

homocysteine thiolactone hydrochloride (30.6 mg, 0.200 mmol, 1.00 eq) was added. The solution was stirred at room temperature overnight. The solvent was removed in vacuo and the product was purified by flash column chromatography on silica gel with the TLC optimized solvent mixture ethyl acetate/iso-hexane 1:1, $R_f = 0.36$. The resulting product was further purified by HPLC yielding 3.9 mg (6 %) of **4** as colourless solid. ^1H NMR (400 MHz, CD_3CN): $\delta = 6.87$ (d, $J = 7.4$ Hz, 1 H, NH), 6.57 (d, $J = 7.7$ Hz, 1 H, NH), 4.55 (dddd, $J = 12.7, 8.1, 7.0, 0.4$ Hz, 1 H, SC(O)-CH-NH), 4.31 (ddd, $J = 9.7, 7.9, 5.2$ Hz, 1 H, NH-C(O)-CH-NH), 3.36 (ddd, $J = 11.9, 11.3, 5.4$ Hz, 1 H, C(O)S-CH_aH_b), 3.25 (dddd, $J = 11.2, 7.0, 1.5, 0.4$ Hz, 1 H, C(O)S-CH_aH_b), 2.51 (dddd, $J = 12.4, 7.0, 5.4, 1.6$ Hz, 1 H, C(O)S-CH₂-CH_aH_b), 2.28 (t, $J = 7.4$ Hz, 2 H, C(O)-CH₂), 2.23 – 2.17 (m, 3 H, HC≡C, HC≡C-CH₂), 2.12 – 2.06 (m, 1 H, C(O)S-CH₂-CH_aH_b), 1.76 (ps. quint, $J = 7.1$ Hz, 2 H, HC≡C-CH₂-CH₂), 1.68 – 1.46 (m, 3 H, CH_aH_b-CH(CH₃)₂, CH_aH_b-CH(CH₃)₂, CH(CH₃)₂), 0.93 (d, $J = 6.5$ Hz, 3 H, CH₃), 0.88 (d, $J = 6.5$ Hz, 3 H, CH₃). ^{13}C NMR (400 MHz, CD_3CN): $\delta = 206.0, 173.5, 173.2, 84.6, 70.1, 59.3, 52.5, 41.5, 35.1, 31.3, 27.8, 25.4, 25.1, 23.2, 21.7, 18.2$. HRMS ESI positive mode (m/z): 325.1572 [M+H]⁺ (calc.: 325.1580), 347.1391 [M+Na]⁺ (calc.: 347.1400), 363.1130 [M+K]⁺ (calc.: 363.1139), 649.3066 [2M+H]⁺ (calc.: 649.3088), 671.2884 [2M+Na]⁺ (calc.: 671.2907), 687.2625 [2M+K]⁺ (calc.: 687.2647). HRMS ESI negative mode (m/z): 323.1477 [M-H]⁻ (calc.: 323.1435), 359.1255 [M+Cl]⁻ (calc.: 359.1202).

***N*-Hex-5-ynoyl-L-phenylalanyl-L-homoserine lactone (2).** *N*-Hex-5-ynoyl-L-phenylalanine (88.2 mg, 0.340 mmol, 1.70 eq) was added to a solution of DIPEA (136 μL , 0.800 mmol, 4.00 eq) in dry DMF (2.0 mL). The mixture was stirred at room temperature for 10 min, treated with *N,N'*-diisopropyl carbodiimide, DIC (52.7 μL , 0.340 mmol, 1.70 eq) and stirred for another 5 min before L-homoserine lactone hydrochloride (27.5 mg, 0.200 mmol, 1.00 eq) was added. The solution was stirred at room temperature overnight. The solvent was removed in vacuo and the product was purified by flash column chromatography on silica gel with the TLC optimized solvent mixture ethyl acetate/iso-hexane 6:1, $R_f = 0.51$. The resulting product was further purified by HPLC yielding 22.1 mg (32 %) of **2** as colourless solid. ^1H NMR (400 MHz, CD_3CN): $\delta = 7.31 - 7.20$ (m, 5 H, H_{arom}), 7.12 (d, $J = 7.1$ Hz, NH-C(O)-CH-NH), 6.63 (d, $J = 7.7$ Hz, NH-C(O)-CH-NH), 4.60 (ddd, $J = 9.0, 8.4, 5.1$ Hz, 1 H, NH-C(O)-CH-NH), 4.46 (ddd, $J = 10.9, 9.1, 7.9$ Hz, 1 H, OC(O)-CH-NH), 4.38 (ps. dt, $J = 9.0, 2.0$ Hz, 1 H, C(O)O-CH_aH_b), 4.22 (ddd, $J = 10.5, 9.0, 6.6$ Hz, 1 H, C(O)O-CH_aH_b), 3.16 (dd, $J = 13.9, 5.1$ Hz, 1 H, Ph-CH_aH_b), 2.83 (dd, $J = 14.0, 9.1$ Hz, 1 H, Ph-CH_aH_b), 2.46 (dddd, $J = 12.3, 9.2, 6.6, 2.0$ Hz, 1 H, C(O)O-CH₂-CH_aH_b), 2.15 – 2.27 (m, 4 H, C(O)O-CH₂-CH_aH_b, C(O)-CH₂, HC≡C), 2.06 (dt, $J = 7.1, 2.7$ Hz, 2 H, HC≡C-CH₂), 1.63 (ps. quint, $J = 7.2$ Hz, 2 H, HC≡C-CH₂-CH₂). ^{13}C NMR (101 MHz, CD_3CN): $\delta = 175.5, 172.7, 171.9, 138.1, 129.9, 129.9, 128.9, 127.2, 117.9, 84.3, 69.8, 66.2, 54.5, 49.0, 37.9, 34.8, 28.7, 24.8, 17.8$. HRMS ESI positive mode (m/z): 343.1643 [M+H]⁺

(calc.: 343.1652), 360.1908 [M+NH₄]⁺ (calc.: 360.1918), 365.1462 [M+Na]⁺ (calc.: 365.1472), 685.3210 [2M+H]⁺ (calc.: 685.3232), 702.3470 [2M+NH₄]⁺ (calc.: 702.3497), 707.3029 [2M+Na]⁺ (calc.: 707.3051). HRMS ESI negative mode (m/z): 341.1539 [M-H]⁻ (calc.: 341.1507), 387.1630 [M+FA-H]⁻ (calc.: 387.1562).

***N*-Hexynoyl-L-phenylalanyl-L-homocysteine thiolactone (5).** *N*-Hex-5-ynoyl-L-phenylalanine (79.0 mg 0.300 mmol, 1.50 eq) was added to a solution of DIPEA (106 μL, 0.620 mmol, 3.10 eq) in dry DMF (1.5 mL). The mixture was stirred at room temperature for 10 min, treated with *N,N'*-diisopropyl carbodiimide, DIC (46.5 μL, 0.300 mmol, 1.50 eq) and stirred for another 5 min before L-homocysteine thiolactone hydrochloride (30.6 mg, 0.200 mmol, 1.00 eq) was added. The solution was stirred at room temperature overnight. The solvent was removed in vacuo and the product was purified by flash column chromatography on silica gel with the TLC optimized solvent mixture ethyl acetate/iso-hexane 3:1, *R*_f = 0.52. The resulting product was further purified by HPLC yielding 7.8 mg (11 %) of **5** as colourless solid. ¹H NMR (600 MHz, CDCl₃): δ = 7.32 – 7.21 (m, 5 H, H_{arom}), 6.42 (d, *J* = 5.9 Hz, 1 H, NH-C(O)-CH-NH), 6.14 (d, *J* = 7.6 Hz, 1 H, NH-C(O)-CH-NH), 4.72 (ps. quart., *J* = 7.0 Hz, 1 H, NH-C(O)-CH), 4.41 (ps. td, *J* = 13.0, 6.6 Hz 1 H, NH-CH-C(O)S), 3.33 (ps. dt, *J* = 11.8, 5.2 Hz, 1 H, C(O)S-CH_aH_b), 3.24 (ddd, *J* = 11.3, 6.9, 1.0 Hz, 1 H, C(O)S-CH_aH_b), 3.10 (dd, *J* = 14.5, 6.8, Hz, 1 H, Ph-CH_aH_b), 3.08 (dd, *J* = 14.5, 6.8, Hz, 1 H, Ph-CH_aH_b), 2.80 (dddd, *J* = 12.5, 6.6, 5.2, 1.2 Hz, 1 H, C(O)S-CH₂-CH_aH_b), 2.31 (t, *J* = 7.4 Hz, 2 H, C(O)-CH₂), 2.12 - 2.23 (m, 2 H, HC≡C-CH₂), 1.96 (t, *J* = 2.6 Hz, 1 H, HC≡C), 1.93 (dq, 12.4, 7.0 Hz, 1 H, C(O)S-CH₂-CH_aH_b), 1.79 (ps. quint., *J* = 7.0 Hz, 2 H, HC≡C-CH₂-CH₂). ¹³C NMR (151 MHz, CDCl₃): δ = 204.2, 172.3, 171.4, 136.0, 129.3, 129.3, 128.8, 128.8, 127.2, 83.3, 69.4, 59.3, 54.2, 38.3, 34.8, 31.3, 27.5, 23.9, 17.7. HRMS ESI positive mode (m/z): 359.1416 [M+H]⁺ (calc.: 359.1424), 376.1681 [M+NH₄]⁺ (calc.: 376.1689), 381.1237 [M+Na]⁺ (calc.: 381.1243), 717.2760 [2M+H]⁺ (calc.: 717.2775), 734.3025 [2M+NH₄]⁺ (calc.: 734.3040), 739.2581 [2M+Na]⁺ (calc.: 739.2594). HRMS ESI negative mode (m/z): 357.1309 [M-H]⁻ (calc.: 357.1278), 403.1401 [M+FA-H]⁻ (calc.: 403.1333).

(*S*)-(5-Oxo-2,5-dihydrofuran-2-yl)methyl hex-5-ynoate (7). *N,N'*-Diisopropylcarbodiimide (DIC) (92.9 μL, 75.7 mg, 0.600 mmol, 1.20 eq) was added to a solution of hex-5-ynoic acid (66.5 μL, 0.600 mmol, 1.20 eq) in dry dichloromethane (5 mL). After 10 min (*S*)-(-)-5-(hydroxymethyl)-2(5*H*)-furanone (57.1 mg, 0.500 mmol, 1.00 eq) was added and the reaction stirred overnight. The solvent was evaporated under reduced pressure and the purification of the resulting oil by HPLC afforded 39.9 mg (38 %) of **7** as colourless solid. ¹H NMR (300 MHz, CDCl₃): δ = 7.42 (dd, *J* = 5.8, 1.6 Hz, 1 H, CH=CH-C(O)O), 6.19 (dd, *J* = 5.8, 2.1 Hz, 1 H, CH=CH-C(O)O), 5.22 (dddd, *J* = 4.9, 4.0, 2.1, 1.7 Hz, 1 H, C(O)O-CH), 4.37 (dd, *J* = 12.1, 3.7 Hz, 1 H, C(O)O-CH-CH_aH_b), 4.31 (dd, *J* = 12.0,

4.8 Hz, 1 H, C(O)O-CH-CH_aH_b), 2.45 (t, *J* = 7.4 Hz, 2 H, C(O)-CH₂), 2.23 (dt, *J* = 6.9, 2.6 Hz, 2 H, HC≡C-CH₂), 1.96 (t, *J* = 2.7 Hz, 1 H, HC≡C), 1.80 (ps. quint, *J* = 7.3 Hz, 2 H, HC≡C-CH₂-CH₂). ¹³C NMR (101 MHz, CDCl₃) δ = 172.6, 172.1, 152.3, 123.3, 82.9, 80.8, 69.6, 62.5, 32.4, 23.3, 17.7. HRMS ESI positive mode (*m/z*): 226.1067 [M+NH₄]⁺ (calc.: 226.1074).

Undec-10-ynal (8b). A 100-mL, one-necked, round-bottomed flask was charged with a solution of Dess-Martin periodinane, DMP (2.32 g, 5.47 mmol, 1.00 eq) in 30 mL of dichloromethane and then cooled in an ice bath while undec-10-ynol (1.05 mL, 5.47 mmol, 1.00 eq) was added dropwise over 1 min. The reaction was stirred for 5 min at 0 °C and after stirring additionally 3 h at room temperature the reaction was completed as monitored by TLC (*n*-pentane/diethyl ether 9:1; *R_f* = 0.32). Thereafter the suspension was transferred with 10 mL diethyl ether to a 50-mL falcon tube and centrifuged (4,000 rpm, 10 min). The supernatant was collected by decantation and the residual pellet was extracted with 20 mL *n*-pentane/diethyl ether (4:1). The combined organic fractions were concentrated under reduced pressure with a rotary evaporator (40 °C, > 200 mbar) and the residue was purified by flash column chromatography on silica gel (*n*-pentane/diethyl ether 9:1). Evaporation of the solvent afforded 658 mg (72 %) of **8b** as colourless liquid. *R_f* (SiO₂, *n*-pentane/diethyl ether 9:1) = 0.32. ¹H NMR (200 MHz, CDCl₃): δ = 9.76 (t, *J* = 1.9 Hz, 1 H, CHO), 2.42 (dt, *J* = 7.3, 1.9 Hz, 2 H, CH₂-CHO), 2.17 (dt, *J* = 6.8, 2.5 Hz, 2 H, HC≡C-CH₂), 1.93 (t, *J* = 2.6 Hz, 1 H, HC≡C), 1.20 (m, 12 H, C₆H₁₂).

4-Hydroxy-2-methylenetetradec-13-ynoic acid ethyl ester (8c). To a suspension of **8b** (193.8 mg, 1.17 mmol, 1.50 eq) and Zn-powder (76.2 mg, 1.17 mmol, 1.50 eq) in 5 mL saturated aqueous NH₄Cl solution THF (4:1) was added ethyl-2-(bromomethyl)-acrylate (107 μL, 0.777 mmol, 1.00 eq) and the reaction mixture was stirred overnight at room temperature. Ethyl acetate (12 mL) was added, the organic layer was separated and the aqueous layer was extracted two times with ethyl acetate (12 mL). The combined organic fractions were washed with brine (10 mL), dried over MgSO₄ and the solvents were evaporated under reduced pressure with a rotary evaporator (40 °C). The mixture was purified by flash column chromatography on silica gel (*i*-hexane/ethyl acetate 6:1). Evaporation of the solvent afforded 84.9 mg (42 %) of **8c** as colourless liquid. *R_f* (SiO₂, *i*-Hex/EtOAc 6:1) = 0.26. ¹H NMR (600 MHz, CDCl₃): δ = 6.24 (d, *J* = 1.1 Hz, 1 H, C=H_aH_b), 5.64 (br, 1 H, C=H_aH_b), 4.21 (q, *J* = 7.1, 2 H, C(O)O-CH₂), 3.72 (br m, 1 H, CH-OH), 2.58 (dd, *J* = 14.0, 2.5 Hz, 1 H, C=C-CH_aH_b), 2.32 (dd, *J* = 14.0, 8.5 Hz, 1 H, C=C-CH_aH_b), 2.17 (dt, *J* = 7.1, 2.4 Hz, 2 H, HC≡C-CH₂), 1.93 (t, *J* = 2.3 Hz, 1 H, HC≡C), 1.51 (ps. quint, *J* = 7.4 Hz, 2 H, HC≡C-CH₂-CH₂), 1.28–1.48 (m, 15 H, C₆H₁₂, CH₃). ¹³C NMR (101 MHz, CDCl₃): δ = 167.7, 137.8, 127.4, 84.8, 70.6, 68.0, 61.0, 40.4,

37.2, 29.5, 29.4, 29.0, 28.7, 28.4, 25.6, 18.4, 14.2. HRMS ESI positive mode (m/z): 281.2104 [M+H]⁺ (calc.: 281.2111), 561.4130 [2M+H]⁺ (calc.: 561.4150).

5-Dec-9-ynyl-3-methylene-dihydrofuran-2-one (8). 4-toluene sulfonic acid monohydrate (18.6 mg, 0.0980 mmol, 0.400 eq) was added to a solution of **8c** (66.6 mg, 0.239 mmol, 1.00 eq) in toluene (2.6 mL). After stirring overnight, the solvent was evaporated under reduced pressure with a rotary evaporator (40 °C, > 100 mbar) and the resulting oil was purified by flash column chromatography on silica gel (*i*-hexane/ethyl acetate 8:1). Evaporation of the solvents afforded 20.0 mg (36 %) of **8** as colourless liquid. *R*_f (SiO₂, *i*-Hex/EtOAc 8:1) = 0.22. ¹H NMR (600 MHz, CDCl₃): δ = 6.22 (ps. t, *J* = 2.8 Hz, 1 H, C=H_aH_b), 5.62 (ps. t, *J* = 2.5 Hz, 1 H, C=H_aH_b), 4.51 (ps. tt, *J* = 7.6, 2.5 Hz, 1 H, CH-O), 3.05 (ps. tdd, *J* = 17.0, 7.7, 2.5 Hz, 1 H, C=C-CH₃H_b), 2.57 (ps. tdd, *J* = 17.0, 6.0, 2.9 Hz, 1 H, C=C-CH_aH_b), 2.18 (dt, *J* = 7.1, 2.6 Hz, 2 H, HC≡C-CH₂), 1.93 (t, *J* = 2.6, 1 H, HC≡C), 1.69–1.76 (m, 1 H, CH_aH_b-CH-O), 1.58–1.64 (m, 1 H, CH_aH_b-CH-O), 1.51 (ps. quint. *J* = 7.2 Hz, 2 H, HC≡C-CH₂-CH₂), 1.28–1.58 (m, 10 H, C₅H₁₀). ¹³C NMR (101 MHz, CDCl₃): δ = 170.3, 134.7, 121.9, 84.7, 77.5, 68.1, 36.2, 33.6, 29.3, 29.1, 28.9, 28.6, 28.4, 24.8, 18.4. HRMS ESI positive mode (m/z): 235.1687 [M+H]⁺ (calc.: 235.1693), 252.1952 [M+NH₄]⁺ (calc.: 252.1958), 257.1505 [M+Na]⁺ (calc.: 257.1512), 486.3563 [2M+NH₄]⁺ (calc.: 486.3578), 491.3117 [2M+Na]⁺ (calc.: 491.3132).

(S)-3-(4-Benzoylphenyl)-2-hex-5-ynamidopropanoic acid (9c). Diazabicycloundecen, DBU (143 μL, 0.0560 mmol, 2.50 eq) was added to a suspension of (*S*)-2-amino-3-(4-benzoylphenyl)propionic acid (103 mg, 0.383 mmol, 1.00 eq) in dry dichloromethane (1.5 mL). After the reaction mixture turned clear, hex-5-ynoyl chloride (66.6 mg, 0.510 mmol, 1.30 eq) was added drop wise and the mixture was stirred overnight. HCl_{aq} (2 M, 300 μL) was added and dichloromethane evaporated under reduced pressure. The residue was purified by HPLC, which resulted in 68.5 mg (49 %) of **9c** as light yellowish solid. ¹H NMR (200 MHz, CDCl₃): δ = 7.82–7.28 (m, 9 H, H_{arom}), 6.30 (d, *J* = 7.6 Hz, 1 H, NH), 4.94 (ps. q, *J* = 6.1 Hz, 1 H, CH-C(O)OH), 3.35 (dd, *J* = 14.1, 5.7, 1 H, C_{arom}-CH_aH_b), 3.19 (dd, 1 H, *J* = 14.0, 6.4 Hz, C_{arom}-CH_aH_b), 2.36 (t, *J* = 7.3, 2 H, NH-C(O)-CH₂), 2.25–2.15 (m, 2 H, HC≡C-CH₂), 1.95 (t, *J* = 2.6 Hz, 1 H, HC≡C), 1.81 (ps. quint, *J* = 6.8 Hz, 2 H, HC≡C-CH₂-CH₂). ¹³C NMR (101 MHz, CDCl₃) δ = 196.6, 173.8, 172.9, 141.0, 137.4, 136.4, 132.6, 130.4, 130.1, 130.0, 129.8, 129.4, 128.5, 128.3, 128.3, 83.2, 69.5, 53.1, 37.4, 34.7, 24.0, 17.7. HRMS ESI positive mode (m/z): 364.1544 [M+H]⁺ (calc.: 364.1543), 381.1809 [M+NH₄]⁺ (calc.: 381.1809), 386.1363 [M+Na]⁺ (calc.: 386.1363), 744.3277 [2M+NH₄]⁺ (calc.: 744.3279), 749.2832 [2M+Na]⁺ (calc.: 749.2833).

***N*-((S)-3-(4-Benzoylphenyl)-1-oxo-1-((S)-2-oxotetrahydrofuran-3-ylamino)propan-2-yl)hex-5-ynamide (9).** Diazabicycloundecen, DBU (21.8 μL, 0.146 mmol, 1.00 eq) and HOBt (25.6 mg, 0.189

mmol, 1.30 eq) were added to a suspension of 9c (52.9 mg, 0.146 mmol, 1.00 eq) in dichloromethane (0.5 mL). After the reaction mixture turned clear, *N,N'*-Diisopropylcarbodiimide, DIC (33.8 μ L, 27.5 mg, 0.218 mmol, 1.5 eq) was added and the reaction mixture was stirred for 3 h at room temperature. The solution was then added drop wise to a solution of 9b (20.0 mg, 0.146 mmol, 1 eq) and DBU (28.4 μ L, 28.9 mg, 0.190 mmol, 1.3 eq) in dry dichloromethane (0.5 mL). The reaction mixture was stirred overnight, the solvents were evaporated under reduced pressure and the residue purified by HPLC. After lyophilisation and purification over silica gel, 6.4 mg (10 %) of 9 were obtained as light yellowish oil. R_f (SiO₂, CH₂Cl₂/MeOH 1:0.5) = 0.38. ¹H NMR (200 MHz, CD₃OD): δ = 7.78-7.40 (m, 9 H, H_{arom}), 4.75 (dd, J = 9.3, 5.7 Hz, 1 H, NH-CH-C(O)), 4.62 (dd, J = 10.9, 9.0 Hz, 1 H, NH-CH-C(O)) 4.58-4.21 (m, 2 H, C(O)O-CH₂), 3.28-3.23 (m, 1 H, CH_aH_b-C_{arom}), 3.06-2.92 (m, 1 H, CH_aH_b-C_{arom}), 2.62-2.42 (m, 1 H, C(O)O-CH₂-CH_aH_b), 2.38-2.24 (m, 3 H, NH-C(O)-CH₂, C(O)O-CH₂-CH_aH_b), 2.21 (t, J = 2.6 Hz, 1 H, HC \equiv C), 2.05 (dt, J = 7.2, 2.6 Hz, 2 H, HC \equiv C-CH₂), 1.68 (ps. quint, J = 7.2, 2 H, HC \equiv C-CH₂-CH₂). ¹³C NMR (101 MHz, CD₃OD) δ = 198.4, 177.1, 175.2, 173.6, 144.1, 139.0, 137.3, 133.7, 131.3, 131.3, 131.0, 131.0, 130.6, 130.6, 129.5, 129.5, 84.2, 70.3, 67.5, 59.1, 55.4, 39.2, 35.6, 29.6, 25.9, 18.5. HRMS ESI positive mode (m/z): 447.1915 [M+H]⁺ (calc.: 447.1915), 464.2180 [M+NH₄]⁺ (calc.: 464.2180), 469.1734 [M+Na]⁺ (calc.: 469.1734), 910.4019 [2M+NH₄]⁺ (calc.: 910.4022).

Solubility of probe 9. The bulky structure of the benzophenone in probe 9 raised questions for its solubility. Serial dilutions of 9 (50.0, 25.0, 12.5, 6.25, 2.50 and 1.25 mM) in water were subjected to transmitting light microscopy. The maximal solubility of 9 in water with 2.5 % DMSO was 2.5 mM.

Preparation of bacterial proteomes. Proteomes of the bacterial strains *Escherichia coli* K12, *Burkholderia cenocepacia* J2315, *Burkholderia thailandensis* E264, *Pseudomonas aeruginosa* PAO1, *Pseudomonas putida* KT2440, *Staphylococcus aureus* NCTC 8325 and *Staphylococcus aureus* Mu50 were prepared from 1 L liquid cultures harvested 1 h after transition in the stationary phase by centrifugation at 13,000 rpm. *Escherichia* and *Pseudomonas* strains were grown in LB (lysogeny broth) medium, *Burkholderia* strains in CASO (casein-soybean broth) medium and *Staphylococcus* strains in BHB (brain-heart broth) medium. The bacterial cell pellets were washed with PBS, resuspended in 20 mL PBS and lysed by French press.

In vitro labelling of bacterial proteomes. Proteome samples were adjusted to a final concentration of 1 mg protein/mL by dilution in PBS prior to probe labelling. Experiments for visualization by 1D SDS-PAGE were carried out in 43 μ L total volume and those for affinity

enrichment in 1892 μ L total volume, such that once CC reagents were added, the total reaction volume was 50 μ L and 2 mL, respectively. Reactions were initiated by addition of the probe and allowed to incubate for 60 min at room temperature. For labelling with the photocrosslinking probes **9/9c**, the reaction mixture was preincubated with the probe for 10 min at room temperature and then incubated for 60 min at 0 °C under UV light (366 nm). For heat controls the proteome was denatured with 1 μ L of 43% SDS at 95 °C for 6 min and cooled to room temperature before the probe was applied. Following incubation, reporter-tagged azide reagents (100 μ M rhodamine-azide for analytical or 20 μ M rhodamine-biotin-azide for preparative scale) were added followed by 1 mM TCEP (1 μ L or 10 μ L) and 100 μ M ligand (3 μ L or 30 μ L). Samples were gently vortexed and the cycloaddition initiated by the addition of 1 mM CuSO_4 (1 μ L or 10 μ L). The reactions were incubated at room temperature for 1 h. For analytical gel electrophoresis, 50 μ L 2 x SDS loading buffer were added and 50 μ L applied on the gel. Fluorescence was recorded in a Fujifilm Las-4000 luminescent image analyser with a Fujinon VRF43LMD3 lens and a 575DF20 filter. Reactions for enrichment were carried out together with a control lacking the probe to compare the results of the biotin-avidin enriched samples with the background of unspecific protein binding on avidin-agarose beads. After CC proteins were precipitated using an equal volume of pre-chilled acetone. Samples were stored on ice for 20 min and centrifuged at 13,000 rpm for 10 min. The supernatant was discarded and the pellet washed two times with 400 μ L of pre-chilled methanol and resuspended by sonication. Subsequently, the pellet was dissolved in 1 mL PBS with 0.2 % SDS by sonication and incubated under gentle mixing with 50 μ L of avidin-agarose beads (Sigma-Aldrich) for 1 h at room temperature. The beads were washed three times with 1 mL of PBS/0.2 % SDS, twice with 1 mL of 6 M urea and three times with 1 mL PBS. 50 μ L of 2 x SDS loading buffer were added and the proteins released for preparative SDS-PAGE by 6 min incubation at 95 °C. Gel bands were isolated, washed and tryptically digested as described previously.

***In situ* labelling of bacteria.** Bacteria were grown in BHB, CASO or LB medium and a quantity equivalent with 2 mL of $\text{OD}_{600} = 2$ was harvested 1 h after reaching stationary phase by centrifugation for analytical and 10 mL for preparative studies, respectively. After washing with PBS, the cells were resuspended in 100 μ L and 500 μ L of PBS for analytical and preparative experiments. Unless indicated otherwise, bacteria were incubated for 2 h with varying concentrations of probe at room temperature. Subsequently, the cells were washed three times with PBS and lysed by sonication with a Bandelin Sonopuls instrument (3 x 30 sec, 60 % maximum intensity) under ice cooling. Membrane and cytosol were separated by centrifugation at 13,000 rpm for 20 min and the membrane fraction was resuspended in 100 μ L and 500 μ L of PBS for

analytical and preparative scale, respectively, followed by click chemistry as described above. Reactions for enrichment were carried out as described for the *in vitro* experiments.

***In situ* labelling of bacteria with probe 9.** *P. putida* was grown to stationary phase in LB medium. Then, 2 mL of the culture were centrifuged at 13,000 rpm for 7 min, the pellet was washed with 1 mL PBS and was resuspended in 100 μ L PBS. Probe 9 (2 μ L, 10 mM) was added (200 μ M final concentration) and the mixture incubated for 1 h at room temperature followed by 1 h UV-exposure (366 nm) for photoreactive probe crosslinking. The cells were washed three times with 1 mL PBS and the pellet resuspended in 100 μ L PBS. Lysis was performed by sonication as described previously and the cytosolic and membrane fractions were subjected to click chemistry.

Mass spectrometry and bioinformatics. Tryptic peptides were loaded onto a Dionex C18 Nano Trap Column (100 μ m) and subsequently eluted and separated by a Dionex C18 PepMap 100 (3 μ m) column for analysis by tandem MS followed by high resolution MS using a coupled Dionex Ultimate 3000 LC-Thermo Finnigan LTQ-FT MS system. The mass spectrometry data were searched using the SEQUEST algorithm against the corresponding databases via the software "bioworks". The search was limited to tryptic peptides, two missed cleavage sites, monoisotopic precursor ions and a peptide tolerance of <10 ppm. Filters were set to further refine the search results. The X_{corr} vs. charge state filter was set to X_{corr} values of 1.5, 2.0 and 2.5 for charge states +1, +2 and +3, respectively. The number of different peptides has to be ≥ 2 and the peptide probability filter was set to < 0.001. These filter values are similar to others previously reported for SEQUEST analysis.¹²³

Nature of the unspecific band in *E. coli*. One band in *E. coli* labelled by γ -butyrolactone probes turned out to be unspecific as shown by a heat denatured control with preincubation of the proteome with 1 % SDS at 95 °C for 6 min prior to addition of probe 5 and in a control with click chemistry but without probe (Figure S1). The identity of this protein was revealed by mass spectrometry to be tryptophanase (Table S4). This protein appeared to be of high abundance and moreover seems to be predestinated to react with diverse probes and functional groups with a total of 7 cysteine and 19 serine residues.

Competitive *in vitro* labelling with reversible binding γ -Lactones. In competitive assays, a 100-, 50- and 10-fold excess of a reversible binding γ -lactone was added to the proteome 15 min prior to addition of the photocrosslinking probe 9.

Recombinant expression. The major hits of MS analysis were recombinantly expressed in *E. coli* as an internal control of the MS results by using the Invitrogen™ Gateway® Technology. Target genes were amplified from the corresponding genomes by PCR with an AccuPrime™ Pfx DNA Polymerase kit with 65 ng of genomic DNA, prepared by standard protocols. *attB1* forward primer and *attB2* reverse primer were designed to yield *attB*-PCR Products needed for Gateway® Technology:

6-Phosphofructokinase, *S. aureus* NCTC 8325

Forward 5'-GGG GAC AAG TTT GTA CAA AAA AGC AGG CTT TAT GAA TGC TGC CGTA

Reverse 5'-GGG GAC CAC TTT GTA CAA GAA AGC TGG GTG TTA TAT AGA TAA CTT GTT AG

Dihydrolipoamide dehydrogenase, *P. aeruginosa* PAO1

Forward 5'-GGG GAC AAG TTT GTA CAA AAA AGC AGG CTT TAT GAG CCA GAA ATT CGA CGT

Reverse 5'-GGG GAC CAC TTT GTA CAA GAA AGC TGG GTG TCA GCG CTT CTT GCG GT

Trigger factor, *B. thailandensis* E264

Forward 5'-GGG GAC AAG TTT GTA CAA AAA AGC AGG CTT TAT GGC TAA CGT TGT TGA AAA CCT
CG

Reverse 5'-GGG GAC CAC TTT GTA CAA GAA AGC TGG GTG TTA CGC TTG CGC CGT TGC G

Trigger factor, *E. coli* K12

Forward 5'-GGG GAC AAG TTT GTA CAA AAA AGC AGG CTT TAT GCA AGT TTC AGT TGA AAC C

Reverse 5'-GGG GAC CAC TTT GTA CAA GAA AGC TGG GTG ATC TTC GTA CGC AGA AGC

Trigger factor, *P. aeruginosa* PAO1

Forward 5'-GGG GAC AAG TTT GTA CAA AAA AGC AGG CTT TAT GCA AGT TTC TGT TGA AAG CAC

Reverse 5'-GGG GAC CAC TTT GTA CAA GAA AGC TGG GTG TCA GGC CGC TTG CGG A

UDP-N-acetylglucosamine 1-carboxyvinyltransferase *murA1*, *S. aureus* NCTC 8325

Forward 5'-GGG GAC AAG TTT GTA CAA AAA AGC AGG CTA CAT GGA TAA AAT AGT AAT CAA AGG

Reverse 5'-GGG GAC CAC TTT GTA CAA GAA AGC TGG GTG TTA ATC GTT AAT ACG TTC AAT GT

UDP-N-acetylglucosamine 1-carboxyvinyltransferase *murA2*, *S. aureus* Mu50

Forward 5'-GGG GAC AAG TTT GTA CAA AAA AGC AGG CTA CAT GGC TCA AGA GGT AAT AAA AAT

Reverse 5'-GGG GAC CAC TTT GTA CAA GAA AGC TGG GTG CTA TAC AGT TTC CGT CCA AA

PCR products were identified on agarose gels and gel bands were isolated and extracted with an E.Z.N.A.™ MicroElute™ Gel Extraction Kit. Concentrations of DNA were measured by a NanoDrop Spectrophotometer ND-1000. 100 fmol of purified *attB*-PCR product and 50 fmol of *attP*-containing donor vector pDONR™ 201 in TE buffer were used for *in vitro* BP recombination reaction with BP Clonase™ II enzyme mix to yield the appropriate *attL*-containing entry clone. After transformation in chemically competent One Shot® TOP10 *E. coli* (Invitrogen), cells were plated on LB agar plates containing 25 µg mL⁻¹ kanamycin. Clones of transformed cells were selected and grown in kanamycin LB medium. Cells were harvested and plasmids were isolated using an E.Z.N.A.™ Plasmid Mini Kit. The corresponding *attB*-containing expression clone was generated by *in vitro* LR recombination reaction of approx. 50 fmol of the *attL*-containing entry clone and 50 fmol of the *attR*-containing destination vector pDest using LR Clonase™ II enzyme mix in TE buffer. The expression clone was transformed in chemically competent BL21 *E. coli* cells (Novagen) and selected on LB agar plates containing 100 µg mL⁻¹ carbenicillin. Validity of the clones was confirmed by plasmid sequence analysis. Recombinant clones were grown in carbenicillin LB medium and target gene expression was induced with anhydrotetracyclin. The bacterial cell pellets were washed with PBS, resuspended in binding buffer (100 mM Tris-HCl, 150 mM NaCl, 1 mM EDTA), lysed by French press and sonication. The protein was then purified with StrepTrap™ HP columns.

Identification of the binding site of probe 8 in dihydrolipoamide dehydrogenase. To a solution of recombinantly expressed and purified *P. aeruginosa* PAO1 dihydrolipoamide dehydrogenase (18 µL, 3.5 µg/µL in PBS) was added probe 8 (1 µL, 1 mM in DMSO) and the mixture was incubated 30 min at room temperature. The buffer was exchanged several times with 25 mM aqueous NH₄HCO₃ to wash away unbound probe leading to a total volume of 100 µL. CaCl₂ (1 µL, 100 mM in H₂O) and Chymotrypsin solution (1 µL, sequencing grade, Roche Diagnostics, Germany) were added and the solution was incubated at room temperature overnight. Formic acid (2 µL, 1 % in H₂O) was added to 18 µL of the chymotryptic digest. The sample was measured by mass spectrometry as specified in chapter “Mass spectrometry and bioinformatics” and accordingly evaluated with a SEQUEST search for chymotryptic peptides.

IC₅₀ measurement. The Pro-Phe bond of the *N*-succinyl-Ala-Ala-Pro-Phe-*p*-nitroanilide substrate can exist in a trans or cis (higher absorption coefficient) form. The substrate was dissolved in a solution of 0.5 M LiCl in trifluoroethanol, TFE (about 50 % cis-peptide) and the re-equilibration of the cis/trans ratio during dilution into Hepes buffer (about 10 % cis-peptide) can be measured by

monitoring the absorption at 330 nm. Because traces of water in the LiCl/TFE solution decrease the cis-content dramatically, LiCl was dried over P_4O_{10} under vacuum and TFE was dried over 4 Å molecular sieve. A solution of the lactone **1**, **2**, **4** or **5** (0-10 mM in DMSO, 20 μ L) was added to a solution containing Hepes (50 mM, pH 7.8, 1950 μ L) and the *E. coli* trigger factor (10 μ L of 100 μ M). After incubation for 10 min at 10 °C, the substrate (20 μ L of 6 mM *N*-succinyl-Ala-Ala-Pro-Phe-*p*-nitroanilide in 0.5 M LiCl in trifluoroethanol) was added and the change in absorption subsequently monitored at 330 nm for 10 min at 10 °C. The data of each measurement was fitted with $A = y_0 A_0 e^{-kt}$ as exponential function leading to the kinetic constant k [s^{-1}]. The mean average kinetic constants (each out of three independent experiments) versus lactone concentration were plotted and the concentration of 50 % inhibition (IC_{50}) was determined.¹¹⁹

Appendix

Table S1: Proteins identified by mass spectrometry.

Species	Protein	ID	MW	R	p Value	X _{corr}	NP
<i>P. aeruginosa</i>	Trigger Factor (TF)	Q9I2U2	48582	1	2.3·10 ⁻⁹	5.57	7
				2	9.3·10 ⁻¹¹	5.58	14
PAO1	Dihydrolipoamide dehydrogenase (DLDH)	Q9I3D1	50165	1	1.8·10 ⁻¹³	5.77	15
				2	5.4·10 ⁻¹²	5.60	16
<i>P. putida</i>	Trigger Factor (TF)	Q88KJ1	48517	1	1.1·10 ⁻¹⁵	6.39	11
				2	2.2·10 ⁻¹⁴	5.76	20
<i>B. thailandensis</i>	Trigger Factor (TF)	Q2SWQ8	49688	1	4.4·10 ⁻⁸	4.50	4
				2	6.7·10 ⁻¹⁰	4.25	9
<i>B. cenocepacia</i>	Trigger Factor (TF)	B4EBM4	49868	1	2.1·10 ⁻⁷	3.85	5
				2	5.6·10 ⁻⁹	4.54	8
<i>S. aureus</i>	Dihydrolipoamide dehydrogenase (DLDH)	POA0E6	49451	1	2.0·10 ⁻⁹	4.74	16
				2	7.7·10 ⁻¹⁵	4.88	24
Mu50	UDP-N-acetylglucosamine-1-carboxyvinyl-transferase 2 (MurA2)	P65456	45075	1	7.7·10 ⁻¹⁵	4.88	24
<i>S. aureus</i>	Dihydrolipoamide dehydrogenase (DLDH)	Q2G2A3	49481	1	1.9·10 ⁻¹¹	4.76	19
				2	6.7·10 ⁻¹¹	4.52	9
NCTC8325	UDP-N-acetylglucosamine-1-carboxyvinyl-transferase 1 (MurA1)	Q2FWF4	44941	1	6.7·10 ⁻¹¹	4.52	9
	6-Phosphofructokinase, putative (PFK)	Q2FXM8	33397	1	3.9·10 ⁻¹⁰	4.62	2
				2	2.4·10 ⁻⁹	4.87	7

This list of proteins shows Protein ID, calculated molecular weight (MW) of the protein referring to ExPASy ProtParam tool, the replicates (R) in which the proteins have been identified, the minimum p values, maximum X_{corr} and the number of peptides (NP) found in each replicate.

Table S2: Proteins identified by mass spectrometry and their observed peptides.

Species	Protein / Peptide	[M+H] ⁺	z	p Value	S _f	Score / X _{corr}	Sequence Coverage / ΔC _n
<i>P. aeruginosa</i>							
PAO1	Trigger Factor (TF)			2.30·10⁻⁰⁹	6.62	70.28	25.20
	K.LNPAGSPSVEPK.S	1195.63171	2	4.89·10 ⁻⁰⁶	0.82	2.34	0.61
	K.ALIGNEVNR.L	985.54254	2	2.36·10 ⁻⁰³	0.95	2.80	0.54
	-.M*QVSVESTSALER.R	1452.70437	2	4.27·10 ⁻⁰⁸	0.98	4.10	0.72
	K.AAEFTVTVNSVAEPK.L	1562.80603	2	1.87·10 ⁻⁰⁴	0.97	4.20	0.74
	K.NQVM*EGLLQANPIEVPK. A	1895.99401	3	6.97·10 ⁻⁰⁶	0.95	3.38	0.51
	R.VQAVQQFGGNIKPDQLPA ELFEEQAK.R	2884.48389	3	2.41·10 ⁻⁰⁷	0.98	5.49	0.68
	R.VLNLTFPEDYQNLDLANK. A	2107.07056	2	2.30·10 ⁻⁰⁹	0.98	5.57	0.78
	Trigger Factor (TF)			9.32·10⁻¹¹	13.27	140.28	42.90
	K.LNPAGSPSVEPK.S	1195.63171	2	2.74·10 ⁻⁰⁷	0.90	2.98	0.73
	K.IDGEAFAGGSAK.G	1122.54260	2	1.45·10 ⁻⁰⁹	0.98	3.93	0.85
	K.ALIGNEVNR.L	985.54254	2	1.44·10 ⁻⁰⁵	0.94	2.74	0.62
	-.M*QVSVESTSALER.R	1452.70437	2	1.84·10 ⁻⁰⁸	0.98	4.44	0.70
	K.QVSYEEAVKPAEAPQAA.-	1787.88098	2	9.32·10 ⁻¹¹	0.97	4.38	0.81
	K.AAEFTVTVNSVAEPK.L	1562.80603	2	1.23·10 ⁻⁰⁵	0.97	4.16	0.71
	K.GTLLVLGSGR.M	972.58368	1	2.45·10 ⁻⁰²	0.68	2.08	0.63
	K.VKNQVM*EGLLQANPIEV PK.A	2123.15739	3	1.69·10 ⁻⁰⁴	0.95	4.32	0.65
	R.AAQNDQLNIDFVGK.I	1647.79724	2	8.47·10 ⁻⁰⁸	0.97	3.22	0.83
	K.NQVM*EGLLQANPIEVPK. A	1895.99401	3	1.62·10 ⁻⁰⁸	0.98	5.12	0.61
	R.LQAEVSDADVDNM*LDVL R.K	2018.97440	3	1.06·10 ⁻⁰⁸	0.98	5.58	0.80
	R.SVVLEEQVVDTVLQK.A	1685.93201	2	1.69·10 ⁻⁰³	0.98	4.47	0.66
	R.QEAM*GDLIQETFYEAVVE	2344.10580	2	5.56·10 ⁻⁰⁸	0.98	4.65	0.68

QK.L						
R.VVLGLIVAEVVK.Q	1238.80823	2	$1.16 \cdot 10^{-09}$	0.99	4.30	0.98
Dihydrolipoamide Dehydrogenase			$1.82 \cdot 10^{-13}$	14.30	150.29	33.30
(DLDH)						
K.ANGVTSFEGHGK.L	1203.57532	2	$3.88 \cdot 10^{-10}$	0.96	3.65	0.86
K.ASEEGVM*VAER.I	1193.55116	2	$4.26 \cdot 10^{-06}$	0.97	3.57	0.60
R.AM*AANDTTGLVK.V	1207.60320	2	$1.08 \cdot 10^{-06}$	0.97	3.89	0.64
K.ASEEGVMVAER.I	1177.55176	2	$7.87 \cdot 10^{-07}$	0.98	3.84	0.68
R.AMAANDTTGLVK.V	1191.60376	2	$3.04 \cdot 10^{-06}$	0.97	3.62	0.53
K.LIVAVGR.R	727.48248	1	$5.44 \cdot 10^{-03}$	0.82	2.13	0.49
K.QVTVTFTDANGEQK.E	1537.74927	2	$7.80 \cdot 10^{-07}$	0.85	2.42	0.58
K.GVTIDVPAM*VAR.K	1244.67122	2	$4.79 \cdot 10^{-07}$	0.96	3.64	0.60
R.RPVTTDLLAADSGVTLDER. G	2029.05603	2	$4.12 \cdot 10^{-08}$	0.97	4.00	0.74
K.TQVLEAENVIIASGSR.P	1686.90210	2	$5.78 \cdot 10^{-11}$	0.99	5.77	0.83
K.GVTIDVPAMVAR.K	1228.67188	2	$8.33 \cdot 10^{-10}$	0.96	3.73	0.63
K.AEGVEVNVGTFPFAASGR. A	1807.89734	2	$1.82 \cdot 10^{-13}$	0.98	5.58	0.75
K.TSVPGVFAIGDVVR.G	1416.78455	2	$1.67 \cdot 10^{-10}$	0.96	3.33	0.63
K.NLTGGIATLFK.A	1134.65173	2	$9.16 \cdot 10^{-07}$	0.97	3.30	0.83
R.LGAEVTVLEALDK.F	1357.75732	2	$1.51 \cdot 10^{-10}$	0.98	4.93	0.67
Dihydrolipoamide Dehydrogenase			$5.41 \cdot 10^{-12}$	15.46	160.28	34.30
(DLDH)						
K.ANGVTSFEGHGK.L	1203.57532	2	$1.10 \cdot 10^{-07}$	0.97	3.42	0.92
R.AM*AANDTTGLVK.V	1207.60320	2	$9.31 \cdot 10^{-07}$	0.97	3.94	0.64
K.ASEEGVMVAER.I	1177.55176	2	$1.76 \cdot 10^{-06}$	0.98	4.15	0.68
K.ASEEGVM*VAER.I	1193.55116	2	$1.38 \cdot 10^{-06}$	0.97	3.49	0.58
K.KQVTVTFTDANGEQK.E	1665.84424	2	$2.04 \cdot 10^{-08}$	0.99	5.57	0.86
R.AMAANDTTGLVK.V	1191.60376	2	$3.43 \cdot 10^{-03}$	0.95	3.10	0.54
K.QVTVTFTDANGEQK.E	1537.74927	2	$1.09 \cdot 10^{-07}$	0.97	4.63	0.69
K.FLPAADEQIAK.E	1202.64160	2	$7.46 \cdot 10^{-07}$	0.92	2.51	0.59
K.GVTIDVPAM*VAR.K	1244.67122	2	$3.63 \cdot 10^{-04}$	0.95	3.53	0.68
R.RPVTTDLLAADSGVTLDER. G	2029.05603	3	$1.39 \cdot 10^{-06}$	0.97	4.82	0.72

K.TQVLEAENVIIASGSR.P	1686.90210	2	$5.41 \cdot 10^{-12}$	0.99	5.59	0.86
K.GVTIDVPAMVAR.K	1228.67188	2	$1.91 \cdot 10^{-09}$	0.97	4.07	0.64
K.AEGVEVNVGTFPFAASGR. A	1807.89734	2	$5.13 \cdot 10^{-11}$	0.98	5.42	0.81
R.LGAEVTVLEALDK.F	1357.75732	2	$1.02 \cdot 10^{-04}$	0.98	4.34	0.64
K.TSVPGVFAIGDVVR.G	1416.78455	2	$2.12 \cdot 10^{-08}$	0.95	2.90	0.74
K.NLTGGIATLFK.A	1134.65173	2	$7.51 \cdot 10^{-07}$	0.97	3.23	0.90

P. putida

KT2446

Trigger Factor (TF) $1.11 \cdot 10^{-15}$ 10.42 110.32 33.20

K.NDQQLNEVR.S	1115.54395	2	$1.54 \cdot 10^{-05}$	0.97	3.45	0.68
K.LNPAGAPAVEPK.S	1163.64185	2	$3.96 \cdot 10^{-07}$	0.95	2.49	0.77
K.VDGEAFAGGSAK.G	1108.52698	2	$7.02 \cdot 10^{-07}$	0.97	3.74	0.70
-.M*QVSVENTSALER.R	1479.71527	2	$1.06 \cdot 10^{-07}$	0.98	4.39	0.61
K.ALLENEVNR.L	1057.56360	1	$1.77 \cdot 10^{-06}$	0.76	2.44	0.61
R.AAQNDDQVNIDFVGK.V	1633.78162	2	$3.51 \cdot 10^{-11}$	0.98	4.90	0.78
R.M*IPGFEEGLVGAK.A	1363.69710	2	$4.30 \cdot 10^{-06}$	0.89	2.83	0.34
K.NQVM*DGLLANPIEVPK. A	1824.95690	2	$3.70 \cdot 10^{-09}$	0.98	5.21	0.71
R.VVNVTFPEDYQNLDLAGK. A	2022.01782	3	$1.11 \cdot 10^{-15}$	0.97	4.82	0.66
R.SVVL EEQVVDTVLQK.A	1685.93201	3	$1.09 \cdot 10^{-07}$	0.98	6.39	0.58
R.VVLGLIVAEVVK.Q	1238.80823	2	$6.30 \cdot 10^{-10}$	0.99	4.85	0.98

Trigger Factor (TF) $2.22 \cdot 10^{-14}$ 18.90 200.29 51.00

K.NDQQLNEVR.S	1115.54395	2	$4.01 \cdot 10^{-06}$	0.97	3.71	0.65
K.VDGEAFAGGSAK.G	1108.52698	2	$5.85 \cdot 10^{-11}$	0.98	4.40	0.80
K.QFELKPDDAK.V	1190.60522	2	$9.12 \cdot 10^{-05}$	0.88	2.91	0.51
-.M*QVSVENTSALER.R	1479.71527	2	$2.38 \cdot 10^{-08}$	0.97	3.82	0.70
K.SVSYEEAVKPAEAPAAAE.-	1818.87561	2	$8.40 \cdot 10^{-08}$	0.97	4.13	0.84
-.MQVSVENTSALER.R	1463.71582	2	$5.59 \cdot 10^{-08}$	0.98	4.49	0.61
K.ESTLEGFR.A	938.45776	1	$4.47 \cdot 10^{-06}$	0.57	1.92	0.63
R.MTIAVPAER.V	987.52917	2	$2.44 \cdot 10^{-03}$	0.91	2.71	0.46
K.LNPAGAPAVEPK.S	1163.64185	2	$8.87 \cdot 10^{-08}$	0.94	3.10	0.70
R.AAQNDDQVNIDFVGK.V	1633.78162	2	$1.82 \cdot 10^{-10}$	0.98	4.73	0.82

K.NQVM*DGLLAANPIEVPK. A	1824.95690	2	$6.10 \cdot 10^{-11}$	0.99	5.76	0.76
K.VKNQVMDGGLLAANPIEVP K.A	2036.12085	3	$4.30 \cdot 10^{-05}$	0.94	3.59	0.68
R.LSAEVADSDLDNM*LEVLR .K	2005.97915	2	$3.72 \cdot 10^{-08}$	0.99	5.44	0.66
R.VVNVTFPEDYQNLDLAGK. A	2022.01782	2	$2.22 \cdot 10^{-14}$	0.98	5.17	0.80
R.VQAVQQFGGNKPEQLPV ELFEEQ AK.R	2926.53101	3	$1.41 \cdot 10^{-06}$	0.97	5.67	0.76
K.NQVMDGGLLAANPIEVPK.A	1808.95752	2	$8.65 \cdot 10^{-10}$	0.98	4.83	0.71
R.SVVLEEQQVVDTVLQK.A	1685.93201	2	$4.14 \cdot 10^{-06}$	0.98	5.20	0.66
R.VVLGLIVAEVVK.Q	1238.80823	2	$5.58 \cdot 10^{-10}$	0.99	4.68	0.96
R.LSAEVADSDLDNMLEVLR. K	1989.97974	2	$5.22 \cdot 10^{-10}$	0.98	5.17	0.74
K.ALLENEVNR.L	1057.56360	2	$1.69 \cdot 10^{-07}$	0.95	2.67	0.66

B. thailandensis

E264

Trigger Factor (TF) $4.40 \cdot 10^{-08}$ 3.80 40.22 10.00

K.ISELDVPK.A	900.50366	2	$4.90 \cdot 10^{-04}$	0.89	2.40	0.38
K.IGDLATAEVER.S	1173.61096	2	$4.40 \cdot 10^{-08}$	0.98	4.50	0.54
K.SLGIEDGDLTK.M	1147.58411	2	$3.54 \cdot 10^{-06}$	0.97	3.43	0.73
K.DAIPVEMFAEQAER.R	1702.81055	2	$5.37 \cdot 10^{-08}$	0.97	3.62	0.84

Trigger Factor (TF) $6.67 \cdot 10^{-10}$ 8.46 90.21 22.90

R.AEVDEFK.S	908.43597	2	$3.34 \cdot 10^{-03}$	0.86	2.33	0.69
R.STTTIGDAEIDR.T	1278.61719	2	$6.86 \cdot 10^{-06}$	0.95	2.62	0.76
K.ISELDVPK.A	900.50366	2	$2.92 \cdot 10^{-03}$	0.89	2.42	0.43
K.IGDLATAEVER.S	1173.61096	2	$2.40 \cdot 10^{-08}$	0.97	4.25	0.54
K.SLGIEDGDLTK.M	1147.58411	2	$2.38 \cdot 10^{-03}$	0.96	3.24	0.72
K.M*VAQQYAGQVEAEVLS K.I	1981.95802	3	$4.97 \cdot 10^{-04}$	0.93	3.37	0.54
K.IGQEFTISR.S	1197.62622	2	$3.00 \cdot 10^{-04}$	0.97	3.15	0.68
K.DAIPVEM*FAEQAER.R	1718.80990	2	$6.67 \cdot 10^{-10}$	0.96	3.92	0.74
K.LGLVLAELVK.A	1054.68701	2	$3.90 \cdot 10^{-05}$	0.96	3.08	0.67

<i>B. cenocepacia</i>				2.08·10⁻⁰⁷	4.69	50.19	10.90
J2315	Trigger Factor (TF)						
	R.STTTIGDAEIDR.T	1278.61719	2	2.08·10 ⁻⁰⁷	0.96	3.14	0.70
	R.WYYSNQQR.L	1144.51709	2	1.82·10 ⁻⁰³	0.90	2.51	0.44
	K.ISELDVPK.A	900.50366	2	8.71·10 ⁻⁰³	0.90	2.33	0.60
	K.SLGIEDGDLTK.M	1147.58411	2	4.12·10 ⁻⁰³	0.96	3.32	0.68
	K.LGLVLAELVK.A	1054.68701	2	8.56·10 ⁻⁰⁷	0.97	3.85	0.77
	Trigger Factor (TF)			5.56·10⁻⁰⁹	7.62	80.23	17.90
	K.ALIEQDQQR.L	1100.56946	2	3.57·10 ⁻⁰⁴	0.91	2.89	0.31
	R.STTTIGDAEIDR.T	1278.61719	2	1.83·10 ⁻⁰⁶	0.96	3.27	0.78
	K.ISELDVPK.A	900.50366	2	1.05·10 ⁻⁰³	0.93	2.48	0.64
	K.IGDLATAEVER.S	1173.61096	2	5.56·10 ⁻⁰⁹	0.98	4.54	0.62
	K.TAQFTVTMK.K	1026.52881	2	4.34·10 ⁻⁰⁴	0.96	2.46	0.76
	K.SLGIEDGDLTK.M	1147.58411	2	5.07·10 ⁻⁰³	0.95	3.15	0.68
	K.IGQEFTISR.A	1197.62622	2	1.02·10 ⁻⁰⁶	0.97	3.37	0.62
	K.LGLVLAELVK.A	1054.68701	2	1.50·10 ⁻⁰⁵	0.97	3.56	0.80
<i>S. aureus</i>	Dihydrolipoamide Dehydrogenase			2.04·10⁻⁰⁹	14.25	160.24	32.30
Mu50	(DLDH)						
	K.ALLHASHR.F	904.51117	2	3.29·10 ⁻⁰⁵	0.88	2.48	0.39
	K.EEGLAIK.A	759.42468	1	2.70·10 ⁻⁰³	0.57	2.13	0.42
	K.EKGVEIVTEAM*AK.S	1420.73969	2	1.62·10 ⁻⁰²	0.90	2.59	0.68
	K.GVEIVTEAM*AK.S	1163.60214	2	9.85·10 ⁻⁰⁴	0.94	3.01	0.69
	R.GLLEVDK.Q	773.44037	1	2.97·10 ⁻⁰⁴	0.88	2.30	0.58
	K.AIGYPIHTM*.-	1018.50711	1	5.05·10 ⁻⁰⁶	0.65	1.89	0.78
	K.GEAYFVDNNSLR.V	1384.64917	2	2.04·10 ⁻⁰⁹	0.98	4.27	0.96
	K.RVIDSTGALNLQEVPGK.L	1796.98645	2	7.02·10 ⁻⁰⁷	0.95	3.66	0.61
	K.GVEIVTEAMAK.S	1147.60278	2	3.29·10 ⁻⁰⁷	0.97	3.33	0.70
	R.VIDSTGALNLQEVPGK.L	1640.88538	2	4.22·10 ⁻⁰⁵	0.94	3.74	0.65
	R.RPNTDELGLEELGVK.F	1669.87549	3	2.83·10 ⁻⁰⁷	0.97	3.58	0.72
	R.ALSLDDTNGFVK.L	1279.65283	2	3.09·10 ⁻⁰⁸	0.97	3.61	0.81
	K.NAIIATGSRPIEIPNFK.F	1841.02795	2	1.10·10 ⁻⁰⁸	0.96	3.88	0.73
	R.PIEIPNFK.F	957.54041	1	6.08·10 ⁻⁰⁴	0.76	2.27	0.31
	R.TSISNIYAIGDIVPGLPLAHK	2179.21216	2	2.01·10 ⁻⁰⁸	0.96	4.74	0.79

.A
K.TIEADYVLTVGR.R 1435.77917 2 6.18·10⁻⁰⁶ 0.98 4.18 0.80

UDP-N-acetylglucosamine 1-carboxyvinyl-transferase 2 (MurA2) **7.66·10⁻¹⁵ 22.87 232.26 43.00**

K.HVEELKR.M 910.51050 2 8.61·10⁻⁰⁵ 0.95 2.80 0.68
K.HVETLTAK.F 898.49927 2 2.47·10⁻⁰⁵ 0.95 2.69 0.75
R.PIDQHIK.G 850.47815 2 8.87·10⁻⁰³ 0.92 2.52 0.55
R.FKHVEELKR.M 1185.67383 2 6.29·10⁻⁰⁴ 0.94 2.69 0.53
K.ALGAIDESSTTSM*K.I 1555.72008 2 2.97·10⁻¹² 0.98 4.48 0.72
R.TLNGEVNISGAK.N 1202.63757 2 2.81·10⁻⁰³ 0.93 2.96 0.60
R.ASYYM*M*GAM*LGR.F 1398.59851 2 8.79·10⁻⁰⁷ 0.97 2.90 0.94
K.ELHGSEYQVIPDR.I 1542.75464 2 1.21·10⁻⁰⁹ 0.97 3.62 0.77
K.ALGAIDESSTTSMK.I 1539.72070 2 7.66·10⁻¹⁵ 0.98 4.88 0.95
R.M*GANIEVDEGTATIK.P 1564.75680 2 1.44·10⁻⁰⁵ 0.97 4.33 0.67
K.PSTLHGAEVYASDLR.A 1615.80750 2 1.02·10⁻⁰⁷ 0.98 3.75 0.74
R.MGANIEVDEGTATIK.P 1548.75745 2 1.35·10⁻⁰⁴ 0.96 3.93 0.56
R.ASYYMM*GAMLGR.F 1366.59971 2 1.24·10⁻⁰⁶ 0.95 4.13 0.09
-.ASYYM*MGAMLGR.- 1366.59971 2 2.13·10⁻⁰⁵ 0.91 3.77 0.26
R.GYTDIVEHLK.A 1174.61023 2 8.58·10⁻⁰⁷ 0.95 3.17 0.61
K.LEGLPQISDVK.T 1198.66772 2 4.08·10⁻⁰⁷ 0.96 3.44 0.53
K.FSELGVNVDVR.D 1234.64258 2 2.01·10⁻⁰⁹ 0.98 4.30 0.57
R.INNNAPYQFVDIK.T 1535.78528 2 5.96·10⁻⁰⁷ 0.97 4.13 0.72
-.ASYYMMGAM*LGR.- 1366.59971 2 1.42·10⁻⁰⁵ 0.88 3.24 0.84
R.ASYYM*MGAMLGR.F 1366.59971 2 2.18·10⁻⁰⁷ 0.94 3.87 0.02
-.ASYYMM*GAMLGR.- 1366.59971 2 2.18·10⁻⁰⁷ 0.93 3.81 0.18
K.NSAVAIIPATLLAQGHVK.L 1803.04871 2 1.44·10⁻⁰⁹ 0.98 5.29 0.85
R.ASYYMMGAMLGR.F 1350.60034 2 5.91·10⁻⁰⁹ 0.98 4.10 0.97
K.ALGADIWTETV.- 1175.59424 2 4.00·10⁻⁰⁵ 0.93 3.09 0.80

***S. aureus* Dihydrolipoamide Dehydrogenase** **1.85·10⁻¹¹ 16.88 190.26 36.10**
NCTC 8325 (DLDH)

K.ALLHASHR.F 904.51117 2 2.31·10⁻⁰⁵ 0.90 2.49 0.35
K.NAIIATGSR.P 902.50543 2 2.74·10⁻⁰⁷ 0.95 2.67 0.70
K.EEGLAIK.A 759.42468 1 5.07·10⁻⁰³ 0.53 2.23 0.35
K.GVEIVTEAM*AK.S 1163.60214 2 3.32·10⁻⁰⁷ 0.97 3.95 0.83

K.AIGYPIHTM*.-	1018.50711	1	$5.09 \cdot 10^{-06}$	0.71	1.81	0.76
K.EKGVEIVTEAMAK.S	1404.74023	2	$1.10 \cdot 10^{-10}$	0.95	3.06	0.73
K.RVIDSTGALNLQEVPGK.L	1796.98645	2	$1.85 \cdot 10^{-11}$	0.97	4.61	0.62
R.GLLEVDK.Q	773.44037	1	$2.52 \cdot 10^{-04}$	0.84	2.24	0.67
R.VIDSTGALNLQEVPGK.L	1640.88538	3	$4.39 \cdot 10^{-08}$	0.98	4.76	0.79
R.ALSLDDTNGFVK.L	1279.65283	2	$1.74 \cdot 10^{-07}$	0.97	3.76	0.81
R.RPNTDELGLEELGVK.F	1669.87549	3	$2.17 \cdot 10^{-07}$	0.98	4.04	0.77
K.DILGGFEK.Q	878.46179	1	$5.93 \cdot 10^{-04}$	0.51	2.00	0.30
K.GVEIVTEAMAK.S	1147.60278	2	$5.42 \cdot 10^{-06}$	0.96	3.15	0.63
K.GEAYFVDNNSLR.V	1384.64917	2	$2.05 \cdot 10^{-09}$	0.98	3.67	-
R.PIEIPNFK.F	957.54041	2	$4.85 \cdot 10^{-05}$	0.95	3.00	0.74
K.NAIIATGSRPIEIPNFK.F	1841.02795	2	$3.49 \cdot 10^{-11}$	0.97	4.57	0.73
K.LTGGVESLLK.G	1016.59863	2	$1.51 \cdot 10^{-04}$	0.81	2.64	0.36
K.TIEADYVLVTVGR.R	1435.77917	2	$4.00 \cdot 10^{-07}$	0.98	4.41	0.82
R.TSISNIYAIGDIVPGLPLAHK	2179.21216	2	$2.46 \cdot 10^{-07}$	0.96	4.47	0.87
.A						
UDP-N-acetylglucosamine 1-carboxyvinyl-			$6.72 \cdot 10^{-11}$	8.72	90.23	19.70
transferase 1 (MurA1)						
K.KDENAVVVDATK.T	1288.67432	2	$4.53 \cdot 10^{-08}$	0.98	3.77	0.79
R.M*NANINVEGR.S	1133.54127	2	$9.94 \cdot 10^{-08}$	0.97	3.69	0.74
K.DENAVVVDATK.T	1160.57935	2	$3.09 \cdot 10^{-06}$	0.97	3.72	0.63
R.AEGELQPVDIK.T	1198.63135	2	$5.53 \cdot 10^{-06}$	0.98	3.89	0.79
K.VVTETVFENR.F	1193.61609	2	$6.72 \cdot 10^{-11}$	0.97	3.98	0.70
K.TLNEEAPYEYVSK.M	1542.73218	2	$7.34 \cdot 10^{-07}$	0.97	3.71	0.79
R.ASILVM*GPLLAR.L	1256.74399	2	$1.92 \cdot 10^{-06}$	0.96	3.69	0.79
R.ASILVMGPLLAR.L	1240.74463	2	$4.56 \cdot 10^{-05}$	0.93	3.63	0.59
R.AAAALILAGLVADGK.T	1353.81006	2	$1.88 \cdot 10^{-09}$	0.98	4.52	0.93
6-Phosphofructokinase, putative (PFK)			$3.86 \cdot 10^{-10}$	1.96	20.23	7.20
K.ELSQYINVDNR.V	1350.66479	2	$3.23 \cdot 10^{-07}$	0.98	3.86	0.68
K.FDYSLYELANK.L	1362.65759	2	$3.86 \cdot 10^{-10}$	0.98	4.62	0.76
6-Phosphofructokinase, putative (PFK)			$2.45 \cdot 10^{-09}$	6.75	70.24	27.00
R.VSVLGHVQR.G	994.57922	2	$6.09 \cdot 10^{-06}$	0.94	2.66	0.79

K.EIADKIEQGIK.R	1243.68921	2	$3.85 \cdot 10^{-07}$	0.93	2.82	0.71
K.ELSQYINVDNR.V	1350.66479	2	$4.17 \cdot 10^{-07}$	0.97	3.89	0.77
K.LELGSVGDTIQR.G	1287.69031	2	$1.18 \cdot 10^{-07}$	0.97	3.84	0.61
K.FDYSLYELANK.L	1362.65759	2	$2.45 \cdot 10^{-09}$	0.98	4.74	0.82
R.LGGYAVDLLMQGETAK.G	1665.85168	2	$1.13 \cdot 10^{-05}$	0.98	4.87	0.64
K.IVATSFDEIFDGK.D	1441.72095	2	$2.35 \cdot 10^{-06}$	0.98	4.00	0.82

*	Refers to an oxidized methionine.
.	Cleavage site.
-	Unspecific cleavage site or C- or N-terminus of protein.
z	Charge of the peptide ion.
p-value	Probability of finding a peptide match as good or better than the observed peptide match by chance. The value displayed for the protein is the probability of the best peptide match (the peptide with the lowest score).
S_f	Score calculated by an algorithm that incorporates the X_{corr} , ΔC_n , S_p , RS_p , peptide mass, charge state, and the number of matched peptides for the search. The higher the value of the S_f score, the better the peptide match. A good score is > 0.7 for peptide ions.
Score	Score of the SEQUEST results; the higher the score, the better the match to the searched sequence.
X_{corr}	A good score is > 1.5 for single charged, > 2.2 for double charged and > 2.8 for triple charged peptide ions.
Sequence Coverage	Coverage of the protein, which is the percentage of the protein sequence covered by the identified peptides.
ΔC_n	Difference between the X_{corr} values for the best match and the second best match. The larger the ΔC_n the better the match with the first sequence compared to the second sequence. A low ΔC_n suggests that the first match is less reliable. A good value is > 0.4 for peptide ions.

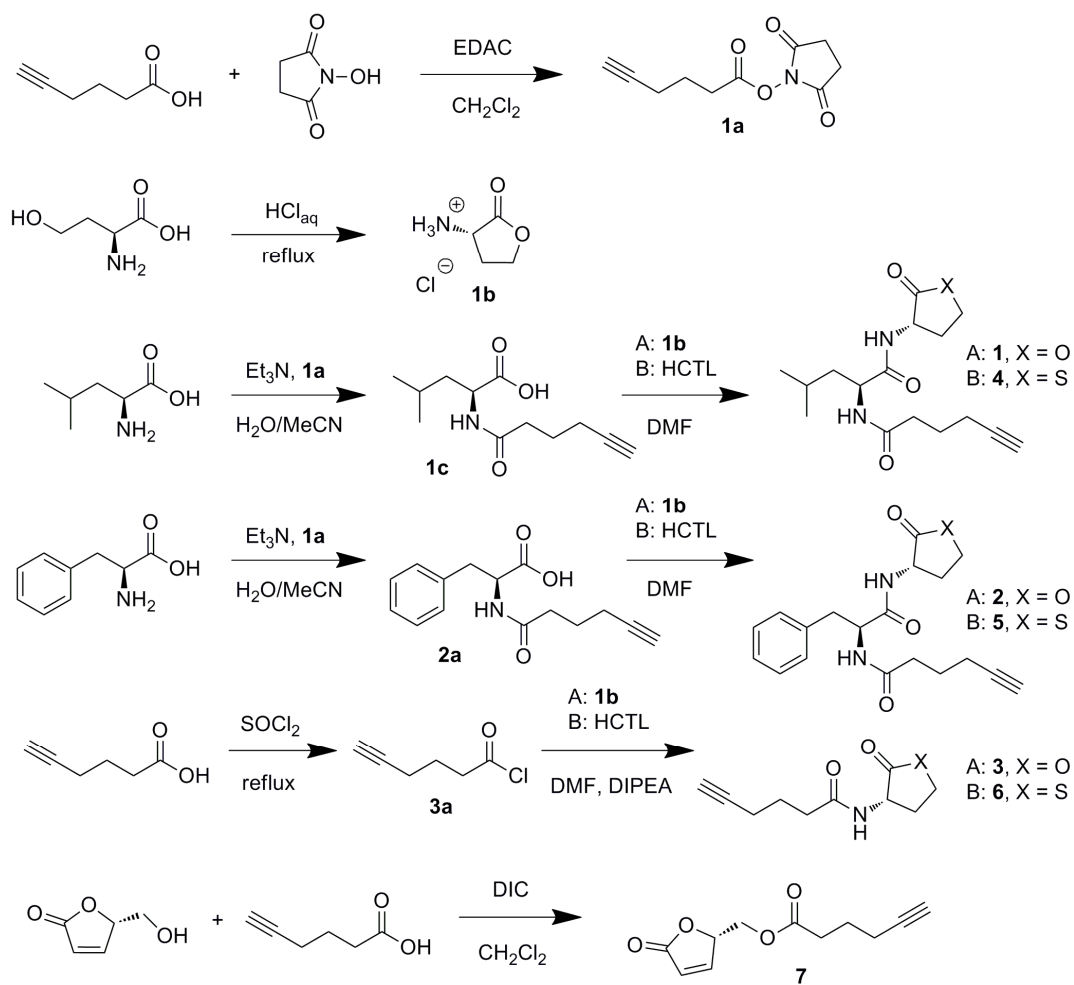
Table S3: Labelled cysteines in *P. aeruginosa* dihydrolipoamide dehydrogenase (DLDH).

Cysteine	Sequence of observed peptide	[M+H] ⁺	z	p Value	S _f	X _{corr}	ΔC _n
Cys#49 & 54	IGKEGKVALGGTC#LNVGC#IPSKAL	2326.26	3	1.3 10 ⁻³	0.85	3.75	0.3
Cys#49 & 54	GGTC#LNVGC#IPSKAL	1430.71	2	4.3 10 ⁻³	0.79	2.85	0.4
Cys*32	GLKTAC*IEKY	1359.76	2	4.8 10 ⁻⁷	0.91	2.79	0.5

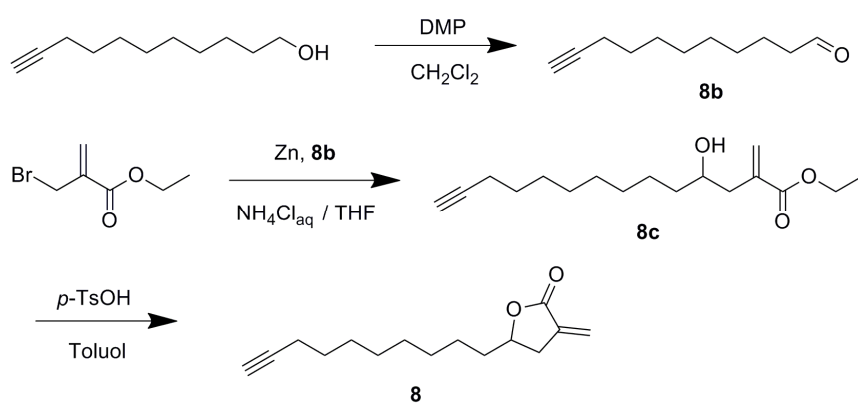
= Disulfide bridge between both cysteine residues. * = 8 labelled cysteine.

Table S4: Identity of the unspecific labelling event in *E. coli*.

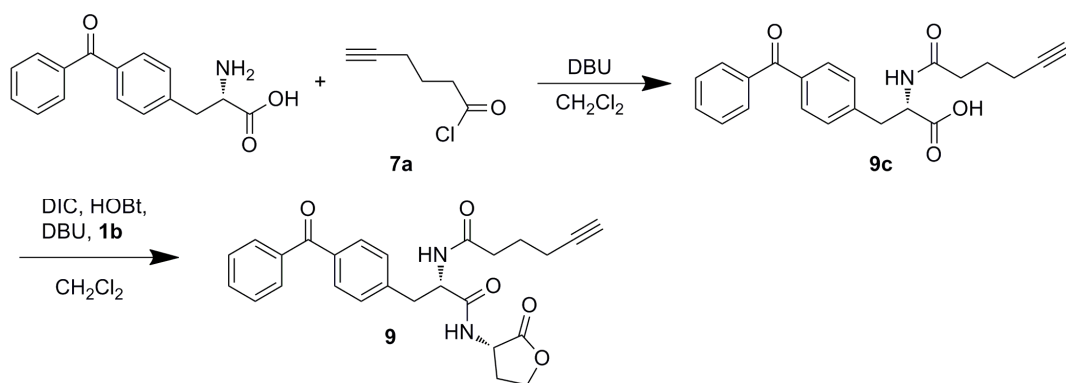
Protein	Protein ID	MW	R	min. p value	Score	NP
Tryptophanase (TnaA)	P0A853	52773	1	1.0 10 ⁻³⁰	230.32	27
			2	1.0 10 ⁻³⁰	190.32	23



Scheme S1: Synthesis of *N*-acylhomoserine lactones **1-6** and the unsaturated γ -butyrolactone probe **7**.



Scheme S2: Synthesis of the α -methylene- γ -butyrolactone probe **8**.



Scheme S3: Synthesis of the γ -lactone photocrosslinking probe **9**.

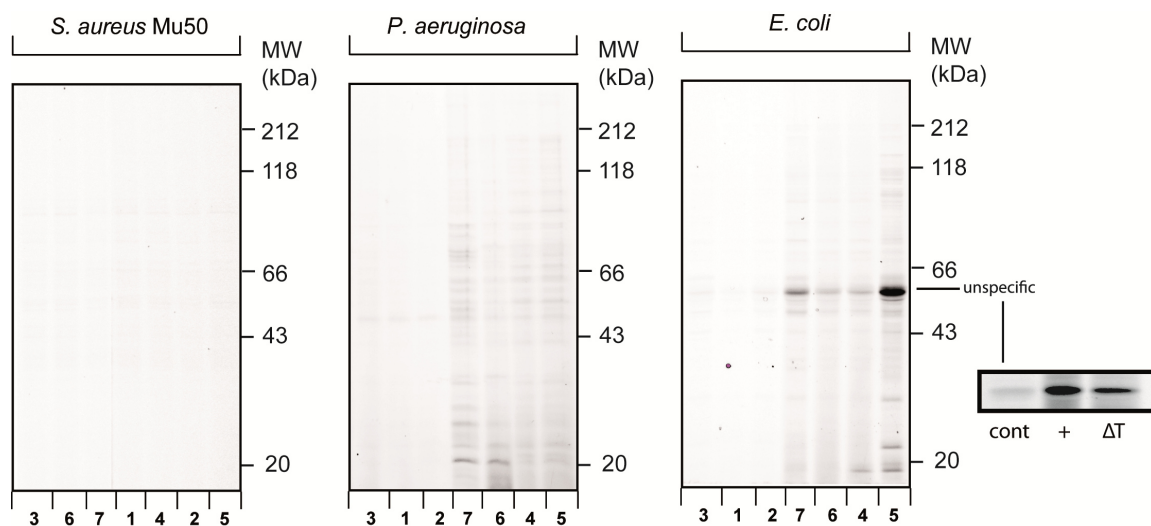


Figure S1: Labelling profiles of γ -butyrolactone probes with living cells of *S. aureus* Mu50, *E. coli* K12, and *P. aeruginosa* PAO1. One band of *E. coli* K12 was proven to be unspecific as shown by a heat control with probe **5** (cont: only click chemistry without probe, +: native proteome, ΔT : heat control).

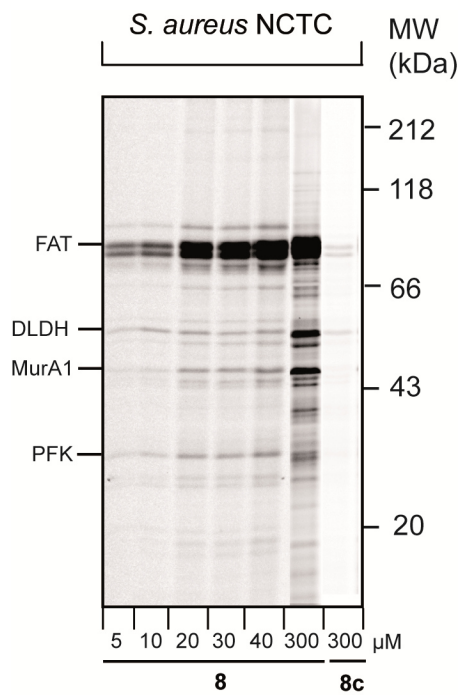


Figure S2: Labelling profile of living *S. aureus* NCTC 8325 with the α -methylene- γ -butyrolactone probe **8** in comparison with **8c**.

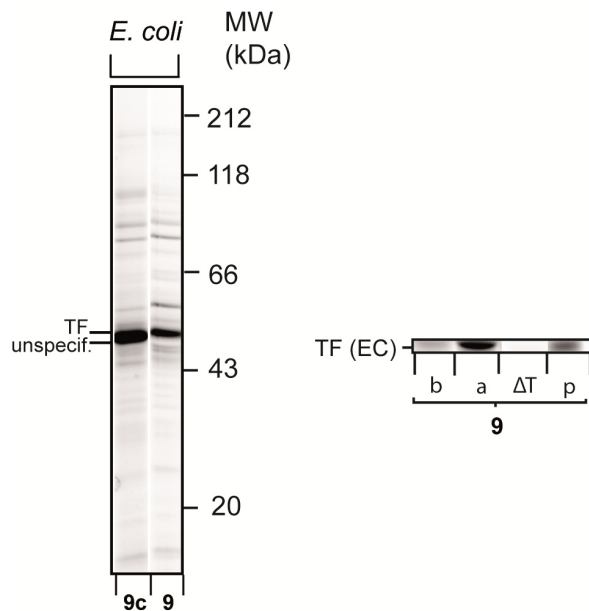


Figure S3: Labelling of *E. coli* K12 *in vitro* proteome with the photocrosslinking probe **9** and *in vitro* labelling of recombinant, overexpressed target enzymes (p: positive control using native proteome, b: not induced, a: induced, ΔT : heat control using induced proteome). Unspecif. = unspecific high abundance protein that is occurring in *E. coli* K12 and migrating at the same height as the trigger factor.

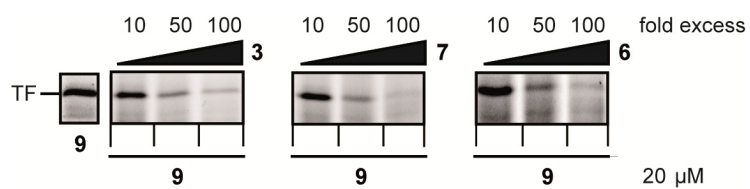


Figure S4: Competitive labelling of the *P. aeruginosa* PAO1 trigger factor (TF) by the photocrosslinking probe 9 and the N-acylhomoserine lactone probes 3, 7 and 6.

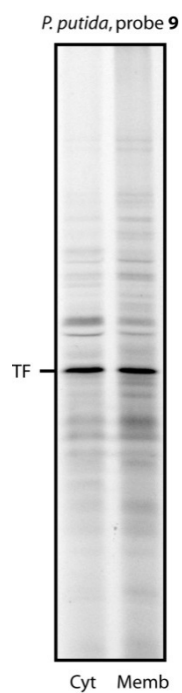
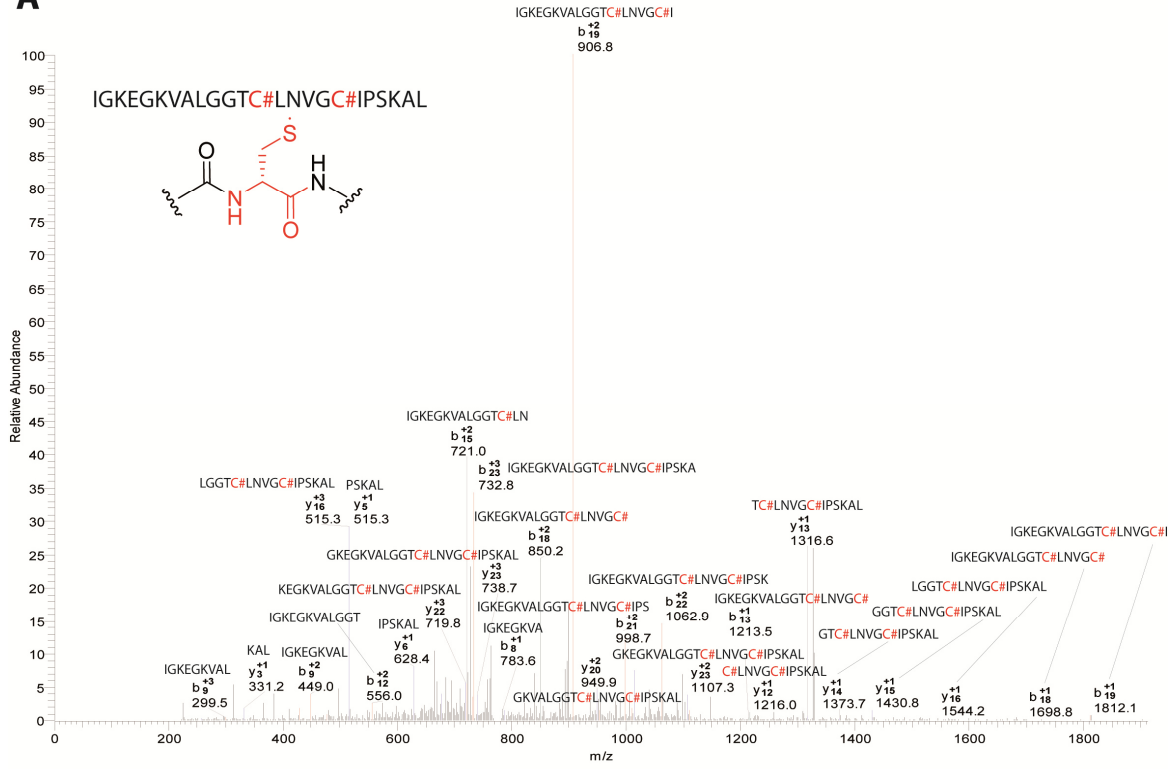
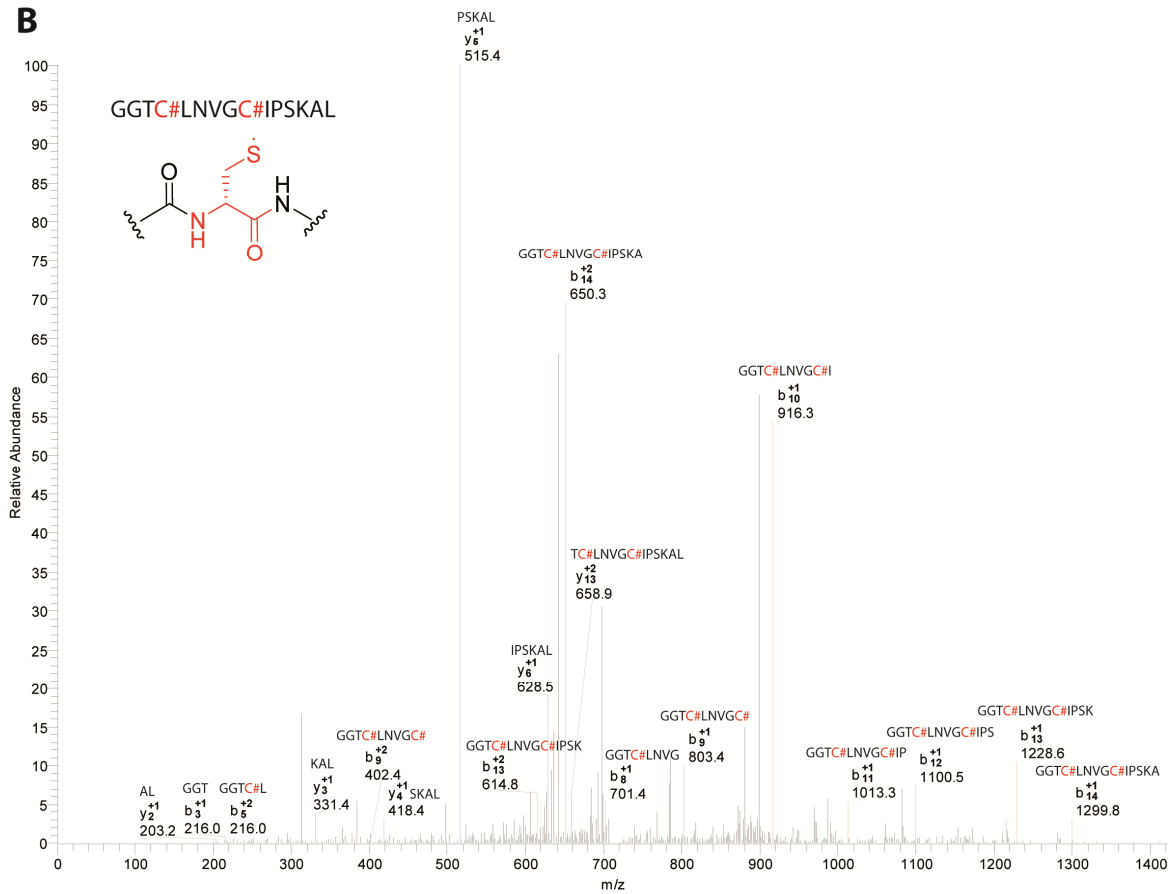


Figure S5: *In situ* labelling of living cells of *P. putida* KT2440 with the photoreactive probe 9.

A**B**

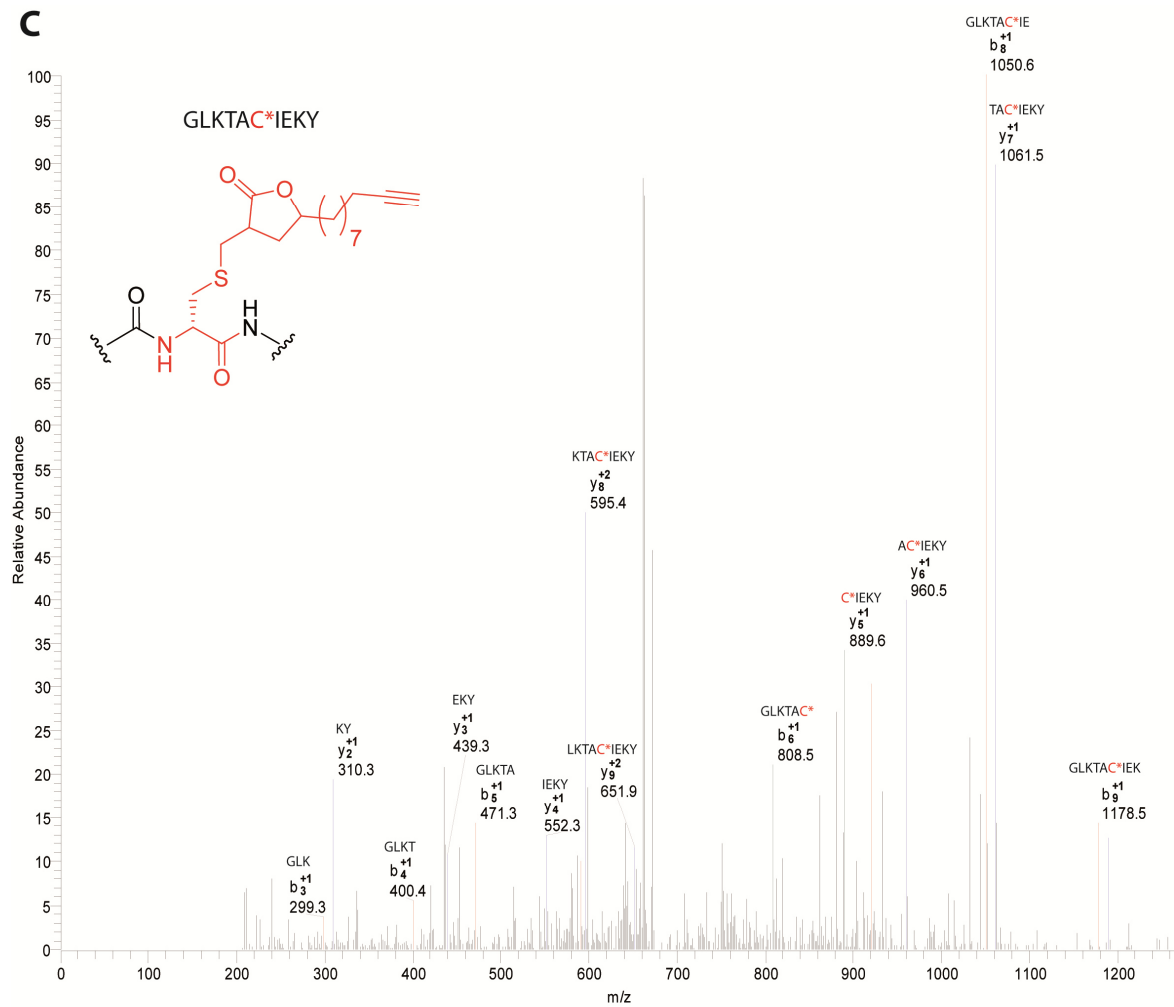
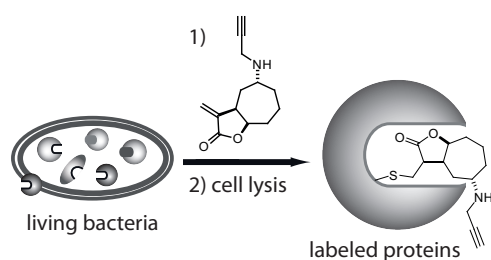


Figure S6: Mass spectra of chymotryptic digested *P. aeruginosa* PAO1 dihydrolipoamide dehydrogenase (DHLD) with disulfide bond (A and B) and modification site by probe **8** (C).

Target analysis of α -alkylidene- γ -butyrolactones in uropathogenic *E. coli*

M. H. Kunzmann, S. A. Sieber. Target analysis of α -alkylidene- γ -butyrolactones in uropathogenic *E. coli*. *Mol. BioSyst.* **2012**, *8*, 3061-3067. DOI: 10.1039/C2MB25313E - Reproduced by permission of The Royal Society of Chemistry



Abstract

α -Alkylidene- γ -butyrolactones are quite common in nature and exhibit a broad spectrum of biological activities. We therefore synthesized a small library of xanthatine inspired α -alkylidene- γ -butyrolactones to screen non-pathogenic and uropathogenic *E. coli* strains by activity based protein profiling (ABPP). The identified targets are involved in cellular redox processes and give first insight into the preferred binding sites of this privileged motif. Furthermore the gene of one protein, C2450, which was only identified in uropathogenic *E. coli*, belongs to a genomic island which encodes a hybrid polyketide/non-ribosomal peptide synthetase (PKS/NRPS). This system is responsible for the synthesis of colibactin, a natural product which causes DNA double strand breaks in eukaryotic cells leading to the activation of the DNA damage checkpoint pathway and subsequent cell cycle arrest. While the role of several proteins that are involved in the colibactin synthesis has been elucidated, the function of C2450 remains elusive. Investigation of the binding site showed that C2450 is modified at a cysteine residue which may be important for the catalytic activity.

Introduction

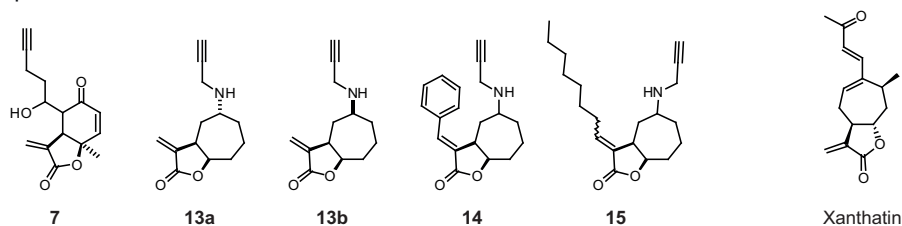
A large number of natural products exhibit electrophilic entities such as epoxides, beta-lactams and Michael acceptors, which are prone to react with enzyme active sites

corresponding to their fine-tuned intrinsic reactivity.^{63, 87, 102} In order to understand the bioactivity and mechanism of action of natural products, methods to dissect and analyse protein reactivity as well as target binding within the context of a whole cellular system are required. We and others have highlighted in previous studies the reactivity of several protein reactive natural products such as beta-lactams and beta-lactones and gained unique insights into target preferences, bioactivity as well as reactivity within several prokaryotic and eukaryotic systems.^{55, 57, 71, 100, 103, 124, 125}

Recently, pilot studies with gamma-lactones and α -methylene- γ -butyrolactones revealed that contrary to β -lactones the intrinsic reactivity of 5-membered γ -lactones is not sufficient to react covalently with enzyme active sites.⁵⁶ However, several specific protein targets could be identified with the substantially more reactive α -methylene- γ -butyrolactones whose intrinsic reactivity is derived from an accessible Michael acceptor system. Corresponding to this unique reactivity, a vast variety of natural products belong to this class of lactones and display a huge structural diversity which is reflected by several potent and wide-ranging bioactivities including anticancer, anti-inflammatory, antibacterial and antifungal.⁷² Since our previous studies focused on general monocyclic γ -butyrolactone reactivity, we obtained an initial picture of their target preferences. However, many γ -lactones are based on polycyclic ring systems which have been little explored for their target preferences. We therefore here extend our studies to bicyclic α -alkylidene- γ -butyrolactones which are inspired from the natural product xanthatine (Figure 1).¹²⁶⁻¹³¹

In previous studies xanthatin was shown to exhibit potent bactericidal and fungicidal activities which were correlated with the privileged α -methylene- γ -lactone scaffold.¹³²⁻¹³⁴ Although a lot of γ -lactones of natural origin contain α -methylene Michael acceptor systems a limited number represents substituted alkylidenes (e.g. kotolactone A and subamolides)^{135, 136} which might be less reactive due to the steric constrain for nucleophilic attack. In order to investigate how xanthatin-derived molecules interact with their dedicated targets in living cells we designed several probe molecules that differed in the structural composition and substitution of the conserved core structure (Figure 1). All molecules were equipped with an alkyne handle for activity-based protein profiling (ABPP)^{39, 104} which allows the attachment of fluorescent azide tags for target identification via the Huisgen-Sharpley-Meldal click chemistry (CC) reaction.^{46, 109, 137}

γ -Lactone probes:



Protein reactive labeling:

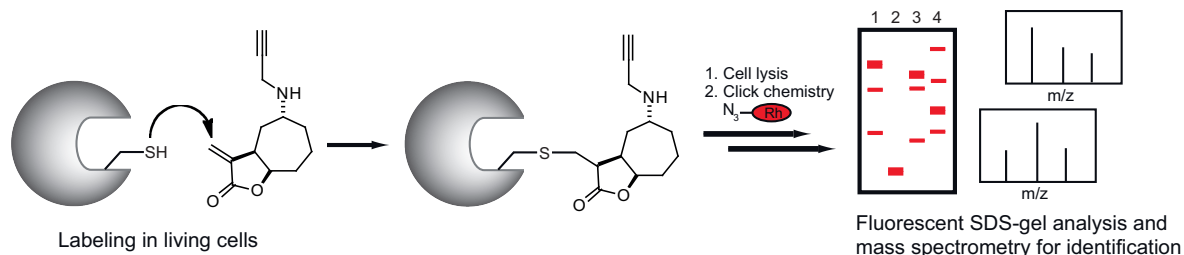


Figure 1: Design of racemic γ -butyrolactone probes and their application in bacterial proteome profiling. Probes are directly incubated with living bacteria to penetrate the cells and label dedicated protein targets *in situ*. The cells are subsequently lysed and the labelled proteins are “clicked” to a fluorescent rhodamine azide dye for visualization by SDS gel electrophoresis and identification by MS. In case of *in vitro* labelling, the cell lysate is incubated with probe.

Several important bacterial enzyme targets have been discovered by this method in the past years. The majority was dedicated to gram positive bacteria such as *S. aureus*, *C. difficile* and *L. monocytogenes*.^{57, 100, 138, 139} Although these organisms represent crucial health threats due to the occurrence of multi-resistances, pathogenic gram negative bacteria such as uropathogenic *E. coli* (UPEC) have been less studied by this approach. UPEC is the cause of severe diseases such as urinary tract infections.¹⁴⁰ These bacteria produce a vast array of virulence factors that are encoded on several pathogenicity islands.

These pathogenic strains therefore contain significantly more genes compared to non-pathogenic *E. coli* and represent candidate organisms for comparative proteome profiling.^{141, 142} We utilized a short array of α -alkylidene- γ -butyrolactone derived probes for target discovery in three pathogenic and one non-pathogenic *E. coli* strains in order to reveal the dedicated targets of this compound class and to screen for pronounced differences between enzymes in pathogenic and non-pathogenic bacteria that could serve as diagnostic marker or putative drug target. Several unique enzymes involved in cellular redox processes as well as in secondary metabolite synthesis were identified. Interestingly, one enzyme of unknown function was only present in uropathogenic but not in non-pathogenic *E. coli*.

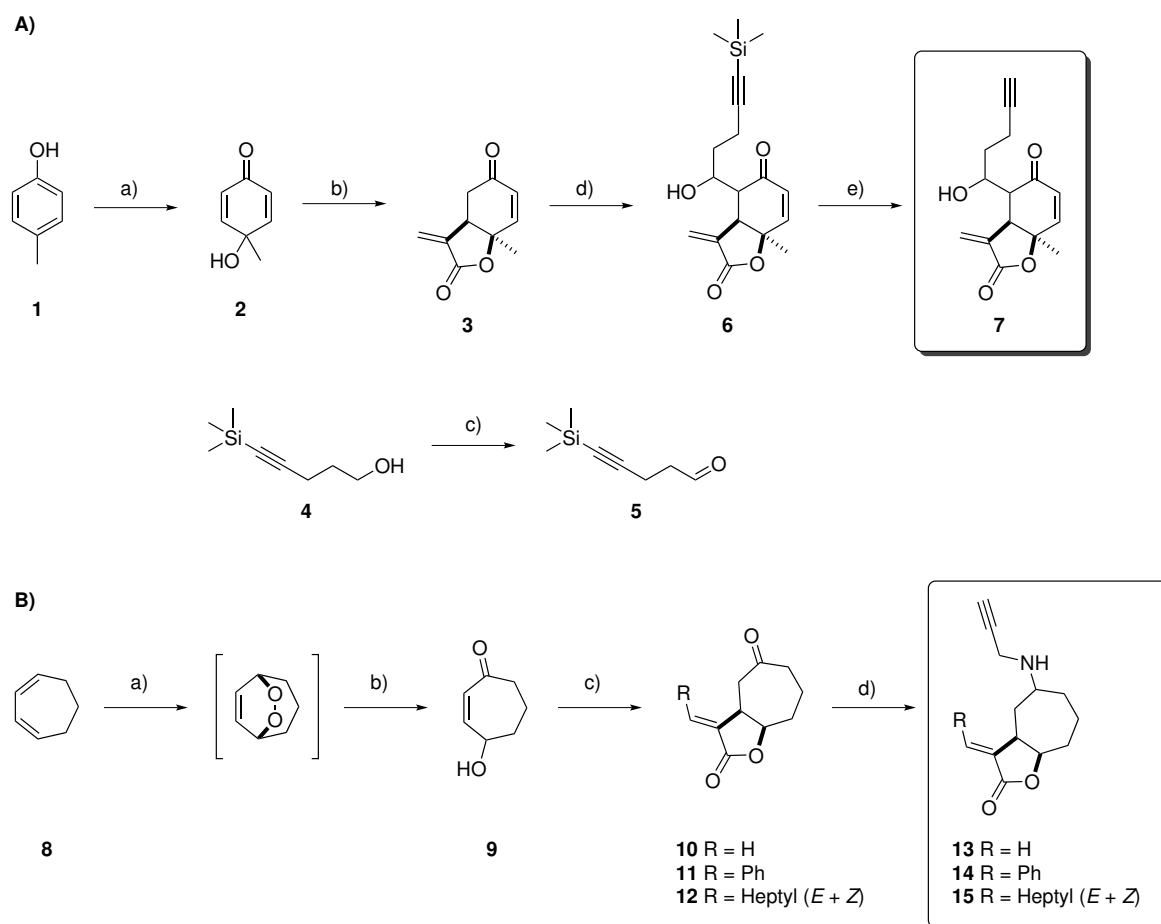
Results and Discussion

Xanthatine derived probe **7** was synthesized by oxidation of *p*-cresol with [bis(trifluoroacetoxy) iodo]-benzene (BTIB) to the dienone **2**.¹⁴³ A one-pot acylation/conjugate addition reaction of **2** with triphenylphosphoranylidene ketene followed by Wittig reaction with paraformaldehyde led to the bicyclic lactone **3** as racemic mixture.¹⁴⁴ Reaction of **3** with the aldehyde **5** yielded the substituted bicyclic lactone **6**, which was deprotected with TBAF/acetic acid to the Michael acceptor probe **7**. Probes **13-15** were synthesized by a dioxygenation reaction of **8** and the intermediate was directly treated with triethylamine to give the enone **9**.¹⁴⁵ Acylation/conjugate addition reactions of **9** with triphenylphosphoranylidene ketene followed by Wittig reaction with different aldehydes yielded the lactones **10-12** as racemic mixtures.¹⁴⁴ Lactone **11** was only observed in *E*-configuration.^{144, 146} A reductive amination of these compounds led to probes **13-15** as diastereomeric mixtures (Scheme 1).¹⁴⁷ Diastereomers **13** were separated by HPLC to yield the compounds **13a** and **13b**, which differ in the stereochemistry of the amine bond (Figure 1).

With these four molecules in hand we tested their protein reactivity against several *E. coli* proteomes including those derived from non-pathogenic *E. coli* K12 and three derived from uropathogenic (536, CFT073 and UTI89) strains (Figure 2). This comparative profiling does not only reveal the dedicated protein targets of individual compounds but in addition may also highlight differences between the four strains with special emphasis on targets that are linked to pathogenicity.

For ABPP studies, *E. coli* cells were grown into stationary phase and subsequently incubated for 2 h with varying amounts of probes. The cells were washed, lysed and the proteomic extract treated with rhodamine azide under CC conditions.⁵⁷ The corresponding SDS gels of these initial studies revealed strong labelling of individual proteins with optimal probe concentrations of 100 μ M (**7**) or 200 μ M (**13a** and **13b**) except two probes **14** and **15** that did not label any proteins even at 400 μ M concentration (Figure S1, Appendix). Interestingly **14** and **15** exhibit a substituted alkylidene γ -lactone scaffold that strongly suggests that these Michael acceptors are shielded from nucleophilic attack and remain unreactive. As this moiety is a common motif in many natural product derived sesquiterpene lactones⁷² we can conclude that these molecules most likely do not exhibit their biological activity via a covalent reaction with enzyme active sites. In contrast, probes **7** and **13a** show a characteristic labelling pattern in all four strains emphasizing that unsubstituted Michael acceptor γ -lactones display a suitable reactivity for dedicated enzyme

active sites (Figure 1). This is in line with previous studies that revealed the importance of α -methylene-Michael acceptors for biological activity.^{148, 149} As there is almost no difference in the labelling pattern of probes **13a** and **13b** it can be concluded that both racemic diastereomers do not influence target preferences (Figure S1, Appendix). We therefore selected probe **13a** as a representative member for all subsequent studies.



Scheme 1: Synthesis of racemic γ -butyrolactone probes. (A) Synthesis of probe **7**: a) BTIB, acetonitrile/water, 0 °C, 5-15 min, 48%; b) Triphenylphosphoranylidene ketene, 1,4-dioxane, reflux, 15 h, paraformaldehyde, reflux, 30 min, 71%; c) Dess-Martin periodinane, dichloromethane, r.t., 3 h, 77%; d) LiHMDS, THF, -78 °C, 1 h, **5**, -78 °C, 4 h, 46%; e) Acetic acid, TBAF, THF, r.t., 15 h, 53%. (B) Synthesis of probes **13-15**: a) TPP (tetraphenylporphyrin), dichloromethane, hv, O₂, 4 °C, 3 h; b) NEt₃, 0 °C, 1 h, r.t., 12 h, 70%; c) Triphenylphosphoranylidene ketene, 1,4-dioxane, reflux, 15 h, paraformaldehyde / benzaldehyde / octanal, reflux, 1.5-48 h, 37% / 60% / 13%; c) propargylamine, acetic acid, THF, r.t., 15 min, sodium triacetoxyborohydride, r.t. 36 h, 28% / 11% / 18%.

Probes **7** and **13a** label several targets in all four proteomes and share a similar labelling pattern suggesting that the additional cyclohexanone Michael acceptor moiety of compound **7** does not significantly alter target selectivity. In fact, compound **13a** with a single Michael

system displays slightly more intense labelling as well as a few more targets compared to compound **7**. Interestingly, a comparison of all four strains shows that both probes label one protein band with a molecular weight of 20 kDa that is only present in uropathogenic strains but absent in the non-pathogenic K12 strain suggesting that this protein could be linked to pathogenicity.

In order to identify this protein as well as other targets we utilized a quantitative enrichment strategy. Cells were labelled with probes, lysed and appended to a rhodamine-biotin-azide tag (Figure S2, Appendix) via CC which allows the enrichment and purification of labelled proteins via avidin binding.⁵⁷ Subsequently, avidin bound proteins were released by heat treatment and separated by fluorescent SDS-PAGE analysis. Enriched protein bands were visualized by fluorescence scanning, isolated, digested and subsequently subjected to mass spectrometric analysis. Peptide fragments were analysed by MS/MS sequencing and proteins predicted via the SEQUEST search algorithm.

Several relevant protein targets were identified including catalase peroxidase (KatG), tRNA sulfurtransferase (Thil), alkyl hydroperoxide reductase subunit C (AhpC) and an uncharacterized protein (C2450) that appears only in uropathogenic strains (Table S1, Appendix). To validate the specificity of the mass spectrometric identification we overexpressed all four identified targets and labelled the recombinant proteins with the corresponding probe (Figure 2B). In all cases a strong protein band could be obtained that almost disappeared if the proteome was heat-denatured prior to labelling emphasizing a specific interaction of the Michael acceptor with the folded enzyme active site.

Thil is involved in the thiamine biosynthesis and catalyses the ATP-dependent transfer of sulphur to cytidine in position 8 of tRNAs to produce 4-thiouridine. The catalytic mechanism involves Cys344 and Cys456 which both are essential for catalytic activity.¹⁵⁰ KatG and AhpC are members of reactive oxygen species defensive genes which are upregulated by the H₂O₂-responsive transactivator OxyR. AhpC cytolyses the reduction of alkyl hydroperoxide and contains two cysteine residues. Cys47 is essential for catalysis whereas Cys166 reduces the susceptibility of AhpC towards inactivation by its own substrates.^{151, 152} C2450 is an uncharacterized protein which lacks functional assignment.

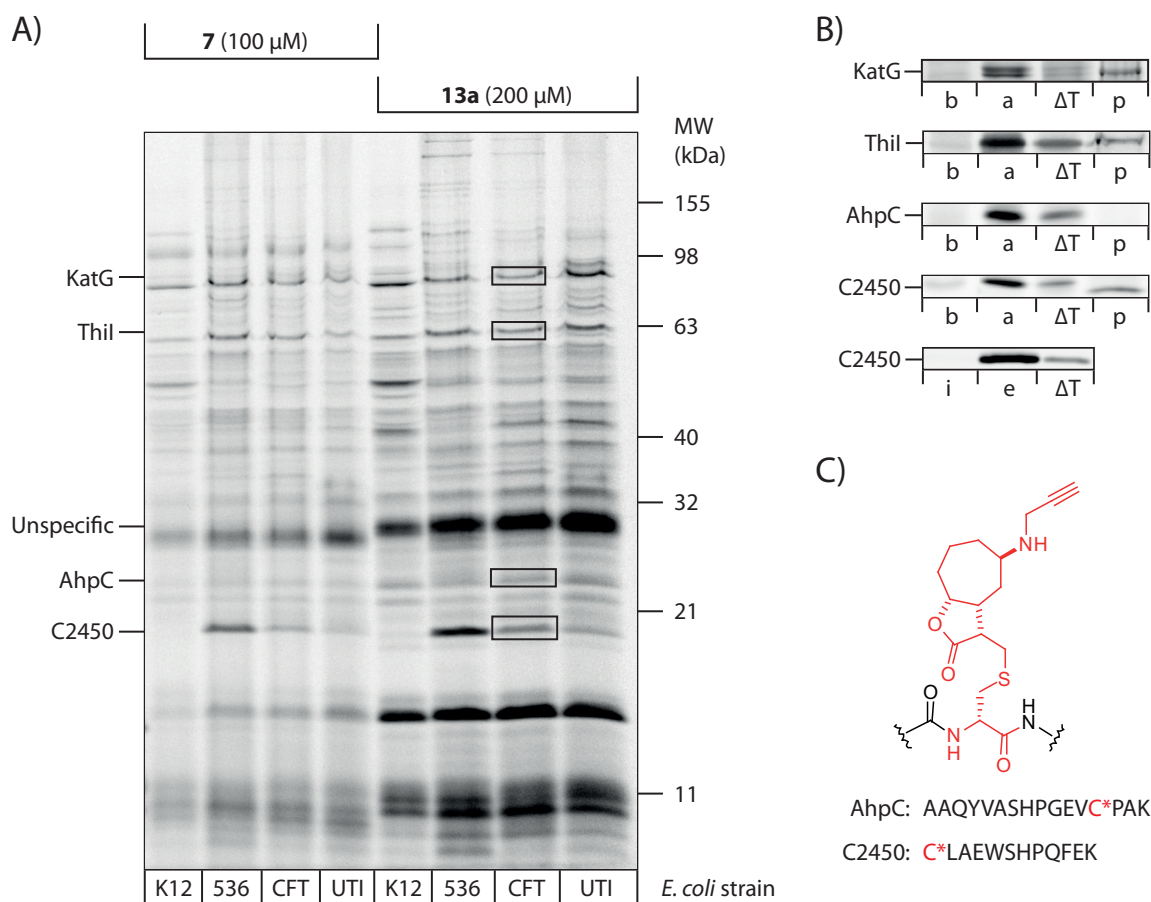


Figure 2: *In situ* labelling of *E. coli* strains with γ -butyrolactone probes **7** and **13a**. (A) Fluorescent SDS gel with labelled proteins. The protein identity is abbreviated next to the gels: KatG, catalase-peroxidase; Thil, tRNA sulfurtransferase; AhpC, alkyl hydroperoxide reductase subunit C and C2450; MW, molecular weight marker. (B) Recombinant expression and labelling of target proteins with **13a** (b, before induction; a, after induction; ΔT , heat control of induced recombinant protein; p, native protein band in the corresponding proteome; i, purified protein preincubated with iodacetamide; e, purified protein). (C) Site of modification of AhpC and C2450 by probe **13a**.

In order to investigate the nature of the interaction of the electrophile with the active site nucleophile we incubated purified AhpC and C2450 with probe **13a** and analysed the tryptic digest via MS/MS sequencing.⁷¹ Interestingly, an active site Cys was the site of attack in both enzymes emphasizing a specificity of probes for dedicated thiol residues of elevated nucleophilicity (Figure 1C, Table S2, Appendix). Contrary to C2450 which is an uncharacterized enzyme, the modified Cys166 of AhpC is one of the two important active site cysteine residues.¹⁵¹

The identified enzymes are likely not essential for *E. coli* viability as shown by a lack of antibiotic activity (no minimal inhibitory concentration values observed) with all molecules under

investigation. A closer inspection of the uncharacterized protein C2450 revealed that this protein is coded by a gene that belongs to a genomic island which encodes a hybrid polyketide/non-ribosomal peptide synthetase (PKS/NRPS).^{153, 154} This PKS/NRPS system is responsible for the synthesis of colibactin, a natural product which causes DNA double strand breaks in eukaryotic cells leading to the activation of the DNA damage checkpoint pathway and subsequent cell cycle arrest. This pathogenic trait of colibactin likely explains its role in devastating uropathogenic *E. coli* infections. While the role of several proteins that are involved in colibactin synthesis has been elucidated the function of C2450 remains elusive. It could be shown that strains with a c2450 deletion still remain pathogenic emphasizing a non-essential role for pathogenesis.¹⁵⁵ C2450 contains only one cysteine residue at position 167 which is selectively targeted by **13a** as shown by MS sequencing (see above). In addition, pre-incubation of C2450 with iodacetamide and subsequent labelling by **13a** (1:1 ratio) revealed a significantly reduced fluorescence signal further validating that this cysteine residue is involved in binding (Figure 2B). Although the knowledge of the active site residue is a first step towards the elucidation of this uncharacterized enzyme, a closer study of its mechanism and function is required. In initial screens for the dedicated substrate we tested the enzymatic turnover of LY-AMC, GGL-AMC und LLVY-AMC (di- or tripeptide 7-amino-4-methylcoumarin) for peptidase, FITC-caseine (casein labelled with fluorescein isothiocyanate) for protease and *para*-nitrophenol acetate for esterase activity. However, we were not able to detect any hydrolytic activity with these substrates; therefore the function of C2450 as an esterase, peptidase or protease is likely to be excluded. Further substrate screens will be required in order to understand its physiological role. Alternatively, our probe could be used as chemical knockout that would allow investigating changes in the metabolome and correlating this with protein function. These follow up studies will be approached in future experiments.

Conclusion

In conclusion, this study aimed to elucidate the intrinsic reactivity of α -alkylidene- γ -butyrolactone derived electrophilic molecules that exhibit a structural similarity to the natural product xanthatine. We synthesized five different molecules that varied in their structural composition. We were able to show that compounds with a substituted α -methylene-Michael acceptor are unreactive, emphasizing that the substituents at this position likely cause a steric clash with the active site nucleophile that prevents covalent modification. It can therefore be concluded that natural products that bear a substitution at the α -methylene-Michael acceptor may not exhibit their biological activity by an irreversible inhibition of the dedicated targets. Vice versa, compounds with an unsubstituted α -methylene-Michael acceptor are reactive as we could

demonstrate by our ABPP experiments and which is also in agreement with previous SAR studies. The targets identified herein contain cysteine residues that are important for catalysis and likely interact with the reactive probes as shown in case of AhpC. In addition, we identified one uncharacterized protein C2450 that is only expressed and active in pathogenic *E. coli*. This shows the potential of our xanthatine-inspired probes which are able to reveal pathogenesis associated enzymes by comparative analysis. Although C2450 is reported to be non-essential for bacteria a further elucidation of its role in the production of the toxin colibactin is an important future task that will help to understand and dissect this crucial bacterial pathogenesis pathway.

Acknowledgements

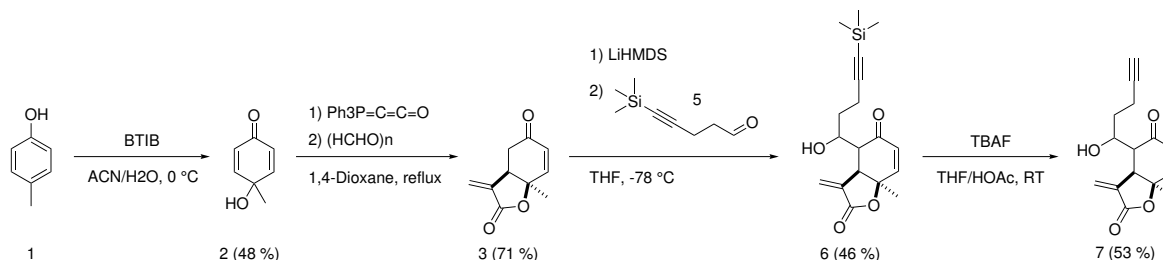
We thank Dr Matthew Nodwell and Dr Vadim Korotkov for important comments and Mona Wolff for excellent scientific support. S.A.S. was supported by the Deutsche Forschungsgemeinschaft, SFB749, FOR1406, an ERC starting grant and the center for integrated protein science, Munich (CIPSM). M.H.K. acknowledges support from the TUM graduate school.

Experimental

Materials. All chemicals were of reagent grade or better and used without further purification. Chemicals and solvents were purchased from Sigma Aldrich or Acros Organics. For all reactions, only commercially available solvents of purissimum grade, dried over molecular sieve and stored under argon atmosphere were used. Solvents for chromatography and workup purposes were generally of reagent grade and purified before use by distillation. In all reactions, temperatures were measured externally. All experiments were carried out under argon. Column chromatography was performed on Merck silica gel (Acros Organics 0.035–0.070 mm, mesh 60 Å). ¹H- and ¹³C-NMR spectra were recorded on a *Bruker Avance I 360* (360 MHz), a *Bruker Avance I* (500 MHz) or a *Bruker Avance III 500* (500 MHz) NMR-System and referenced to the residual proton and carbon signal of the deuterated solvent, respectively. HR-ESI-MS, HR-LC-ESI-MS, HR-APCI-MS and HR-LC-APCI-MS mass spectra were recorded with a *Thermo Finnigan LTQ FT Ultra* coupled with a *Dionex UltiMate 3000* HPLC system. ESI-MS and LC-ESI-MS mass spectra were recorded with a *Thermo Finnigan LCQ ultrafleet* coupled with a *Dionex UltiMate 3000* HPLC system. HPLC analysis was accomplished with a *Waters 2695 separations module*, an *X-Bridge™ C18 3.5 μm OBD™* column (4.6 x 100 mm) and a *Waters 2996 PDA detector*. HPLC separation was accomplished with a *Waters 2545 quaternary gradient module*, an *X-Bridge™ Prep C18 10 μm*

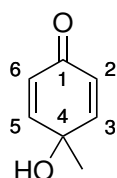
OBDTM (50 x 250 mm), an X-BridgeTM Prep C18 5 μ m OBDTM (30 x 150 mm) or an YMC Triart C18 5 μ m column (10 x 250 mm), a Waters 2998 PDA detector and a Waters Fraction Collector III.

Synthesis of 7



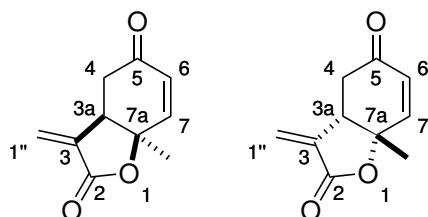
Compounds **3**, **6** and **7** were isolated as racemic mixtures.

4-hydroxy-4-methylcyclohexa-2,5-dienone (**2**)



[Bis(trifluoroacetoxy)iodo] benzene (BTIB) (4.73 g, 11.0 mmol, 1.10 eq.) was added to a stirred solution of *p*-cresol (**1**) (1.08 g, 10.0 mmol, 1.00 eq.) in acetonitrile/water (3:1, 40 mL) at 0 °C and stirring was continued until TLC analysis (diethyl ether) showed completion of the reaction after 5-15 min. The brown reaction mixture was quenched by addition of water (40 mL) and the resulting mixture was extracted with dichloromethane (4 x 50 mL). The combined extracts were dried (Na₂SO₄) and evaporated under reduced pressure. This crude product was purified by column chromatography (diethyl ether/hexane 3:1) followed by recrystallization (hexane/ethyl acetate) to give **2** (518 mg, 4.82 mmol, 48 %) as a brown solid. *R*_f = 0.20 (diethyl ether/hexane, 3:1). ¹H-NMR (500 MHz, CDCl₃) δ = 6.90 (d, ³J_{2,3} = ³J_{5,6} = 9.9 Hz, 2 H, 2-H, 6-H), 6.14 (d, ³J_{2,3} = ³J_{5,6} = 9.9 Hz, 2 H, 3-H, 5-H), 2.19 (br s, 1 H, OH), 1.50 (s, 3 H, Me). ¹³C-NMR (90 MHz, CDCl₃) δ = 185.4, 152.1, 127.2, 67.2, 26.7. Data is consistent with that reported in the literature.¹⁴³

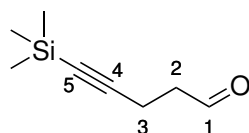
(3aR*,7aR*)-7a-Methyl-3-methylidene-3a,7a-dihydro-3H,4H-benzofuran-2,5-dione (**3**)



Triphenylphosphoranylidene ketene (Bestmann's ylide) (317 mg, 1.05 mmol, 1.05 equiv.), handled under an atmosphere of argon, was added in one portion to a stirred solution of 4-hydroxy-4-

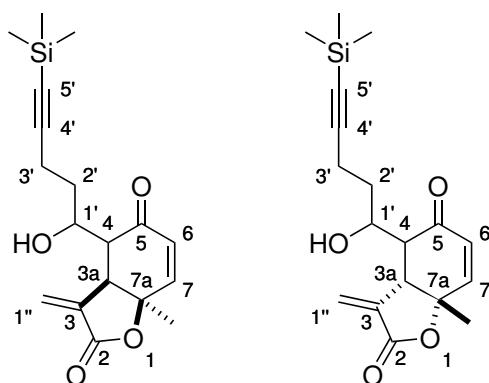
methylcyclohexa-2,5-dienone (**2**) (124 mg, 1.00 mmol, 1.00 equiv.) in 1,4-dioxane (20 mL) at r.t. under argon and the resulting solution was heated to reflux for 15 h. The septum was removed and paraformaldehyde (300 mg, 10.0 mmol, 10.0 equiv.) was added in one portion, rapidly replacing the septum once the addition was complete. The mixture was then heated to reflux for 30 min before being cooled and the solvent was removed in vacuo. The residue was purified by flash column chromatography on SiO₂ eluting with EtOAc/hexane (2:1) to afford compound **3** (127 mg, 0.713 mmol, 71 %) as a colourless solid. *R*_f = 0.66 (EtOAc/hexane, 2:1). ¹H-NMR (500 MHz, CDCl₃) δ = 6.60 (d, ³J_{6,7} = 10.3 Hz, 1 H, 7-H), 6.31 (d, ⁴J_{1''a,3a} = 3.4 Hz, 1 H, 1''_a-H), 5.99 (d, ³J_{6,7} = 10.3 Hz, 1 H, 6-H), 5.59 (d, ⁴J_{1''b,3a} = 3.0 Hz, 1 H, 1''_b-H), 3.35-3.39 (m, 1 H, 3a-H), 2.85 (d, ³J_{3a,4} = 4.2 Hz, 2 H, 4-H), 1.75 (s, 3 H, CH₃). ¹³C-NMR (90 MHz, CDCl₃) δ = 194.3, 168.1, 146.7, 137.5, 128.8, 122.4, 80.0, 45.1, 36.0, 23.9. MS-ESI (m/z): C₁₀H₁₁O₃ [M+H]⁺, calc.: 179.1, found: 179.0. Data is consistent with that reported in the literature.¹⁴⁴

5-(Trimethylsilyl)pent-4-ynal (**5**)



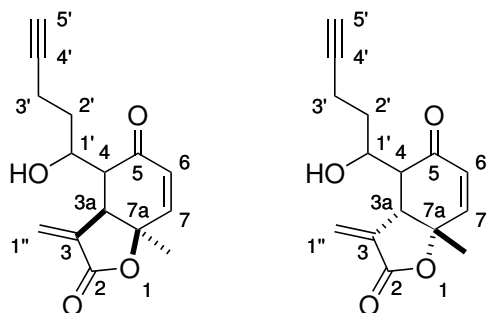
5-(Trimethylsilyl)-4-pentyn-1-ol (**4**) (16.5 mmol, 2.58 g, 3.00 mL, 1.00 eq.) was added slowly to a suspension of Dess-Martin periodinane (7.21 g, 17.0 mmol, 1.03 eq.) in dichloromethane (80 mL). The mixture was stirred for 3 h and the solvent was removed in vacuo (500 mbar). The residue was purified by flash column chromatography on SiO₂ eluting with hexane/diethyl ether (6:1) to afford **5** (1.95 g, 12.7 mmol, 77 %) as colourless oil. *R*_f = 0.40 (hexane/diethyl ether, 6:1). ¹H-NMR (500 MHz, CDCl₃) δ = 9.82 (s, 1 H, 1-H), 2.69 (t, ³J_{2,3} = 7.2 Hz, 2 H, 2-H), 2.57 (t, ³J_{2,3} = 7.2 Hz, 2 H, 3-H), 0.16 (s, 9 H, TMS). ¹³C-NMR (90 MHz, CDCl₃) δ = 200.4, 104.7, 85.8, 42.5, 13.1, 0.0. Data is consistent with that reported in the literature.¹⁵⁶

(3aR*7aR*)-4-(1-hydroxy-5-(trimethylsilyl)pent-4-yn-1-yl)-7a-methyl-3-methylidene-3a,7a-dihydro-3H,4H-benzofuran-2,5-dione (**6**)



To **3** (40.0 mg, 0.224 mmol, 1.00 eq.) in THF (10 mL) was added LiHMDS (1 M in THF, 0.224 mL, 0.224 mmol, 1.00 eq.) at $-78\text{ }^{\circ}\text{C}$ and the mixture was stirred for 1 h. **5** (45.0 mg, 0.291 mmol, 1.30 eq.) was added and the mixture was stirred for further 4 h. The reaction mixture was quenched with saturated $\text{NH}_4\text{Cl}_{\text{aq}}$ (10 mL) and extracted with EtOAc (3 x 20 mL). The organic phase was dried with MgSO_4 and the solvents were removed in vacuo. The residue was purified by flash column chromatography on SiO_2 eluting with hexane/EtOAc (2:1) to afford **6** (34.5 mg, 0.104 mmol, 46 %) as colourless oil. $R_f = 0.29$ (hexane/EtOAc, 2:1). $^1\text{H-NMR}$ (500 MHz, CDCl_3) $\delta = 6.66$ (d, $^3J_{6,7} = 10.4$ Hz, 0.86 H, 7-H), 6.55 (d, $^3J_{6,7} = 10.4$ Hz, 0.14 H, 7-H), 6.33-6.36 (m, 1 H, $1''_a$ -H), 6.14 (d, $^4J_{1''b,3a} = 3.0$ Hz, 0.14 H, $1''_b$ -H), 6.00 (d, $^3J_{6,7} = 10.4$ Hz, 0.86 H, 6-H), 5.98 (d, $^3J_{6,7} = 10.4$ Hz, 0.14 H, 6-H), 5.60 (d, $^4J_{1''b,3a} = 3.0$ Hz, 0.86 H, $1''_b$ -H), 4.50-4.56 (m, 0.14 H, $1'$ -H), 4.10-4.17 (m, 0.86 H, $1'$ -H), 3.76-3.78 (m, 0.14 H, 3a-H), 3.75-3.73 (m, 0.86 H, 3a-H), 2.86-2.90 (m, 0.14 H, 4-H), 2.80-2.85 (m, 0.86 H, 4-H), 2.48-2.56 (m, 1 H, $3'_a$ -H), 2.37-2.45 (m, 1 H, $3'_b$ -H), 1.93-2.00 (m, 0.14 H, $2'$ -H), 1.82-1.89 (m, 0.86 H, $2'$ -H), 1.83 (s, 2.58 H, CH_3), 1.66-1.80 (m, 1 H, $2'$ -H), 1.77 (s, 0.42 H, CH_3), 0.18 (s, 1.26 H, TMS), 0.17 (s, 7.74 H, TMS). $^{13}\text{C-NMR}$ (90 MHz, CDCl_3) $\delta = 196.8, 168.1, 146.7, 138.34, 129.1, 128.60, 125.6, 122.8, 106.0, 87.2, 79.9, 70.3, 67.6, 54.5, 51.0, 47.5, 44.6, 34.7, 33.3, 26.88, 25.9, 22.3, 17.0, 0.05, 0.0, -0.03$. HRMS-ESI (m/z): $\text{C}_{18}\text{H}_{25}\text{O}_4\text{Si}$ $[\text{M}+\text{H}]^+$, calc.: 333.15219, found: 333.15166, $\delta = 1.6$ ppm.

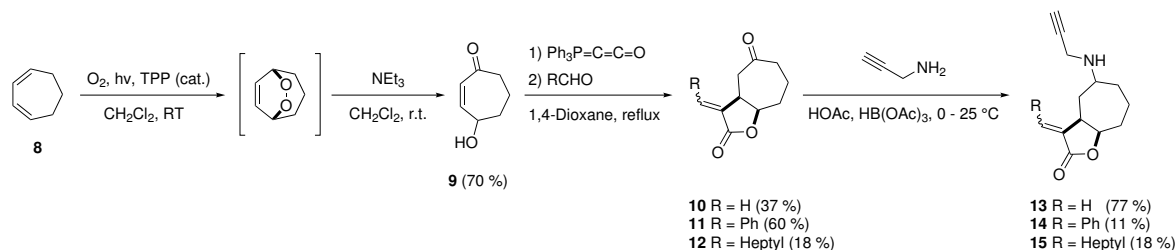
(3aR*7aR*)-4-(1-hydroxypent-4-yn-1-yl)-7a-methyl-3-methylidene-3a,7a-dihydro-3H,4H-benzofuran-2,5-dione (7)



To **6** (20.0 mg, 60.0 μmol , 1.00 eq.) in THF (5 mL) was added acetic acid (1 mL) and TBAF (200 μmol , 3.33 eq.) at r.t. and the reaction was stirred until TLC analysis showed completion of the reaction. Saturated $\text{NH}_4\text{Cl}_{\text{aq}}$ (20 mL) was added and the reaction mixture was extracted with EtOAc. The organic phase was washed with saturated NaCl_{aq} , dried with MgSO_4 and the solvents were removed in vacuo. The residue was purified by flash column chromatography on SiO_2 eluting with hexane/EtOAc (2:1) to afford **7** (8.20 mg, 31.8 μmol , 53 %) as colourless oil. $R_f = 0.34$ (hexane/EtOAc, 2:1). $^1\text{H-NMR}$ (500 MHz, CDCl_3) $\delta = 6.69$ (dd, $^3J_{6,7} = 10.3$ Hz, $^4J_{3a,7} = 0.8$ Hz, 1 H, 7-H), 6.41 (d, $^4J_{1''a,3a} = 2.6$ Hz, 1 H, $1''_a$ -H), 6.08 (d, $^3J_{6,7} = 10.3$ Hz, 1 H, 6-H), 5.74 (d, $^4J_{1''b,3a} = 2.3$ Hz, 1 H, $1''_b$ -H), 4.05 (dt, $J = 9.3, 4.0$ Hz, 1 H, $1'$ -H), 3.42 (dtd, $^3J_{3a,4} = 5.8$ Hz, $^4J_{1''b,3a} = 2.4$ Hz, $^4J_{3a,7} = 0.8$ Hz,

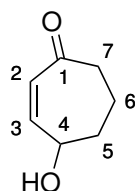
1 H, 3a-H), 2.65 (dd, $^3J_{3a,4} = 6.1$ Hz, $^3J_{4,1'} = 4.3$ Hz, 1 H, 4-H), 2.41-2.46 (m, 2 H, 3'-H), 2.02-2.08 (m, 1 H, 2'-H), 2.00 (t, $^4J_{3',5'} = 2.7$ Hz, 1 H, 5'-H), 1.84-1.92 (m, 1 H, 2'-H), 1.73 (s, 3 H, CH₃). **¹³C-NMR** (90 MHz, CDCl₃) $\delta = 197.8, 167.9, 145.5, 137.9, 129.6, 124.5, 83.2, 79.2, 69.8, 69.6, 52.1, 47.2, 34.0, 26.9, 15.0$. **HRMS-ESI** (m/z): C₁₅H₁₇O₄ [M+H]⁺, calc.: 261.11214, found: 261.11210, $\delta = 0.2$ ppm.

Synthesis of 13a, 13b, 14 and 15



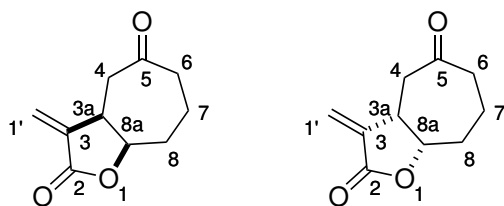
All compounds were isolated as racemic mixtures.

4-hydroxycyclohept-2-enone (9)



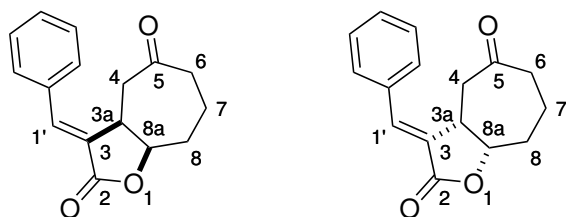
A solution containing 1,3-cycloheptadiene (**8**) (942 mg, 10.0 mmol, 1.09 mL, 1.00 eq.) and tetraphenylporphyrin (6.0 mg, 9.8 μ mol) in dry CH₂Cl₂ (30 mL) was irradiated with a tungsten halogen lamp at 4 °C while oxygen was continuously bubbled through it. The reaction was monitored by TLC analysis and after completion (3 h) the solvent was evaporated in vacuo. The residue was dissolved in CH₂Cl₂ (10 mL) and NEt₃ (2.80 mL, 20.0 mmol, 2.00 eq.) was added over 20 min at 0 °C. The mixture was stirred 1 h at 0 °C, 12 h at r.t. and HCl_{aq} (2 M, 15 mL) was added. The reaction mixture was extracted with CH₂Cl₂ (2 \times 15 mL, the organic phase was dried over MgSO₄ and the solvent was removed in vacuo. The residue was purified by flash column chromatography on SiO₂ eluting with hexane/EtOAc (1:1) to afford **9** (873 mg, 6.92 mmol, 70 %) as colourless oil. $R_f = 0.47$ (hexane/EtOAc, 1:1). **¹H-NMR** (500 MHz, CDCl₃) $\delta = 6.59$ (ddd, $J = 12.6, 3.1, 1.2$ Hz, 1 H, 3-H), 5.97 (ddd, $J = 12.6, 2.2, 0.7$ Hz, 1 H, 2-H), 4.56-4.63 (m, 1 H, 4-H), 2.54-2.67 (m, 2 H, 7-H), 2.18-2.28 (m, 1 H, 5_a-H), 2.09-2.18 (s, 1 H, OH), 1.81-1.91 (m, 3 H, 5_b-H, 6-H). **¹³C-NMR** (90 MHz, CDCl₃) $\delta = 203.1, 149.0, 129.9, 70.5, 43.1, 35.2, 18.3$. **HRMS-ESI** (m/z): C₇H₁₁O₂ [M+H]⁺, calc.: 127.07536, found: 127.07527, $\delta = 0.7$ ppm. Data is consistent with that reported in the literature.¹⁴⁵

(3aR*8aR*)-3-methylenehexahydro-2H-cyclohepta[b]furan-2,5(3H)-dione (10)



Triphenylphosphoranylidene ketene (720 mg, 2.39 mmol, 1.05 eq.) was added to a stirred solution of **9** (288 mg, 2.29 mmol, 1.00 eq.) in 1,4-dioxane (45 mL) at r.t. and the reaction was heated to reflux for 15 h. Paraformaldehyde (684 mg, 22.8 mmol, 10.0 eq.) was added and the reaction mixture heated to reflux for additional 1.5 h. After the reaction cooled to r.t. the solvent was removed in vacuo and the residue was purified by flash column chromatography on SiO₂ eluting with hexane/EtOAc (1:1 → 1:2). The resulting product was further purified by HPLC yielding **10** (152 mg, 0.844 mmol, 37 %) as colourless solid. *R*_f = 0.67 (hexane/EtOAc, 1:2). ¹H-NMR (500 MHz, CDCl₃) δ = 6.37 (d, *J* = 2.7 Hz, 1 H, 1'_a-H), 5.71 (d, *J* = 2.4 Hz, 1 H, 1'_b-H), 4.73 (ddd, *J* = 9.5, 7.9, 3.8 Hz, 1 H, 8a-H), 3.39 (dddd, *J* = 14.4, 7.0, 4.6, 2.5 Hz, 1 H, 3a-H), 2.85 (dd, *J* = 13.0, 11.5 Hz, 1 H, 4_a-H), 2.59 (dd, *J* = 13.0, 4.3 Hz, 1 H, 4_b-H), 2.53 (t, *J* = 6.8 Hz, 2 H, 6-H), 2.23 (dddd, *J* = 14.4, 8.3, 3.8, 2.1 Hz, 1 H, 8_a-H), 1.95-2.10 (m, 2 H, 7_a-H, 8_b-H), 1.57-1.68 (m, 1 H, 7_b-H). ¹³C-NMR (90 MHz, CDCl₃) δ = 208.8, 169.0, 138.0, 123.7, 79.7, 44.4, 43.8, 38.5, 29.9, 18.0. HRMS-ESI (*m/z*): C₁₀H₁₃O₃ [M+H]⁺, calc.:181.08592, found: 181.08608, δ = 0.9 ppm. Data is consistent with that reported in the literature.¹⁴⁴

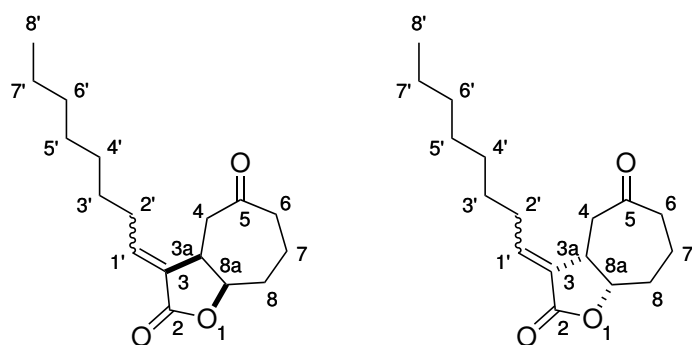
(3aR*8aR*E)-3-benzylidenehexahydro-2H-cyclohepta[b]furan-2,5(3H)-dione (11)¹⁴⁴



Triphenylphosphoranylidene ketene (500 mg, 1.65 mmol, 1.05 eq.) was added to a stirred solution of **9** (199 mg, 1.58 mmol, 1.00 eq.) in 1,4-dioxane (40 mL) at r.t. and the reaction was heated to reflux for 15 h. Benzaldehyde (838 mg, 7.90 mmol, 5.00 eq.) was added and the reaction mixture heated to reflux for additional 48 h. After the reaction cooled to r.t. the solvent was removed in vacuo and the residue was purified by flash column chromatography on SiO₂ eluting with hexane/EtOAc (2:1 → 1:2). The resulting product was further purified by HPLC yielding **11** (243 mg, 0.948 mmol, 60 %) as colourless solid. *E/Z* > 95:5 based on comparison of chemical shift and coupling constant of 1'-H with related compounds.¹⁴⁶ *R*_f = 0.34 (hexane/EtOAc, 1:2). ¹H-NMR (500 MHz, CDCl₃) δ = 7.57 (d, *J* = 7.4 Hz, 2 H, *o*-Ar-H) 7.55 (d, *J* = 1.9 Hz, 1 H, 1'-H), 7.48 (t, *J* = 7.4 Hz, 2 H, *m*-Ar-H), 7.43 (t, *J* = 7.3 Hz, 1 H, *p*-Ar-H), 4.69 (ddd, *J* = 8.9, 6.5, 4.7 Hz, 1 H, 8a-H), 3.72

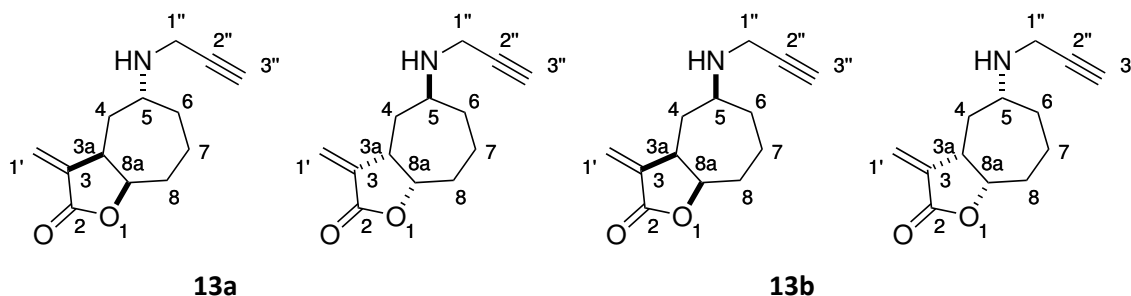
(dddd, $J = 11.9, 6.4, 3.0, 1.9$ Hz, 1 H, 3a-H), 2.80 (t, 12.8 Hz, 1 H, 4_a-H), 2.51-2.64 (m, 3 H, 4_b-H, 6-H), 2.28 (dddd, $J = 15.2, 8.8, 4.7, 2.0$ Hz, 1 H, 8_a-H), 2.20 (dddd, $J = 15.0, 10.6, 8.8, 1.9$ Hz, 1 H, 8_b-H), 2.05-2.15 (m, 1 H, 7_a-H), 1.59-1.69 (m, 1 H, 7_b-H). ¹³C-NMR (90 MHz, CDCl₃) $\delta = 209.4, 171.2, 137.9, 133.3, 130.5, 129.4, 128.6, 79.3, 77.4, 44.7, 40.3, 39.1, 29.4, 17.3$. HRMS-ESI (m/z): C₁₆H₁₇O₃ [M+H]⁺, calc.: 257.11722, found: 257.11687, $\delta = 1.4$ ppm.

(3aR*8aR*)-3-octylidenehexahydro-2H-cyclohepta[b]furan-2,5(3H)-dione (12) ¹⁴⁴



Triphenylphosphoranylideneketene (500 mg, 1.65 mmol, 1.05 eq.) was added to a stirred solution of **9** (199 mg, 1.58 mmol, 1.00 eq.) in 1,4-dioxane (40 mL) at r.t. and the reaction was heated to reflux for 15 h. Octanal (1.01 g, 7.90 mmol, 5.00 eq.) was added and the reaction mixture heated to reflux for additional 48 h. After the reaction cooled to r.t. the solvent was removed in vacuo and the residue was purified by flash column chromatography on SiO₂ eluting with hexane/EtOAc (10:1 → 1:2). The resulting product was further purified by HPLC yielding **12** (57.0 mg, 0.205 mmol, 13 %) as colourless solid. E/Z = 1:5 based on comparison of chemical shift and coupling constant of 1'-H with related compounds. ¹⁴⁶ $R_f = 0.42$ (hexane/EtOAc, 1:2). ¹H-NMR (500 MHz, CDCl₃) $\delta = 6.77$ (td, $J = 7.7, 2.0$ Hz, 0.8 H, 1'-H(Z)), 6.25 (td, $J = 7.7, 2.0$ Hz, 0.2 H, 1'-H(E)), 4.63 (ddd, $J = 8.4, 7.0, 4.6$ Hz, 1 H, 8a-H(E+Z)), 3.31 (ddt, $J = 12.1, 5.7, 2.5$ Hz, 0.8 H, 3a-H(Z)), 3.21-3.28 (m, 0.2 H, 3a-H(E)), 2.85 (t, $J = 12.4$ Hz, 0.2 H, 4_a-H(E)) 2.80 (t, $J = 13.0$ Hz, 0.8 H, 4_a-H(Z)), 2.69-2.76 (m, 0.4 H, 2'-H(E)), 2.48-2.61 (m, 2 H, 6-H(E+Z)), 2.43 (dd, $J = 12.9, 4.1$ Hz, 0.2 H, 4_b-H(E)), 2.35 (dd, $J = 13.3, 3.6$ Hz, 0.8 H, 4_b-H(Z)), 2.21-2.32 (m, 1.6 H, 2'-H(Z)), 2.10-2.21 (m, 2 H, 8-H(E+Z)), 1.99-2.10 (m, 1 H, 7_a-H(E+Z)), 1.57-1.68 (m, 1 H, 7_b-H(E+Z)), 1.40-1.54 (m, 2 H, 3'-H(E+Z)), 1.22-1.38 (m, 8 H, 4'-H(E+Z), 5'-H(E+Z), H6'-H(E+Z), 7'-H(E+Z)), 0.87-0.92 (m, 3 H, 8'-H(E+Z)). ¹³C-NMR (90 MHz, CDCl₃) $\delta = 209.5, 209.4, 169.9, 168.8, 146.5, 142.9, 130.0, 128.0, 79.1, 78.9, 44.7, 44.5, 44.2, 42.8, 40.2, 37.7, 31.8, 31.7, 29.8, 29.5, 29.3, 29.2, 29.2, 29.1, 29.0, 28.5, 27.7, 22.6, 22.6, 17.6, 17.0, 14.1, 14.1$. HRMS-ESI (m/z): C₁₇H₂₇O₃ [M+H]⁺, calc.: 279.19547, found: 279.19510, $\delta = 1.3$ ppm.

(3aR*5R*8aR*)-3-methylene-5-(prop-2-yn-1-ylamino)-octahydro-2H-cyclohepta[b]furan-2-one (13a) and (3aR*5S*8aR*)-3-methylene-5-(prop-2-yn-1-ylamino)-octahydro-2H-cyclohepta[b]furan-2-one (13b)¹⁴⁷



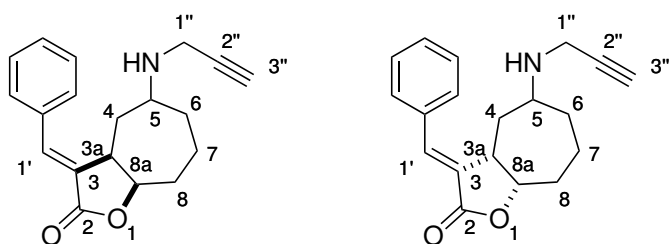
To a solution of **10** (18.0 mg, 0.100 mmol, 1.00 eq.) in THF (10 mL) were added propargylamine (6.06 mg, 7.05 μ L, 0.110 mmol, 1.10 eq.) and acetic acid (6.01 mg, 5.72 μ L, 0.100 mmol, 1.00 eq.) at r.t. and the reaction was stirred for 15 min. Sodium triacetoxyborohydride (31.8 mg, 0.150 mmol, 1.50 eq.) was added and the reaction mixture was stirred at r.t. for further 36 h. Saturated NaHCO_3 (15 mL) and H_2O (5 mL) were added and the mixture was extracted with EtOAc (3 \times 20 mL). The organic phase was dried over MgSO_4 , the solvents were removed in vacuo and the residue was purified by flash column chromatography on SiO_2 eluting with EtOAc. The product was separated by HPLC yielding **13a** (11.5 mg, 52.4 μ mol, 49 %) and **13b** (6.50 mg, 29.6 μ mol, 28 %) as colourless solids.

Diastereomer 13a (for determination of relative stereochemistry see 2D-NMR spectrum): $R_f = 0.36$ (hexane/EtOAc, 1:2). **$^1\text{H-NMR}$** (500 MHz, CDCl_3) $\delta = 6.31$ (d, $J = 3.2$ Hz, 1 H, $1'_a\text{-H}$), 5.58 (d, $J = 2.8$ Hz, 1 H, $1'_b\text{-H}$), 4.79 (ddd, $J = 10.0, 8.7, 3.5$ Hz, 1 H, $8a\text{-H}$), 3.38-3.52 (m, 3 H, $3a\text{-H}$, $1''\text{-H}$), 3.18-3.23 (m, 1 H, 5-H), 2.24 (t, $J = 2.4$ Hz, 1 H, $3''\text{-H}$), 2.00-2.07 (m, 2 H, 4_a-H , 8_a-H), 1.87 (ddd, $J = 14.9, 10.1, 1.4$ Hz, 1 H, 4_b-H), 1.71-1.81 (m, 1 H, 8_b-H), 1.55-1.70 (m, 4 H, 6-H , 7-H), 1.34 (br s, 1 H, NH). **$^{13}\text{C-NMR}$** (90 MHz, CDCl_3) $\delta = 170.3, 140.2, 121.8, 81.7, 77.3, 71.7, 52.2, 37.44, 35.7, 35.7, 34.6, 31.5, 18.8$. **HRMS-ESI** (m/z): $\text{C}_{13}\text{H}_{18}\text{NO}_2$ [$\text{M}+\text{H}$] $^+$ calc.: 220.13321 found: 220.13360, $\delta = 1.8$ ppm.

Diastereomer 13b (for determination of relative stereochemistry see 2D-NMR spectrum): $R_f = 0.25$ (hexane/EtOAc, 1:2). **$^1\text{H-NMR}$** (500 MHz, CDCl_3) $\delta = 6.31$ (d, $J = 3.0$ Hz, 1 H, $1'_a\text{-H}$), 5.62 (d, $J = 2.6$ Hz, 1 H, $1'_b\text{-H}$), 4.64 (ddd, $J = 12.2, 8.4, 4.1$ Hz, 1 H, $8a\text{-H}$), 3.51 (d, $J = 2.5$ Hz, 2 H, $1''\text{-H}$), 3.25-3.33 (m, 1 H, $3a\text{-H}$), 2.82 (ddd, $J = 10.0, 9.0, 2.6$ Hz, 1 H, 5-H), 2.25 (t, $J = 2.4$ Hz, 1 H, $3''\text{-H}$), 2.14-2.21 (m, 1 H, 8_a-H), 1.98-2.02 (m, 3 H, 4_a-H , 6_a-H , 7_a-H), 1.58-1.73 (m, 2 H, 4_b-H , 8_b-H), 1.50 (br s, 1 H, NH), 1.22-1.41 (m, 2 H, 6_b-H , 7_b-H). **$^{13}\text{C-NMR}$** (90 MHz, CDCl_3) $\delta = 169.9, 140.0, 122.5, 81.7, 77.2, 71.7, 56.8, 40.2, 37.5, 36.8, 35.4, 30.8, 21.5$. **HRMS-ESI** (m/z): $\text{C}_{13}\text{H}_{18}\text{NO}_2$ [$\text{M}+\text{H}$] $^+$ calc.: 220.13321 found: 220.13360, $\delta = 1.8$ ppm.

(3a*R8a*R***E*)-3-benzylidene-5-(prop-2-yn-1-ylamino)octahydro-2*H*-cyclohepta-[*b*]furan-2-one**

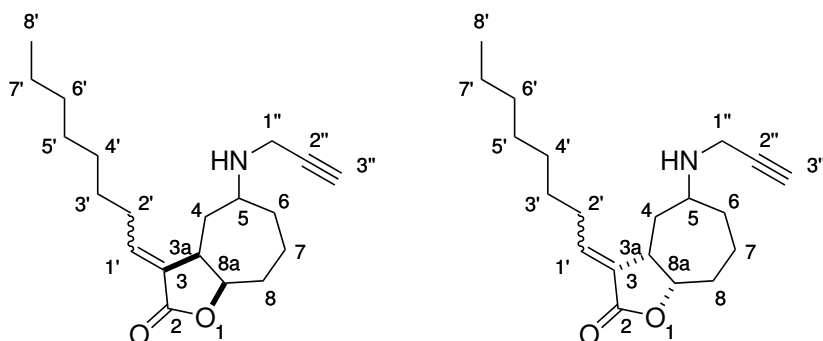
(14)¹⁴⁷



To a solution of **11** (81.0 mg, 0.316 mmol, 1.00 eq.) in THF (40 mL) were added propargylamine (19.1 mg, 22.3 μ L, 0.348 mmol, 1.10 eq.) and acetic acid (19.0 mg, 18.1 μ L, 0.316 mmol, 1.00 eq.) at r.t. and the reaction was stirred for 15 min. Sodium triacetoxyborohydride (100 mg, 0.474 mmol, 1.50 eq.) was added and the reaction mixture was stirred at r.t. for further 36 h. Saturated NaHCO_3 (40 mL) and H_2O (20 mL) were added and the mixture was extracted with EtOAc (3 \times 40 mL). The organic phase was dried over MgSO_4 , the solvents were removed in vacuo and the residue was purified by flash column chromatography on SiO_2 eluting with hexane/EtOAc (2:1 \rightarrow 0:1). The resulting product was further purified by HPLC yielding **14** (12.5 mg, 33.9 μ mol, 11 %) as colourless solid. $R_f = 0.14$ (EtOAc). $^1\text{H-NMR}$ (500 MHz, CDCl_3) $\delta = 7.59\text{--}7.65$ (m, 2 H, Ar-H), 7.49–7.54 (m, 2 H, Ar-H), 7.43–7.49 (m, 2 H, Ar-H, 1'-H), 4.93 (ddd, $J = 8.7, 6.7, 2.2$ Hz, 0.15 H, 8a-H, Isomer 2), 4.67 (ddd, $J = 11.2, 7.1, 6.2$ Hz, 0.85 H, 8a-H, Isomer 1), 4.17 (ddt, $J = 8.8, 6.2, 3.3$ Hz, 0.15 H, 3a-H, Isomer 2), 3.84 (ddt, $J = 9.7, 7.0, 2.5$ Hz, 0.85 H, 3a-H, Isomer 1), 3.72 (ddd, $J = 29.7, 17.0, 2.6$ Hz, 1.7 H, 1''-H, Isomer 1), 3.48–3.56 (m, 0.85 H, 5-H, Isomer 1), 3.20 (ddd, $J = 103.2, 16.8, 2.6$ Hz, 0.3 H, 1''-H, Isomer 2), 2.94–3.00 (m, 0.15 H, 5-H, Isomer 2), 2.88 (t, $J = 2.5$ Hz, 0.85 H, 3''-H, Isomer 1), 2.71 (t, $J = 2.6$ Hz, 0.15 H, 3''-H, Isomer 2), 2.36 (ddd, $J = 14.4, 8.7, 6.1$ Hz, 1 H, 8_a-H), 2.19–2.29 (m, 1 H, 6_a-H), 1.86–2.02 (m, 3 H, 4-H, 7_a-H), 1.69 (m, 1 H, 8_b-H), 1.56–1.65 (m, 1 H, 6_b-H), 1.33–1.43 (m, 1 H, 7_b-H). $^{13}\text{C-NMR}$ (90 MHz, CDCl_3) $\delta = 170.8, 160.6, 137.4, 136.3, 133.64, 133.59, 130.4, 130.1, 130.1, 130.0, 129.3, 129.1, 79.6, 79.0, 77.4, 74.1, 57.8, 55.3, 39.0, 36.7, 33.8, 33.7, 32.9, 32.8, 31.7, 29.8, 29.5, 29.4, 29.0, 28.6, 22.4, 18.3, 17.5, 13.4$. **HRMS-ESI** (m/z): $\text{C}_{19}\text{H}_{22}\text{NO}_2$ [M+H]⁺, calc.: 296.16451, found: 296.16427, 0.8 ppm.

(3a*R8a*R**)--3-octylidene-5-(prop-2-yn-1-ylamino)octahydro-2*H*-cyclohepta[*b*]-furan-2-one**

(15)¹⁴⁷



To a solution of **12** (57.0 mg, 0.205 mmol, 1.00 eq.) in THF (20 mL) were added propargylamine (12.4.1 mg, 14.5 μ L, 0.226 mmol, 1.10 eq.) and acetic acid (12.3 mg, 11.7 μ L, 0.205 mmol, 1.00 eq.) at r.t. and the reaction was stirred for 15 min. Sodium triacetoxyborohydride (65.3 mg, 0.308 mmol, 1.50 eq.) was added and the reaction mixture was stirred at r.t. for further 36 h. Saturated NaHCO₃ (20 mL) and H₂O (10 mL) were added and the mixture was extracted with EtOAc (3 \times 30 mL). The organic phase was dried over MgSO₄, the solvents were removed in vacuo and the residue was purified by flash column chromatography on SiO₂ eluting with hexane/EtOAc (1:1 \rightarrow 0:1). The resulting product was further purified by HPLC yielding **15** (12.0 mg, 37.8 μ mol, 18 %) as colourless solid. R_f = 0.23 (EtOAc). **¹H-NMR** (500 MHz, CDCl₃) δ = 6.90 (ddd, J = 9.5, 5.6, 2.4 Hz, 0.30 H, 1'-H), 6.80 (ddd, J = 8.6, 6.4, 2.0 Hz, 0.47 H, 1'-H), 6.35 (dt, J = 8.0, 7.9, 2.3 Hz, 0.12 H, 1'-H), 6.25 (dt, J = 7.9, 7.7, 2.0 Hz, 0.09 H, 1'-H), 4.81-4.87 (m, 0.43 H, 8a-H), 4.54-3.63 (m, 0.57 H, 8a-H), 3.71-3.92 (m, 2 H, 1''-H), 3.16-3.56 (m, 2 H), 2.78-2.94 (m, 0.22 H), 2.60-2.74 (m, 0.22 H), 2.51-2.58 (m, 1 H, 3''-H), 2.40-2.48 (m, 0.50 H), 2.19-2.40 (m, 3 H), 2.08-2.19 (m, 1 H), 1.97-2.06 (m, 1.5 H), 1.82-1.93 (m, 0.41 H), 1.59-1.82 (m, 2.29 H), 1.40-1.59 (m, 2 H), 1.22-1.39 (m), 0.87-0.94 (m, 3 H). **¹³C-NMR** (90 MHz, CDCl₃) δ = 170.4, 170.1, 169.3, 168.9, 162.9, 162.7, 162.4, 162.1, 147.8, 147.1, 144.8, 143.7, 130.4, 128.8, 128.5, 126.8, 117.4, 115.1, 79.5, 79.5, 78.8, 78.4, 78.4, 77.99, 77.96, 77.94, 72.7, 72.6, 72.5, 72.3, 57.9, 57.5, 54.2, 54.0, 41.4, 39.1, 38.6, 36.8, 34.7, 34.0, 33.9, 33.8, 33.6, 33.6, 33.2, 32.7, 32.4, 32.2, 31.9, 31.9, 31.8, 31.6, 30.5, 30.4, 30.3, 29.6, 29.5, 29.5, 29.4, 29.4, 29.3, 29.3, 29.2, 29.22, 29.21, 29.1, 29.1, 28.6, 27.9, 27.8, 22.8, 22.6, 20.2, 18.9, 17.6, 17.5, 14.2, 14.2. **HRMS-ESI** (m/z): C₂₀H₃₂NO₂ [M+H]⁺, calc.: 318.24276, found: 318.24255, δ = 0.6 ppm.

Preparation of *in vitro* proteomes. Proteomes of the bacterial strains were prepared from 1 L liquid cultures harvested 1 h after transition in the stationary phase by centrifugation at 13,000 rpm. Bacterial strains were grown in LB (lysogeny broth) medium, bacterial cell pellets were washed with PBS (20 mL), resuspended in PBS (20 mL) and lysed by ultrasound or French press.

***In vitro* labelling of bacterial proteomes.** Proteome samples were adjusted to a final concentration of 1 mg protein/mL by dilution in PBS prior to probe labelling. Experiments for visualization by 1D SDS-PAGE were carried out in 43 μ L total volume and those for affinity enrichment in 1892 μ L total volume, such that once CC reagents were added, the total reaction volume was 50 μ L and 2 mL, respectively. Reactions were initiated by addition of the probe and allowed to incubate for 1 h at room temperature. For heat controls the proteome was denatured with 2 μ L of 21.5% SDS at 96 °C for 6 min and cooled to room temperature before the probe was applied. Following incubation, reporter-tagged azide reagents (100 μ M rhodamine-azide for analytical or 20 μ M rhodamine-biotin-azide for preparative scale) were added followed by 1 mM TCEP (1 μ L or 10 μ L) and 100 μ M ligand (3 μ L or 30 μ L). Samples were gently vortexed and the cycloaddition initiated by the addition of 1 mM CuSO_4 (1 μ L or 10 μ L). The reactions were incubated at room temperature for 1 h.

For analytical gel electrophoresis, 50 μ L 2 x SDS loading buffer were added and 50 μ L applied on the gel. Fluorescence was recorded in a Fujifilm Las-4000 luminescent image analyser with a Fujinon VRF43LMD3 lens and a 575DF20 filter.

Reactions for enrichment were carried out together with a control lacking the probe to compare the results of the biotin-avidin enriched samples with the background of unspecific protein binding on avidin-agarose beads. After CC proteins were precipitated using an equal volume of pre-chilled acetone. Samples were stored on ice for 20 min and centrifuged at 13,000 rpm for 10 min. The supernatant was discarded and the pellet washed two times with 400 μ L of pre-chilled methanol and resuspended by sonication. Subsequently, the pellet was dissolved in 1 mL PBS with 0.2 % SDS by sonication and incubated under gentle mixing with 50 μ L of avidin-agarose beads (Sigma-Aldrich) for 1 h at room temperature. The beads were washed three times with 1 mL of PBS/0.2 % SDS, twice with 1 mL of 6 M urea and three times with 1 mL PBS. 50 μ L of 2 x SDS loading buffer were added and the proteins released for preparative SDS-PAGE by 6 min incubation at 96 °C. Gel bands were isolated, washed and typically digested as described previously.

***In situ* labelling of bacterial proteomes.** Bacteria were grown in LB medium and a quantity equivalent with 2 mL of $OD_{600} = 2$ was harvested 1 h after reaching stationary phase by centrifugation for analytical and 10 mL for preparative studies, respectively. After washing with PBS, the cells were resuspended in 100 μ L and 500 μ L of PBS for analytical and preparative experiments. Unless indicated otherwise, bacteria were incubated for 2 h with varying concentrations of probe at room temperature. Subsequently, the cells were washed three times with PBS and lysed by sonication with a Bandelin Sonopuls instrument (4 x 20 sec, 60 % maximum intensity) under ice cooling. Membrane and cytosol were separated by centrifugation at 13,000 rpm for 20 min and the membrane fraction was resuspended in 100 μ L and 500 μ L of PBS for analytical and preparative scale, respectively, followed by click chemistry as described above. Reactions for enrichment were carried out as described for the *in vitro* experiments.

Mass spectrometry and bioinformatics. Tryptic peptides were loaded onto a Dionex C18 NanoTrap Column (100 μ m) and subsequently eluted and separated by a Dionex C18 PepMap 100 (3 μ m) column for analysis by tandem MS followed by high resolution MS using a Dionex UltiMate 3000 LC coupled to a Thermo Finnigan LTQ-FT MS. The mass spectrometry data were searched using the SEQUEST algorithm against the corresponding databases via the software “bioworks”. The search was limited to tryptic peptides, two missed cleavage sites, monoisotopic precursor ions and a peptide tolerance of <10 ppm. Filters were set to further refine the search results. The X_{corr} vs. charge state filter was set to X_{corr} values of 1.5, 2.0 and 2.5 for charge states +1, +2 and +3, respectively. The number of different peptides has to be ≥ 2 and the peptide probability filter was set to < 0.001. These filter values are similar to others previously reported for SEQUEST analysis. Minimum p-values and maximum X_{corr} values of each run as well as the total number of obtained peptides are reported in Table S2.

Recombinant expression. The major hits of MS analysis were recombinantly expressed in *E. coli* as an internal control of the MS results by using the Invitrogen™ Gateway® Technology. Target genes were amplified from the corresponding genomes by PCR with an AccuPrime™ Pfx DNA Polymerase kit with 65 ng of genomic DNA, prepared by standard protocols. *attB1* forward primer and *attB2* reverse primer were designed to yield *attB*-PCR Products needed for Gateway® Technology. PCR products were identified on agarose gels and gel bands were isolated and extracted with an E.Z.N.A.™ MicroElute™ Gel Extraction Kit. Concentrations of DNA were measured by a Tecan Infinite® M200 PRO plate reader. 100 fmol of purified *attB*-PCR product and 50 fmol of *attP*-containing donor vector pDONR™ 201 in TE buffer were used for *in vitro* BP recombination reaction with BP Clonase™ II enzyme mix to yield the appropriate *attL*-containing

entry clone. After transformation in chemically competent One Shot[®] TOP10 *E. coli* (Invitrogen), cells were plated on LB agar plates containing 25 µg mL⁻¹ kanamycin. Clones of transformed cells were selected and grown in kanamycin LB medium. Cells were harvested and plasmids were isolated using an E.Z.N.A.[™] Plasmid Mini Kit. The corresponding *attB*-containing expression clone was generated by *in vitro* LR recombination reaction of approx. 50 fmol of the *attL*-containing entry clone and 50 fmol of the *attR*-containing destination vector pDest using LR Clonase[™] II enzyme mix in TE buffer. The expression clone was transformed in chemically competent BL21 *E. coli* cells (Novagen) and selected on LB agar plates containing 100 µg mL⁻¹ ampicillin. Validity of the clones was confirmed by plasmid sequence analysis. Recombinant clones were grown in ampicillin LB medium and target gene expression was induced with anhydrotetracyclin. The bacterial cell pellets were washed with PBS, resuspended in binding buffer (100 mM Tris-HCl, 150 mM NaCl, 1 mM EDTA), lysed by French press and sonication. The protein was then purified with StrepTrap[™] HP columns.

Primer for recombinant expression.

KatG, *E. coli* CFT073

Forward 5'-GGGGACAAGTTTGTACAAAAAGCAGGCTTTATGAGCACGTCAGACGAT
Reverse 5'-GGGGACCACTTTGTACAAGAAAGCTGGGTGTTACAGCAGGTCGAAACG

Thil, *E. coli* CFT073

Forward 5'-GGGGACAAGTTTGTACAAAAAGCAGGCTTTATGAAGTTTATCATTAAATTGTTCCCG
Reverse 5'-GGGGACCACTTTGTACAAGAAAGCTGGGTGTTACGGGCGATACACCTTCA

AhpC, *E. coli* CFT073

Forward 5'-GGGGACAAGTTTGTACAAAAAGCAGGCTTTATGTCCTTGATTAACACCAA
Reverse 5'-GGGGACCACTTTGTACAAGAAAGCTGGGTGTTAGATTTTACCAACCAGGT

C2450, *E. coli* CFT073

Forward 5'-GGGGACAAGTTTGTACAAAAAGCAGGCTTTATGGCTGTTCCATCATCAAAA
Reverse 5'-GGGGACCACTTTGTACAAGAAAGCTGGGTGCTATTCTGCAAGACATTTCTG

Identification of the binding site of probe 13a and C2450. To a solution of recombinantly expressed and purified protein (20 µL, 50 µM in PBS) the corresponding probe (1 µL, 10 mM in DMSO) was added and the mixture incubated 1 h at room temperature. The buffer was exchanged several times with 25 mM aqueous NH₄HCO₃ to wash away unbound probe leading to a

total volume of 100 μL . CaCl_2 (1 μL , 100 mM in H_2O) and trypsin or chymotrypsin solution (1 μL , 0.5 $\mu\text{g}/\mu\text{L}$, sequencing grade) were added and the solution was incubated at 37 $^\circ\text{C}$ (trypsin) or 25 $^\circ\text{C}$ (chymotrypsin) overnight. The sample was measured by mass spectrometry as specified in chapter “Mass spectrometry and bioinformatics” and accordingly evaluated with a SEQUEST search for tryptic or chymotryptic peptides. The modified peptides are given in **Table S2**.

Determination of MIC Values. Bacteria were grown in 5 mL LB media at 37 $^\circ\text{C}$ overnight. 2 μL of this culture were added to each well of a 96 well plate containing wells with 97 μL fresh LB media and 1 μL probe in DMSO (50 mM, final probe concentration 500 μM). Control wells containing no probe or no bacteria were included. The plate was incubated at 37 $^\circ\text{C}$ overnight and the resulting optical density was measured by a Tecan Infinite[®] M200 PRO plate reader.

Assay for esterase activity. For detection of esterase activity the enzymatic cleavage of *p*-nitrophenyl acetate to *p*-nitrophenol and acetate was monitored by measuring the absorption at 405 nm with a Tecan Infinite[®] M200 PRO plate reader. Each well contained of 245 μL buffer (100 mM Tris-HCl, 150 mM NaCl, pH 7.5), 2.5 μL enzyme (up to 100 μM in 100 mM Tris-HCl, 150 mM NaCl, pH 7.5) and 2.5 μL *p*-nitrophenyl acetate (25 mM in acetonitrile). The absorption at 405 nm was recorded for 10 min by a Tecan Infinite[®] M200 PRO plate reader. Control wells without *p*-nitrophenyl acetate, without enzyme and with 0.1 M NaOH instead of buffer have been included.

Assay for peptidase activity. For detection of peptidase activity the enzymatic cleavage of LY-AMC, GGL-AMC and LLVY-AMC (di- or tripeptide aminomethylcoumarin) was monitored by measuring the fluorescence emission at 440 nm after excitation at 365 nm. To 40 μL of enzyme (0.1 $\mu\text{g}/\mu\text{L}$ in 100 mM Tris-HCl, 150 mM NaCl, pH 7.5) were added 10 μL of the AMC substrate (100 mM stock solution in DMSO, diluted to 1 mM in 100 mM Tris-HCl, 150 mM NaCl, pH 7.5) and the fluorescence emission at 440 nm was measured for 30 min.

Assay for protease activity. Protease activity was determined with the Sigma-Aldrich[®] Protease Fluorescent Detection Kit (product number PF0100-1KT). Briefly casein labelled with fluorescein isothiocyanate (FITC-casein) is incubated with the putative protease (up to 5 μM final concentration). Protease activity leads to the cleavage of the FITC-casein into smaller fragments. Acidification with trichloroacetic acid leads to precipitation of undigested FITC-casein while cleaved smaller fragments remain in solution. After centrifugation, the supernatant is neutralized and the fluorescence of the FITC-labelled fragments is measured by a Tecan Infinite[®] M200 PRO plate reader. Addition of trypsin instead of the putative protease is used as positive control.

Appendix

Table S1: Proteins identified by mass spectrometry in *E. coli* K12, CFT073 and UTI89.

Protein	Prot. ID	Score	Coverage [%]	Unique peptides	PSMs
	P13029	108.43	32.02	19	33
Catalase-peroxidase (KatG)	Q8FBA9	282.53	48.21	28	87
	Q1R3X0	251.28	50.96	30	84
	P77718	15.35	9.75	4	5
tRNA sulfurtransferase (ThiI)	Q8FKB7	5.55	4.98	2	2
	Q1RFB7	8.64	5.60	2	3
	P0AE08	9.52	21.39	3	3
Alkyl hydroperoxide reductase subunit C (AhpC)	P0AE09	23.27	24.06	4	8
	Q1REV6	21.48	31.55	5	8
Only in pathogenic <i>E. coli</i>					
C2450 (identical to C2206)	Q8FGD0	267.26	55.29	10	97
C2206 (identical to C2450)	Q1RAE0	122.74	52.35	9	43

This list of proteins shows Protein ID, Score, Sequence coverage in percent, number of unique peptides and number of PSMs in the *E. coli* strains K12, CFT73 and UTI89.

Table S2: Labelled cysteines in *E. coli* AhpC and C2450.

Cysteine	Sequence of peptide	X _{corr}	Probability	Charge	MH ⁺ [Da]	ΔM [ppm]
AhpC: C166	AAQYVASHPGEVCA*PAK	2.27	27.46	3	1846.917	0.95
AhpC: C166	AAQYVASHPGEVCA*PAK	2.30	19.68	3	1846.899	9.06
C2450: C167	C*LAEWSHPQFEK	3.08	25.30	3	1693.804	0.18
C2450: C167	C*LAEWSHPQFEK	2.87	33.35	2	1693.809	3.10

* = **13a** labelled cysteine

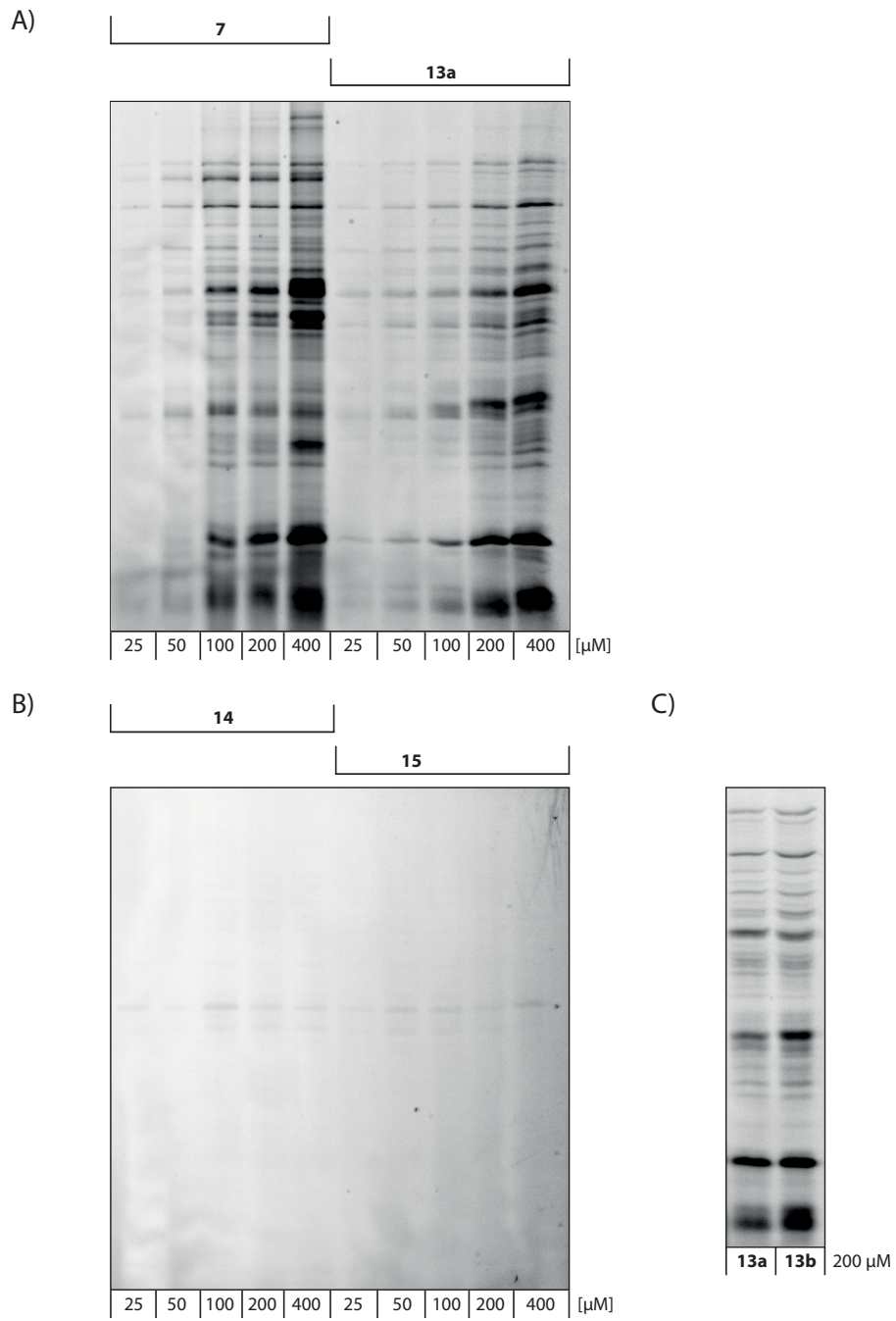
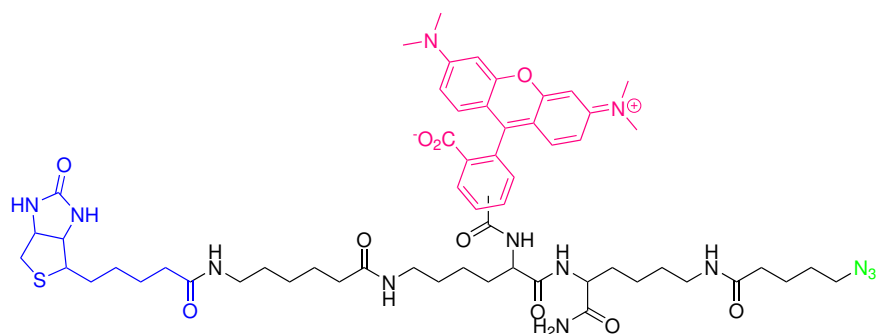
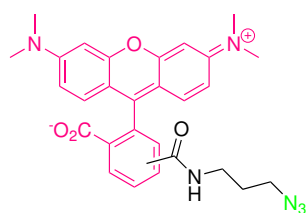


Figure S1: *In situ* labelling of *E. coli* K12 to determine the optimal labelling concentration of the corresponding probe.



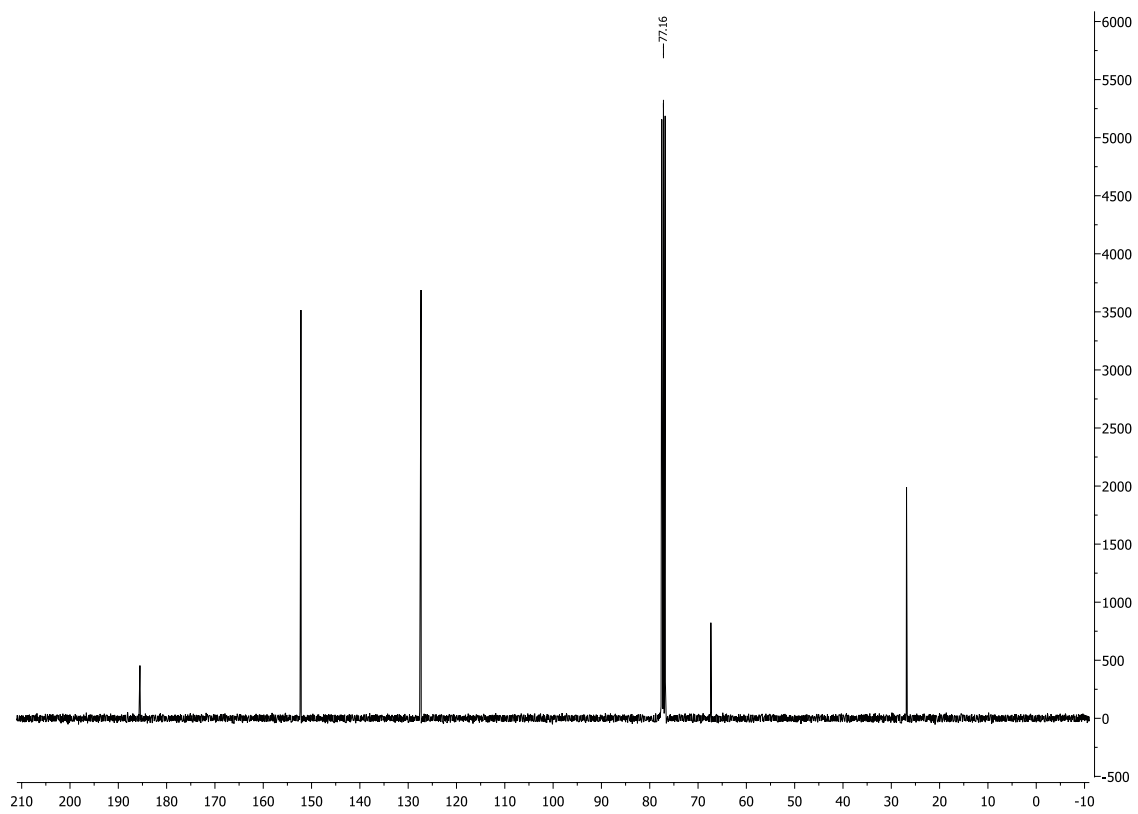
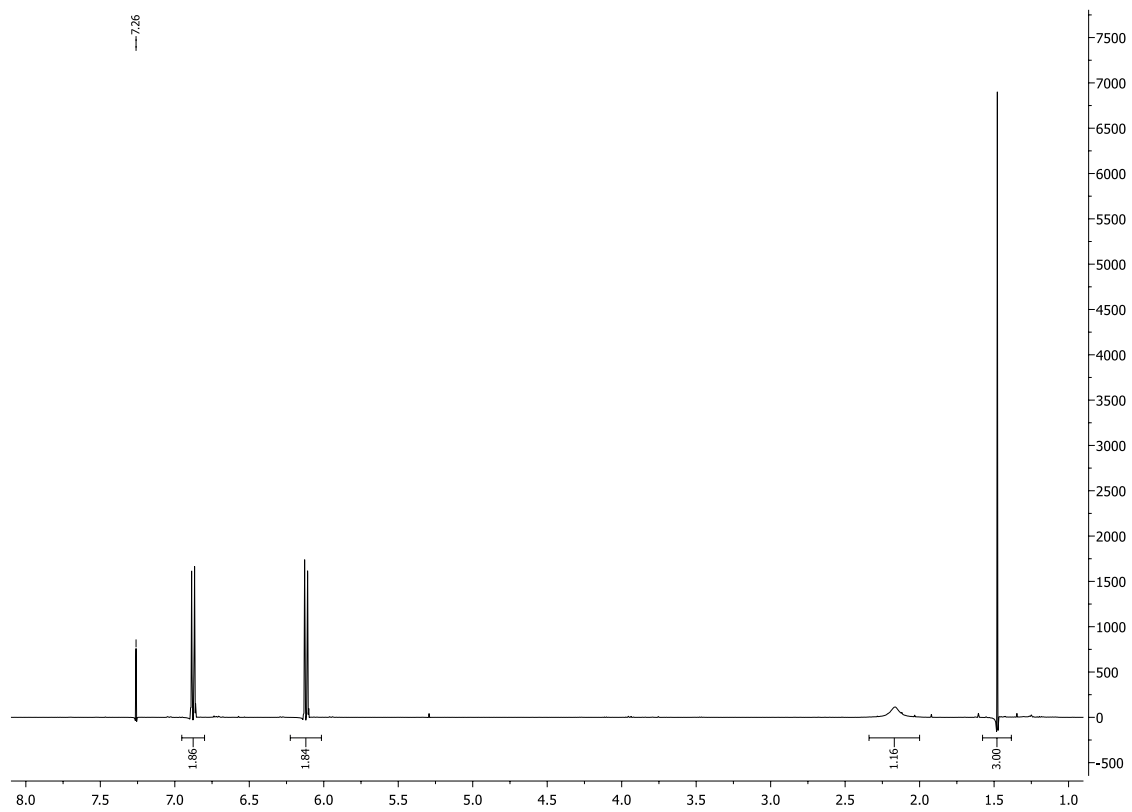
biotin-rhodamine-azide



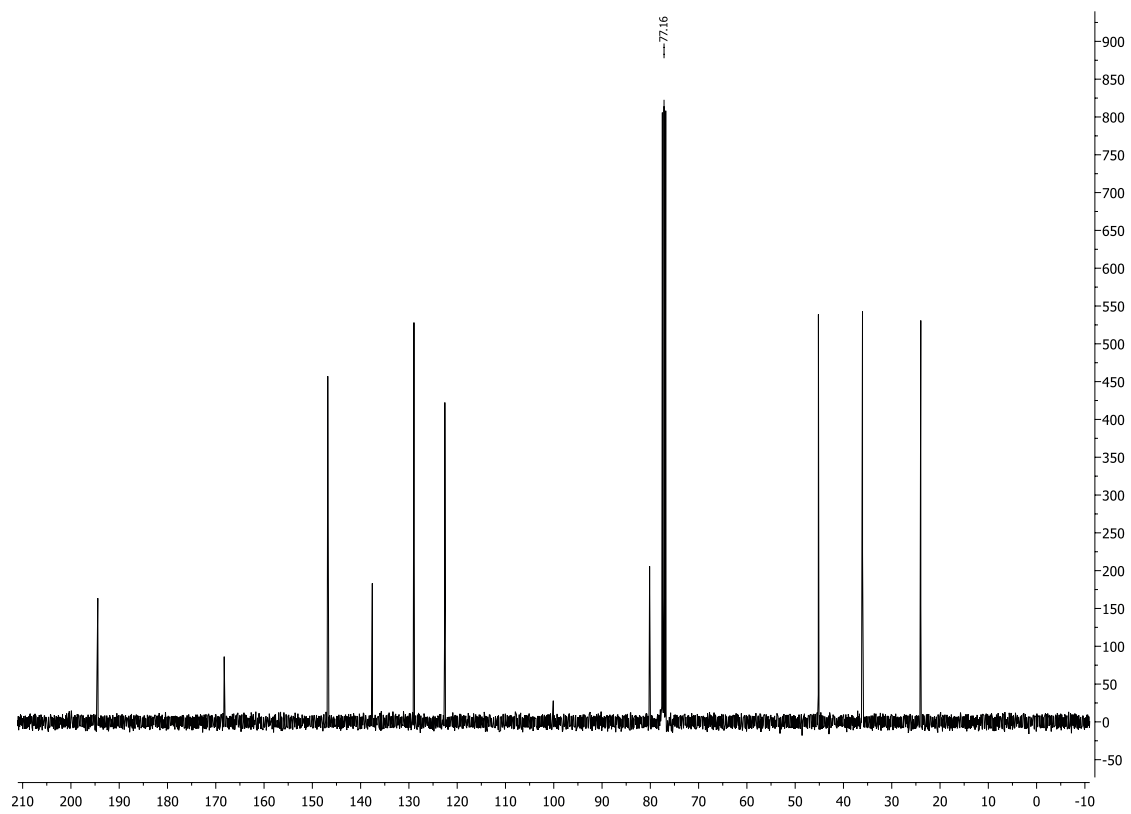
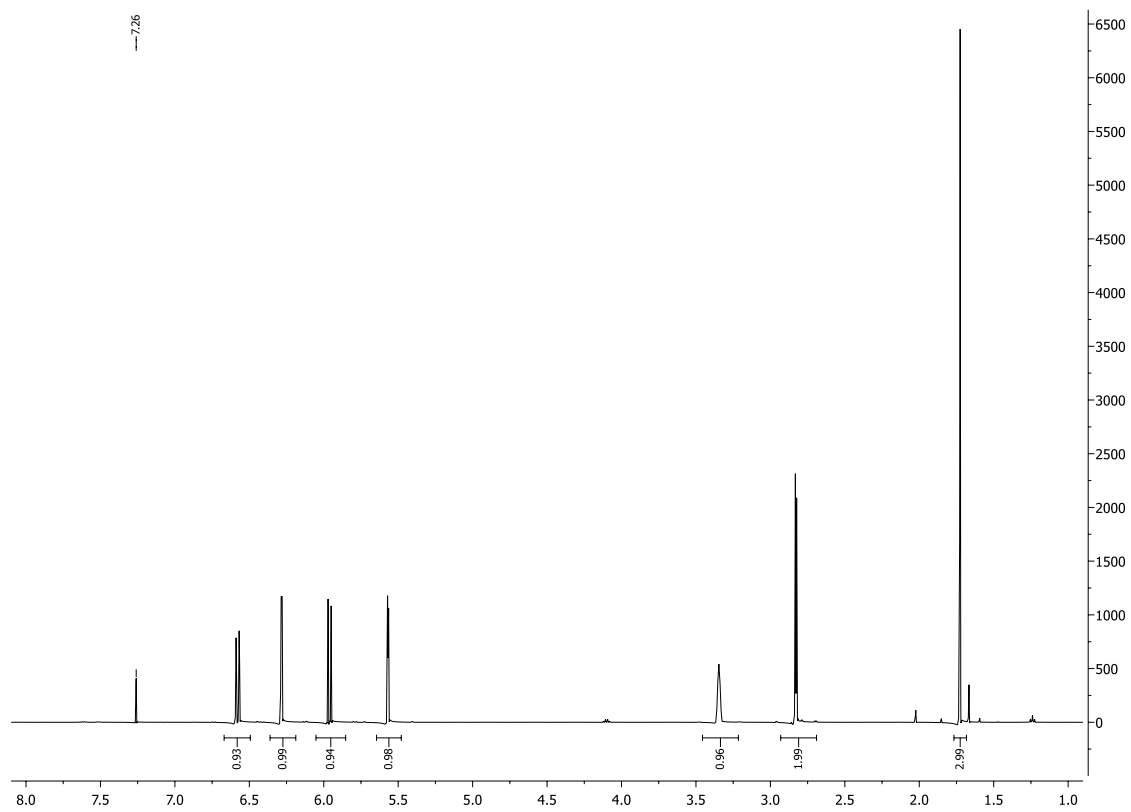
rhodamine-azide

Figure S2: Structure of rhodamine-azide and biotin-rhodamine-azide (trifunctional linker).¹⁵⁷

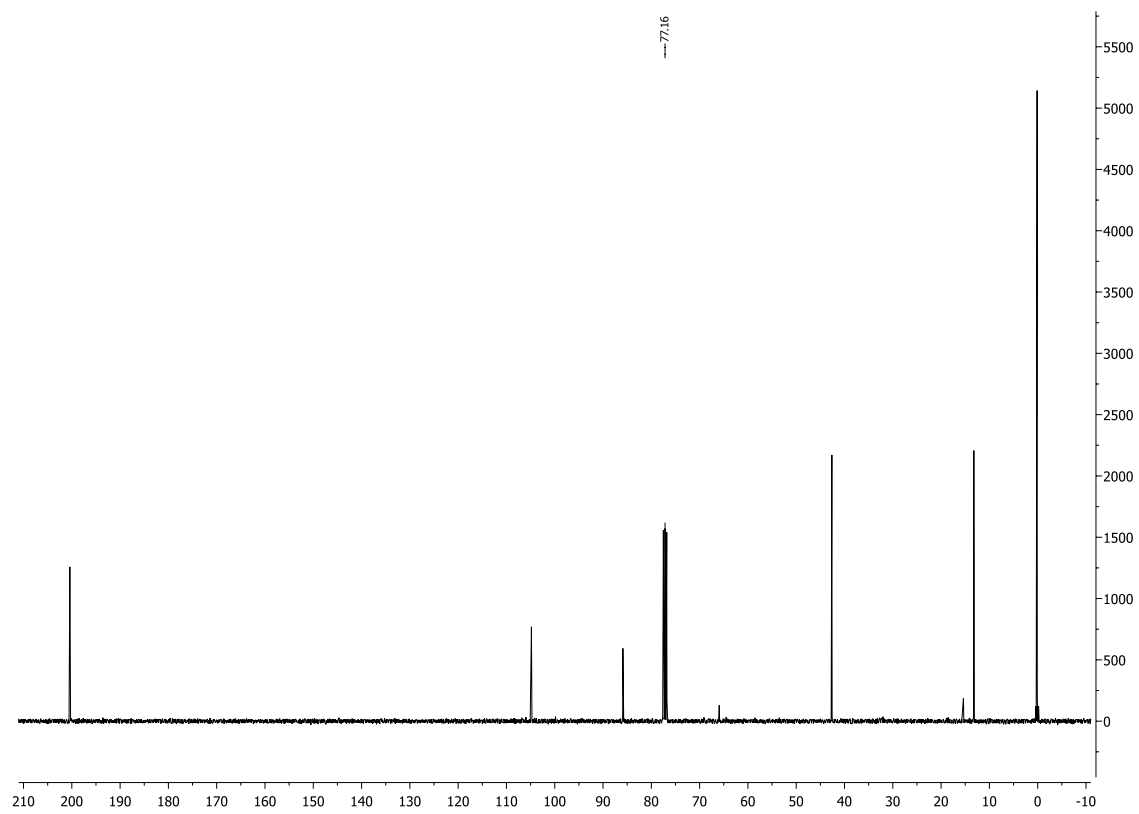
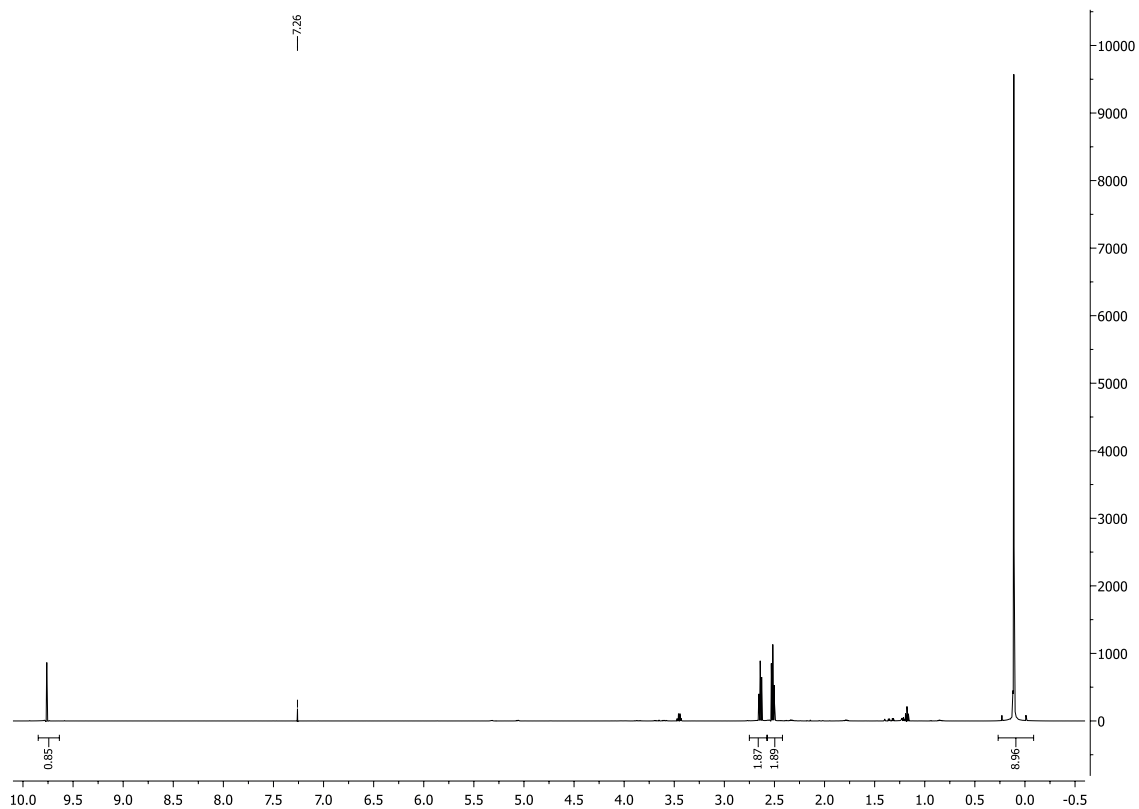
$^1\text{H-NMR}$ (500 MHz, CDCl_3) and $^{13}\text{C-NMR}$ (90 MHz, CDCl_3) of compound 2



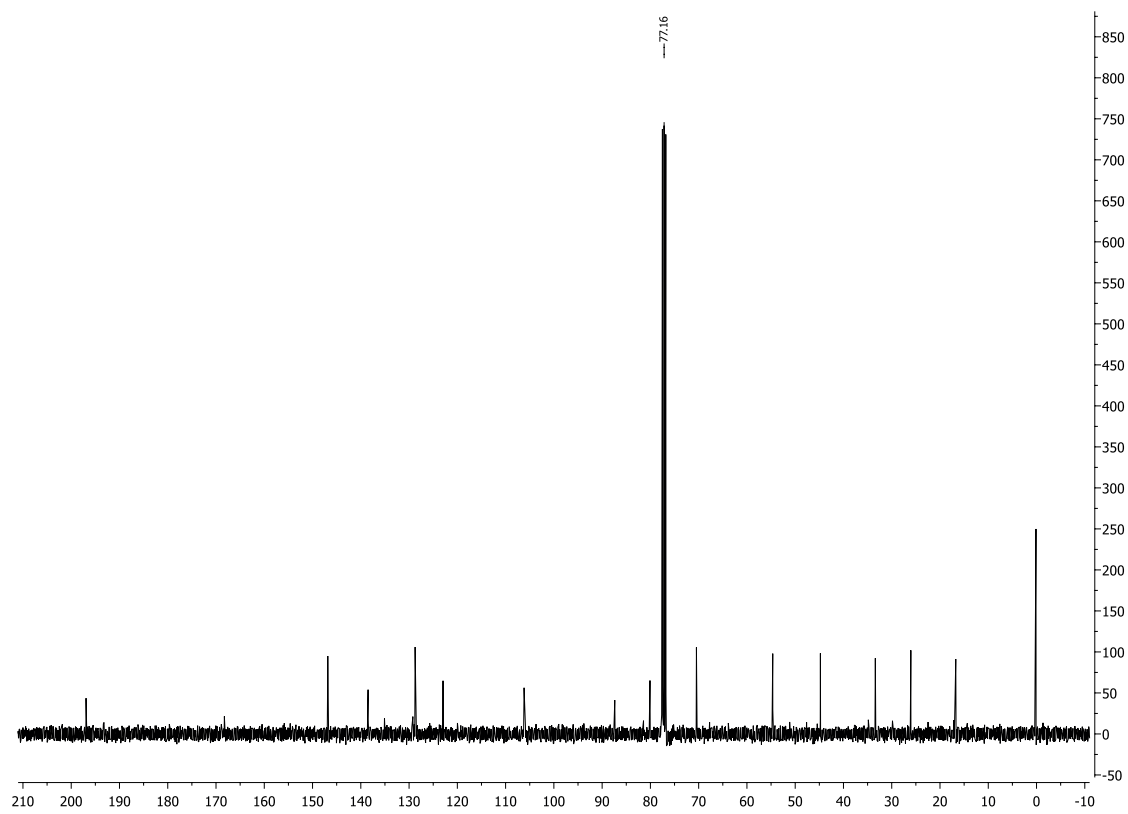
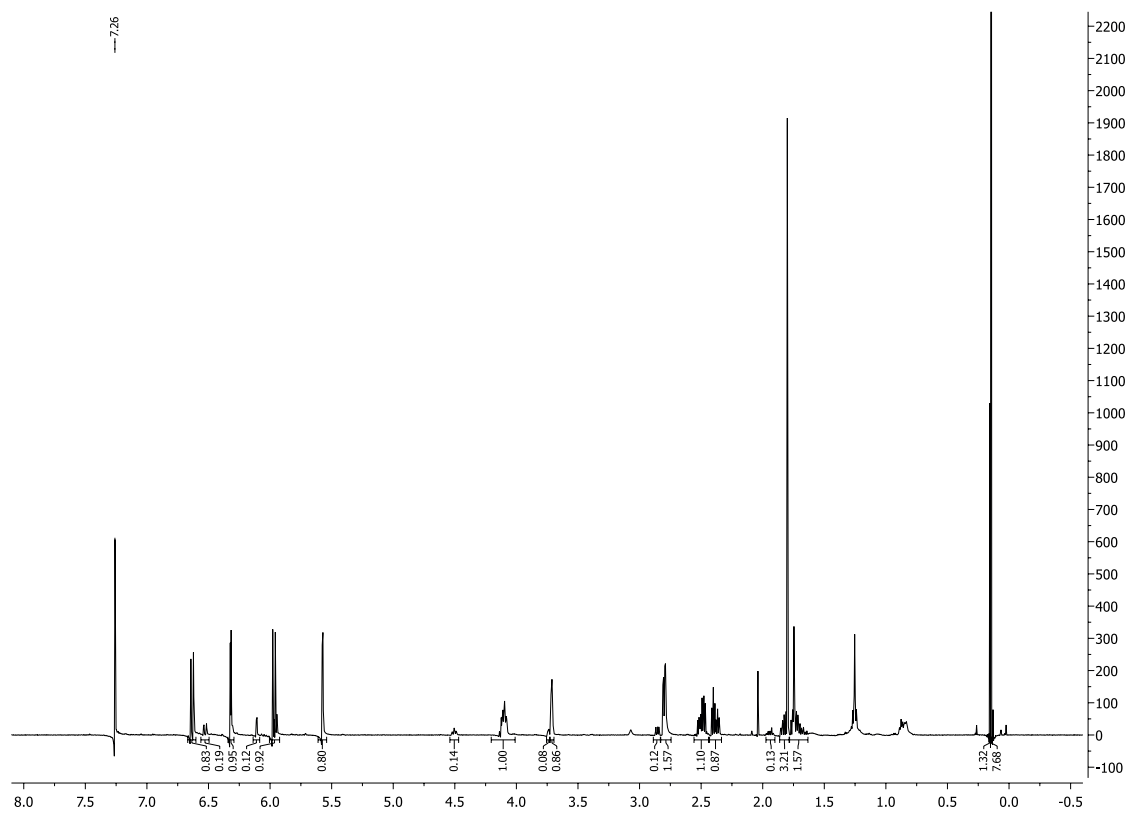
$^1\text{H-NMR}$ (500 MHz, CDCl_3) and $^{13}\text{C-NMR}$ (90 MHz, CDCl_3) of compound 3



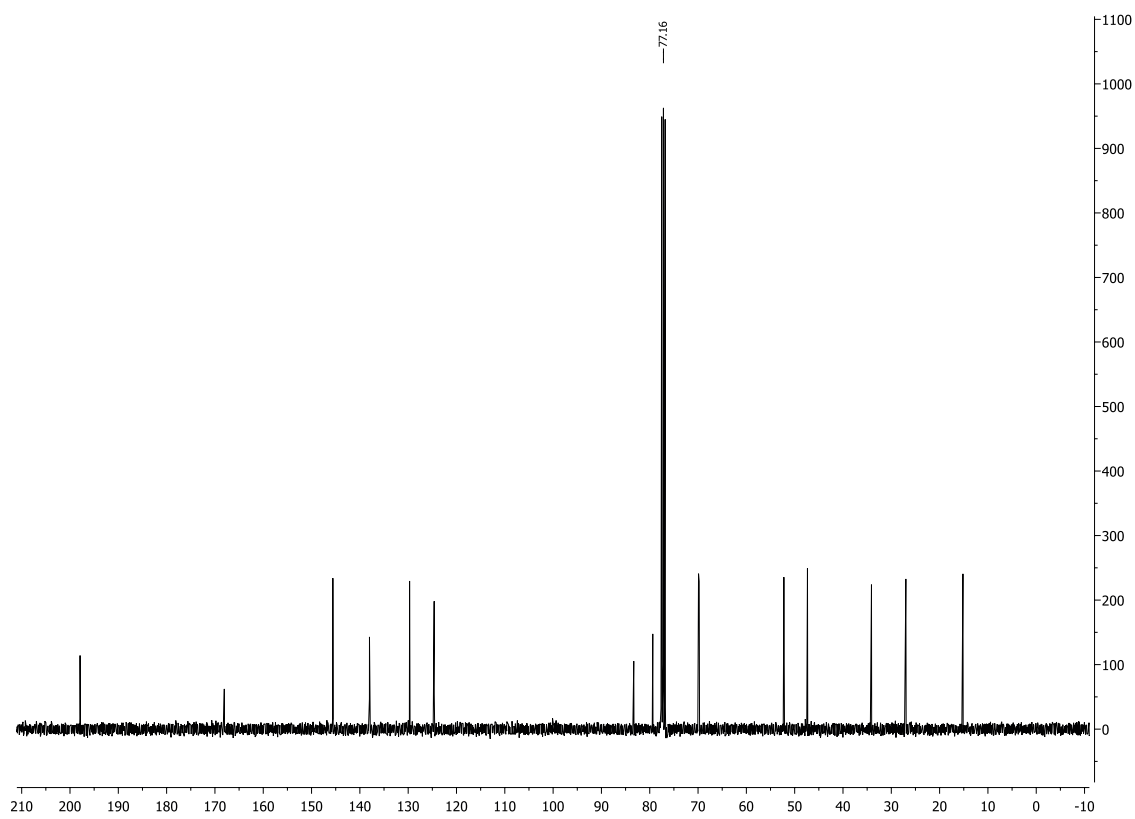
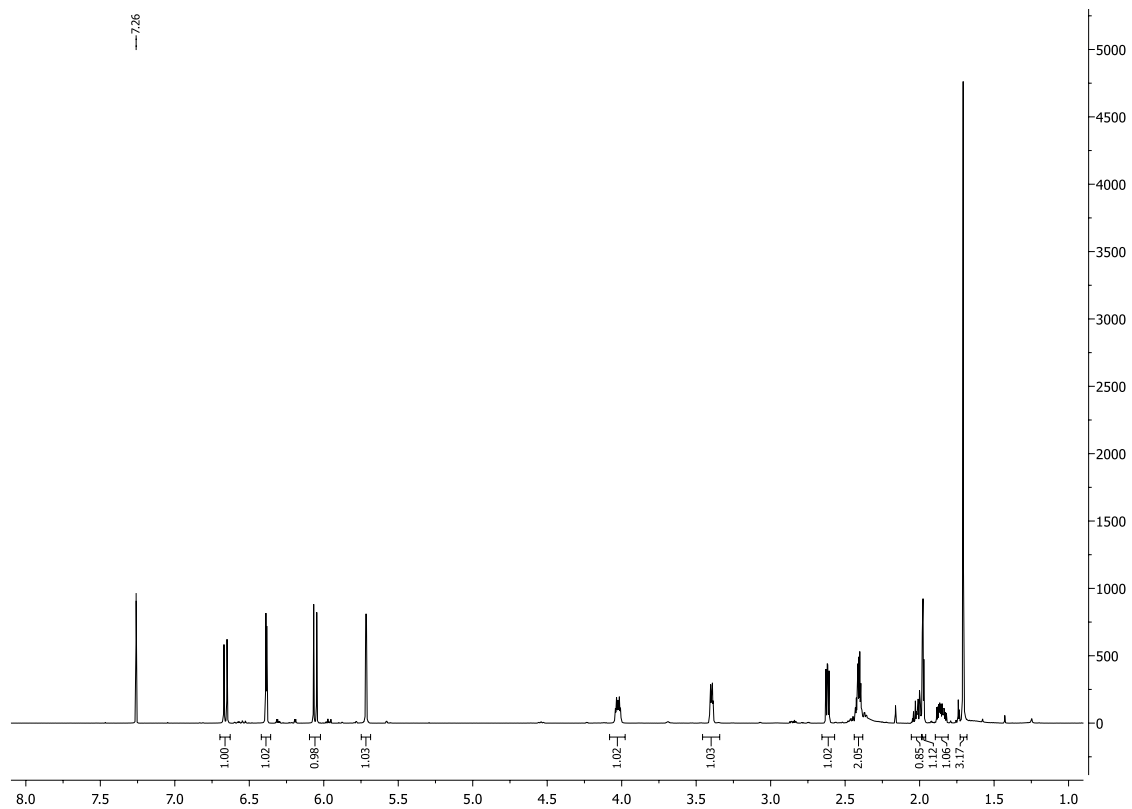
$^1\text{H-NMR}$ (500 MHz, CDCl_3) and $^{13}\text{C-NMR}$ (90 MHz, CDCl_3) of compound 5



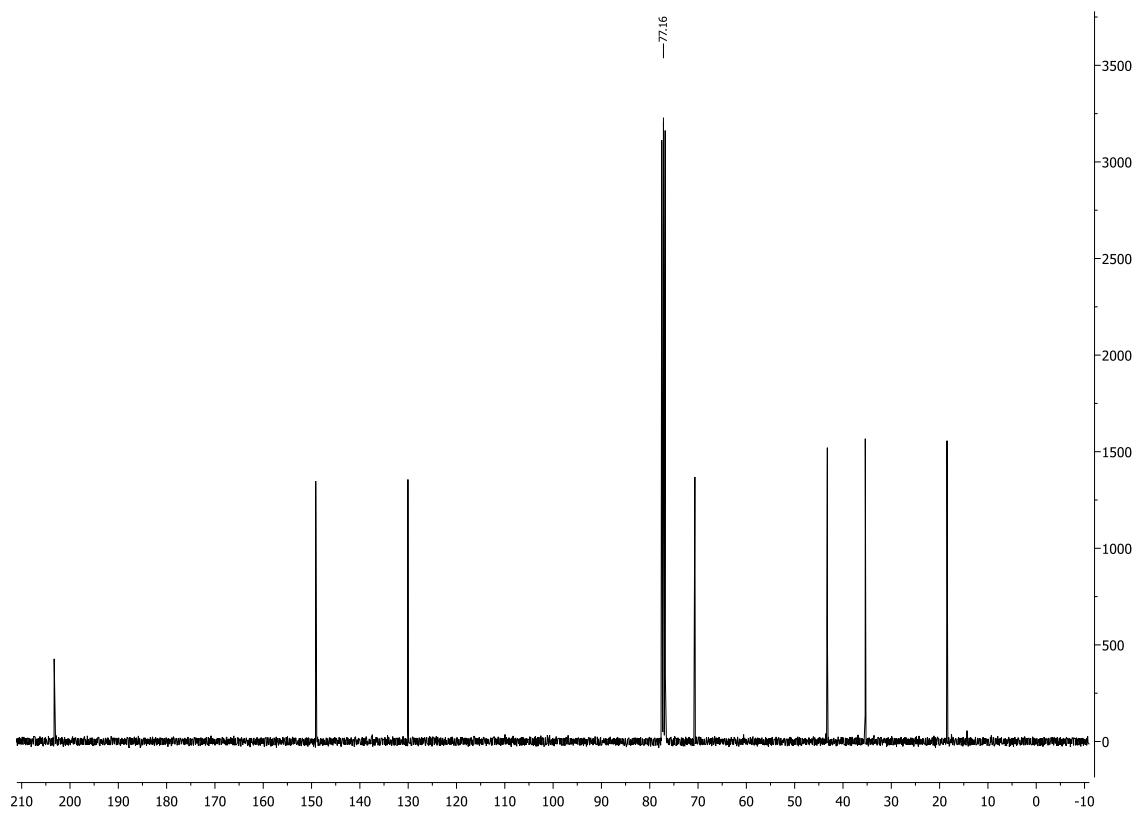
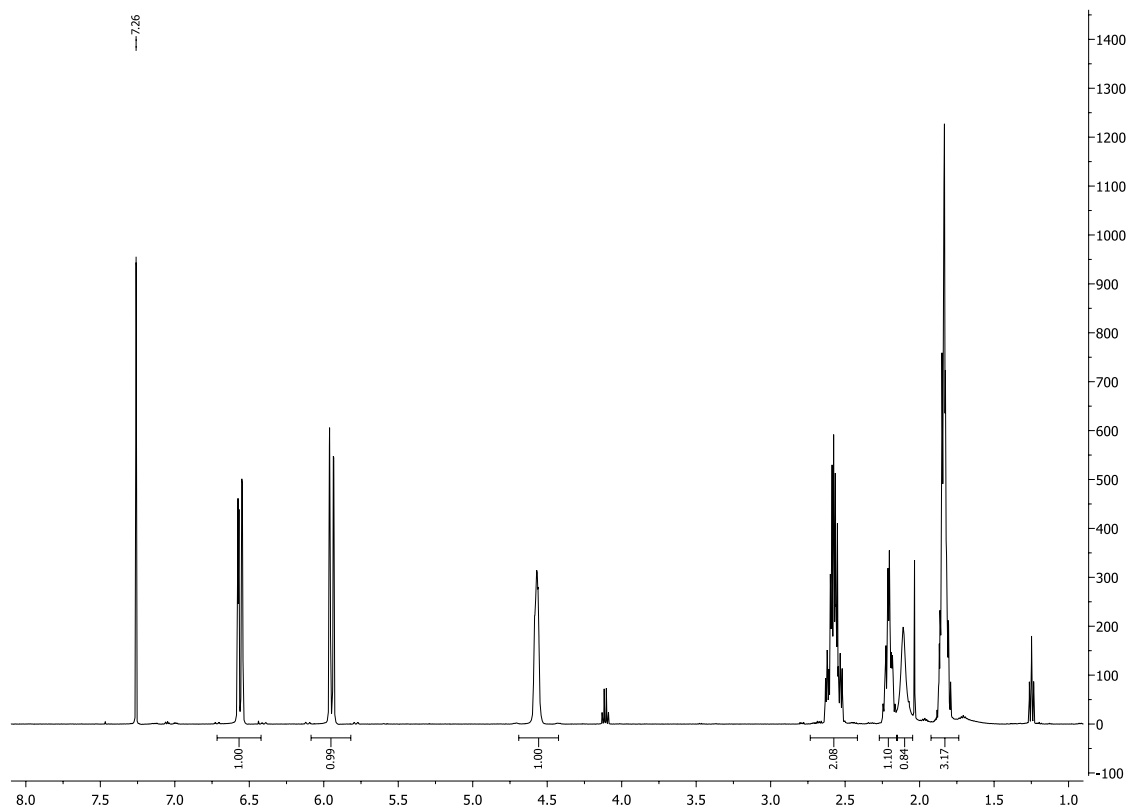
$^1\text{H-NMR}$ (500 MHz, CDCl_3) and $^{13}\text{C-NMR}$ (90 MHz, CDCl_3) of compound 6



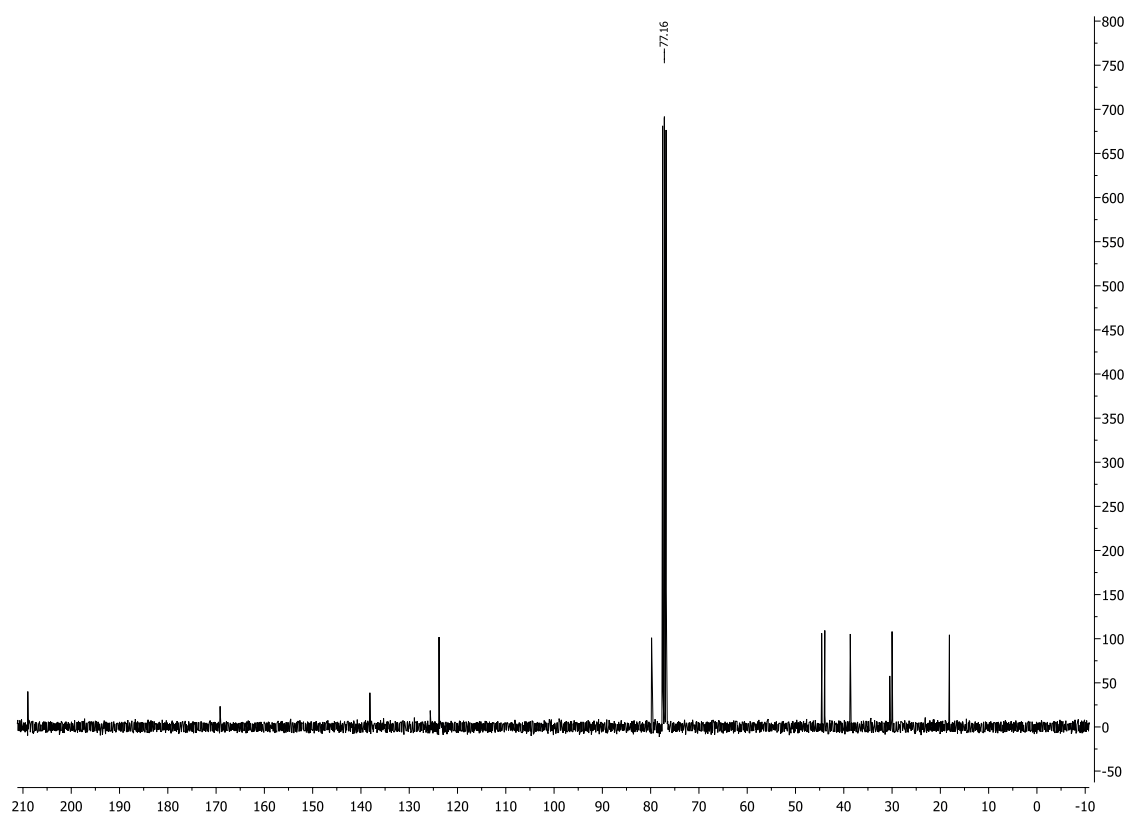
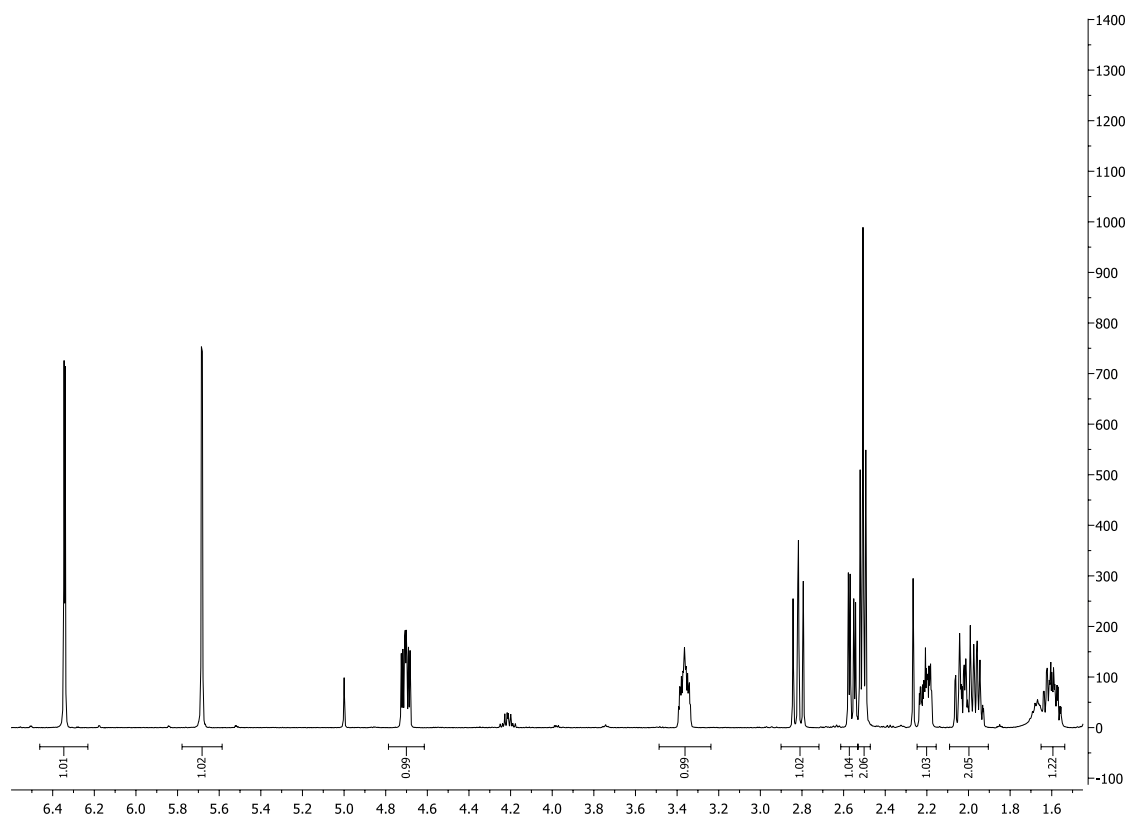
$^1\text{H-NMR}$ (500 MHz, CDCl_3) and $^{13}\text{C-NMR}$ (90 MHz, CDCl_3) of compound 7



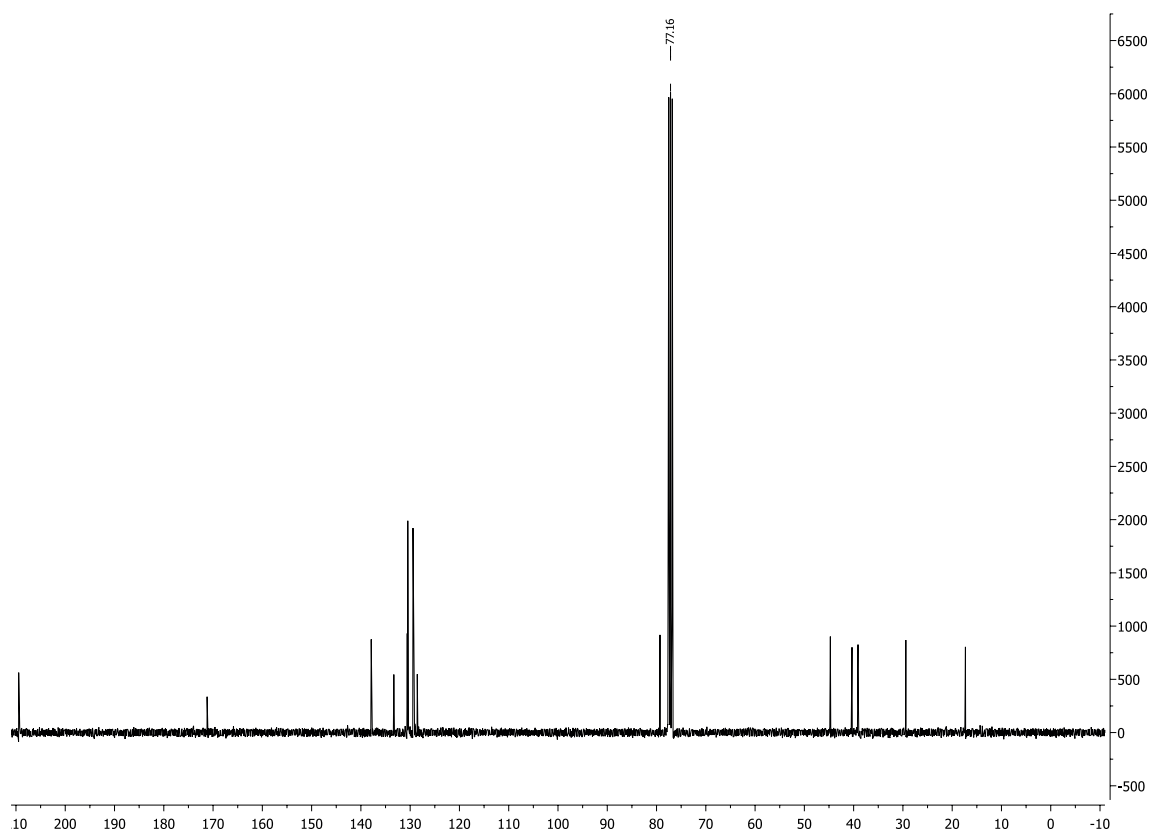
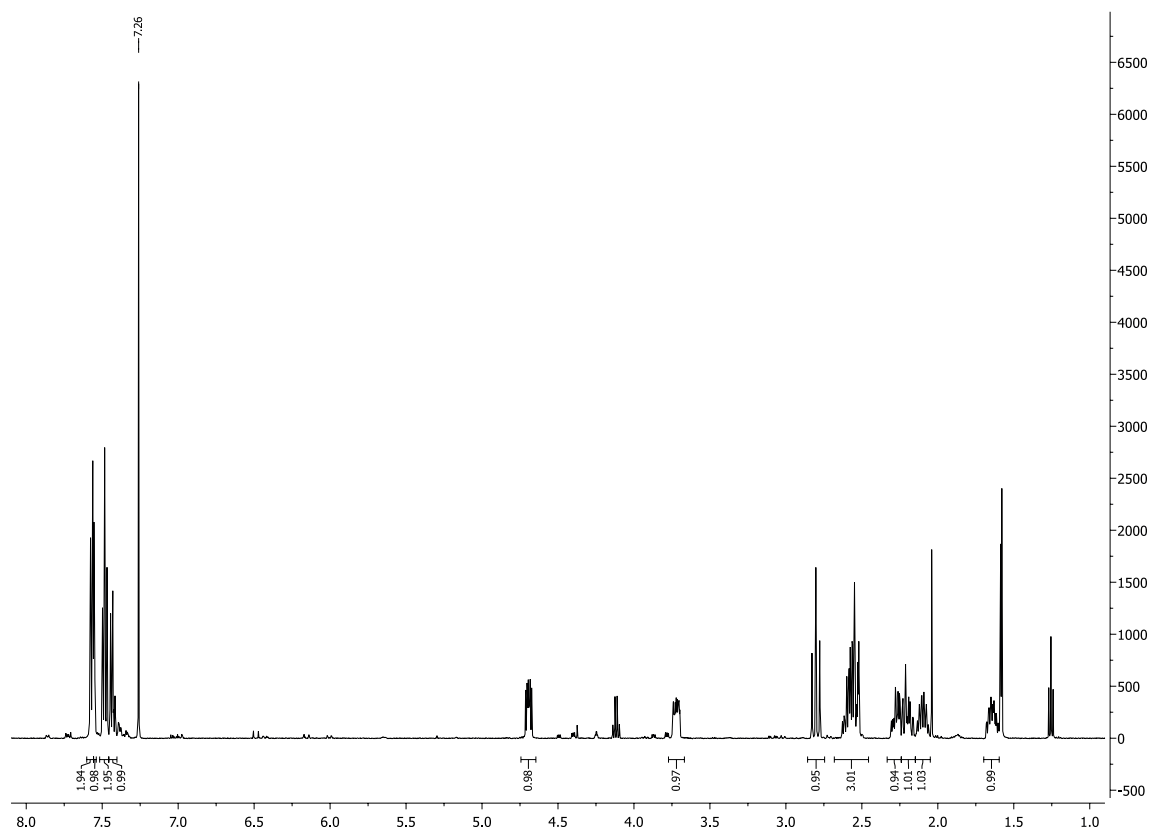
$^1\text{H-NMR}$ (500 MHz, CDCl_3) and $^{13}\text{C-NMR}$ (90 MHz, CDCl_3) of compound 9



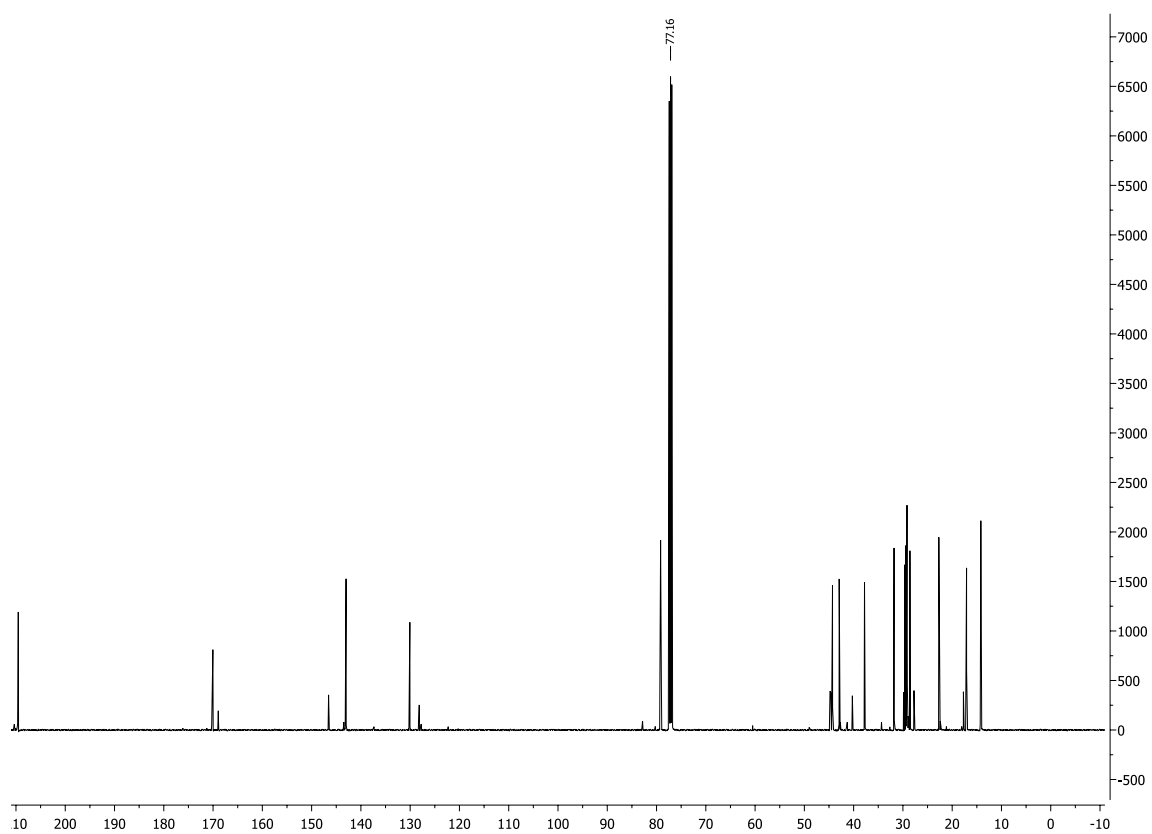
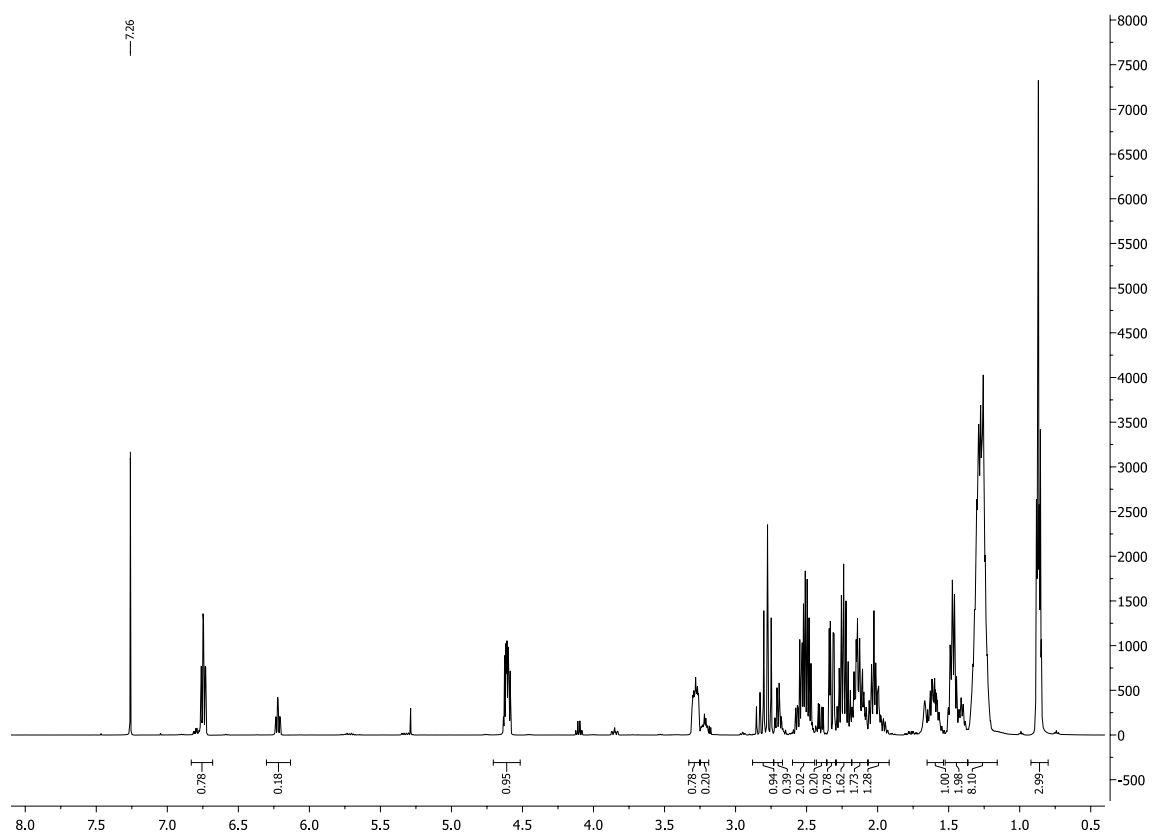
$^1\text{H-NMR}$ (500 MHz, CDCl_3) and $^{13}\text{C-NMR}$ (90 MHz, CDCl_3) of compound 10



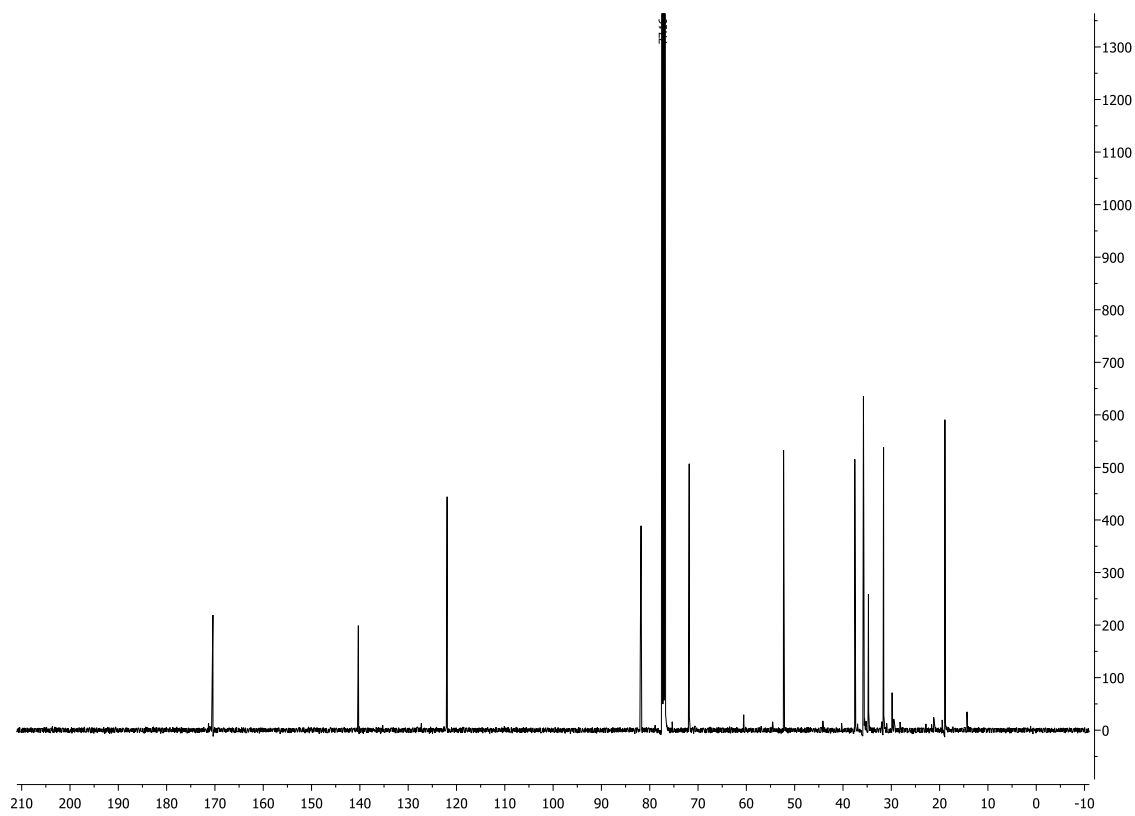
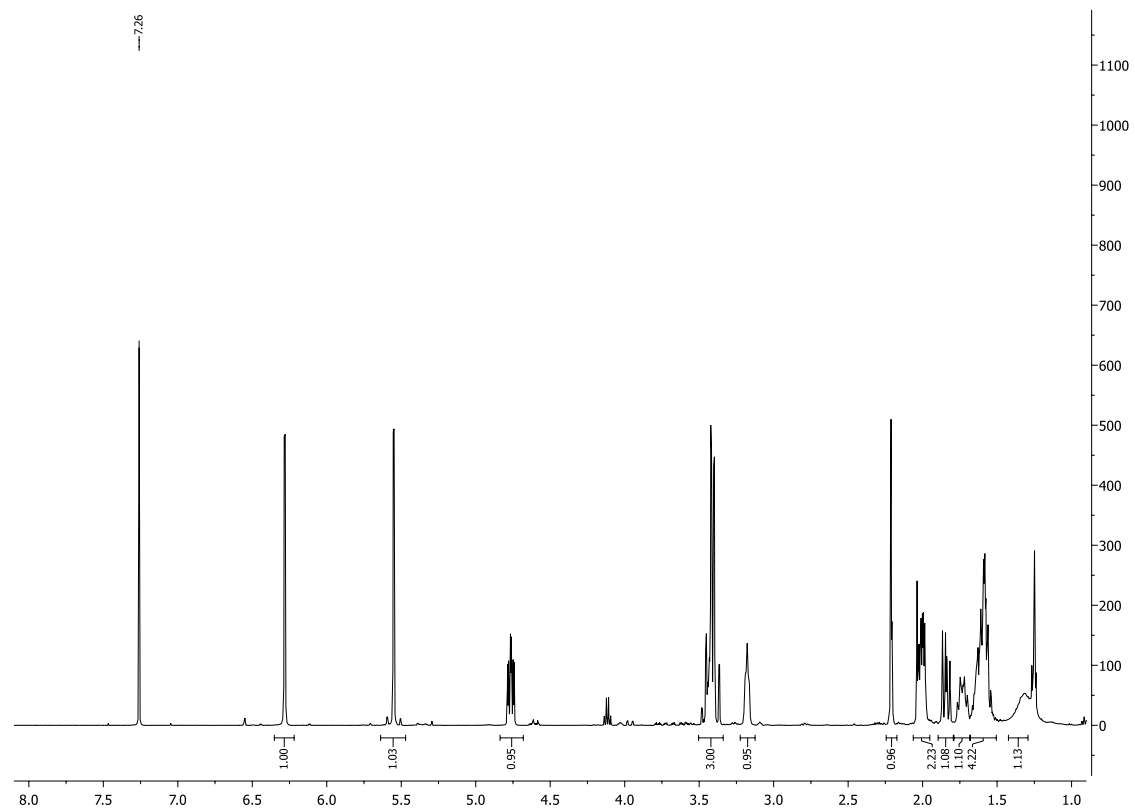
$^1\text{H-NMR}$ (500 MHz, CDCl_3) and $^{13}\text{C-NMR}$ (90 MHz, CDCl_3) of compound 11



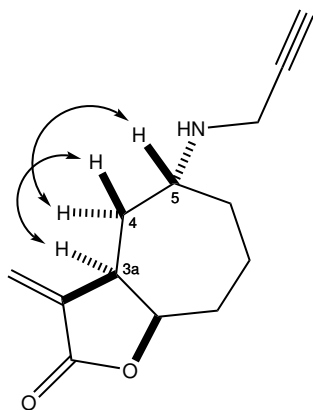
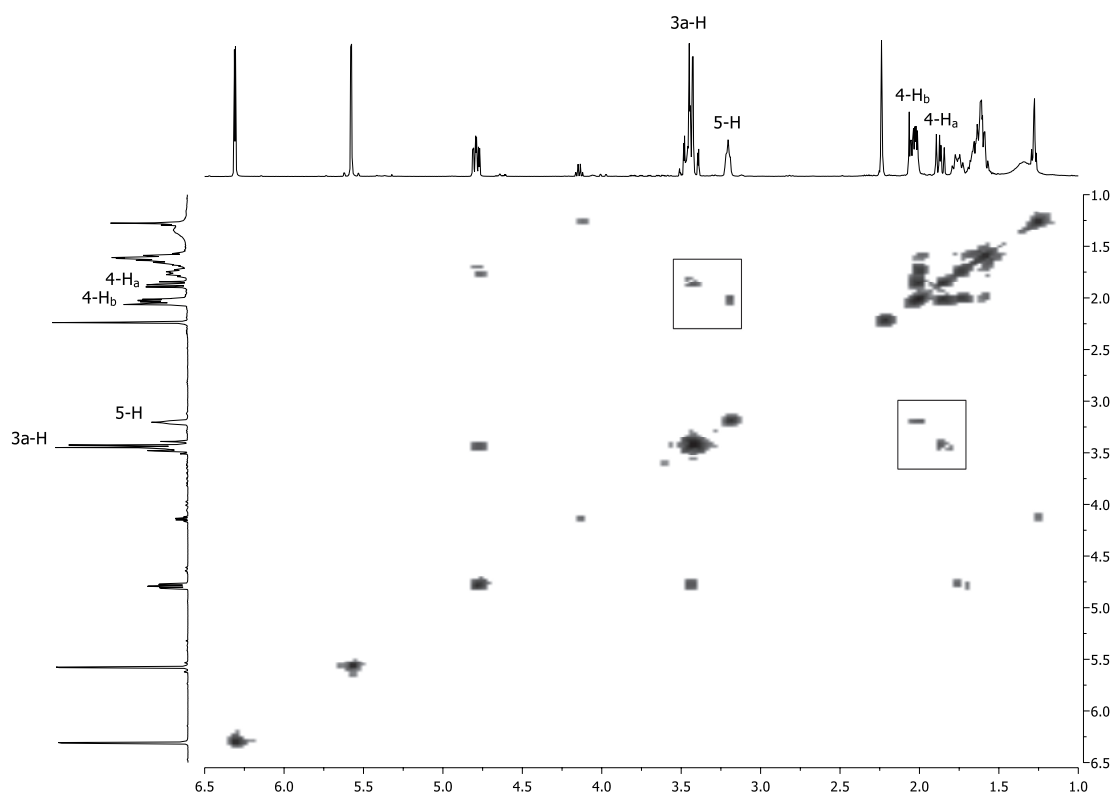
$^1\text{H-NMR}$ (500 MHz, CDCl_3) and $^{13}\text{C-NMR}$ (90 MHz, CDCl_3) of compound 12



$^1\text{H-NMR}$ (500 MHz, CDCl_3) and $^{13}\text{C-NMR}$ (90 MHz, CDCl_3) of compound 13a

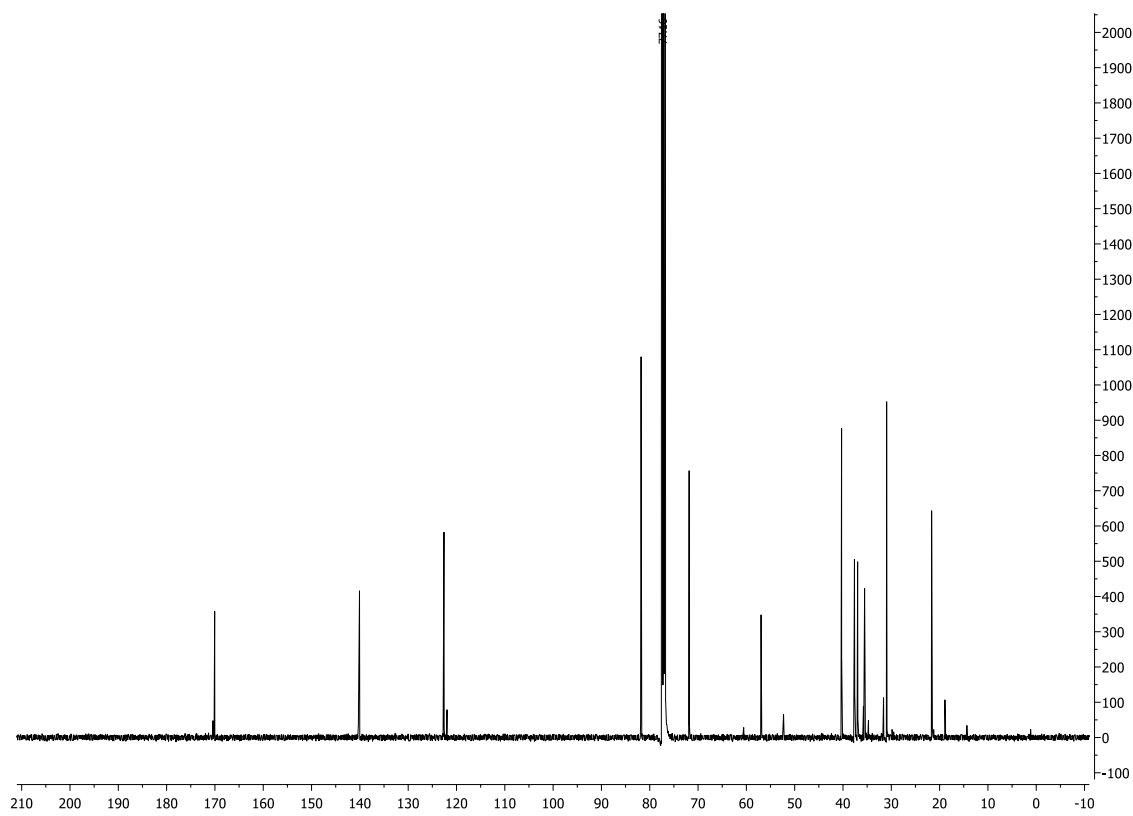
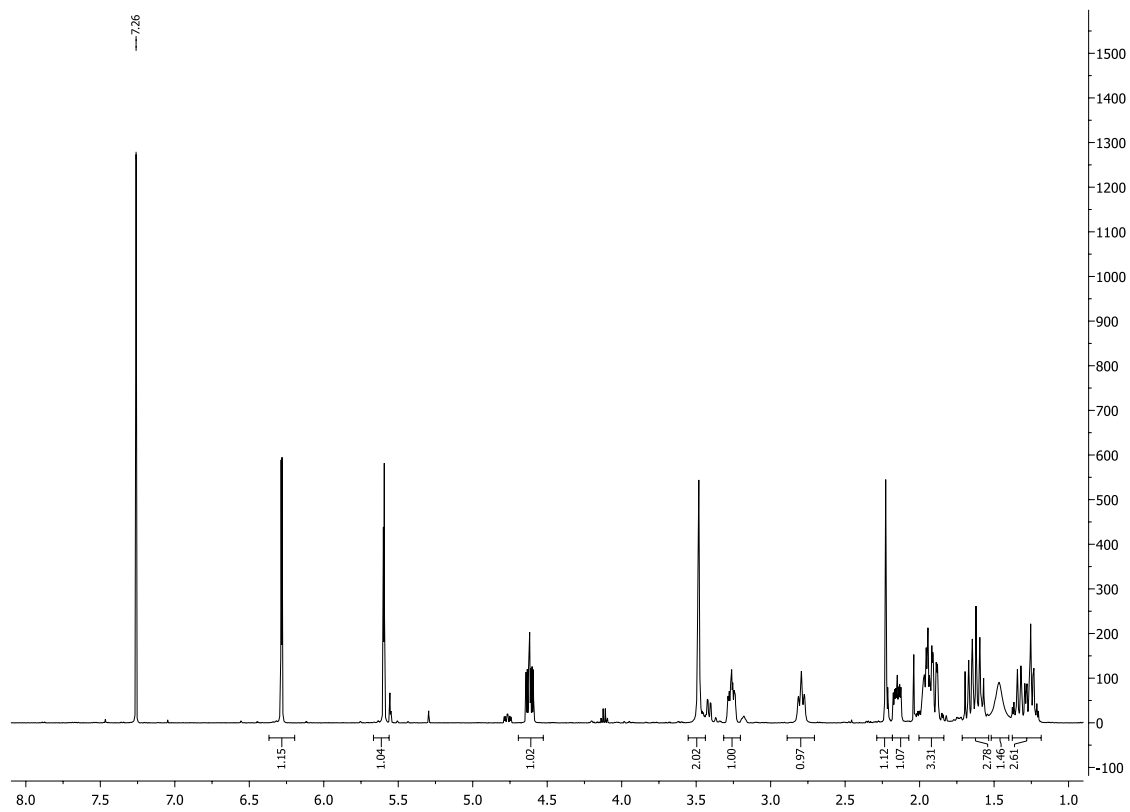


$^1\text{H}, ^1\text{H}$ -COSY-NMR (500 MHz, CDCl_3) of 13a

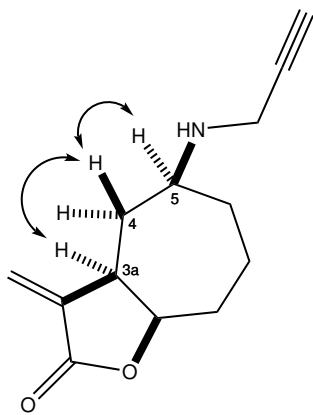
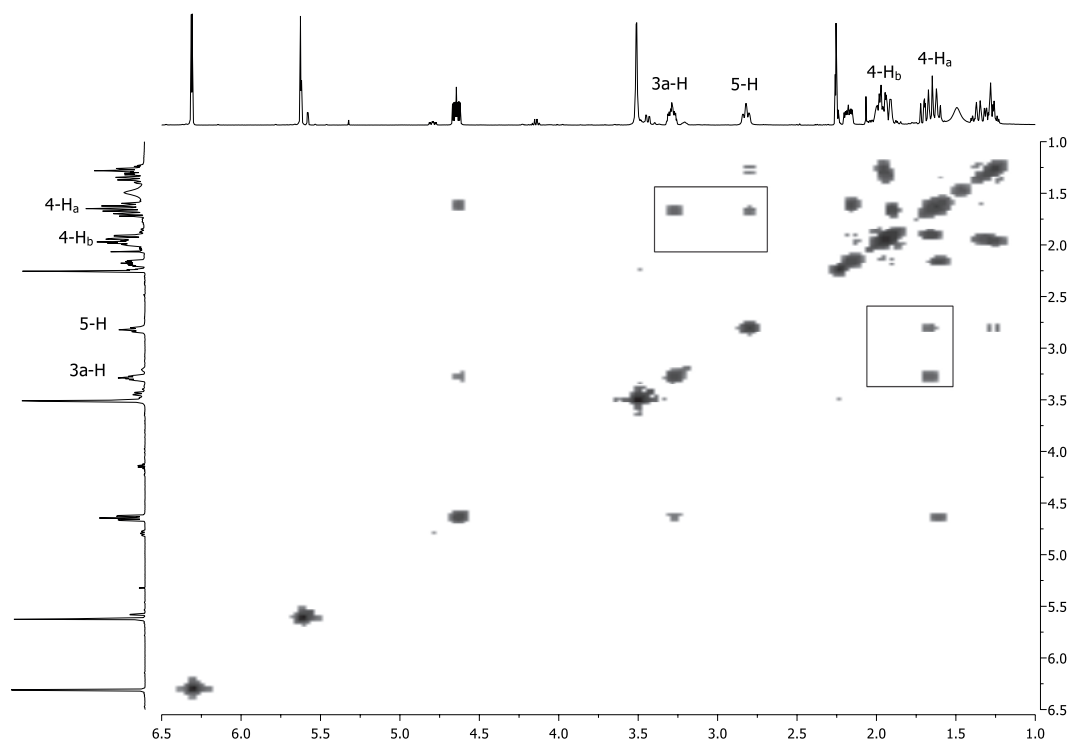


3a-H couples to 4-H_a, 5-H to 4-H_b

$^1\text{H-NMR}$ (500 MHz, CDCl_3) and $^{13}\text{C-NMR}$ (90 MHz, CDCl_3) of compound 13b

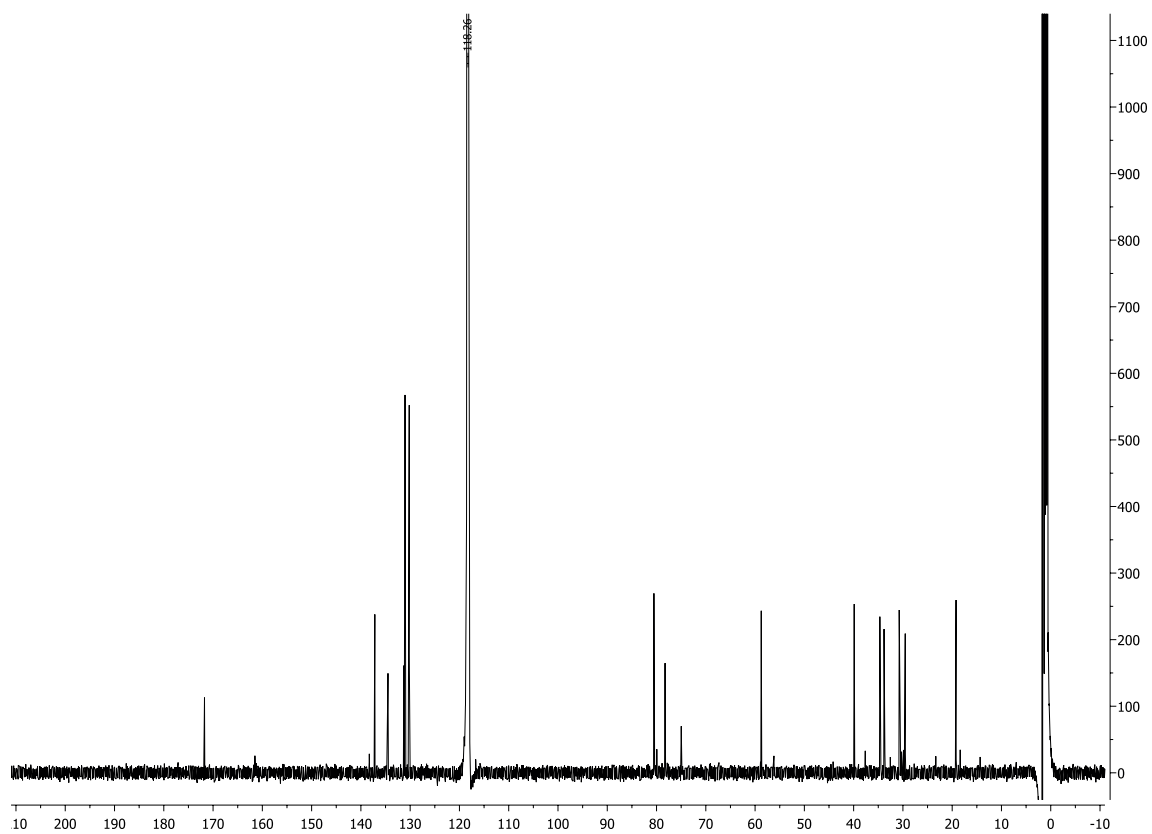
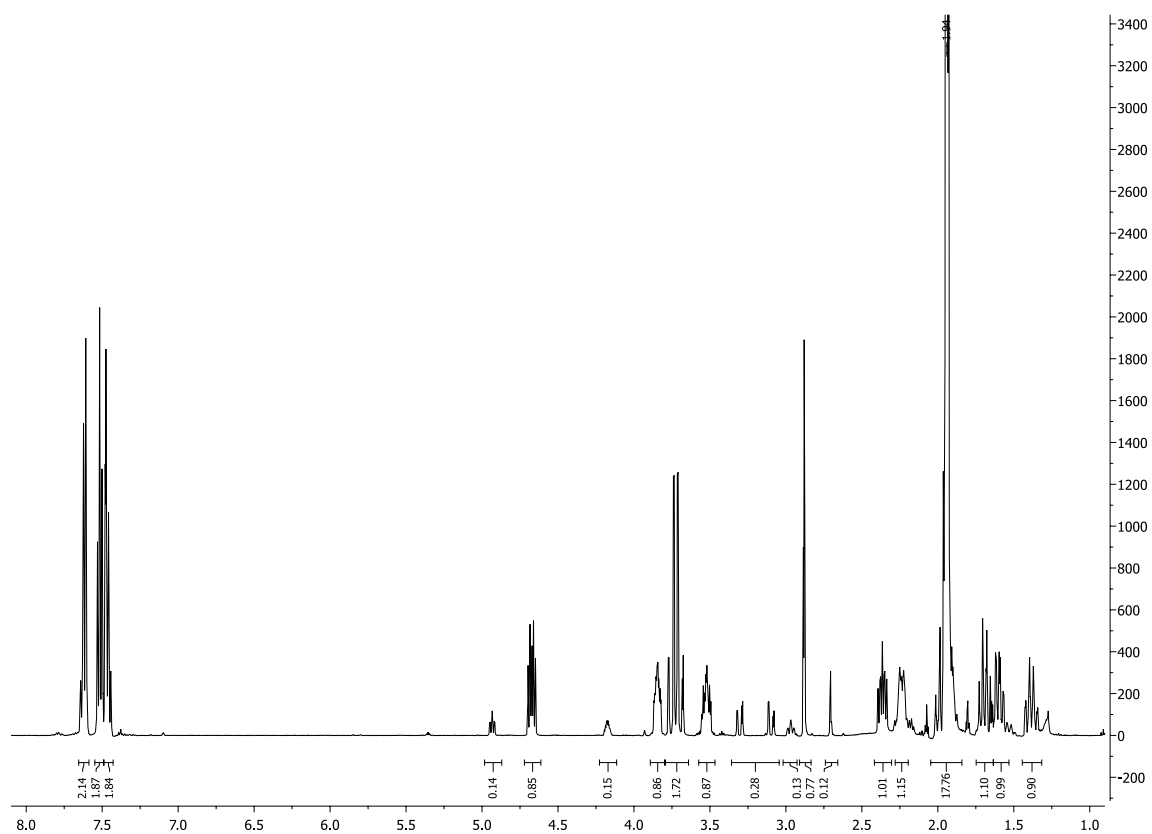


$^1\text{H}, ^1\text{H}$ -COSY-NMR (500 MHz, CDCl_3) of 13b

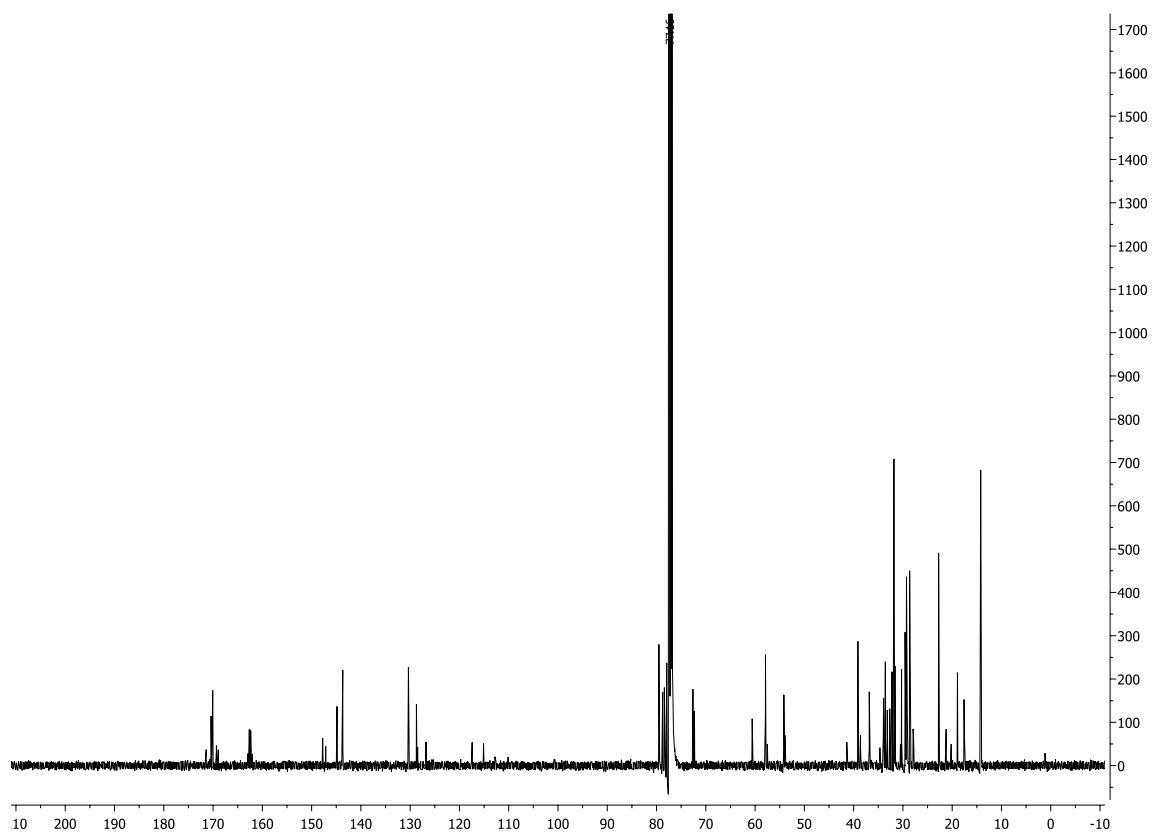
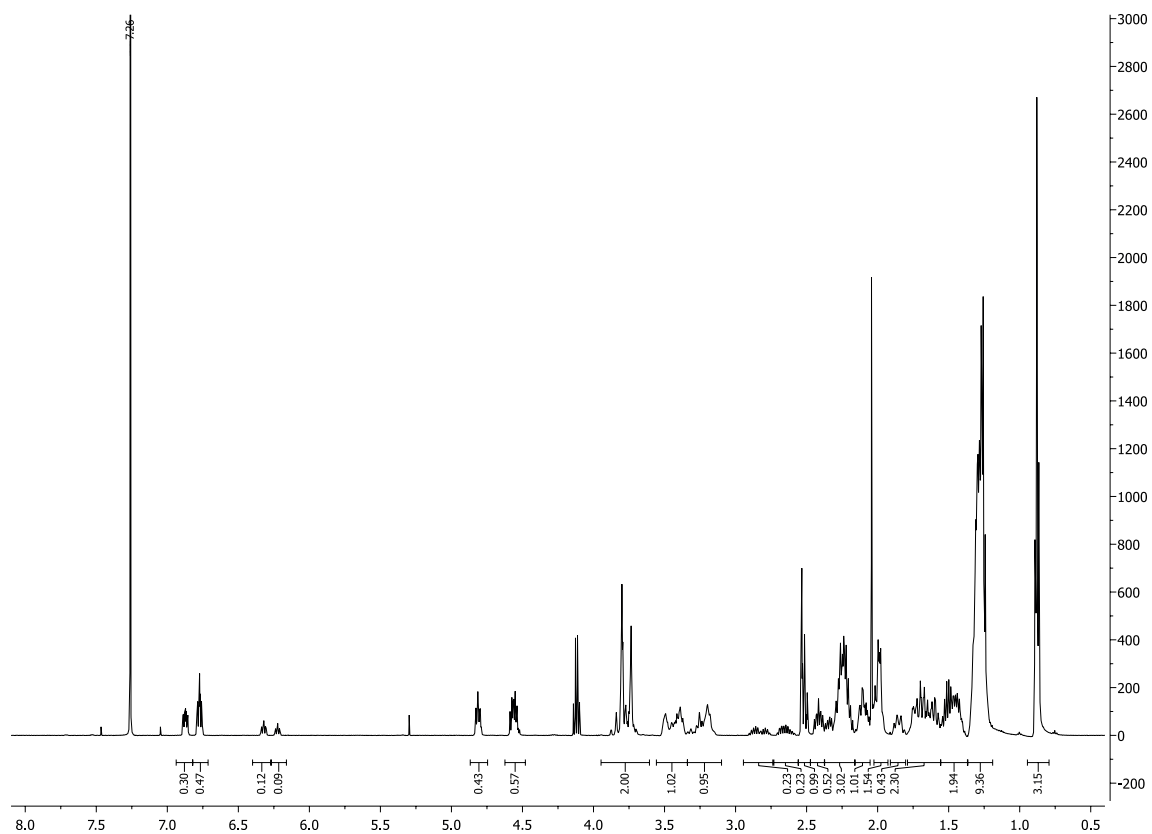


3a-H and 5-H couple to 4-H_a

$^1\text{H-NMR}$ (500 MHz, CDCl_3) and $^{13}\text{C-NMR}$ (90 MHz, CDCl_3) of compound 14

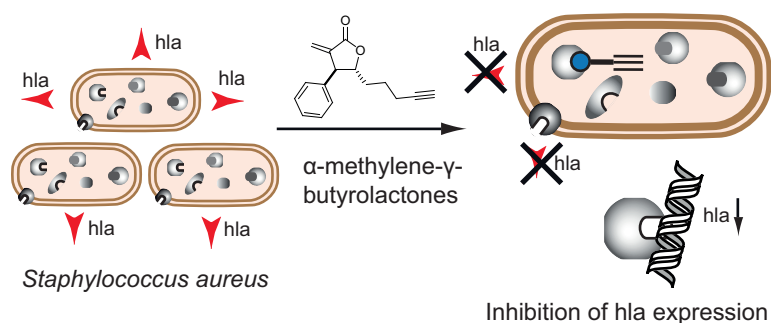


$^1\text{H-NMR}$ (500 MHz, CDCl_3) and $^{13}\text{C-NMR}$ (90 MHz, CDCl_3) of compound 15



α -Methylene- γ -butyrolactones attenuate *Staphylococcus aureus* virulence by inhibition of transcriptional regulation

M. H. Kunzmann, N. C. Bach, B. Bauer, S. A. Sieber. α -Methylene- γ -butyrolactones attenuate *Staphylococcus aureus* virulence by inhibition of transcriptional regulation. *Chem. Sci.* **2013**, Accepted Manuscript. DOI: 10.1039/C3SC52228H - Reproduced by permission of The Royal Society of Chemistry



Abstract

Bacterial pathogenesis is triggered by complex molecular mechanisms that sense bacterial density within an infected host and induce the expression of toxins for overriding the immune response. Virulence is controlled by a set of transcriptional regulators that directly bind to DNA promoter regions of toxin-encoding genes. Here, we identified an α -methylene- γ -butyrolactone as potent inhibitor of *Staphylococcus aureus* virulence. Treatment of bacteria not only resulted in a markedly decreased expression of one of the most prominent virulence factors α -hemolysin (Hla) but also caused attenuated invasion efficiency. Mass spectrometry (MS) based target identification revealed this biological effect originating from the consolidated binding to three important transcriptional regulators SarA, SarR and MgrA. MS investigation of the binding site uncovered a conserved cysteine in all three proteins which gets covalently modified. Intriguingly, investigation of DNA binding demonstrated an impaired DNA-protein interaction upon compound treatment. The functional correlation between target binding, inhibition and the observed biological effect was proven by gene knockouts and confirmed the expected mode of action.

Introduction

Staphylococcus aureus represents an opportunistic pathogen that infects a variety of human organs and causes severe diseases such as endocarditis, pneumonia and toxic shock syndrome.⁴ Tissue infection is promoted by a variety of bacterial virulence factors including hemolysins, leukocidins and immune modulators that support bacterial propagation within the host and attenuation of the immune response.¹⁵⁸

Due to the lack of novel and effective antibiotic drugs and the rising concern about multidrug-resistant bacteria, the targeting of virulence received increasing interest in the past years as an alternative treatment strategy.^{14, 28, 159, 160} Virulence factors are not essential for bacterial viability and thus inhibition of virulence reduces selective pressure, which is a major cause of resistance development. Recent genomic and proteomic studies have revealed insights into the complex pathways by which bacteria control the expression of several virulence factors.¹⁶¹ Multiple two component systems sense environmental conditions and transduce extracellular signals inside the cell, thereby initiating selective molecular responses including virulence gene expression via transcriptional regulators.^{162, 163} In *S. aureus* virulence expression is controlled by global regulatory elements such as staphylococcal accessory regulators (Sar).^{161, 164, 165} The SarA protein binds to several target gene promoters including α -hemolysin (Hla), protein A and fibronectin binding protein (FnBP).¹⁶⁶⁻¹⁶⁸ Analysis of multiple *S. aureus* genomes revealed the existence of additional members of this regulatory family including SarR and MgrA which share a high structural similarity to SarA.^{161, 169-171} Recent studies emphasized the existence of a central Cys based redox sensor which is crucial for DNA binding and thus regulatory activity.¹⁷² In addition, SarA activity is controlled by phosphorylation of the same Cys residue.¹⁷³ Genetic deletion of *sarA*, *sarR* and *mgrA* regulators revealed dramatic changes in the production of several toxins, including Hla, that result in strains that cannot cause infection within murine abscess models.^{174, 175} The regulation of toxin expression by transcriptional regulators, however, is highly complex and inactivation of individual proteins such as SarA can result in the up- or downregulation of Hla toxin expression depending on the corresponding *S. aureus* strain.¹⁷⁶⁻¹⁷⁸

In the search for novel therapies against multidrug-resistant *S. aureus* (MRSA) strains, anti-virulence concepts become more and more important. We previously described the inhibition of ClpP, a central bacterial protease, which in addition to the transcriptional regulators, controls the expression of crucial virulence factors.^{179, 180} β -lactones were found to be specific inhibitors which downregulate the expression of several toxins including toxic shock syndrome toxin, Hla and

enterotoxin B.²⁸ More recently, He *et al.* screened a library of compounds for dedicated MgrA inhibitors and identified 5,5-methylenedisalicylic acid (MDSA) that efficiently blocked DNA binding.¹⁸¹

In our search for novel antibacterial compounds we screened a distinct collection of α -methylene- γ -butyrolactones to reduce the expression of Hla (Figure 1). α -Methylene- γ -butyrolactones represent a potent and privileged structural motif that exhibits a huge diversity of bioactivities and is present in about 3% of all known natural products.^{72, 182}

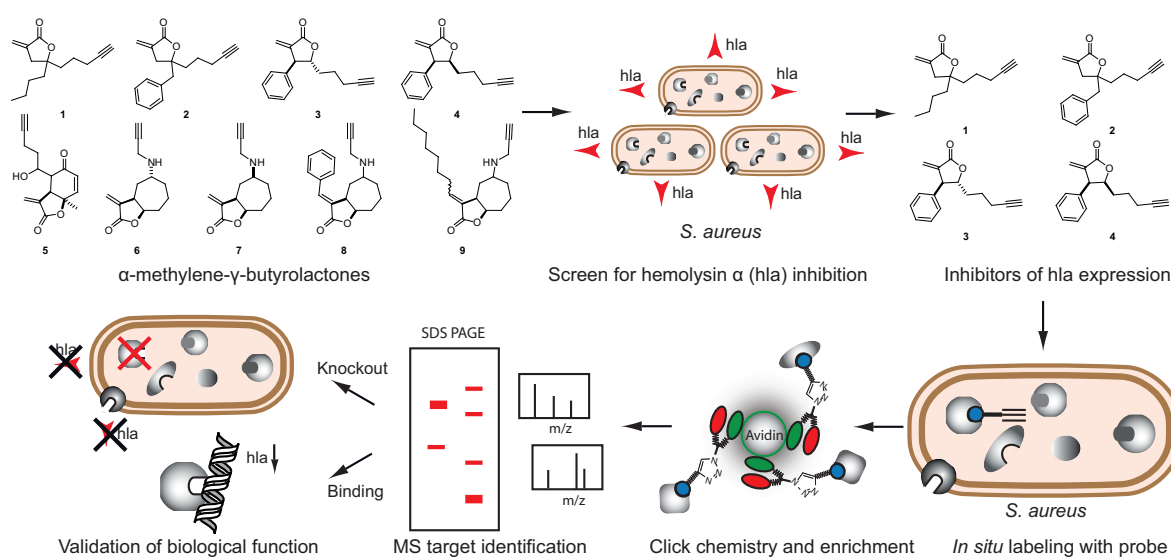


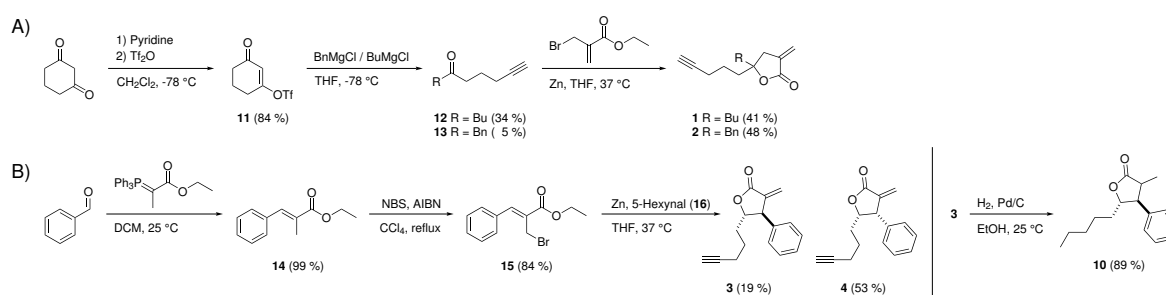
Figure 1: An α -methylene- γ -butyrolactone library was screened for hemolysis inhibition of *S. aureus*. The cellular targets of potent compounds were identified by incubation with living *S. aureus* cells, subsequent lysis, click chemistry with rhodamine biotin azide and enrichment with biotin-avidin beads followed by SDS page and mass spectrometric analysis (MS). *In vitro* assays and knockout studies were performed to verify the identified proteins and the biological effect.

We identified two compounds that revealed a significant reduction in toxin expression and subsequently started target deconvolution by activity based protein profiling (ABPP) (Figure 1).^{39, 102, 104} Proteomic profiling and mass spectrometric analysis showed that all active compounds exhibited binding and reactivity preferences for the three transcriptional virulence regulators SarA, SarR and MgrA via the conserved Cys redox sensing residue. Moreover, subsequent EMSA assays demonstrated that covalent binding to these particular regulatory proteins induced protein-DNA dissociation. Concordantly with previous reports,^{167, 183-185} the relevance of these targets for virulence in *S. aureus* was verified by genetic knockouts. Thus, these results not only expand the scope of virulence inhibition but also emphasize the drugability of multiple response regulators for medical applications.

Results and Discussion

Synthesis of α -methylene- γ -butyrolactones

Inspired by the diversity of α -methylene- γ -butyrolactones in nature we extended our existing collection of xanthatine inspired molecules (Scheme 1, Appendix) by four additional molecules that bear the core structure but are equipped with different side chains.¹⁸² All molecular structures exhibit a terminal alkyne handle which serves as a tag for downstream target identification by activity based protein profiling (ABPP).^{39, 104, 138, 177, 186} In this strategy the small probe molecules penetrate cells and bind to dedicated target(s) within a native environment (Figure 1). Subsequent cell lysis, Huisgen-Sharpless-Meldal cycloaddition (click chemistry) with functionalized azides allow the binding, enrichment and visualization of proteins of interest for subsequent identification by SDS-gel electrophoresis and mass spectrometry, respectively (Figure 1).^{46, 109, 137}



Scheme 1: Synthesis of A) aliphatic substituted and B) phenyl substituted α -methylene- γ -butyrolactone probes and the hydrated compound **10**. For synthetic details please refer to the appendix.

The synthesis followed two different procedures in order to account for aliphatic as well as aromatic substituted α -methylene- γ -butyrolactones (Scheme 1).

For aliphatic substituted lactones, compound **11** was synthesized as described by Kamijo *et al.* and a subsequent reaction with the indicated Grignard reagent lead to the precursors **12** and **13**.¹⁸⁷ A Reformatsky reaction with ethyl 2-(bromo-methyl)acrylate yielded the final aliphatic substituted lactone probes **1** and **2** as a racemic mixtures.¹⁸⁸ In case of phenyl substituted lactones, a Wittig reaction of benzaldehyde with (carbethoxyethylidene) triphenylphosphorane led to the formation of compound **14** which was brominated at its allylic position by using NBS and AIBN to yield lactone precursor **15**.¹⁸⁹ The final phenyl substituted lactones **3** and **4** (each racemic) were obtained by a Reformatsky reaction of **15** with 5-hexynal.¹⁸⁸ Compound **3** was reduced by hydration with Pd/C to yield probe **10**.

Test for anti-hemolytic and antibiotic activity

All compounds including the previously established α -methylene- γ -butyrolactones were tested for bioactivities against several *S. aureus* strains including antibiotic sensitive (NCTC8325) as well as MRSA (Mu50 and USA300) (Table S1). First, all compounds were investigated for their ability to inhibit *S. aureus* hemolysis of sheep derived erythrocytes. Compound **3** exhibited the most potent IC_{50} value of 4 μ M in NCTC8325 and 2 μ M in USA 300 followed by compound **4** that was slightly less active (Figure 2A and Figure S1, Appendix). In order to verify if the anti-hemolytic effect is based on the direct inhibition of virulence rather than an indirect consequence of antibiotic activity, we additionally determined the minimal inhibitory (MIC) concentration of all molecules (Figure 2B). Interestingly, only weak antibiotic activity could be obtained for compound **3** (100 μ M) which is 25-50 fold higher than the IC_{50} for hemolytic activity. All other compounds did not show any antibiotic effects below 100-500 μ M. In addition, compounds **3** and **4** were added to NCTC8325 at various concentrations close to their hemolysis IC_{50} . No adverse effect on the bacterial growth was observed that could explain their anti-hemolytic effects (Figure 2C) emphasizing that the molecules directly target virulence gene expression.

Although all structures share the same α -methylene- γ -butyrolactone scaffold, the side chain decoration seems to significantly alter and influence the corresponding bioactivity. The anti-hemolytic compounds **3** and **4** for instance represent the only scaffolds with a substituent in 4-position. Interestingly, the conversion of **3** from *trans* to *cis* **4** reduces the anti-hemolytic effect emphasizing a precise structure activity relationship (SAR) for target interactions.

All molecules were further tested for cytotoxicity in human HeLa cells via the MTT assay (Figure S2, Appendix). Compound **3** showed a toxic effect with an EC_{50} of 12 μ M, which is 3-6-fold above its anti-hemolytic effect. Thus further optimization of the compounds is desired in order to improve their toxicity profile for pharmacological application. This could be achieved by a fine tuning of the electrophilic exocyclic double bond as a fully reduced α -methyl group in compound **10** revealed a toxicity EC_{50} of > 100 μ M. However, the presence of an electrophile seems mandatory since no reduction of Hla expression with compound **10** was observed (Figure S1, Appendix). A better understanding of this SAR data would be achieved by the knowledge of the corresponding cellular targets.

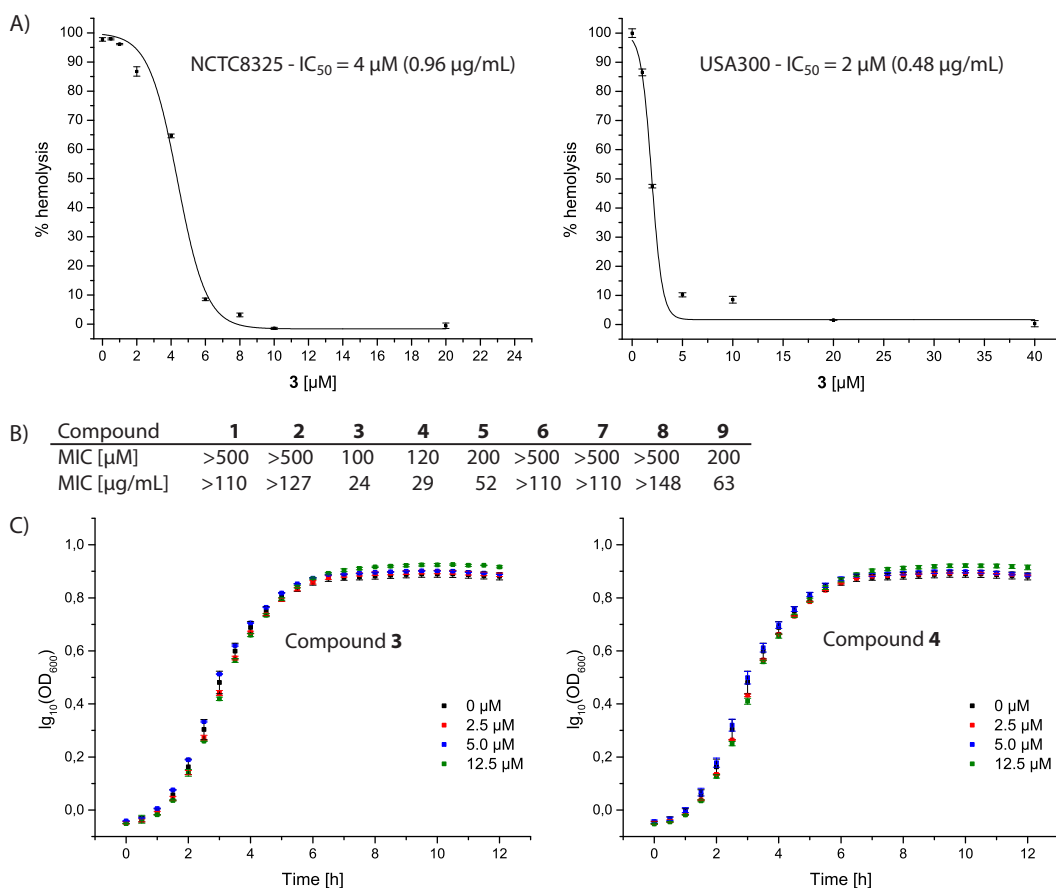


Figure 2: A) Inhibition of sheep blood hemolysis caused by *S. aureus* NCTC8325 and USA300 by probe **3**. Data were fitted to the dose-response function $f(x) = A_1 + (A_2 - A_1) / (1 + 10^{(\text{LOG}(x_0 - x))^p})$ with a variable Hill-slope given by parameter p . B) MIC values for NCTC8325 strain of the corresponding lactone probes in μM and μg/ml. C) NCTC8325 growth curves based on OD₆₀₀ with compounds **3** or **4**. Each compound was tested in at least three independent trials in triplicates; average values are shown and error bars display standard deviations from the mean.

Target deconvolution by ABPP

To unravel the molecular basis for the anti-hemolytic activity of **3** we utilized a proteomic approach by which the compounds were incubated with living bacteria of three different strains (antibiotic sensitive NCTC8325, and two MRSA strains: Mu50 and USA300) at various concentrations. The cells were lysed and the alkyne was subsequently modified with a rhodamine azide tag by click chemistry. The labeled cytosolic and cell envelope proteomes were individually separated by SDS-gel electrophoresis and analysed by fluorescent scanning. Due to the reactive Michael acceptor system, several fluorescently labeled proteins could be detected and a concentration of 5-10 μM seemed optimal for saturated labelling (Figure 3A, Figure S3A and C, Appendix). The target pattern can roughly be divided in high molecular weight (hmw) proteins and low molecular weight (lmw).

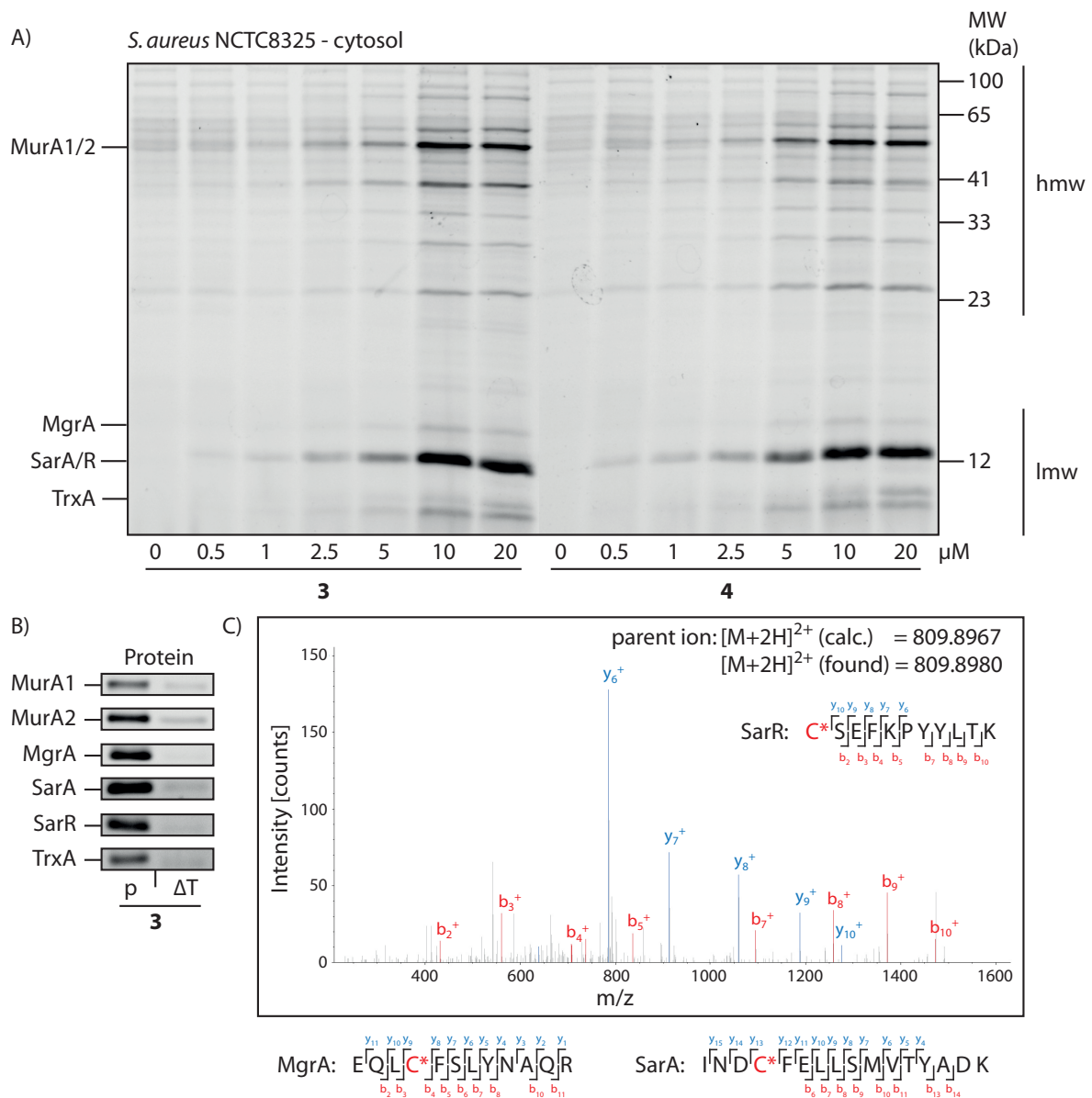


Figure 3: Target identification of α -methylene- γ -butyrolactones. A) *In situ* labelling of *S. aureus* NCTC8325 with probes **3** and **4** at indicated concentrations. Identified proteins of the corresponding gel bands are shown on the left. For details about the protein abbreviations please refer to Table S2. B) Target validation by labelling of recombinant proteins with the probes (p = recombinant protein, ΔT = heat denatured protein). C) MS/MS spectrum for the identification of the modified binding site (C* = compound **3** modified cysteine residue).

While some lmw protein bands were characteristic for the majority of compounds others were specific to **3** and **4**, the compounds that exhibited the best anti-hemolytic activity (Figure S3B, Appendix). This emphasizes that the corresponding proteins could be involved in virulence. Another interesting observation derived from the comparison of all three strains in the hmw

segment of the gel. One additional protein band at a molecular weight of 60 kDa appears only in Mu50 and thus might be resistance associated (Figure S4, Appendix).

In order to identify these particular cytosolic protein bands we next applied gel-based and gel-free MS identification methods. Labeled proteins were attached to a trifunctional tag consisting of azide, rhodamine and biotin via click chemistry.¹⁹⁰ Biotinylated proteins were enriched on avidin beads, washed and released by heat denaturation. The proteins were then either separated via SDS-PAGE, isolated, tryptically digested and analysed by LC-MS/MS or directly digested and analysed by LC-MS/MS. MS/MS fragmentation revealed peptide sequences that were investigated by the SEQUEST search algorithm in order to obtain protein identities. Analysis of the low molecular weight protein IDs suggested thioredoxin A (TrxA), a staphylococcal disulfide reductase, as well as three transcriptional regulators, SarA, SarR and MgrA as the most likely hits over several runs (Tables S2 and S3, Appendix).

This result is in line with the observed phenotype of compounds **3** and **4** as SarA, SarR and MgrA are involved in virulence regulation and *hla* expression.^{175-178, 191, 192} Interestingly, all other compounds did not or only weakly label SarA, SarR and/or MgrA in the proteome which provides a link to the observed phenotype (Figure S3 and S4, Appendix). In addition, the distinct 60 kDa protein specific for Mu50 was identified as bifunctional AAC/APH, an enzyme that is involved in propagating resistance to several antibiotics including gentamycin and kanamycin (Figure S4, Appendix).¹⁹³ The protein band below at about 55 kDa was identified as MurA1 and MurA2 – two enzymes that are involved in cell wall biosynthesis and are crucial for bacterial viability.^{71, 194} Their putative inhibition by α -methylene- γ -butyrolactones could explain the observed antibiotic activity at higher concentrations. All other bands in the 90 kDa region correspond to characteristic reactive proteins in *S. aureus* that are unspecifically labeled at concentrations above 20 μ M.¹⁹⁵ One predominant member has been assigned as formate acetyltransferase before by several MS experiments.^{71, 195} Since this study focuses on the anti-hemolytic activity of α -methylene- γ -butyrolactones we commenced with target validation for proteins that are characteristic for the observed biological effects.

Target validation

Before we started with the functional studies of the transcriptional regulators we first analysed MurA1 and MurA2 inhibition by **3** in order to evaluate their potential contribution to the observed anti-hemolytic effects at sub-MIC concentrations. Incubation of recombinant MurA proteins⁷¹ with **3** and subsequent modification with the fluorescent dye via click chemistry revealed a strong

fluorescent band on SDS-PAGE (Figure 3B). No labelling was observed if the proteins were heat denatured prior to compound addition emphasizing a specific interaction with the folded and active enzyme. Enzyme activity of the cell wall biogenesis regulating enzymes MurA1 and MurA2 was measured by monitoring the enolpyruvyl transfer reaction with phosphoenolpyruvate (PEP) and UDP-*N*-acetylglucosamine (UDPAG)⁷¹. Here, 100 μ M compound **3** was required to significantly impair enzyme activity (Figure S5, Appendix). This is comparable to the corresponding MIC value (100 μ M) suggesting that inhibition of these essential enzymes is related to the observed antibiotic activity. To evaluate the contribution of MurA1/2 inhibition to the reduction of hemolysis we utilized the well characterized MurA1/2 inhibitor fosfomycin and applied it at sub-MIC concentrations to *S. aureus* NCTC8325.¹⁹⁴ No effect on the hemolysis production was observed at a concentration of 0.55 μ M (MIC < 2.75 μ M) emphasizing that these targets are not responsible for the observed anti-hemolytic effects (Figure S6, Appendix). Therefore, we focused our attention to the functional characterization of the low molecular weight proteins with special emphasis on the transcriptional regulators.

TrxA, *sarA*, *sarR* and *mgrA* were cloned into strep-tag expression vector systems and expressed as recombinant proteins in *E. coli* BL21 DE3. Specific interactions of the probe molecules with the corresponding proteins were confirmed via *in situ* labelling with living cells before and after induction, *in vitro* labelling with heat denatured cell lysates containing the proteins as well as heat denaturation of the purified proteins prior to labelling (Figure 3B, Figure S7, Appendix). The denatured proteins did not bind the compound emphasizing the importance of a properly folded binding pocket for recognition.

In order to identify the site of binding we incubated the purified proteins with 4-fold excess of **3** for 30 min, digested with trypsin and analysed the resulting peptides via HPLC-MS/MS. In case of SarA, SarR and MgrA a single cysteine residue (Cys9, Cys57 and Cys12) was identified as site of covalent attachment (Figure 3C and Figure S8, Appendix). The identified cysteines are highly conserved in all three structurally related proteins and located at the dimerization interface.^{171, 172, 196} They form H-bonds with residues from the adjacent monomer thus likely explaining their elevated nucleophilicity and reactivity towards the electrophilic α -methylene- γ -butyrolactones. These cysteine residues are important regulatory switches. For instance, Cys12 in MgrA is an important sensor for oxidative stress.¹⁷² Peroxides cause oxidation of the thiol to sulfenic acid and subsequent dissociation from the DNA.^{172, 197} In case of SarA, recent studies show phosphorylation of Cys9 as an additional regulation principle reducing DNA binding affinity.^{173, 198}

It is known that *S. aureus* adapts to changes of external oxygen concentrations by redox dependent processes regulating the expression of genes. Small thiol specific proteins such as thioredoxin (TrxA) maintain the intracellular thiol-disulfide balance.^{199, 200} TrxA is an oxidoreductase enzyme featuring a conserved active site Trp-Cys-Gly-Pro-Cys sequence that forms or breaks disulfide bonds by inter-protein exchange reactions.²⁰¹ As this regulation also indirectly triggers the redox state of transcriptional regulators we were interested if **3** is able to inhibit the reductase activity of TrxA.¹⁹⁹ The inhibition of TrxA by **3** was evaluated by an assay system which measures the reduction of disulfide bonds within insulin.²⁰² Reduced insulin becomes insoluble and enzyme turnover is followed by increasing turbidity. Concentration-dependent inhibition of TrxA activity was observed and an IC₅₀ value of 17 μM obtained (Figure S9, Appendix). Apart from its function in the cellular redox pathway not much is known about the biological impact of TrxA inhibition. A *trxA* deletion in *Salmonella enterica* exhibited a reduction in intracellular replication and mouse virulence emphasizing a possible role in virulence regulation that would correlate with the above-mentioned function.²⁰³

These examples highlight the importance of a fine tuned cellular redox mechanism that among other duties, maintains cysteine oxidation states in transcriptional regulators for DNA binding. In order to evaluate if covalent modification with a small molecule induces DNA displacement effects we utilized electrophoretic mobility shift assays (EMSA) and obtained corresponding IC₅₀ values (Figure 4 and Figure S10, Appendix).

Based on previous studies we selected the *agr* promoter DNA region as a confirmed binding site for SarA, SarR and MgrA.^{191, 204} A fluorescent AlexaFluor488 dye at the 5' site allowed us to monitor protein-DNA interaction via fluorescence scanning of the corresponding native polyacrylamide gels. All three proteins were incubated in the presence of the fluorescent DNA and various concentrations of compounds. Unspecific binding was reduced by the addition of an excess of salmon sperm DNA.

The corresponding mobility shift gels are shown in Figure 4 and Figure S10 (Appendix). Interestingly, SarA, SarR and MgrA showed mobility shifts at low molar excess of **3** (0.5-fold for SarR and 4-fold for SarA and MgrA). This emphasizes that the binding to all three transcriptional regulators could be responsible for the phenotypic effect. Importantly, compounds not exhibiting any anti-virulence activity, except compound **5**, did not show mobility shifts with SarA, SarR and MgrA, thereby demonstrating a lack of interaction (Figure 4 and Figure S10, right panel,

Appendix). This is also in line with labelling studies of the three recombinant proteins (Figure S11, Appendix).

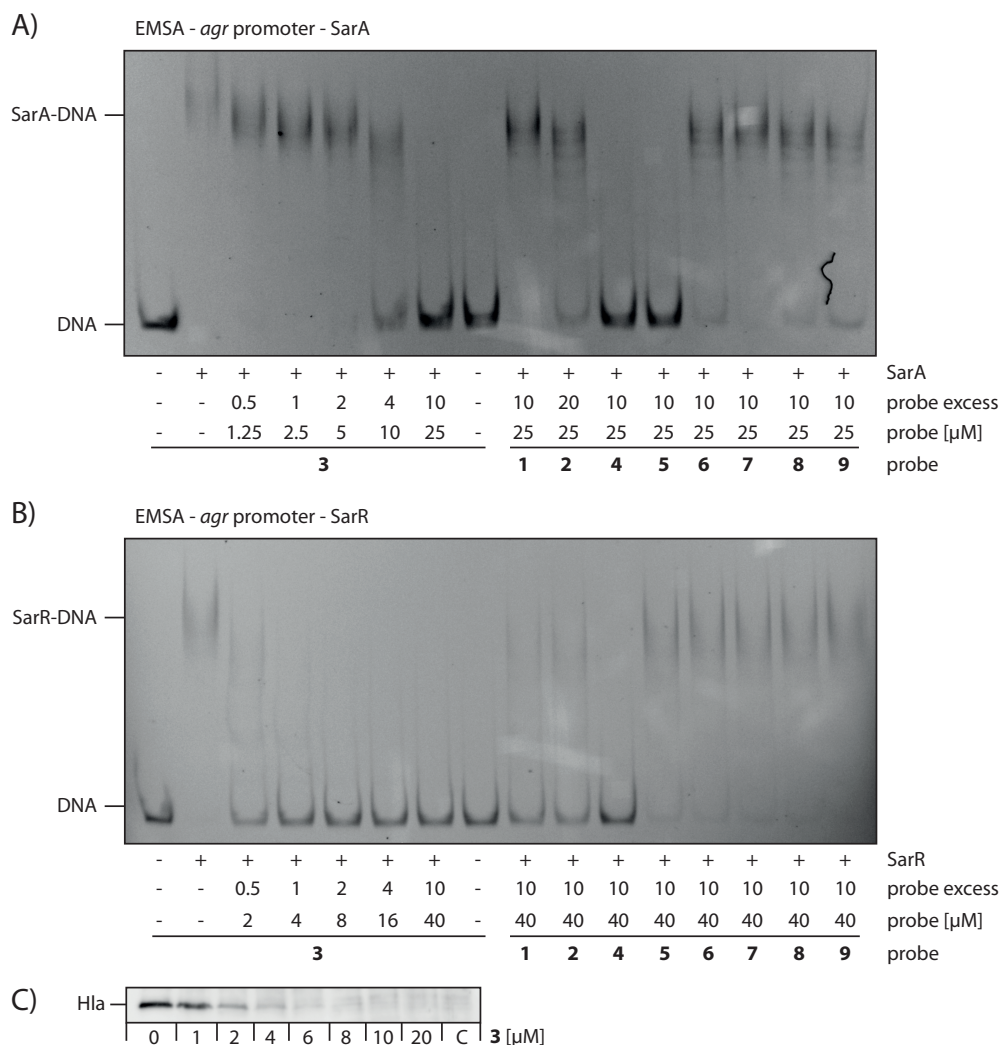


Figure 4: Electrophoretic mobility shift assay (EMSA) with A) SarA and B) SarR (for MgrA please refer to Figure S10, Appendix). The left part of the gel shows a concentration dependent analysis with anti-virulence compound **3**, the right part displays a single concentration analysis with all other compounds. DNA = unbound fluorescent promoter DNA; SarA/SarR-DNA = protein bound DNA. C) Luminescent western blot of *S. aureus* NCTC8325 supernatant (grown with increasing concentrations of probe **3**) incubated with a primary anti-Hla (α -hemolysin) and a secondary (HRP) antibody.

Several previous studies show that SarA, SarR and MgrA regulate *hla* expression.^{161, 164} This regulation principle, however, is highly complex and strain specific. For instance, a *sarA* knockout in *S. aureus* strain 8325-4 downregulates *hla* expression^{167, 205, 206} while the same knockout in strains V8 or SH1000 upregulates Hla levels.¹⁷⁷ Several reasons for this observation have been discussed and a strong link to the Sar family protein amount (including SarS) has been suggested.^{177, 179} In order to further elucidate if the observed anti-hemolytic effect correlates

indeed with reduced expression levels of Hla we utilized western blot analysis with anti-Hla antibodies. In agreement with the results of the blood hemolysis assay as well as the EMSA assay the expression of Hla was significantly diminished at a concentration of 2 μM **3** and abolished at concentrations above 4 μM (Figure 4C). This strongly suggests that at least the cumulative inhibition of all three transcriptional regulators reduces *hla* expression in the *S. aureus* strains investigated here (NCTC8325 and USA3000). However, the individual role of each regulator has to be investigated with the corresponding *mgrA*, *sarA* and *sarR* knockout strains.

Functional analysis by gene knockouts

In order to validate the relevance of transcriptional regulator inhibition by α -methylene- γ -butyrolactone **3** we obtained previously established knockout strains of *sarA*, *sarR*, *mgrA* as well as a *sarA/R* double knockout. Phage mediated transduction of the selective resistance cassettes into the corresponding genes of the *S. aureus* NCTC8325 genome revealed corresponding knockout strains for further functional investigations.^{167, 183-185}

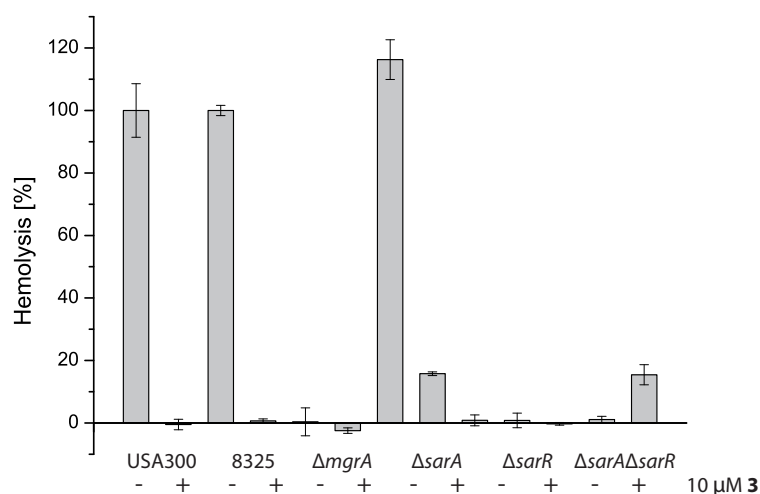


Figure 5: Hemolysis of sheep red blood cells upon incubation with supernatants of *S. aureus* USA300, NCTC8325 and the corresponding NCTC8325 knockout strains $\Delta mgrA$, $\Delta sarA$, $\Delta sarR$ and $\Delta sarA\Delta sarR$ with and without 10 μM probe **3**.

Subsequent hemolysis assays with the parental strain and the knockouts revealed a significant reduction in Hla production in case of $\Delta sarR$ and $\Delta mgrA$ (Figure 5). Contrary, the $\Delta sarA$ strain showed an increase in hemolysis as described for several strains previously¹⁷⁷, thereby indicating SarA as being not a responsible target for the anti-hemolytic effect of compound **3**. Interestingly, addition of compound **3** decreased hemolysis production of $\Delta sarA$ bacteria, thus emphasizing SarR and MgrA as the responsible anti-virulence-determining targets. In order to investigate which of

the two effects –activation of hemolysis by $\Delta sarA$ or reduction of hemolysis by $\Delta sarR$ is dominating we investigated a $\Delta sarA\Delta sarR$ double mutant. Interestingly, this double mutation resulted in no detectable hemolysis demonstrating that inactivation of at least these two transcriptional regulators is sufficient to match the chemical phenotype of α -methylene- γ -butyrolactone **3**. Thus, the results of ABPP, EMSA studies as well as functional knockouts clearly support a mechanism of action by which compound **3** covalently attaches to a functional relevant cysteine in all three transcriptional regulators, preventing DNA binding and downstream hemolysis production.

Reduction of *S. aureus* invasion into human THP-1 cells

Previous studies with *sarA* deletion strains in *S. aureus* indicated a reduced binding to fibronectin, an important membrane associated protein in eukaryotic cells and a trigger for bacterial invasion.^{207, 208} Therefore, we finally investigated if binding of **3** to the transcriptional regulators would reduce the phagocytosis mediated invasion of *S. aureus* into human macrophages for which we performed a compound-based assay.²⁰⁹ Bacterial cells were grown in the presence of 20 μM **3** for 16 h, and incubated with differentiated THP-1 cells in the presence of 2 μM **3** for 2 h. In order to interrupt cellular uptake mechanisms cells were washed with cold PBS and subsequently incubated in medium supplemented with 50 $\mu\text{g}/\text{ml}$ gentamycin to kill all remaining extracellular, non-internalized bacteria. The cells were lysed, lysates were plated and intracellular bacteria were counted as colony forming units (CFU) after one day of incubation at 37°C. Interestingly, compound **3** significantly reduced the invasiveness of *S. aureus* by 40% emphasizing that the pathogen is not only disarmed in its Hla mediated virulence but also weakened in its general pathogenicity (Figure S12, Appendix). This further highlights the relevance of these proteins as putative targets against bacterial infections.

Conclusion

Inhibition of virulence is a powerful approach to reduce the pathogenicity of bacteria. The expression of toxins that contribute to the devastating effects of bacterial infections is regulated by a complex network of proteins that mediate a precise timing in the initiation of virulence. This timing is important, as bacteria need a certain density in order to overrun the host. Several transcriptional regulators are activated by quorum sensing and initiate toxin production. SarA, SarR and MgrA are DNA binding proteins that attach to a promoter region important for *hla* transcription. Once their central cysteine is modulated by e.g. phosphorylation or oxidation these proteins show reduced DNA affinity and therefore alter transcription of the target genes. We

were able to show that the covalent modification of this particular central cysteine residues by suitably designed α -methylene- γ -butyrolactones not only reduced DNA affinity but induced DNA dissociation that resulted in a strong decrease of Hla expression. In addition, the invasion of *S. aureus* into human THP-1 cells was significantly reduced demonstrating that bacteria are weakened in multiple aspects of pathogenesis. This approach is novel and exhibits several advantages compared to a previous MgrA specific inhibitor (MDSA).¹⁸¹ α -Methylene- γ -butyrolactone **3** abolishes Hla production at 2-4 μ M concentration and is thus more potent compared to MSDA, which exhibits a hemolysis IC₅₀ of 0.2 mM. Combined inhibition of several targets might be an advantageous strategy as the effects are likely additive leading to a more efficient depletion of Hla mediated virulence. Due to the structural similarity of all three transcriptional regulators it is not surprising that one compound with a suitable decoration binds all proteins via the sensing cysteine. This irreversible binding also exhibits the advantage of a stable link that is long lasting and only reversed by protein turnover.

Acknowledgement

We thank Mona Wolff for excellent technical support, David C. Hooper, Simon J. Foster and Erik Gustafsson for providing *S. aureus* knockout strains and Matt Nodwell and Katrin Lorenz-Baath for scientific discussions. S. A. Sieber was supported by the Deutsche Forschungsgemeinschaft SFB749, SFB1035, FOR1406, an ERC starting grant (259024) and the Center for Integrated Protein Science Munich CIPSM. M. H. Kunzmann thanks the TUM Graduate School for project funding and the ERC for financial support.

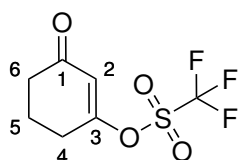
Experimental

Materials. All chemicals were of reagent grade or better and used without further purification. Chemicals and solvents were purchased from Sigma Aldrich or Acros Organics. For all reactions, only commercially available solvents of purissimum grade, dried over molecular sieve and stored under argon atmosphere were used. Solvents for chromatography and workup purposes were generally of reagent grade and purified before use by distillation. In all reactions, temperatures were measured externally. All experiments were carried out under argon. Column chromatography was performed on Merck silica gel (Acros Organics 0.035–0.070 mm, mesh 60 Å). ¹H- and ¹³C-NMR spectra were recorded on a *Bruker Avance I 360* (360 MHz), a *Bruker Avance I* (500 MHz) or a *Bruker Avance III 500* (500 MHz) NMR-System and referenced to the residual proton and carbon signal of the deuterated solvent, respectively. HR-ESI-MS, HR-LC-ESI-MS, HR-122

APCI-MS and HR-LC-APCI-MS mass spectra were recorded with a *Thermo Finnigan LTQ FT Ultra* coupled with a *Dionex UltiMate 3000* HPLC system. ESI-MS and LC-ESI-MS mass spectra were recorded with a *Thermo Finnigan LCQ ultrafleet* coupled with a *Dionex UltiMate 3000* HPLC system. HPLC analysis was accomplished with a *Waters 2695 separations module*, an *X-Bridge™ C18 3.5 μm OBD™* column (4.6 x 100 mm) and a *Waters 2996 PDA detector*. HPLC separation was accomplished with a *Waters 2545 quaternary gradient module*, an *X-Bridge™ Prep C18 10 μm OBD™* (50 x 250 mm), an *X-Bridge™ Prep C18 5 μm OBD™* (30 x 150 mm) or an *YMC Triart C18 5 μm* column (10 x 250 mm), a *Waters 2998 PDA detector* and a *Waters Fraction Collector III*.

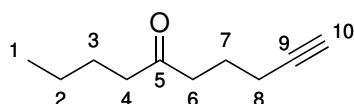
Synthesis of the γ -lactone probe library

3-(Trifluoromethanesulfonyloxy)-2-cyclohexen-1-one (**11**)²¹⁰



A solution of cyclohexane-1,3-dione (1.12 g, 10.0 mmol, 1.00 eq.) and pyridine (1.57 g, 1.6 mL, 20.0 mmol, 2.00 eq.) in dichloromethane (50 mL) was cooled to -78 °C. Trifluoromethanesulfonic anhydride (1 M in dichloromethane, 12.0 mL, 12.0 mmol, 1.20 eq.) was added slowly and the reaction mixture was stirred for 10 min at -78 °C. The reaction mixture was warmed to 0 °C and after consumption of the diketone (monitored by TLC) HCl_{aq} (1 M, 20 mL) was added. The reaction mixture was extracted with diethyl ether (3 x 50 mL), the organic layer was washed with saturated $\text{Na}_2\text{CO}_{3\text{aq}}$ (100 mL), water (100 mL), dried over Na_2SO_4 , filtered and the solvents were evaporated under reduced pressure. The residue was purified by column chromatography (silica gel, hexane/ethyl acetate = 10:1) to yield compound **11** (2.04 g, 8.35 mmol, 84%) as yellowish oil. Data is consistent with that reported in the literature.¹⁸⁷ R_f (hexane/ethyl acetate = 10:1) = 0.16. R_f (hexane/ethyl acetate = 5:1) = 0.31. $^1\text{H-NMR}$ (500 MHz, CDCl_3) δ = 6.05 (s, 1 H, 2-H), 2.68 (td, $^3J_{4,5}$ = 6.3 Hz, $^4J_{2,4}$ = 1.2 Hz, 2 H, 4-H), 2.44 (t, $^3J_{5,6}$ = 6.3 Hz, 2 H, 6-H), 2.12 (p, $^3J_{4,5}$ = $^3J_{5,6}$ = 6.3 Hz, 2 H, 5-H). $^{13}\text{C-NMR}$ (91 MHz, CDCl_3) δ = 197.6, 167.6, 119.3, 36.4, 28.6, 20.9.

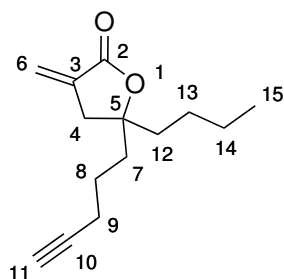
Dec-9-yn-5-one (**12**)²¹⁰



To a solution of butylmagnesium bromide (1.82 M in toluene, 2.25 mL, 4.10 mmol, 1.00 eq.) in toluene (15 mL) was added compound **11** (1.10 g, 4.50 mmol, 1.10 eq.) in toluene (15 mL) at -78 °C. The reaction mixture was stirred for 10 min at -78 °C, 10 min at 0 °C, 30 min at room

temperature and 30 min at 60 °C. Saturated $\text{NH}_4\text{Cl}_{\text{aq}}$ (15 mL) was added and the reaction mixture was extracted with diethyl ether (3 x 30 mL). The organic layer was washed with water (30 mL), brine (30 mL), dried over Na_2SO_4 , filtered and the solvents were evaporated under reduced pressure. The residue was purified by column chromatography (silica gel, hexane/ethyl acetate = 20:1) to yield compound **12** (211 mg, 1.39 mmol, 34%) as colourless oil. R_f (hexane/ethyl acetate = 20:1) = 0.20. R_f (hexane/ethyl acetate = 10:1) = 0.32. $^1\text{H-NMR}$ (500 MHz, CDCl_3) δ = 2.54 (t, $^3J_{6,7}$ = 7.2 Hz, 2 H, 6-H), 2.40 (t, $^3J_{3,4}$ = 7.5 Hz, 2 H, 4-H), 2.21 (td, $^3J_{7,8}$ = 6.9 Hz, $^4J_{8,10}$ = 2.7 Hz, 2 H, 8-H), 1.94 (t, $^4J_{8,10}$ = 2.7 Hz, 1 H, 10-H), 1.78 (p, $^3J_{6,7}$ = $^3J_{7,8}$ = 7.1 Hz, 2 H, 7-H), 1.55 (h, $^3J_{2,3}$ = $^3J_{3,4}$ = 7.5 Hz, 2 H, 3-H), 1.30 (t, $^3J_{1,2}$ = $^3J_{2,3}$ = 7.5 Hz, 2 H, 2-H), 0.89 (t, $^3J_{1,2}$ = 7.5 Hz, 3 H, 1-H). $^{13}\text{C-NMR}$ (91 MHz, CDCl_3) δ = 210.7, 83.8, 69.1, 42.8, 41.1, 26.1, 22.5, 22.4, 17.9, 14.0. **HRMS-ESI** (m/z): $\text{C}_{10}\text{H}_{17}\text{O}^+$ $[\text{M}+\text{H}]^+$, calc.: 153.12739, found: 153.12714, δ = 1.63 ppm.

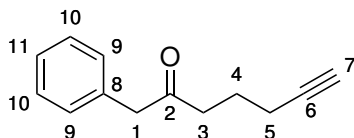
5-Butyl-3-methylene-5-(pent-4-yn-1-yl)dihydrofuran-2(3H)-one (**1**)²¹¹



Zinc dust (1.0 g) was activated by rinsing with 0.5 M HCl_{aq} (10 mL), then water (10 mL), anhydrous ethanol (10 mL), and diethyl ether (10 mL), then dried in vacuo (0.05 mbar at 150 °C) overnight and cooled to room temperature under argon atmosphere. To a solution of compound **12** (100 mg, 0.657 mmol, 1.00 eq.) in THF (5 mL) was added freshly activated zinc dust (51.5 mg, 0.788 mmol, 1.20 eq.) and the mixture was stirred for 15 min at 37 °C. Ethyl 2-(bromomethyl)acrylate (109 μL , 152 mg, 0.788 mmol, 1.20 eq.) in THF (5 mL) was added and the mixture stirred for 24 h at 37 °C. The reaction mixture was cooled to room temperature, HCl_{aq} (10% w/v, 2 mL) was added and the mixture was stirred for 30 min at room temperature. The solution was filtered and extracted with ethyl acetate (3 x 20 mL). The organic layer was washed with water (40 mL), brine (40 mL), dried over Na_2SO_4 , filtered and the solvents were evaporated under reduced pressure. The residue was purified by column chromatography (silica gel, hexane/ethyl acetate = 10:1) to yield racemic compound **1** (59.0 mg, 0.268 mmol, 41%) as colourless oil. R_f (hexane/ethyl acetate = 10:1) = 0.28. $^1\text{H-NMR}$ (500 MHz, CDCl_3) δ = 6.21 (t, $^4J_{4,6-Z}$ = 2.9 Hz, 1 H, 6-Z-H), 5.60 (t, $^4J_{4,6-E}$ = 2.5 Hz, 1 H, 6-E-H), 2.69-2.80 (m, 1 H, 4-H), 2.22 (td, $^3J_{8,9}$ = 6.9 Hz, $^4J_{9,11}$ = 2.6 Hz, 2 H, 9-H), 1.96 (t, $^4J_{9,11}$ = 2.6 Hz, 1 H, 11-H), 1.72-1.84 (m, 2 H, 7-H), 1.63-1.69 (m, 2 H, 12-H), 1.51-1.63 (m, 2 H, 8-H), 1.24-1.36 (m, 4 H, 13-H, 14-H), 0.90 (t, $^3J_{14,15}$ = 7.0 Hz, 3 H, 15-H). $^{13}\text{C-NMR}$ (91 MHz, CDCl_3) δ =

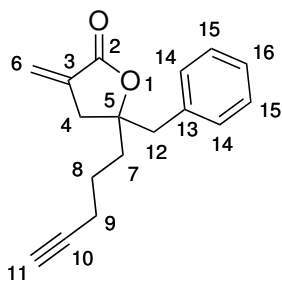
170.0, 135.9, 122.1, 85.5, 83.7, 69.1, 39.2, 38.5, 37.6, 25.5, 23.0, 22.5, 18.7, 14.1. **HRMS-ESI** (m/z): $C_{14}H_{21}O_2^+$ [M+H]⁺, calc.: 221.15361, found: 221.15353, δ = 0.34 ppm.

1-Phenylhept-6-yn-2-one (**13**)²¹⁰



To a solution of benzylmagnesium bromide (2.00 M in toluene, 3.67 mL, 7.34 mmol, 1.00 eq.) in toluene (15 mL) was added compound **11** (1.97 g, 8.07 mmol, 1.10 eq.) in toluene (15 mL) at -78 °C. The reaction mixture was stirred for 10 min at -78 °C, 10 min at 0 °C, 30 min at room temperature and 30 min at 60 °C. Saturated NH_4Cl_{aq} (15 mL) was added and the reaction mixture was extracted with diethyl ether (3 x 30 mL). The organic layer was washed with water (30 mL), brine (30 mL), dried over Na_2SO_4 , filtered and the solvents were evaporated under reduced pressure. The residue was purified by column chromatography (silica gel, hexane/ethyl acetate = 50:1 to 1:1) to yield compound **13** (61.2 mg, 0.329 mmol, 5%) as colourless oil. R_f (hexane/diethyl ether = 2:1) = 0.24. **¹H-NMR** (500 MHz, $CDCl_3$) δ = 7.33 (m, 2 H, 10-H), 7.26 (m, 1 H, 11-H), 7.21 (m, 2 H, 9-H), 3.70 (s, 2 H, 1-H), 2.61 (t, $^3J_{3,4}$ = 7.2 Hz, 2 H, 3-H), 2.19 (td, $^3J_{4,5}$ = 6.9 Hz, $^4J_{5,7}$ = 2.7 Hz, 2 H, 5-H), 1.93 (t, $^4J_{5,7}$ = 2.7 Hz, 1 H, 7-H), 1.77 (t, $^3J_{3,4}$ = $^3J_{4,5}$ = 7.0 Hz, 2 H, 4-H). **¹³C-NMR** (91 MHz, $CDCl_3$) δ = 207.9, 134.3, 129.5, 128.9, 127.2, 83.6, 69.1, 50.4, 40.5, 22.3, 17.8. **HRMS-ESI** (m/z): $C_{13}H_{15}O^+$ [M+H]⁺, calc.: 187.11174, found: 187.11198, δ = 1.28 ppm.

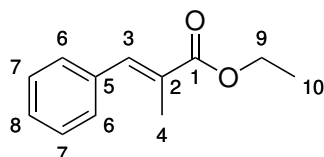
5-Benzyl-3-methylene-5-(pent-4-yn-1-yl)dihydrofuran-2(3H)-one (**2**)²¹¹



Zinc dust (1.0 g) was activated by rinsing with 0.5 M HCl_{aq} (10 mL), water (10 mL), anhydrous ethanol (10 mL), and diethyl ether (10 mL). The substance was then dried in vacuo (0.05 mbar at 150 °C) overnight and cooled to room temperature under argon atmosphere. To a solution of compound **13** (61.2 mg, 0.329 mmol, 1.00 eq.) in THF (2.5 mL) was added freshly activated zinc dust (25.8 mg, 0.394 mmol, 1.20 eq.) and the mixture was stirred for 15 min at 37 °C. Ethyl 2-(bromomethyl)acrylate (54.4 μ L, 76.1 mg, 0.394 mmol, 1.20 eq.) in THF (2.5 mL) was added and the mixture stirred for 2 h at 37 °C. The reaction mixture was cooled to room temperature, HCl_{aq} (10% w/v, 1 mL) was added and the mixture was stirred for 30 min at room temperature. The

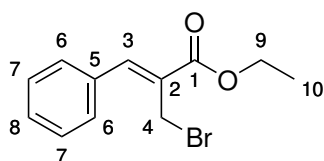
solution was filtered and extracted with ethyl acetate (3 x 10 mL). The organic layer was washed with water (20 mL), brine (20 mL), dried over Na₂SO₄, filtered and the solvents were evaporated under reduced pressure. The residue was purified by column chromatography (silica gel, hexane/ethyl acetate = 7:1) to yield racemic compound **2** (40.0 mg, 0.157 mmol, 48%) as colourless oil. R_f (hexane/ethyl acetate = 7:1) = 0.26. ¹H-NMR (500 MHz, CDCl₃) δ = 7.26-7.30 (m, 2 H, 15-H), 7.19-7.26 (m, 3 H, 14-H, 16-H), 6.00 (t, ⁴J_{4,6-Z} = 2.9 Hz, 1 H, 6-Z-H), 5.40 (t, ⁴J_{4,6-E} = 2.6 Hz, 1 H, 6-E-H), 3.06 (d, ²J_{12,12} = 14.0 Hz, 1 H, 12-H_a), 2.87 (d, ²J_{12,12} = 14.1 Hz, 1 H, 12-H_b), 2.85 (dt, ²J_{4,4} = 17.2 Hz, ⁴J_{4,6-Z} = ⁴J_{4,6-E} = 2.7 Hz, 1 H, 4-H_a), 2.68 (dt, ²J_{4,4} = 17.2 Hz, ⁴J_{4,6-Z} = ⁴J_{4,6-E} = 2.8 Hz, 1 H, 4-H_b), 2.23 (td, ³J_{8,9} = 6.9 Hz, ⁴J_{9,11} = 2.7 Hz, 2 H, 9-H), 1.97 (t, ⁴J_{9,11} = 2.7 Hz, 1 H, 11-H), 1.77-1.92 (m, 2 H, 7-H), 1.64-1.71 (m, 2 H, 8-H). ¹³C-NMR (91 MHz, CDCl₃) δ = 169.9, 135.4, 135.0, 130.9, 128.6, 127.2, 121.7, 84.9, 83.6, 69.2, 45.2, 39.3, 36.4, 22.5, 18.7. HRMS-ESI (m/z): C₁₆H₁₇O₂⁺ [M+H]⁺, calc.: 255.13796, found: 255.13801, δ = 0.22 ppm.

Ethyl 2-methyl-3-phenylacrylate (**14**)²¹²



To a solution of benzaldehyde (531 mg, 510 μL, 5.00 mmol, 1.00 eq.) in dichloromethane (15 mL) was added (carbethoxyethylidene)triphenylphosphorane (2.17 g, 6.00 mmol, 1.20 eq.) and the reaction mixture was stirred for 12 h at room temperature. The solvent was evaporated under reduced pressure and the residue was purified by column chromatography (silica gel, hexane/diethyl ether = 3:1) to yield compound **14** (943 mg, 4.96 mmol, 99%) as colourless oil. R_f (hexane/diethyl ether, 3:1) = 0.41. ¹H-NMR (500 MHz, CDCl₃) δ = 7.69 (q, ⁴J_{3,4} = 1.5 Hz, 1 H, 3-H), 7.37-7.41 (m, 4 H, 6-H, 7-H), 7.30-7.34 (m, 1 H, 8-H), 4.28 (q, ³J_{9,10} = 7.1 Hz, 2 H, 9-H), 2.12 (d, ⁴J_{3,4} = 1.5 Hz, 3 H, 4-H), 1.35 (t, ³J_{9,10} = 7.1 Hz, 3 H, 10-H). ¹³C-NMR (91 MHz, CDCl₃) δ = 168.8, 138.8, 136.1, 129.8, 128.8, 128.5, 128.4, 61.0, 14.5, 14.2. HRMS-ESI (m/z): C₁₂H₁₅O₂⁺ [M+H]⁺, calc.: 191.10666, found: 191.10666, δ = 0.19 ppm.

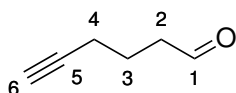
Ethyl 2-(bromomethyl)-3-phenylacrylate (**15**)²¹²



To a solution of compound **14** (500 mg, 2.63 mmol, 1.00 eq.) in tetrachloromethane (35 mL) was added *N*-bromosuccinimide (NBS, 517 mg, 2.90 mmol, 1.10 eq.) and azobisisobutyronitrile (AIBN,

17.2 mg, 0.105 mmol, 0.0345 eq.) and the reaction mixture was stirred for 18 h under reflux. The reaction was cooled to room temperature and dichloromethane (35 mL) was added. The reaction mixture was washed with water (30 mL) and brine (30 mL), dried over Na₂SO₄ and the solvents were evaporated under reduced pressure. The residue was purified by column chromatography (silica gel, hexane/diethyl ether = 5:1) to yield compound **15** (566 mg, 2.22 mmol, 84%) as colourless oil. R_f (hexane/diethyl ether, 5:1) = 0.32. ¹H-NMR (500 MHz, CDCl₃) δ = 7.82 (s, 1 H, 3-H), 7.56-7.60 (m, 2 H, 6-H), 7.44-7.49 (m, 2 H, 7-H), 7.38-7.43 (m, 1 H, 8-H), 4.40 (s, 2 H, 4-H), 4.35 (q, ³J_{9,10} = 7.1 Hz, 2 H, 9-H), 1.38 (t, ³J_{9,10} = 7.1 Hz, 3 H, 10-H). ¹³C-NMR (91 MHz, CDCl₃) δ = 166.3, 142.8, 134.5, 129.8, 129.7, 129.2, 129.0, 61.6, 27.0, 14.4. HRMS-ESI (m/z): C₁₂H₁₄⁷⁹BrO₂⁺ [M+H]⁺, calc.: 269.01717, found: 269.01696, δ = 0.79 ppm. C₁₂H₁₄⁸¹BrO₂⁺ [M+H]⁺, calc.: 271.01512, found: 271.01493, δ = 0.70 ppm.

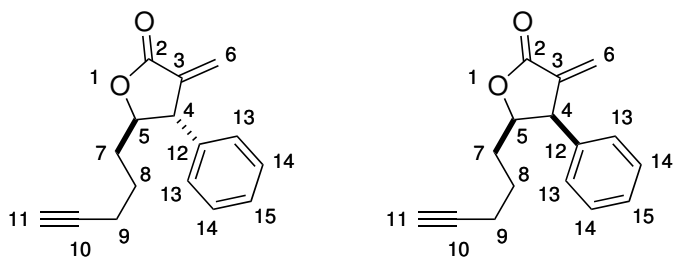
5-Hexyn-1-ol (16)²¹³



Dichloromethane (20 mL) was cooled to -78 °C, oxalyl chloride (1.65 g, 1.12 mL, 13.0 mmol, 2.50 eq.) was added and the reaction mixture was stirred for 5 min at -78 °C. Dimethyl sulfoxide (1.02 g, 923 μL, 13.0 mmol, 2.50 eq.) was added and after gas evolution ceased, the reaction mixture was stirred for further 5 min at -78 °C. 5-Hexyn-1-ol (510 mg, 573 μL, 5.20 mmol, 1.00 eq.) was added and the reaction mixture was stirred for 5 min at -78 °C. Subsequently, triethylamin (2.63 g, 3.63 mL, 26.0 mmol (5.00 eq.)) was added and the reaction mixture was stirred for 15 min at -78 °C. The reaction mixture was warmed to room temperature, washed with HCl_{aq} (0.5 M, 15 mL), saturated NaHCO₃ (15 mL), dried over MgSO₄, filtered and solvents were evaporated under reduced pressure. The residue was purified by fractional vacuum distillation to yield compound **16** (1.02 g, 8.06 mmol, 62%) as colourless oil. Data is consistent with that reported in the literature.²¹³ R_f (hexane/diethyl ether, 4:1) = 0.45. ¹H-NMR (500 MHz, CDCl₃) δ = 9.81 (s, 1 H, 1-H), 2.61 (td, ³J_{2,3} = 7.2 Hz, ³J_{1,2} = 1.4 Hz, 2 H, 2-H), 2.27 (td, ³J_{3,4} = 6.9 Hz, ⁴J_{4,6} = 2.7 Hz, 2 H, 4-H), 1.98 (t, ⁴J_{4,6} = 2.7 Hz, 1 H, 6-H), 1.85 (p, ³J_{2,3} = ³J_{3,4} = 7.1 Hz, 2 H, 3-H). ¹³C-NMR (91 MHz, CDCl₃) δ = 201.89, 83.31, 69.50, 42.67, 20.92, 17.91.

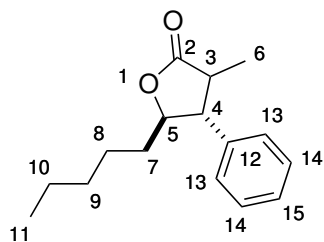
(4*S**,5*R** and 4*R**,5*R**)-3-methylene-5-(pent-4-yn-1-yl)-4-phenyldihydrofuran-2(3*H*)-one (3, 4)²¹¹,

214



Zinc dust (1.0 g) was activated by rinsing with 0.5 M HCl_{aq} (10 mL), water (10 mL), anhydrous ethanol (10 mL), and diethyl ether (10 mL). The substance was then dried in vacuo (0.05 mbar at 150 °C) overnight and cooled to room temperature under argon atmosphere. To a solution of compound **16** (45.2 mg, 0.470 mmol, 1.20 eq.) in THF (7 mL) was added freshly activated zinc dust (30.8 mg, 0.470 mmol, 1.20 eq.) and the mixture was stirred for 15 min at 37 °C. Compound **15** (100 mg, 0.392 mmol, 1.00 eq.) in THF (7 mL) was added and the mixture stirred for 15 h at 37 °C. The reaction mixture was cooled to room temperature, HCl_{aq} (10% w/v, 7 mL) was added and the mixture was stirred for 30 min at room temperature. The solution was filtered and extracted with ethyl acetate (3 x 30 mL). The organic layer was washed with water (60 mL), brine (60 mL), dried over Na₂SO₄, filtered and the solvents were evaporated under reduced pressure. The residue was purified by column chromatography (silica gel, hexane/ethyl acetate = 10:1 to 3:1) to yield racemic compounds **3** (17.7 mg, 0.074 mmol, 19%) and **4** (49.7 mg, 0.207 mmol, 53%) as colourless oils. **Diastereomer 3:** *R*_f(hexane/Et₂O, 3:1) = 0.46. **¹H-NMR** (500 MHz, CDCl₃) δ = 7.36-7.40 (m, 2 H, 14-H), 7.30-7.35 (m, 1 H, 15-H), 7.19-7.23 (m, 2 H, 13-H), 6.36 (d, ⁴*J*_{4,6-Z} = 3.3 Hz, 1 H, 6-Z-H), 5.39 (d, ⁴*J*_{4,6-E} = 2.8 Hz, 1 H, 6-E-H), 4.40 (td, ³*J*_{4,5} = ³*J*_{5,7a} = 7.9 Hz, ³*J*_{5,7b} = 4.0 Hz, 1 H, 5-H), 3.79 (dt, ³*J*_{4,5} = 6.8 Hz, ⁴*J*_{4,6-Z} = ⁴*J*_{4,6-E} = 3.2 Hz, 1 H, 4-H), 2.22 (td, ³*J*_{8,9} = 6.9 Hz, ⁴*J*_{9,11} = 2.6 Hz, 2 H, 9-H), 1.73-1.1.96 (m, 4 H, 7-H, 8-H_a, 11-H), 1.56-1.65 (m, 1 H, 8-H_b). **¹³C-NMR** (91 MHz, CDCl₃) δ = 169.8, 140.3, 139.0, 129.3, 128.5, 128.0, 123.9, 85.1, 83.5, 69.2, 52.8, 33.8, 24.4, 18.3. **HRMS-ESI** (m/z): C₁₆H₁₇O₂⁺ [M+H]⁺, calc.: 241.12231, found: 241.12211, δ = 0.80 ppm. **Diastereomer 4:** *R*_f(hexane/Et₂O, 3:1) = 0.35. **¹H-NMR** (500 MHz, CDCl₃) δ = 7.33-7.37 (m, 2 H, 14-H), 7.29-7.33 (m, 1 H, 15-H), 7.13-7.16 (m, 2 H, 13-H), 6.45 (d, ⁴*J*_{4,6-Z} = 2.8 Hz, 1 H, 6-Z-H), 5.62 (d, ⁴*J*_{4,6-E} = 2.5 Hz, 1 H, 6-E-H), 4.73 (ddd, ³*J*_{5,7a} = 9.9 Hz, ³*J*_{4,5} = 7.9 Hz, ³*J*_{5,7b} = 3.8 Hz, 1 H, 5-H), 4.37 (dt, ³*J*_{4,5} = 7.8 Hz, ⁴*J*_{4,6-Z} = ⁴*J*_{4,6-E} = 2.6 Hz, 1 H, 4-H), 2.04-2.16 (m, 2 H, 9-H), 1.86 (t, ⁴*J*_{9,11} = 2.7 Hz, 1 H, 11-H), 1.65-1.74 (m, 1 H, 8-H_a), 1.42-1.52 (m, 1 H, 8-H_b), 1.31-1.39 (m, 1 H, 7-H_a), 1.22-1.30 (m, 1 H, 7-H_b). **¹³C-NMR** (91 MHz, CDCl₃) δ = 170.4, 139.0, 137.5, 129.2, 128.9, 127.9, 124.6, 83.6, 81.3, 69.0, 49.5, 31.5, 24.8, 18.1. **HRMS-ESI** (m/z): C₁₆H₁₇O₂⁺ [M+H]⁺, calc.: 241.12231, found: 241.12211, δ = 0.80 ppm.

(4*R,5*R**)-3-methyl-5-pentyl-4-phenyldihydrofuran-2(3*H*)-one (10)**



To a solution of compound **3** (100 mg, 0.406 mmol, 1.00 eq.) in ethanol (10 mL) was added 5% Pd on carbon (5.00 mg) and the mixture was stirred for 24 h at room temperature under hydrogen atmosphere. The solvent was evaporated under reduced pressure and the residue was purified by column chromatography (silica gel, hexane/ethyl acetate = 10:1) to yield inseparable racemic diastereomers **10** (89.0 mg, 0.361 mmol, 89%) as colourless oil. R_f (hexane/EtOAc, 5:1) = 0.49. $^1\text{H-NMR}$ (500 MHz, CDCl_3) δ = 7.37-7.42 (m, 2 H, 14-H, major diastereomer), 7.36-7.29 (m, 1.2 H, 15-H major, 14-H minor), 7.23-7.27 (m, 2.1 H, 13-H major, 15-H minor), 7.13-7.16 (m, 0.2 H, 13-H minor), 4.68-4.73 (m, 0.1 H, 5-H minor), 4.36-4.41 (m, 1 H, 5-H major), 3.37-3.42 (m, 0.1 H, 4-H minor), 2.99-3.07 (m, 0.1 H, 3-H minor), 2.77-2.86 (m, 2 H, 3-H major, 4-H major), 1.6-1.68 (m, 2.2 H, 7-H both), 1.45-1.56 (m, 1.1 H, 8_b-H both), 1.17-1.37 (m, 8.8 H both, 6-H both, 8_a-H both, 9-H both, 10-H both), 0.88-0.92 (m, 0.3 H, 11-H, minor), 0.82-0.87 (m, 3 H, 11-H, major). $^{13}\text{C-NMR}$ (91 MHz, CDCl_3) δ = 179.35, 178.18, 138.33, 137.48, 129.25, 129.01, 128.02, 127.85, 127.59, 84.50, 84.15, 56.92, 50.62, 43.96, 39.00, 34.79, 33.67, 31.61, 25.59, 25.53, 22.63, 22.55, 14.10, 14.07, 13.41, 11.60. **HRMS-ESI** (m/z): $\text{C}_{16}\text{H}_{23}\text{O}_2^+$ $[\text{M}+\text{H}]^+$, calc.: 247.16926, found: 247.16920, δ = 0.22 ppm.

Hemolysis Assay. *S. aureus* was grown in B broth shaking at 37 °C until cell density reached OD_{600} = 0.6-0.8. Fresh B broth was inoculated with 2×10^6 bacteria/mL and to 1 mL aliquots was added probe in DMSO (1 μL). The cultures were incubated overnight (16 h) shaking at 37 °C. The OD_{600} was measured to check the effect of substances on bacterial growth. Cultures were centrifuged (10 min, 13,000 g) and 100 μL of each supernatant (triplicates for each culture) were pipetted into 96 well plates. Positive controls (1 μL DMSO) and negative controls (1 mL sterile broth) were included. Erythrocyte suspension (50 μL) was added to each well and the plate was incubated for 10 min shaking at 37 °C. The OD_{600} , which correlates with the amount of intact erythrocytes, was measured by a Tecan Infinite® M200 PRO plate reader.

Determination of MIC-Values. *S. aureus* was grown in B broth shaking at 37 °C until cell density reached OD_{600} = 0.6-0.8. Fresh B broth (Yeast extract (5.0 g), tryptic peptone (10.0 g), NaCl (5.0 g), K_2HPO_4 (1.0 g), H_2O (1.0 l)) was inoculated with 2×10^6 bacteria/mL and 99 μL

of this culture were added to each well of a 96 well plate. Probe in DMSO (1 μ L, varying concentrations) was added and control wells containing no probe (1 μ L DMSO) or no bacteria (99 μ L B broth) were included. The plate was incubated at overnight (16 h) shaking at 37 °C and the resulting optical density was measured by a Tecan Infinite® M200 PRO plate reader.

MTT assay for cytotoxicity determination. HeLa cells were cultured in RPMI 1640 medium supplemented with 2 mM L-glutamine and 10% FCS (fetal calf serum). Cells were plated in 96 well flat-bottom plates (4,500 cells in 100 μ L medium for each well) and cultured for 24 h at 37 °C and 5% CO₂. Culture medium was removed and probes (DMSO stocks) were diluted 1:1,000 in new culture medium and added to cells. After 24 h incubation at 37 °C and 5% CO₂, MTT solution (20 μ L, 5mg/mL in PBS) was added followed by incubation for 2 h at 37 °C, 5% CO₂. The culture medium was removed and DMSO added (200 μ L) to dissolve the formazan salt (metabolic product of MTT). The resulting optical density was measured at 579 nm (background subtraction at 630 nm) by a TECAN Infinite M200 pro plate reader. All measurements were performed in triplicates and EC₅₀ values were calculated from curve fittings.

In situ labelling. Bacteria were grown in lysogeny broth (LB, for *E. coli* strains) or in brain heart broth (BHB, for *S. aureus* strains) and a quantity equivalent with 1 mL of OD₆₀₀ = 4 was harvested 1 h after reaching stationary phase by centrifugation (10 min, 4,000 g, 4 °C) for analytical and 5 mL for preparative studies, respectively. After washing with PBS, the cells were resuspended in 200 μ L and 500 μ L of PBS for analytical and preparative experiments. Unless indicated otherwise, bacteria were incubated for 2 h with varying concentrations of probe (1 μ L in DMSO) at RT. Subsequently, the cells were washed three times with 1 mL PBS and lysed with a cell homogenizer (Precellys 24 and Precellys Glas-Kit 0.5 mm Small, PEQLAB Biotechnologies GmbH). Membrane and cytosol were separated by centrifugation (30 min, 21,000 g, 4 °C). For heat controls, the cells were lysed, the proteins were denatured with 2 μ L of SDS (21.5 % in ddH₂O) at 96 °C for 6 min and cooled to RT before the probe was applied.⁵⁶

Click reaction and analytical gel-based analysis. In case of analytical labelling, the click reaction was carried out with 44 μ L of proteome, so that after addition of all reagents a total volume of 50 μ L was reached. Both, cytosol fraction and membrane fraction were analysed separately. Therefore, 1 μ L RhN₃ (5 mM in DMSO) was added to 44 μ L of proteome, followed by 1 μ L TCEP solution (53 mM in ddH₂O) and 3 μ L ligand TBTA (83 mM in DMSO/*tert*-butanol). Samples were gently vortexed and the cycloaddition was initiated by the addition of 1 μ L CuSO₄ solution (50 mM

in ddH₂O). The reaction was incubated for 1 h at RT. For analytical gel electrophoresis, 50 µL 2×SDS loading buffer were added and 50 µL were applied on the gel. Roti[®]-Mark STANDARD (*Carl Roth GmbH & Co. KG*, for Coomassie staining) and BenchMark™ Fluorescent Protein Standard (*Life Technologies Corp.*) were applied as markers to determine the protein mass. After application of the protein samples, the gels were developed for 4-5 h with 300 V. Fluorescence scans of SDS gels were performed with a *Fujifilm* Las-4000 luminescent image analyser containing a VRF43LMD3 lens and a 575DF20 filter.

Click reaction and preparative gel-based analysis. The cytosol fraction was used for preparative analysis. 3 µL trifunctional linker¹⁹⁰ (10 mM in DMSO) was added to 500 µL labelled proteome, followed by 10 µL TCEP solution (53 mM in ddH₂O) and 30 µL ligand TBTA (83 mM in DMSO/*tert*-butanol). The samples were gently vortexed and the cycloaddition was initiated by the addition of 10 µL CuSO₄ solution (50 mM in ddH₂O). The reaction was allowed to proceed for 1 h at RT. Reactions for enrichment were carried out together with a control lacking the probe to compare the results of the biotin-avidin enriched samples with the background of unspecific protein binding on avidin-agarose beads. The proteins were precipitated by addition of cold acetone (1 mL, -80 °C) and incubation for 18 h at -20 °C. Then the proteins were pelletized (15 min, 21,000 g, 4 °C) and the supernatant was discarded. The proteins were washed with prechilled methanol (2 × 200 mL, -80 °C, resuspension by sonication, 5-10 sec, 10 % max. intensity; 15 min, 21,000 g, 4 °C). Subsequently, the pellet was dissolved at RT in 1 mL 0.4 % SDS in PBS by sonication and incubated under gentle mixing with 50 µL of prewashed (3 × 1 mL 0.4 % SDS in PBS) avidin-agarose beads (avidin-agarose from egg white, 1.1 mg/mL in aqueous glycerol suspension, *Sigma-Aldrich Co. LLC*) for 2 h at RT. The beads were washed with 0.4 % SDS in PBS (3 × 1 mL), aqueous urea (6 M, 2 × 1 mL) and PBS (3 × 1 mL). 50 µL of 2×SDS loading buffer were added and the proteins were released for preparative SDS-PAGE by incubation for 6 min at 96 °C. The beads were pelletized (3 min, 21,000 g) and the supernatant was isolated and stored at -80 °C. The supernatant was applied on a preparative gel, and developed for 4-5 h (300 V). After gel electrophoresis, the bands were visualized using a *Fujifilm* Las-4000 luminescent image analyser containing a VRF43LMD3 lens and a 575DF20 filter. The observed bands were cut out, isolated and reduced to small pieces, prior to further processing.

Click reaction and preparative gel-free analysis. The cytosol fraction was used for preparative analysis. 3 µL trifunctional linker (10 mM in DMSO) were added to 500 µL labelled proteome, followed by 10 µL TCEP solution (53 mM in ddH₂O) and 30 µL TBTA (83 mM in DMSO/*tert*-butanol). The samples were gently vortexed and the cycloaddition was initiated by the addition of 10 µL

CuSO₄ solution (50 mM in ddH₂O). The reaction was allowed to proceed for 1 h at RT. Reactions for enrichment were carried out together with a control lacking the probe to compare the results of the biotin-avidin enriched samples with the background of unspecific protein binding on avidin-agarose beads. The proteins were precipitated by addition of cold acetone (1 mL, -80 °C) and incubation for 18 h at -20 °C. Then the proteins were pelletized (15 min, 21,000 g, 4 °C) and the supernatant was discarded. The proteins were washed with prechilled methanol (2 × 200 mL, -80 °C, resuspension by sonication, 5-10 sec, 10 % max. intensity; 15 min, 21,000 g, 4 °C). Subsequently, the pellet was dissolved at RT in 1 mL 0.4 % SDS by sonication and incubated under gentle mixing with 50 µL of prewashed (3 × 1 mL 0.4 % SDS) avidin-agarose beads (avidin-agarose from egg white, 1.1 mg/mL in aqueous glycerol suspension, *Sigma-Aldrich Co. LLC*) for 2 h at RT. The beads were washed with 0.4 % SDS in PBS (4 × 1 mL), aqueous urea (6 M in ddH₂O, 4 × 1 mL) and PBS (4 × 1 mL). The beads were suspended in HEPES buffer (20 mM, pH = 7.5) containing urea (7 M) and thiourea (2 M). The proteins were reduced by addition of DTT (1 M in ddH₂O, 0.2 µL, 45 min, RT) and then alkylated by addition of iodoacetamide (0.55 M in ddH₂O, 2 µL, 30 min, RT, in the dark). The reaction was quenched by addition of DTT (1 M in ddH₂O, 30 min, RT). The proteins were first digested with Lys-C (0.5 µg/µL in 50 mM HEPES in ddH₂O, pH = 8, 1 µL, 4 h in the dark, RT). The digest was then diluted with TEAB (50 mM in ddH₂O, 600 µL) and trypsin (0.5 µg/µL in 50 mM acetic acid in ddH₂O, 1.5 µL) was added. After incubation for 18 h at 37 °C the reaction was stopped by addition of formic acid (4 µL). The beads were pelletized (1 min, 1000 g) and the supernatant was transferred into LoBind tube (*Eppendorf AG*). The beads were once washed with 0.1 % FA (100 µL, 1 min, 21,000 g) and the supernatant was transferred into the LoBind tube. The samples were desalted using Sep-Pak C18 1 cc Vac Cartridges (*Waters Corp.*). The cartridges were first equilibrated with ACN (1 × 1 mL), elution buffer (ACN/H₂O/FA = 80:19.5:0.5 v/v/v, 1 × 1 mL) and 0.1 % TFA (in ddH₂O, 1 × 1 mL). Then the sample was applied to the cartridge and the proteins were washed with 0.1 % TFA (in ddH₂O, 1 × 1 mL) and 0.5 % FA (in ddH₂O, 1 × 0.5 mL). The proteins were eluted into a LoBind tube (ACN/H₂O/FA = 80:19.5:0.5 v/v/v, 2 × 250 µL) and concentrated *in vacuo* in a vacuum centrifuge (4 h, 1 mbar, RT). The remaining peptides were stored at -20 °C.

In gel digestion. The gel pieces corresponding to fluorescent bands were directly cut on the gel and washed with ddH₂O (100 µL, 15 min, 550 rpm, RT), MeCN/50 mM ammonium bicarbonate (200 µL, 15 min, 550 rpm, RT) and MeCN (100 µL, 10 min, 550 rpm, RT). The shrunken gel pieces were swollen in 50 mM ammonium bicarbonate (100 µL, 5 min, 550 rpm, RT), before additional MeCN (100 µL, 15 min, 550 rpm, RT) was added. The supernatant was removed and the gel pieces were again washed with MeCN (100 µL, 10 min, 550 rpm, RT) and then dried under vacuum in a

centrifugal evaporator (15 min, 1 mbar, RT). The proteins were reduced by addition of DTT solution (10 mM in 50 mM ammonium bicarbonate, 100 μ L, 45 min, 550 rpm, 56 °C) to the gel pieces. The pieces were then washed with MeCN (100 μ L, 10 min, 550 rpm, RT), prior to alkylation with iodacetamide solution (55 mM in 50 mM ammonium bicarbonate, 100 μ L, 30 min in the dark, 550 rpm, RT). The gel pieces were afterwards washed with MeCN/50 mM ammonium bicarbonate (100 μ L, 15 min, 550 rpm, RT) and MeCN (100 μ L, 10 min, 550 rpm, RT) and then dried *in vacuo* in a centrifugal evaporator (15 min, 1 mbar, RT). Digest solution was added (100 μ L, 10 min, 4 °C then 37 °C, 300 rpm overnight). The next day the supernatant was transferred into a LoBind tube (*Eppendorf AG*) and 25 mM ammonium bicarbonate (100 μ L, 15 min sonication, RT) was added to the gel pieces. Then MeCN (100 μ L) was added and the sample sonicated for 15 min. The supernatant was then transferred into the same LoBind tube. 5 % FA (100 μ L, 15 min sonication, RT) was added to the gel pieces, followed by additional MeCN (100 μ L, 15 min sonication, RT). The supernatant was then transferred into the same LoBind tube and replaced by MeCN (100 μ L, 15 min sonication, RT). The supernatant was transferred into the LoBind tube and the solvent was removed *in vacuo* in a vacuum centrifuge (4 h, 1 mbar, RT). The remaining peptides were stored at -80°C.¹¹²

Sample preparation for mass spectrometry. Centrifugal filters (modified Nylon, 0.45 μ m, low protein binding, *VWR International, LLC*) were pre-rinsed with ddH₂O (1 \times 500 μ L, 13000 rpm, 1 min, RT), aqueous NaOH (1 \times 500 μ L, 13000 rpm, 1 min, RT), ddH₂O (2 \times 500 μ L, 13000 rpm, 1 min, RT) and 1 % FA (1 \times 500 μ L, 13000 rpm, 1 min, RT). The peptides were dissolved in 1 % FA (20 μ L, 15 min sonication, RT) and added to the pre equilibrated filters and centrifuged (13000 rpm, 1 min, RT). The filtrate was transferred into a vial and stored at 4 °C until the measurement was performed.

Identification of binding sites. To analyse the binding sites of **3** and to identify the respective sites, recombinant proteins were incubated with a 10-fold excess of inhibitor for 30 min at RT. Unbound probe was removed during three buffer exchange steps with 25 mM ammonium hydrogen carbonate using size exclusion filters (5 kDa, *Sartorius Stedim Biotech S.A.*). Labelled proteins were digested overnight with trypsin or chymotrypsin (*Promega Corp.*), which were added at a ratio of 1:100 (w/w) of the protein amount. Acidifying the sample with trifluoroacetic acid to a final concentration of 0.5 % stopped the digest. Samples were filtered and directly used for MS analysis.

Mass spectrometry and bioinformatics. Measurements were performed using an Orbitrap XL coupled online to an Ultimate 3000 nano HPLC system (*Thermo Fisher Scientific Inc.*). Samples were loaded on a trap column and separated on a 15 cm C18 column (2 μm , 100 \AA , *Thermo Fisher Scientific Inc.*) during a 50 min gradient from 5 to 30 % acetonitrile, 1 % formic acid. For protein identification either the five most intense ions of the full scan were fragmented using CID or a combination of CID of the three most intense ions and HCD of the two most intense ions was performed. The mass spectrometry data were searched using the SEQUEST algorithm against the corresponding databases via the Proteome Discoverer Software 1.3 (*Thermo Fisher Scientific Inc.*). Protein *N*-terminal acetylation, oxidation on methionine and additional masses for the specific inhibitors were added as variable modifications. Depending on the enzyme used for the digest, enzyme specificity was set to trypsin or chymotrypsin and mass tolerances of the precursor and fragment ions to 10 ppm and 0.5 Da, respectively. Only sites found with high confidence and localization probabilities better than 0.99 that were identified with the most spectra were considered as binding sites. Results are shown in Table S2 and S3.

Recombinant expression. The major hits of MS analysis were recombinantly expressed in *E. coli* as an internal control of the MS results by using the Invitrogen™ Gateway® Technology. Target genes were amplified from the corresponding genomes by PCR with an AccuPrime™ Pfx DNA Polymerase kit with 65 ng of genomic DNA, prepared by standard protocols. *attB1* forward primer and *attB2* reverse primer were designed to yield *attB*-PCR Products needed for Gateway® Technology. PCR products were identified on agarose gels and gel bands were isolated and extracted with an E.Z.N.A.™ MicroElute™ Gel Extraction Kit. Concentrations of DNA were measured by a Tecan Infinite® M200 PRO plate reader. 100 fmol of purified *attB*-PCR product and 50 fmol of *attP*-containing donor vector pDONR™ 201 in TE buffer were used for *in vitro* BP recombination reaction with BP Clonase™ II enzyme mix to yield the appropriate *attL*-containing entry clone. After transformation in chemically competent One Shot® TOP10 *E. coli* (Invitrogen), cells were plated on LB agar plates containing 25 $\mu\text{g mL}^{-1}$ kanamycin. Clones of transformed cells were selected and grown in kanamycin LB. Cells were harvested and plasmids were isolated using an E.Z.N.A.™ Plasmid Mini Kit. The corresponding *attB*-containing expression clone was generated by *in vitro* LR recombination reaction of approx. 50 fmol of the *attL*-containing entry clone and 50 fmol of the *attR*-containing destination vector pDest using LR Clonase™ II enzyme mix in TE buffer. The expression clone was transformed in chemically competent BL21 *E. coli* cells (Novagen) and selected on LB agar plates containing 100 $\mu\text{g mL}^{-1}$ ampicillin. Validity of the clones was confirmed by plasmid sequence analysis. Recombinant clones were grown in ampicillin LB and target gene

expression was induced with anhydrotetracyclin. The bacterial cell pellets were washed with PBS, resuspended in binding buffer (100 mM Tris-HCl pH 8.0, 150 mM NaCl, 1 mM EDTA), lysed by French press and sonication. The protein was then purified with StrepTrap™ HP columns and stored in the corresponding buffer.

Primer for recombinant expression.

MgrA, *S. aureus* NCTC 8325

Forward 5'-GGGGACAAGTTTGTACAAAAAAGCAGGCTTTATGTCTGATCAACATAATTTAAAAGA

Reverse 5'-GGGGACCACTTTGTACAAGAAAGCTGGGTGTTATTTTCCTTTGTTTCATCAAATG

SarA, *S. aureus* NCTC 8325

Forward 5'-GGGGACAAGTTTGTACAAAAAAGCAGGCTTTATGGCAATTACAAAAATCAATGATTG

Reverse 5'-GGGGACCACTTTGTACAAGAAAGCTGGGTGTTATAGTTCAATTCGTTGTTTGCTT

SarR, *S. aureus* NCTC 8325

Forward 5'-GGGGACAAGTTTGTACAAAAAAGCAGGCTTTATGAGTAAAATTAATGACATTAATGATTT

Reverse 5'-GGGGACCACTTTGTACAAGAAAGCTGGGTGTTAATTTTAAATGTATTCTTCTAATTCTG

TrxA, *S. aureus* NCTC 8325

Forward 5'-GGGGACAAGTTTGTACAAAAAAGCAGGCTTTATGGCAATCGTAAAAGTAACAGA

Reverse 5'-GGGGACCACTTTGTACAAGAAAGCTGGGTGTTATAAATGTTTATCTAAACTTCAGCTA

MurA inhibition assay.^{71, 194} The inhibition of MurA1 and MurA2 by probe **3** was measured by examining the release of pyrophosphate from the MurA-catalysed enolpyruvyl transfer reaction with phosphoenolpyruvate (PEP) and UDP-*N*-acetylglucosamine (UDPAG) in a malachite green heptamolybdate assay. MurA1 and MurA2 from *S. aureus* NCTC 8325 were purified as described in “Recombinant Expression” and immediately desalted into 50 mM Hepes buffer pH 7.5. To MurA1 and MurA2 (5 μM and 1 μM in 60 μL 50 mM Hepes buffer pH 7.5) was added 1.2 μL probe **3** (DMSO solution) and the well plate was incubated 30 min at room temperature. 53.8 μL UDPAG-Solution (in 50 mM Hepes pH 7.5, final UDPAG concentration 1 mM) was added and the plate incubated for 10 min at room temperature. Then to each well was added 5 μL of 24 mM PEP (in 50 mM Hepes buffer pH 7.5, final PEP concentration 1 mM). The plate was shaken for 10 min, and allowed to sit at room temperature for 30 min. 20 μL from each well was withdrawn and mixed in another well plate with 80 μL of a 3:1 mixture of 0.045% malachite green in H₂O and 4.2% ammonium heptamolybdate in 4 M HCl. After 10 min, the absorption at 660 nm was read with a

Tecan Infinite® M200 PRO plate reader. Each concentration was tested in at least three independent trials in triplicates.

TrxA-Assay.²⁰² The TrxA-catalysed reduction of disulfide bonds within insulin was measured by a well-established assay (Holmgren, 1979). Insulin becomes therefore insoluble and the enzyme turnover can be followed by increasing turbidity. Insulin solutions were prepared by suspending insulin (50 mg, Sigma Aldrich) in 50 mM Tris-HCl (4 mL, pH 8.0) followed by addition of HCl_{aq} (1 M) until pH 2-3 and rapid addition of NaOH_{aq} (1 M) until pH 8.0 was reached. Finally the volume was adjusted to 5 mL with water. The insulin stocks were stored at -20 °C. DTT in (100 mM in H₂O) was prepared fresh each day and was stored at 4 °C. TrxA buffer consisted of 100 mM KH₂PO₄ pH 7.0 and 2 mM EDTA. Measurements were done in 96 well plates at room temperature in a total volume of 200 µL. Thioredoxin (170 µM in TrxA buffer) was reduced by 10-fold molar excess of DTT solution for 1 h on ice and diluted in TrxA buffer to a final concentration of 1 µM. 176 µL of TrxA dilution were added to each well of a 96 well plate (triplicates) and increasing concentration of probe **3** (2 µL in DMSO) was added. The plate was incubated for 2 h at room temperature. Insulin solution (20 µL) and DTT solution (2 µL) were added and the absorption at 650 nm was recorded on a Tecan Infinite® M200 PRO plate reader every 2 min for 30 min at room temperature. Each concentration was tested in at least three independent trials in triplicates.

Electrophoretic Mobility Shift Assay (EMSA).¹⁷⁸ The Alexa Fluor 488 (AF488) labeled *agr* promoter fragment of NCTC8325 was generated by PCR and then purified by an Omega Bio-Tek MicroElute Cycle-Pure Kit. MgrA, SarA and SarR were purified as described in the Supplementary Information and aliquots were stored in 100 mM Tris-HCl pH 8.0, 150 mM NaCl and 1 mM EDTA at -80 °C. To 10.8 µL EMSA-Binding-Buffer (100 mM Tris-HCl pH 8.0, 150 mM NaCl, 1 mM EDTA, 5% Glycerol) containing MgrA (1.75 µM), SarA (2.50 µM) or SarR (4.00 µM) were added 0.2 µL probe of the desired concentration in DMSO and the mixture was incubated 1.5 h at room temperature. Then 1 µL of *agr* promoter fragment mixed with salmon sperm DNA (Carl Roth, Karlsruhe) was added leading to final concentrations of 5 nM (7.5 ng) *agr* promoter fragment and 2 µg/µL salmon sperm DNA (Carl Roth, Karlsruhe). After incubation for 15 min at room temperature, 2 µL EMSA-Loading-Buffer (100 mM Tris-HCl pH 8.0, 150 mM NaCl, 1 mM EDTA, 5% Glycerol, 0.1% bromphenol blue) were added and the samples were applied on 5% TBE polyacrylamide gels (150 V, 45 min). Fluorescence was recorded in a Fujifilm Las-4000 luminescent image analyser with a Fujinon VRF43LMD3 lens and an Y515-Di filter. Forward primer: 5'-caattttacaccactctcctc (5'-AF488), Reverse primer: 5'-catcaactattttccatcacatct (5'-AF488).

Construction of NCTC8325 mutants.²¹⁵ We constructed *mgrA*, *sarA*, *sarR* and *sarA/sarR* mutants from strain NCTC8325 by phage ϕ 11 transduction of *mgrA::cat*, *sarA::kan* and *sarR::erm* as described previously. Colonies of interest were selected on BHI agar plates containing sodium citrate (10 g/ml) and the corresponding antibiotics (chloramphenicol 5 μ g/ml, kanamycin 50 μ g/mL or erythromycin 5 μ g/mL). Mutations were confirmed by PCR reactions of the corresponding genes and their flanking regions.

Invasion assay for *S. aureus* infected human macrophages. Human THP-1 monocytes were seeded in a 6-well plate (1×10^6 cells/well in 2 mL RPMI1640 medium containing 10% fetal calf serum and 5 mM L-glutamine) and PMA (phorbol 12-myristate 13-acetate, 40 ng/well) was added. Cells were incubated for 2 days (37°C; 5% CO₂), medium was removed, cells were washed three times with PBS (RT) and fresh medium was added. Bacteria (*S. aureus* NCTC8325) were inoculated in fresh B-medium (1:100), incubated to an OD₆₀₀ of 0.4-0.5 and diluted to 3.4×10^7 bacteria/mL (formula $y = 4E+07e^{1.0958x}$). Bacteria were supplemented with respective inhibitory compounds (1000 x DMSO stocks) and incubated for 16 h (37 °C, 200 rpm). Bacterial culture was diluted in B-medium (1:10) and OD₆₀₀ was measured. CFU was calculated (see formula) and 5×10^7 bacteria (MOI 50, confluent monolayer in 6-well plate 1×10^6 cells) were diluted in 2 mL RPMI1640/10% FCS/5 mM L-glutamine. The respective compound (non-lethal concentration, 2 μ M, 1000 x DMSO stocks) was added to bacterial suspensions and 2 mL of the bacterial suspension was added to the cells (2 mL without bacteria as control). Infected cells were incubated for 2 h (37 °C, 5% CO₂), supernatant was removed and collected for CFU-plating assay of the inoculum. Cells were washed four times with ice cold PBS and 2 ml medium containing gentamycin (50 μ g/mL) was added. Cells were incubated for 24 h with gentamycin to kill all extracellular bacteria and proceed intracellular replication of invaded bacteria. Afterwards cells were washed once with PBS (1 mL) and 0.5% saponin (1 mL)/B-medium was added. Incubation of cells proceeded for 10 min at 37 °C (5% CO₂) and then the lysate was plated out by using different dilutions. Quantitative analysis of bacterial concentrations was performed by counting CFUs one day after plating. Dilutions for CFU-plating assay: inoculum: 10^{-2} , 10^{-3} , 10^{-4} ; supernatants: 10^0 ; lysed cells: 10^{-1} , 10^{-2} in B-medium. Plates were incubated overnight (37°C) and colonies counted subsequently.²⁰⁹

Appendix

Table S1: *S. aureus* strains used in this study.

Strain	Relevant Characteristics	Source or Reference
RN4220	Restriction-deficient transformation recipient	Kreiswirth et al. (1983) ²¹⁶
RN6390	Laboratory strain related to 8325-4, <i>rsbU</i> ⁻	Novick (1993) ²¹⁷
NCTC8325	Standard laboratory strain, <i>rsbU</i> ⁻	Novick (1967) ²¹⁸
NCTC8325-4	NCTC8325 strain cured of three prophages	Novick (1967) ²¹⁸
Mu50	Aminoglycosides and tetracycline resistant strain	Hiramatsu et al. (1997) ²¹⁹
USA300 FPR3757	Clinically associated strain	LGS Standards (Wesel, Germany)
RN6390 $\Delta mgrA$	RN6390, <i>mgrA::cat</i> (Cm ^r)	Troung-Balduc et al. (2008) ¹⁸³
PC1839	NCTC8325-4, <i>sarA::km</i> (Km ^r)	Chan & Foster (1998) ¹⁶⁷
WA1396	NCTC8325-4, <i>sarR::ermB</i> (Em ^r)	Gustafsson & Oscarsson (2008) ¹⁸⁴
WA1461	NCTC8325-4, <i>sarA::km, sarR::ermB</i> (Km ^r Em ^r)	Gustafsson & Oscarsson (2008) ¹⁸⁵
NCTC8325 $\Delta mgrA$	NCTC8325, <i>mgrA::cat</i> (Cm ^r)	this study
NCTC8325 $\Delta sarA$	NCTC8325, <i>sarA::km</i> (Km ^r)	this study
NCTC8325 $\Delta sarR$	NCTC8325, <i>sarR::ermB</i> (Em ^r)	this study
NCTC8325 $\Delta sarA/R$	NCTC8325, <i>sarA::km, sarR::ermB</i> (Km ^r Em ^r)	this study

Cm^r, resistance to chloramphenicol; Em^r, resistance to erythromycin; Km^r, resistance to kanamycin; Tc^r, resistance to tetracyclin.

Table S2: Proteins identified by gel-based analysis.

Strain	Protein Abbreviation	Protein Description	Accession Number	Replicates	Sequence Coverage	Unique Peptides	PSMs	Scores of individual experiments				AAs	MW
Mu50	AacA-AphD	Bifunctional AAC/APH	P0A0C0	2	36	15	42	47.5	65.8	-	-	479	56.8
	MurA1	UDP-N-acetylglucosamine 1-carboxyvinyltransferase 1	Q931H5	2	11	4	7	8.0	11.3	-	-	421	45.0
	MurA2	UDP-N-acetylglucosamine 1-carboxyvinyltransferase 2	P65456	4	53	14	81	87.3	102.7	27.4	30.8	419	45.0
	MgrA	HTH-type transcriptional regulator	Q99VT5	4	42	5	13	25.2	7.2	6.3	ni	147	17.1
	SarA	Transcriptional regulator	Q7A2W5	4	31	4	10	7.8	8.6	11.6	ni	124	14.7
	SarR	HTH-type transcriptional regulator	Q7A2M3	4	32	4	25	19.8	33.1	14.7	10.1	115	13.7
	TrxA	Thioredoxin	P0A0K4	4	36	3	10	9.6	16.8	5.4	ni	104	11.4
NCTC8325	MgrA	HTH-type transcriptional regulator	Q2G0B1	4	50	7	27	11.0	5.9	34.7	23.7	147	17.1
	SarA	Transcriptional regulator	Q2G2U9	4	31	4	10	6.0	13.3	9.2	ni	124	14.7
	SarR	HTH-type transcriptional regulator	Q9F0R1	4	46	5	43	29.5	51.6	43.7	13.5	115	13.7
	TrxA	Thioredoxin	Q2FZD2	4	48	4	18	11.9	21.4	22.2	ni	104	11.4
USA300	MgrA	Transcriptional regulator MarR family	Q2FIV3	2	31	5	9	5.9	21.3	-	-	147	17.1
	SarA	Transcriptional regulator	Q2FJ20	2	46	6	13	14.9	24.4	-	-	124	14.7
	SarR	HTH-type transcriptional regulator	Q2FEJ8	2	32	4	14	19.3	25.0	-	-	115	13.7
	TrxA	Thioredoxin	Q2FHT6	2	36	3	4	7.8	5.9	-	-	104	11.4

This list shows strain, protein abbreviation, protein description, accession number, number of replicates, sequence coverage in percent, number of unique peptides, number of peptide spectral matches (PSM's), scores of individual experiments (-, no further experiment; ni, not identified), number of amino acids and molecular weight in kDa.

Table S3: Proteins identified by gel-free analysis in *S. aureus* USA300.

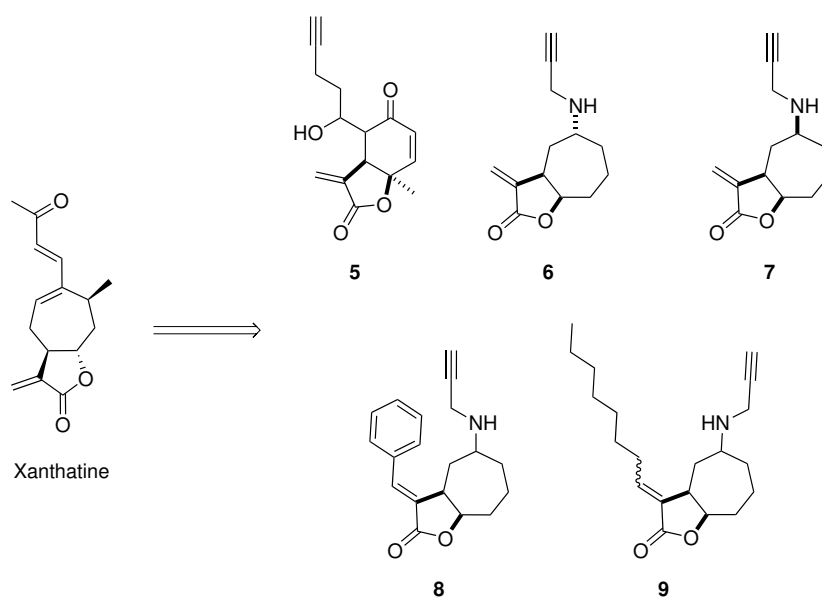
Protein Description (Abbreviation)	Accession	Sequence	Unique	PSMs	Mean Score	Scores			Scores			AAs	MW
		Coverage	Peptides			5 μ M probe 3	20 μ M Probe 3	20 μ M Probe 3	20 μ M Probe 3				
Thioredoxin (TrxA)	Q2FHT6	60	9	64	32,8	15,1	22,8	32,4	47,5	26,7	52,4	104	11,4
HTH-type transcriptional regulator (SarR)	Q2FEJ8	62	11	51	29,3	12,1	11,4	19,2	41,1	33,0	59,2	115	13,7
Iron-sulphur cluster repair protein (ScdA)	Q2FK11	44	11	39	21,7	11,7	7,1	13,2	40,3	23,0	34,6	224	25,5
Methylenetetrahydrofolate-tRNA-(uracil-5-)-methyltransferase (TrmFO)	Q2FHI7	33	10	45	21,4	14,9	13,6	15,4	28,6	28,8	27,4	435	48,3
Nitric oxide synthase oxygenase	Q2FFI1	43	13	46	20,3	20,5	31,1	13,2	25,1	25,1	6,8	358	41,7
Thioredoxin reductase	Q2FIM9	54	15	42	19,6	9,8	7,3	5,5	38,9	29,6	26,6	311	33,6
UDP-N-acetylglucosamine 1-carboxyvinyltransferase (MurA)	Q2FF27	35	8	27	15,1	ni	9,9	10,4	5,5	15,4	34,3	421	45,0
Respiratory nitrate reductase, beta subunit	Q2FEA1	27	8	28	13,8	9,5	15,4	4,8	25,9	11,0	16,3	481	55,2
Staphylococcal accessory regulator (SarS)	Q2FKE7	22	7	26	12,3	8,0	8,8	5,5	17,4	23,7	10,3	250	29,9
Fructose-1,6-bisphosphatase class 3	Q2FDY9	15	8	19	12,0	ni	9,3	6,6	16,0	17,7	10,1	654	76,1
Glutathione peroxidase	Q2FHD4	46	6	25	11,9	5,1	13,3	5,7	16,0	24,9	6,4	158	18,1
2-C-methyl-D-erythritol 4-phosphate cytidyltransferase	Q2FK15	33	4	17	11,0	5,5	5,0	ni	9,4	16,9	18,2	238	26,6
DNA-directed RNA polymerase subunit alpha	Q2FER5	25	5	16	11,0	ni	6,7	20,4	14,3	6,4	7,3	314	35,0
Transcriptional regulator, MarR family (MgrA)	Q2FIV3	37	6	20	10,1	11,8	4,8	5,2	ni	15,8	12,9	147	17,1
Pyridine nucleotide-disulfide oxidoreductase	Q2FGW2	38	8	14	8,1	5,7	ni	9,1	10,0	10,6	5,0	328	36,7
30S ribosomal protein S12	Q2FJ95	36	5	14	7,0	4,7	7,7	5,8	ni	9,2	7,7	137	15,3

This list shows protein description, accession number, protein abbreviation, sequence coverage in percent, number of unique peptides, number of peptide spectral matches (PSM's), mean score, scores of individual experiments (ni, not identified), number of amino acids and molecular weight in kDa. Only proteins which were identified in 5 out of 6 experiments and are not appearing in the DMSO controls are listed.

Table S4: Labeled cysteines in *S. aureus* NCTC8325 proteins MgrA, SarA and SarR

Protein	Labeled cysteine	Sequence of peptide	X _{corr}	Probability	Charge	MH+ [Da]	ΔM [ppm]
MgrA	Cys12	EQLC*FSLYNAQR	4.15	51.15	3	1711,815	0.33
		EQLC*FSLYNAQR	2.70	69.25	2	1711,820	3.05
SarA	Cys9	INDC*FELLSMVTYADK	2.65	106.76	2	2101,994	3.82
SarR	Cys57	C*SEFKPYYLTK	3.72	57.95	2	1618,789	1.56

* **3** labeled cysteine



Scheme S1: Chemical structure of xanthatine and xanthatine inspired γ -lactone probes.

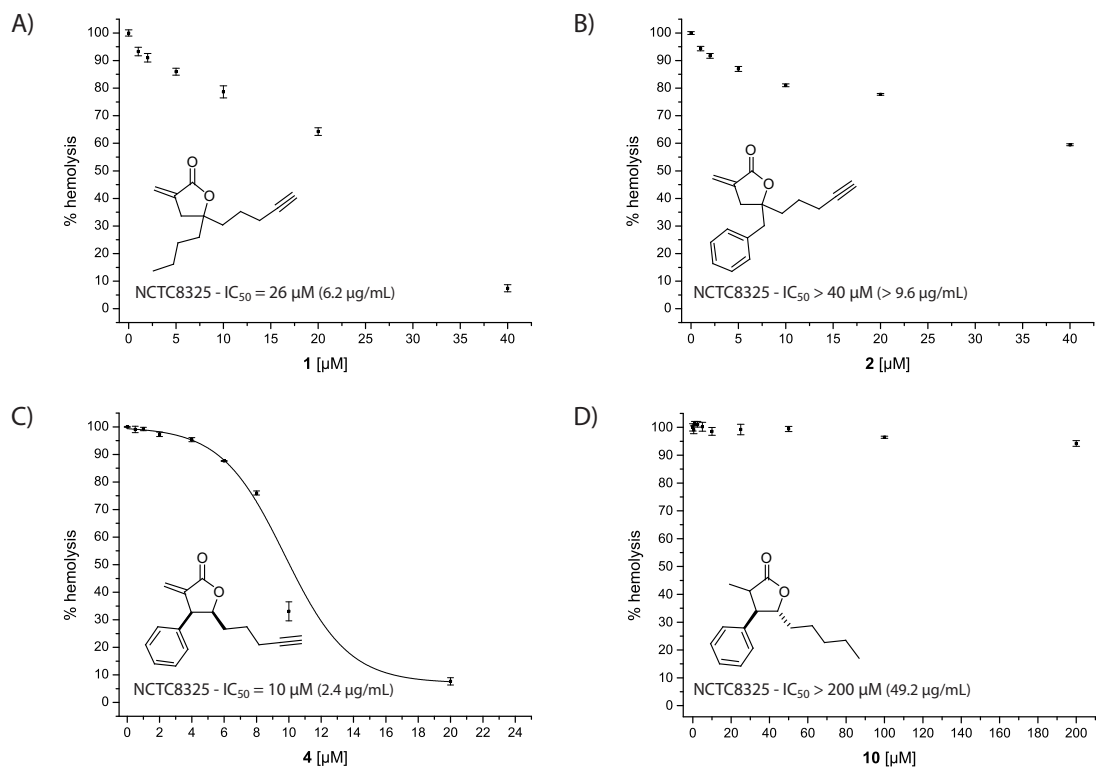


Figure S1: Hemolysis inhibition of *S. aureus* NCTC8325 by lactone probes **1** (A), **2** (B), **4** (C) and **10** (D). Each compound was tested in at least three independent trials in triplicates; average values are shown and error bars display standard deviations from the mean. Data were fitted to the dose-response function $f(x) = A_1 + (A_2 - A_1) / (1 + 10^{(\text{LOG}(x_0 - x))p})$ with a variable Hill-slope given by parameter p .

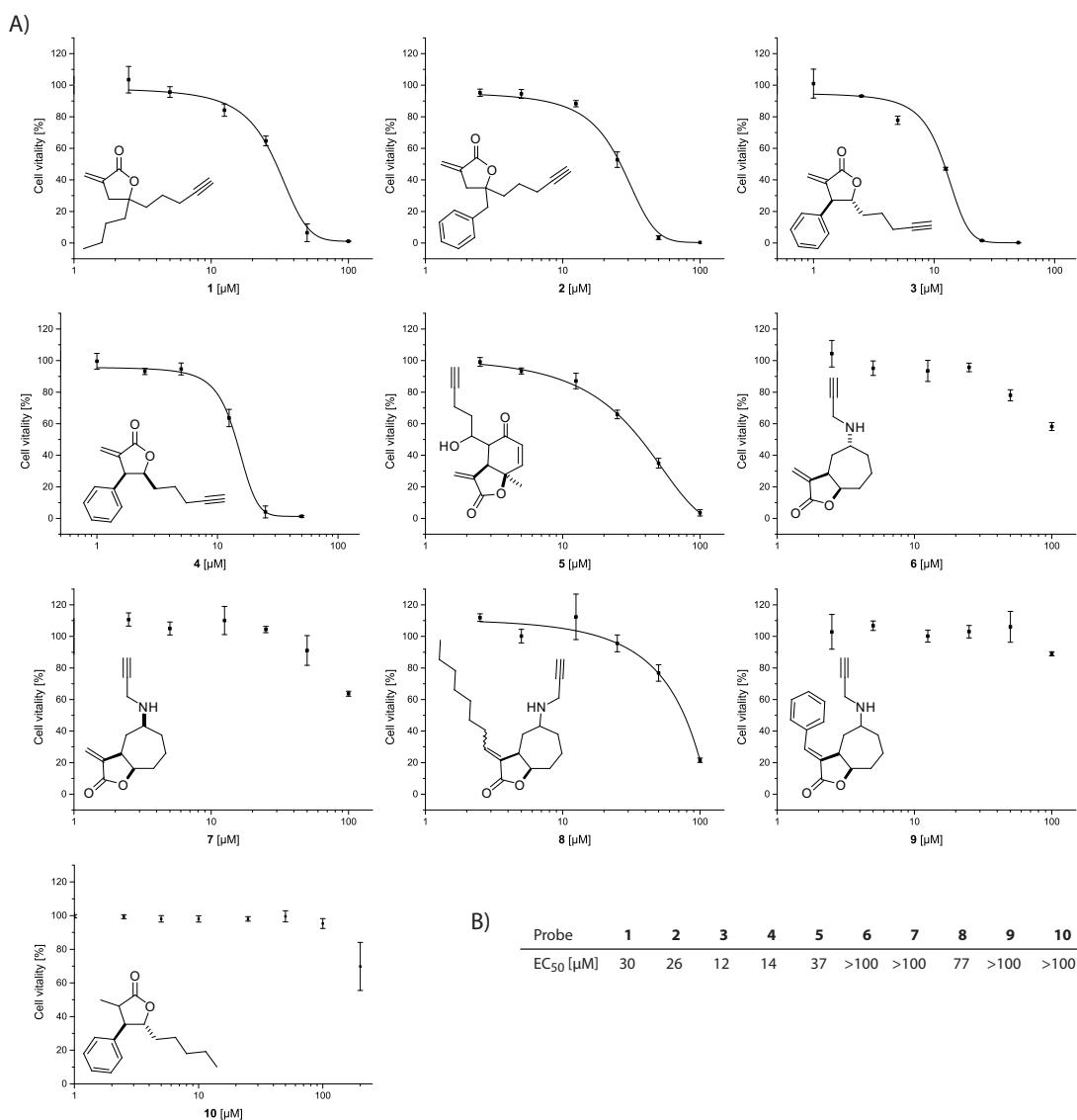


Figure S2: A) MTT assay with lactone probes. Each compound was tested in at least three independent trials in triplicates; average values are shown and error bars display standard deviations from the mean. Data were fitted to the dose-response function $f(x) = A_1 + (A_2 - A_1) / (1 + 10^{(\text{LOG}(x_0 - x))p})$ with a variable Hill-slope given by parameter p . B) EC₅₀ values of compounds **1-10** obtained by curve fitting.

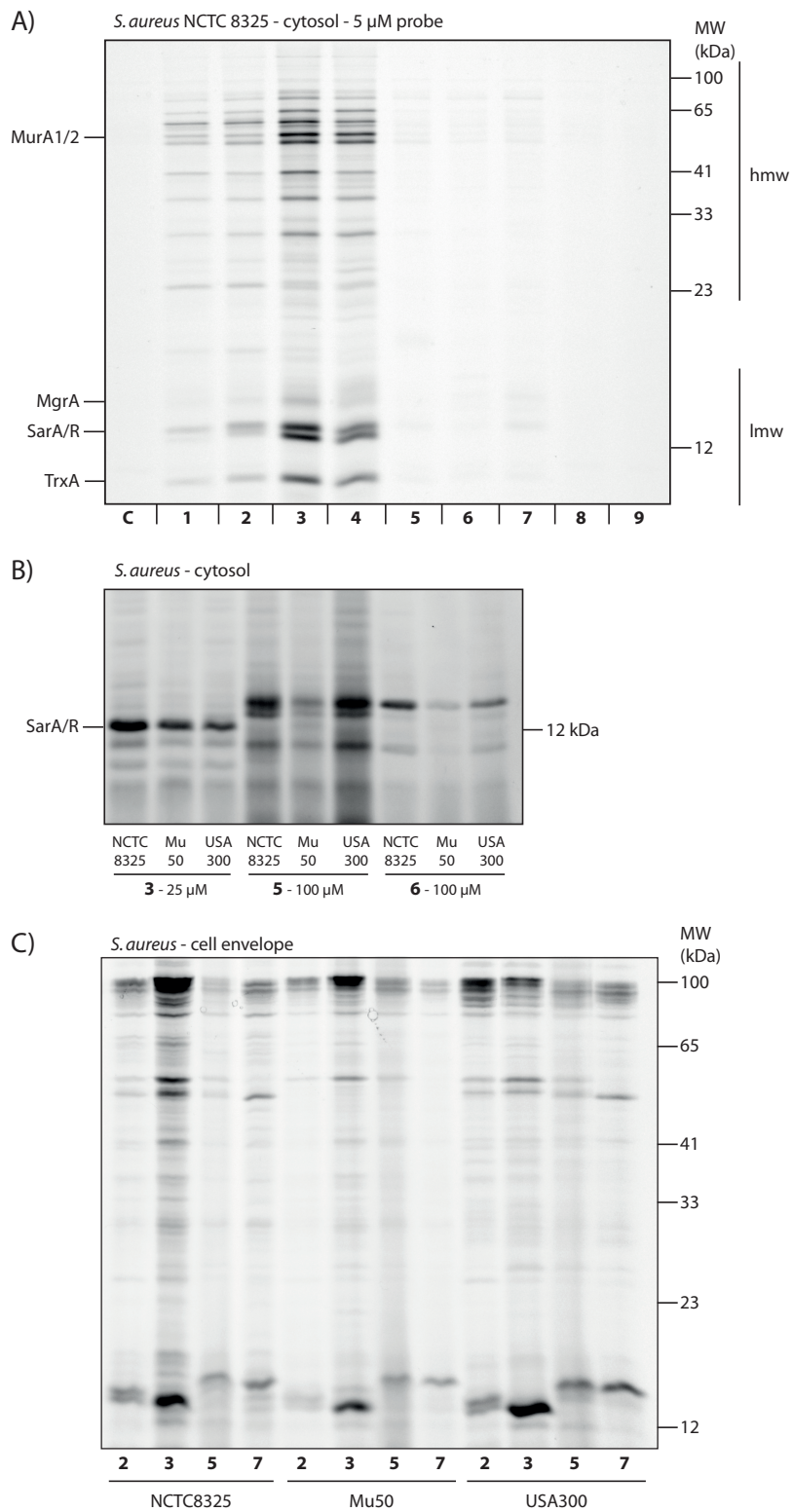


Figure S3: A) *In situ* labelling of *S. aureus* NCTC8325 with 5 μ M probe 1-9. Names of proteins are listed on the left side (please refer to Table S2 for full names). hmw = high molecular weight; lmw = low molecular weight. B) *In situ* labelling of *S. aureus* NCTC8325 with higher concentrations of probe 3, 5 and 6 in order to compare lmw labelling pattern. C) *In situ* labelling of *S. aureus* NCTC8325 membrane fraction with 5 μ M probe 2, 3, 5 and 7.

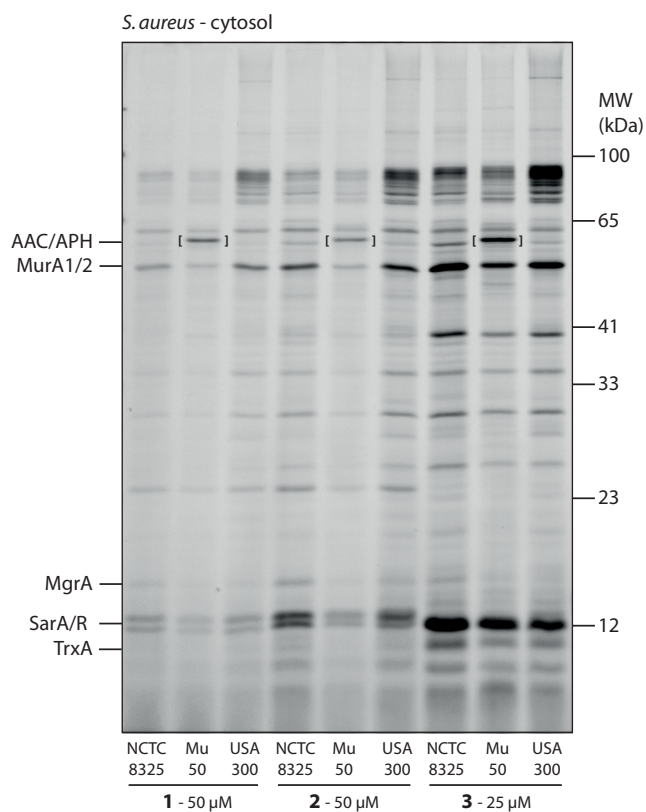


Figure S4: *In situ* labelling of *S. aureus* NCTC8325, Mu50 and USA300 with lactone probes **1**, **2** and **3**. Names are listed on the left side (full names in Table S2). The resistance associated hmw protein is indicated on the gel.

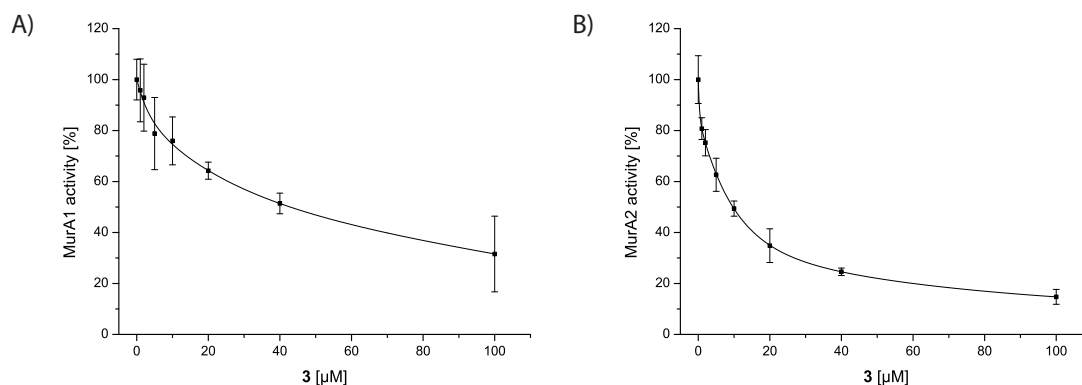


Figure S5: Inhibition of MurA1- and MurA2-catalyzed enolpyruvyl transfer reaction by lactone probe **3**. Each concentration was tested in at least three independent trials in triplicates; average values are shown and error bars display standard deviations from the mean. Data were fitted to the dose-response function $f(x) = A_1 + (A_2 - A_1) / (1 + 10^{(\text{LOG}(x_0 - x))p})$ with a variable Hill-slope given by parameter p .

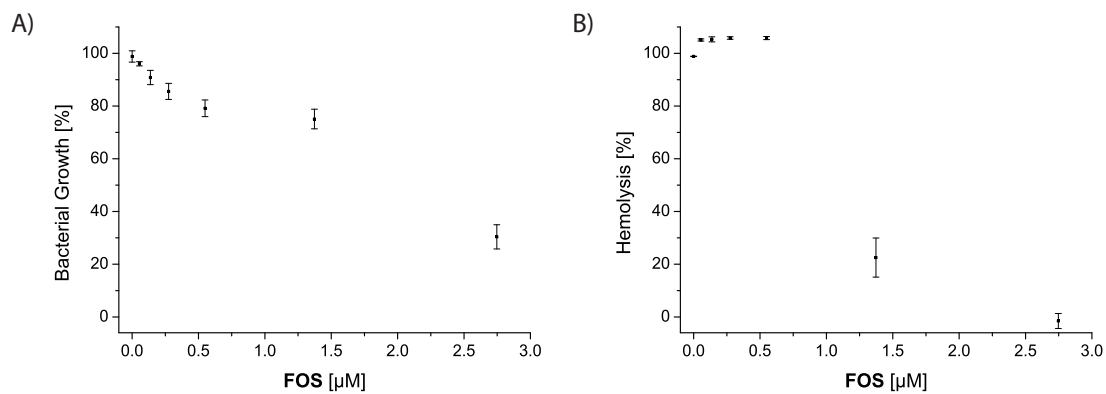


Figure S6: A) Growth and B) hemolysis-inhibition of *S. aureus* NCTC8325 by the antibiotic fosfomycin (FOS). Each compound was tested in at least three independent trials in triplicates; average values are shown and error bars display standard deviations from the mean.

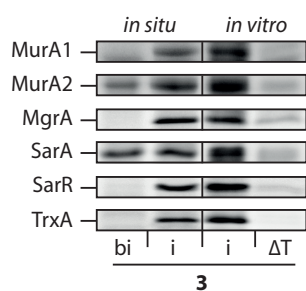


Figure S7: A) Recombinant expression and *in situ/vitro* labelling of target proteins with probe **3** (bi, before induction; i, after induction; ΔT , heat control of induced recombinant proteins).

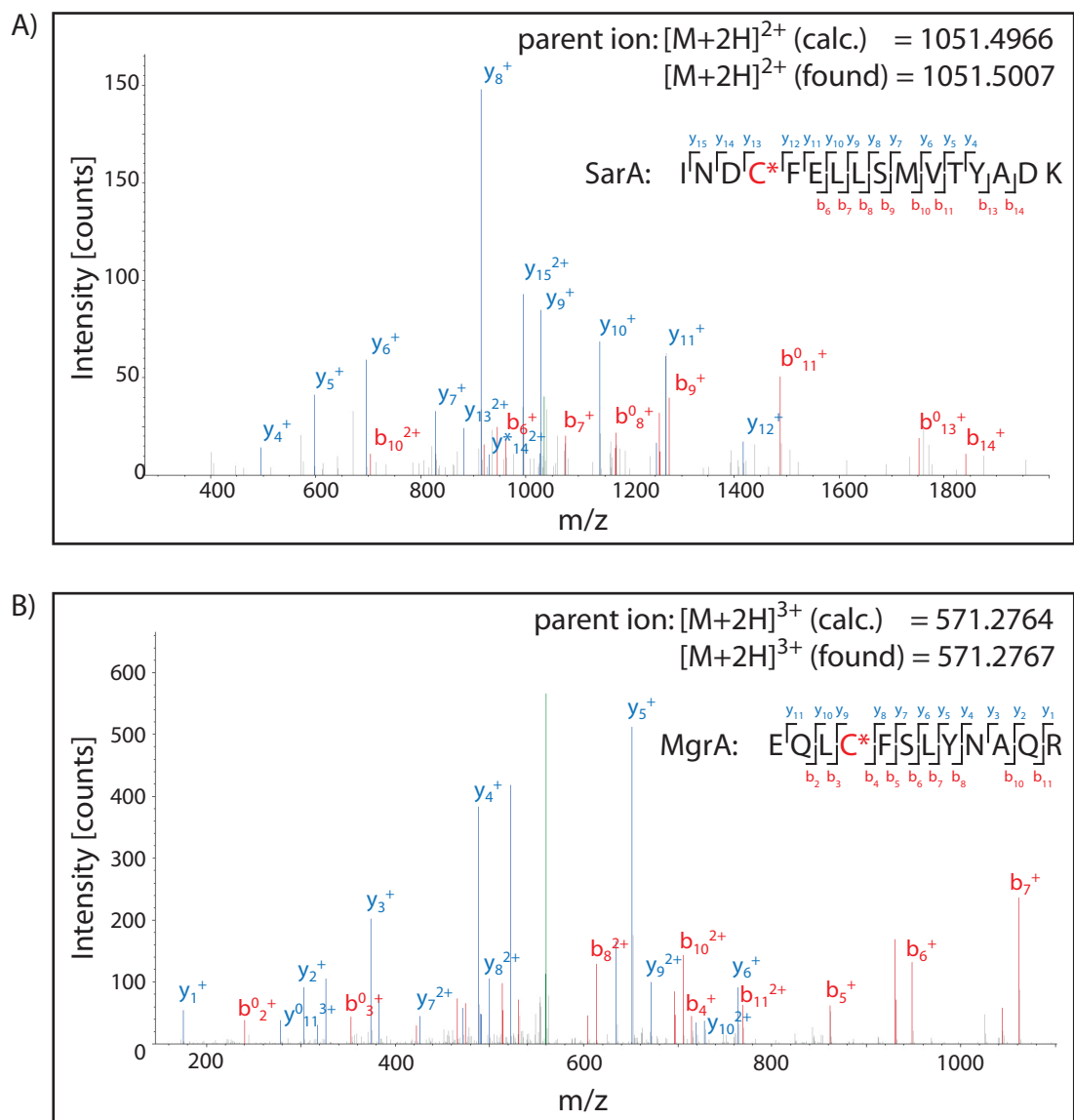


Figure S8: Mass spectra of **3** labeled and digested SarA (A) and MgrA (C). Y-ions are shown in blue, b-ions in red. The fragmentation of the corresponding peptide is shown and the modified cysteine indicated with *.

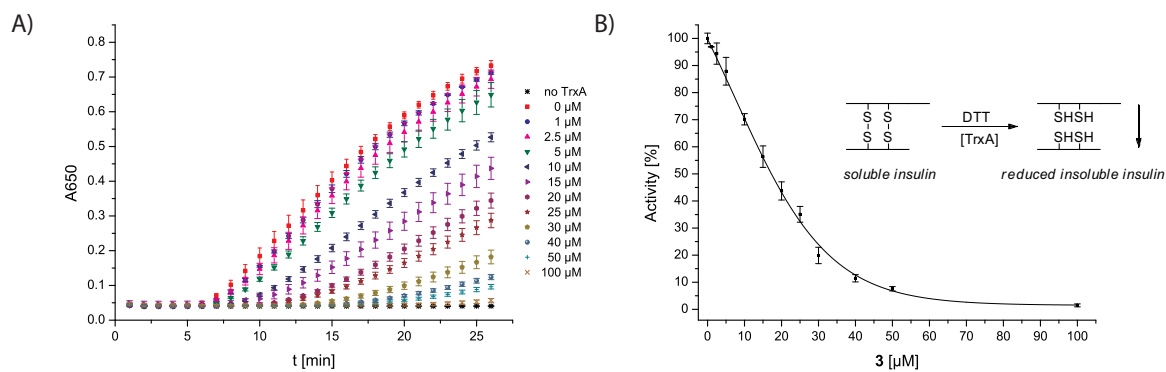


Figure S9: Inhibition of TrxA-catalysed insulin reduction by lactone probe **3**. A) Increase in absorption caused by reduced and turbid insulin. Addition of **3** leads to a concentration dependent inhibition of the TrxA-catalysed reduction. B) The total absorption changes were plotted against the corresponding probe concentrations to determine the remaining TrxA-activity compared to the DMSO treated positive control (100% activity). Each concentration was tested in at least three independent trials in triplicates; average values are shown and error bars display standard deviations from the mean. Data were fitted to the dose-response function $f(x) = A_1 + (A_2 - A_1) / (1 + 10^{(\text{LOG}(x_0 - x))p})$ with a variable Hill-slope given by parameter p .

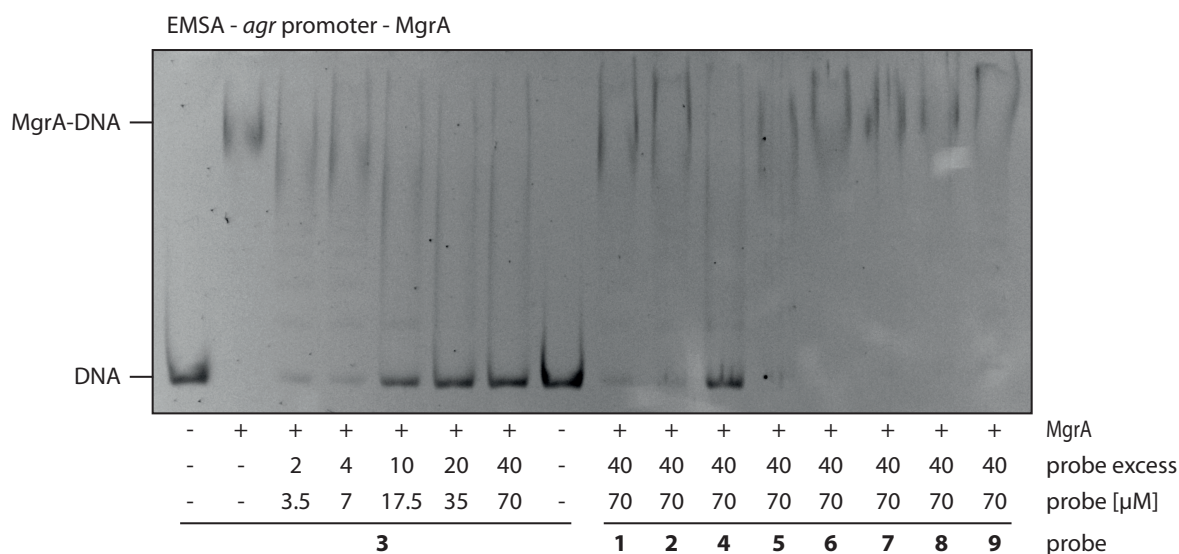


Figure S10: Electrophoretic mobility shift assay (EMSA) with *agr* promoter DNA and MgrA. The left part of the gel shows a concentration dependent analysis with anti-virulence compound **3**, the right part displays a single concentration analysis with all other compounds. DNA = unbound fluorescent promoter DNA; MgrA-DNA = protein bound DNA.

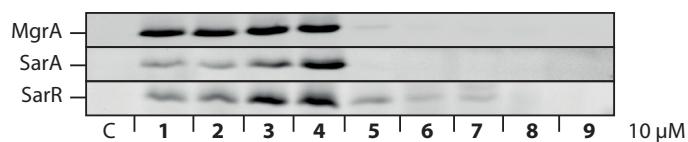


Figure S11: Fluorescent SDS-gel of purified recombinant proteins (10 μM) labeled with the corresponding lactone probes (10 μM) and “clicked” to rhodamine azide.

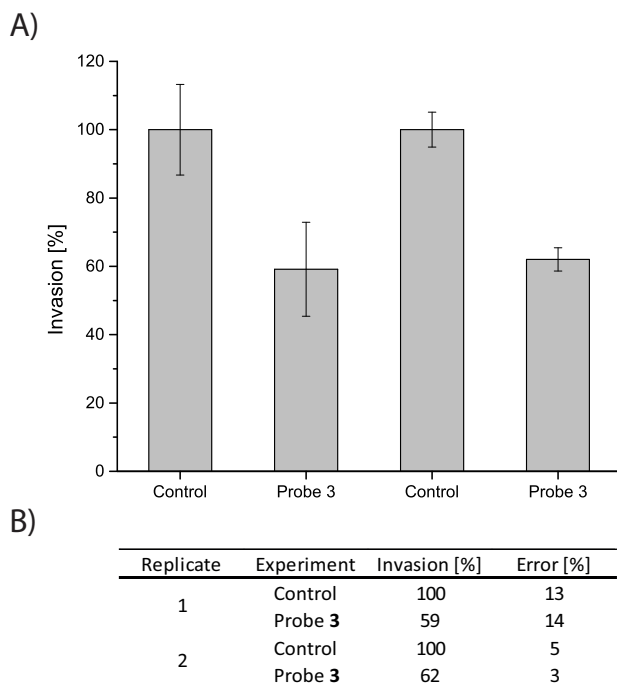
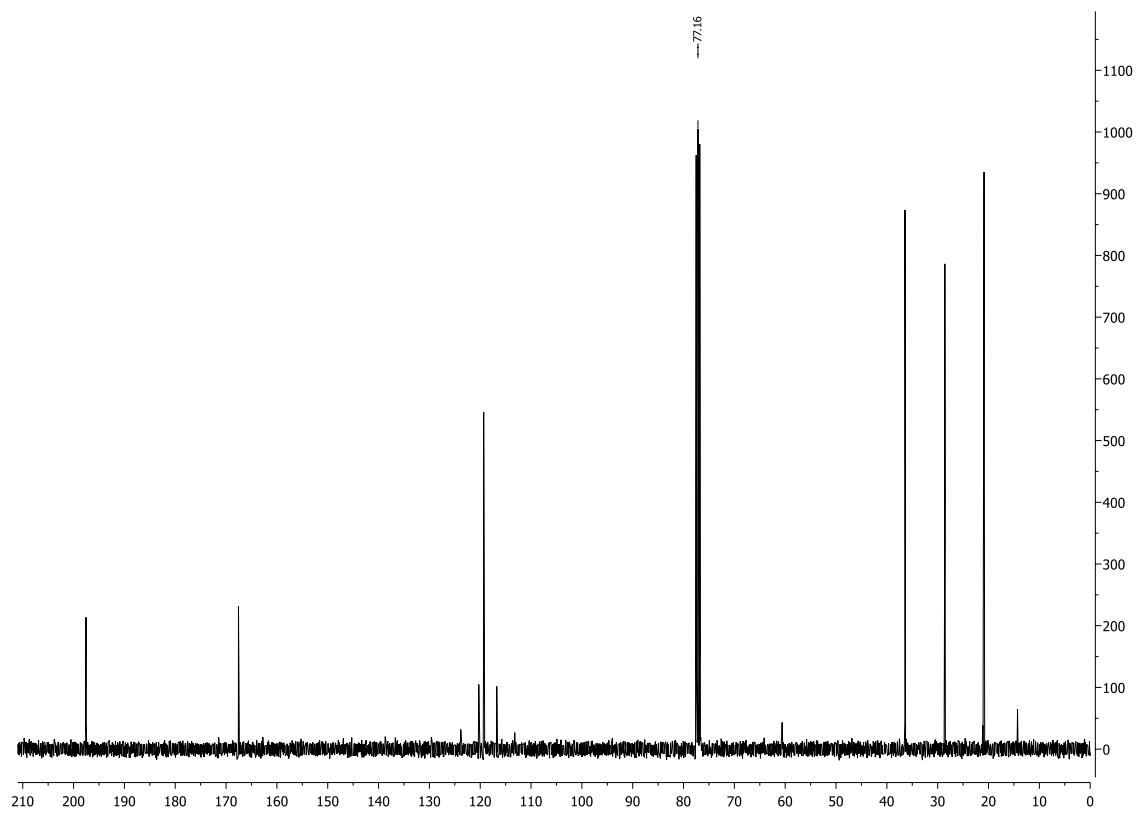
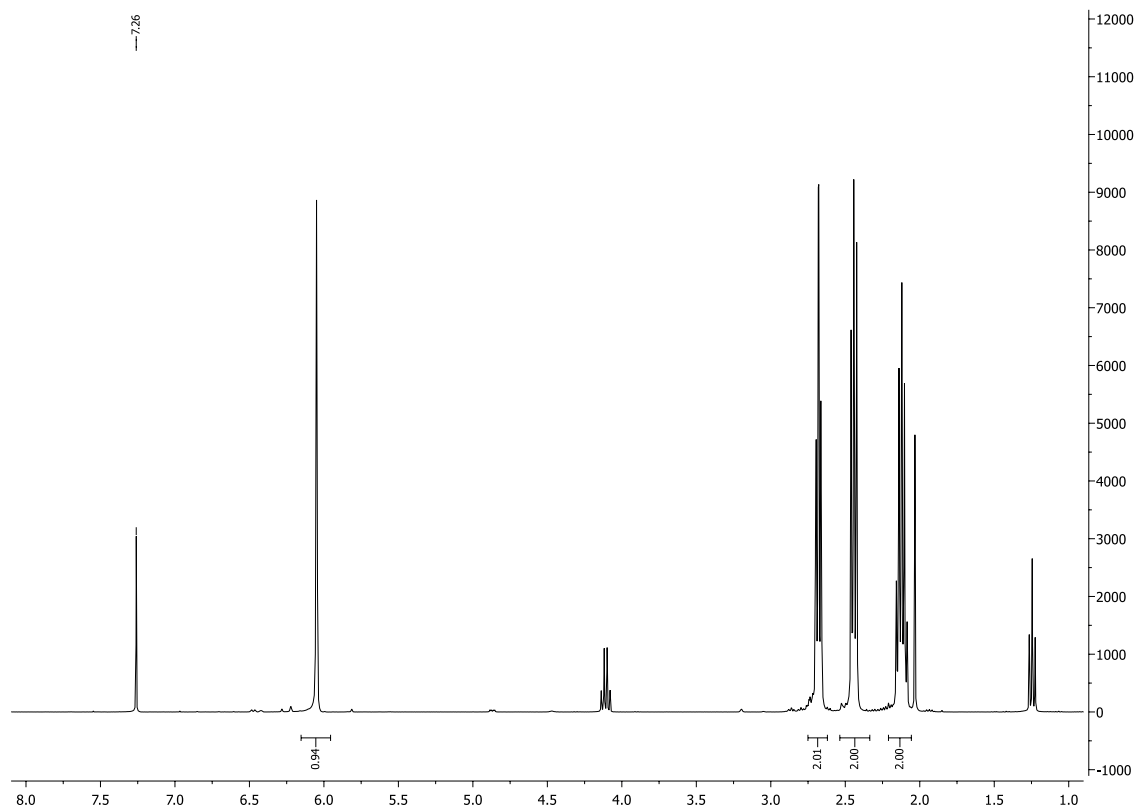
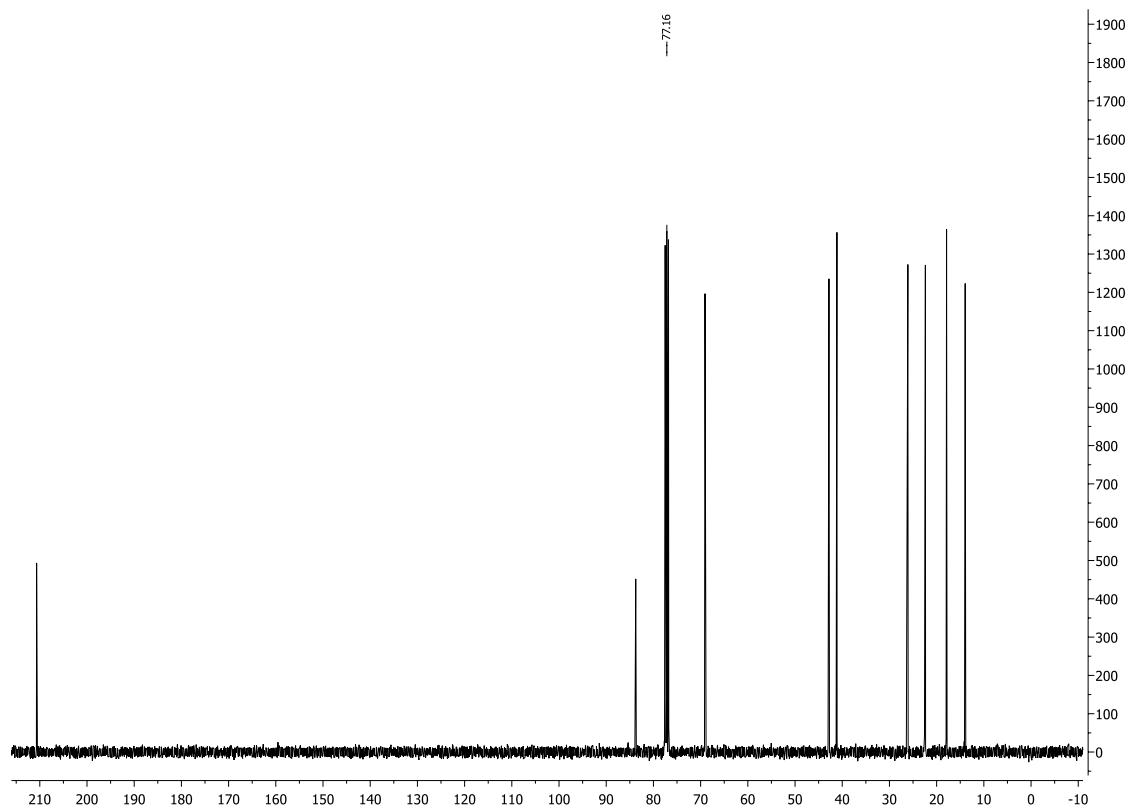
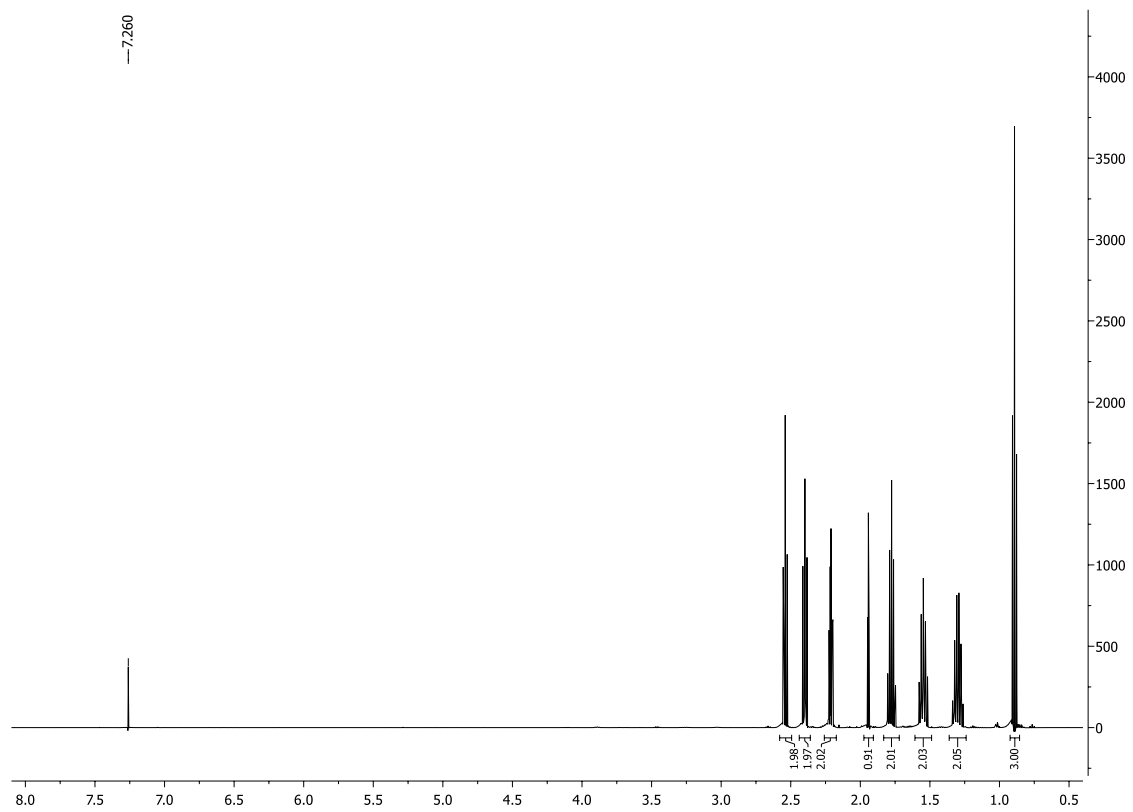


Figure S12: Invasion of THP-1 cells by *S. aureus*. Addition of **3** leads to decreased invasion of THP-1 cells compared to the DMSO treated positive control (100% invasion). The experiment was done in two independent trials in triplicates; average values are shown and error bars display standard deviations from the mean.

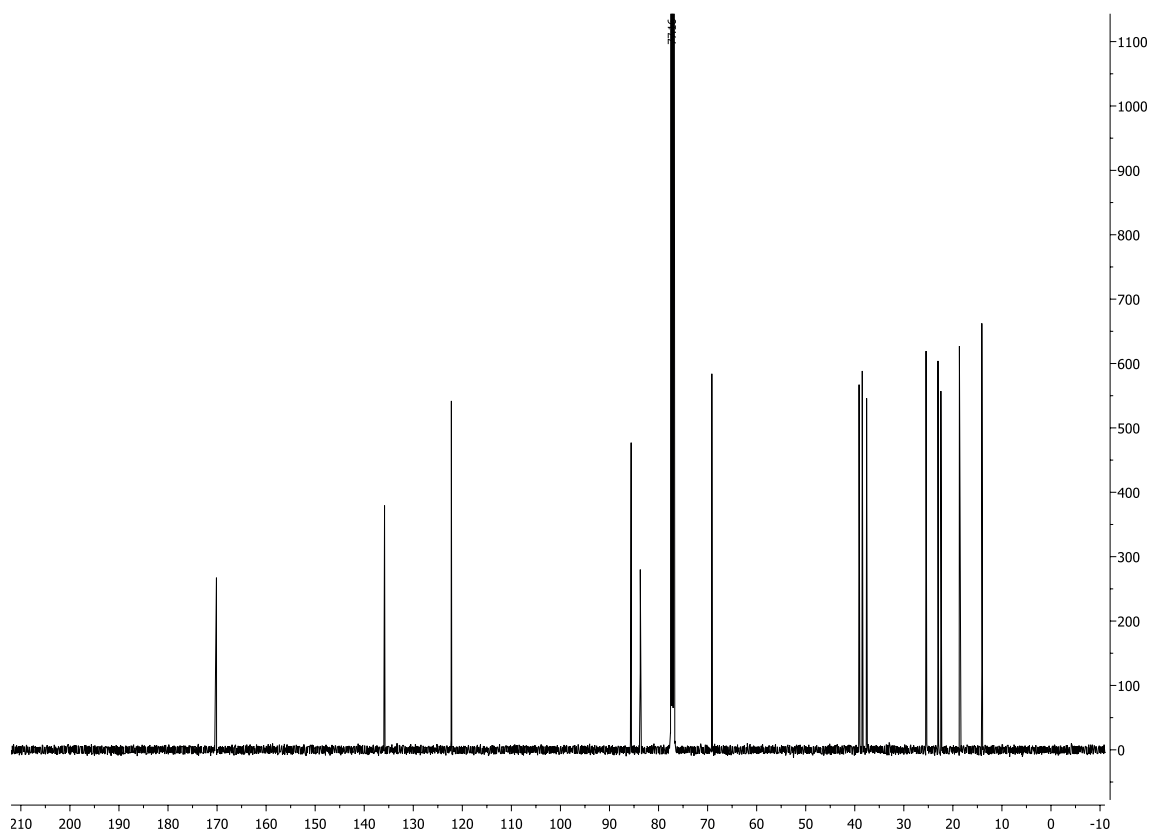
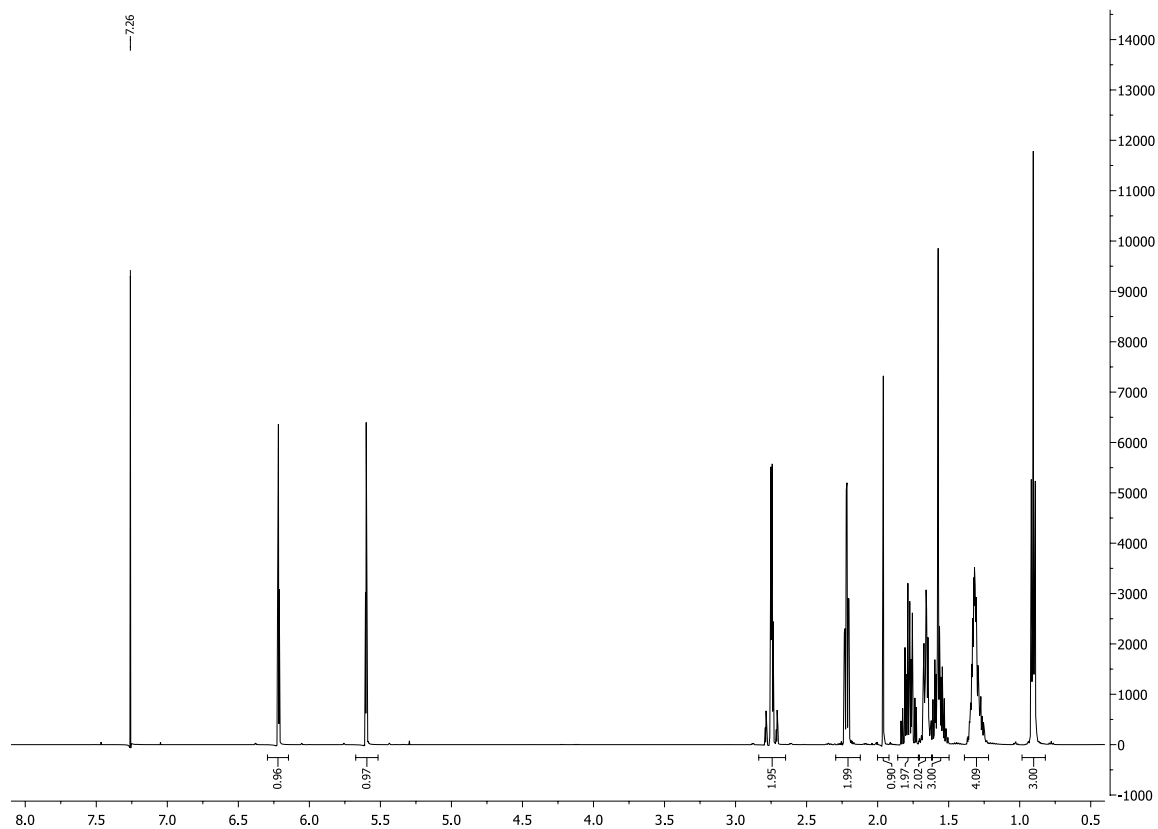
¹H- und ¹³C-NMR of 11



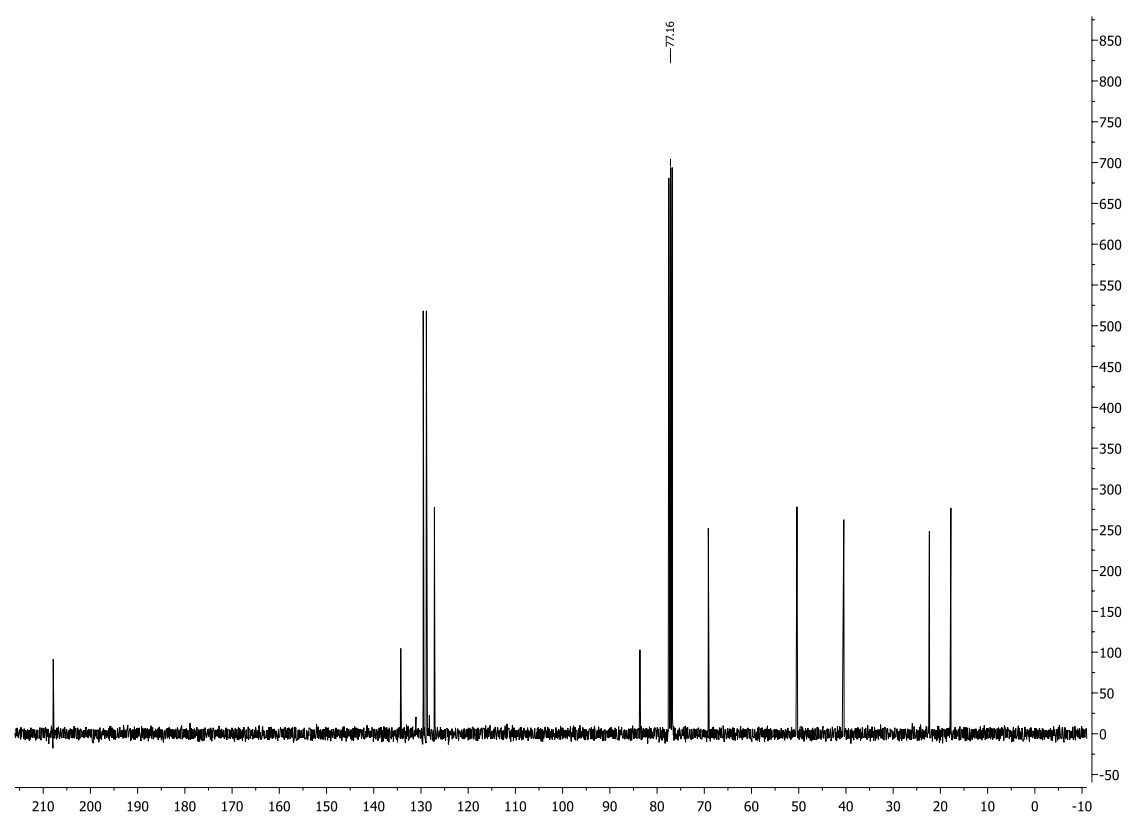
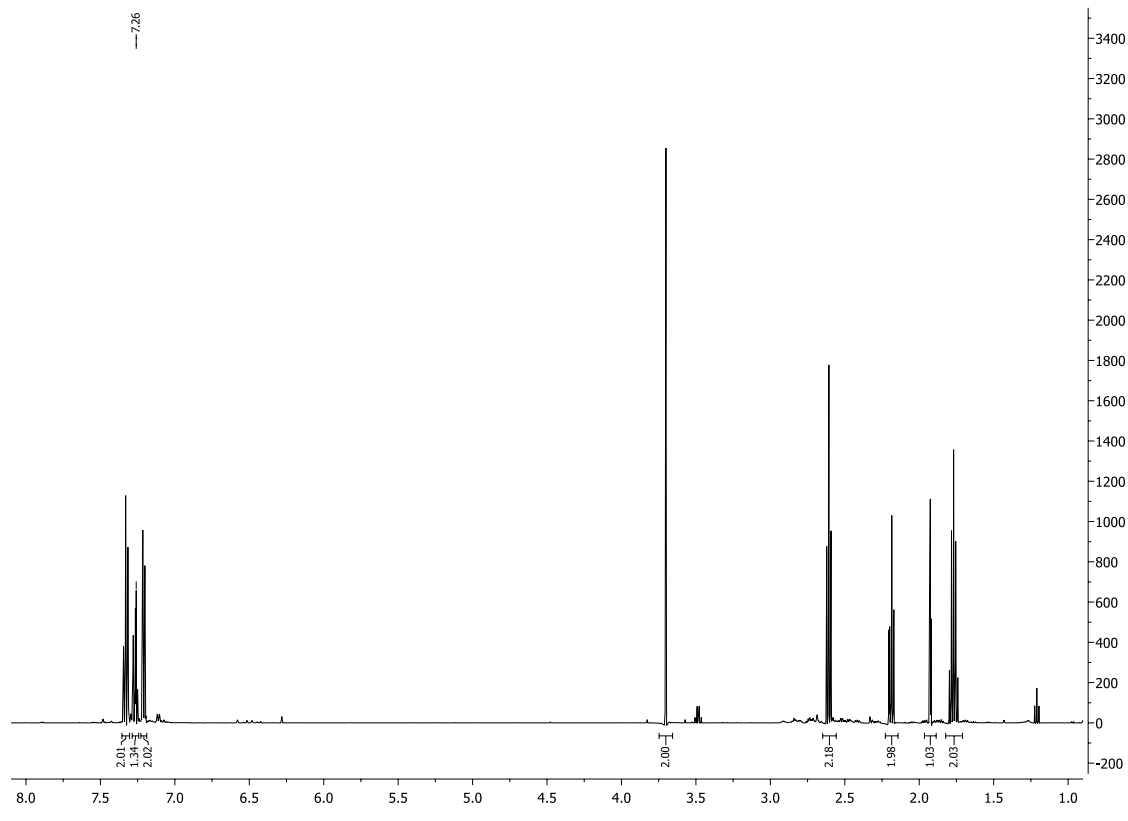
¹H- und ¹³C-NMR of 12



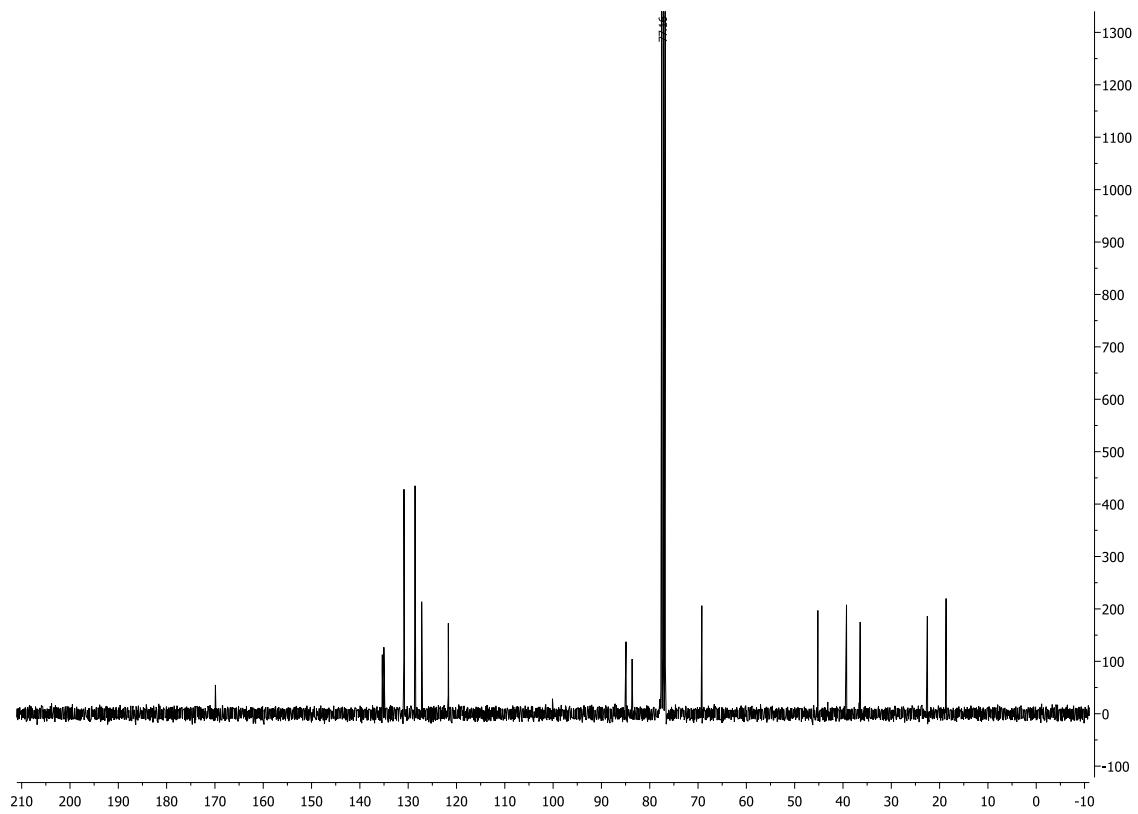
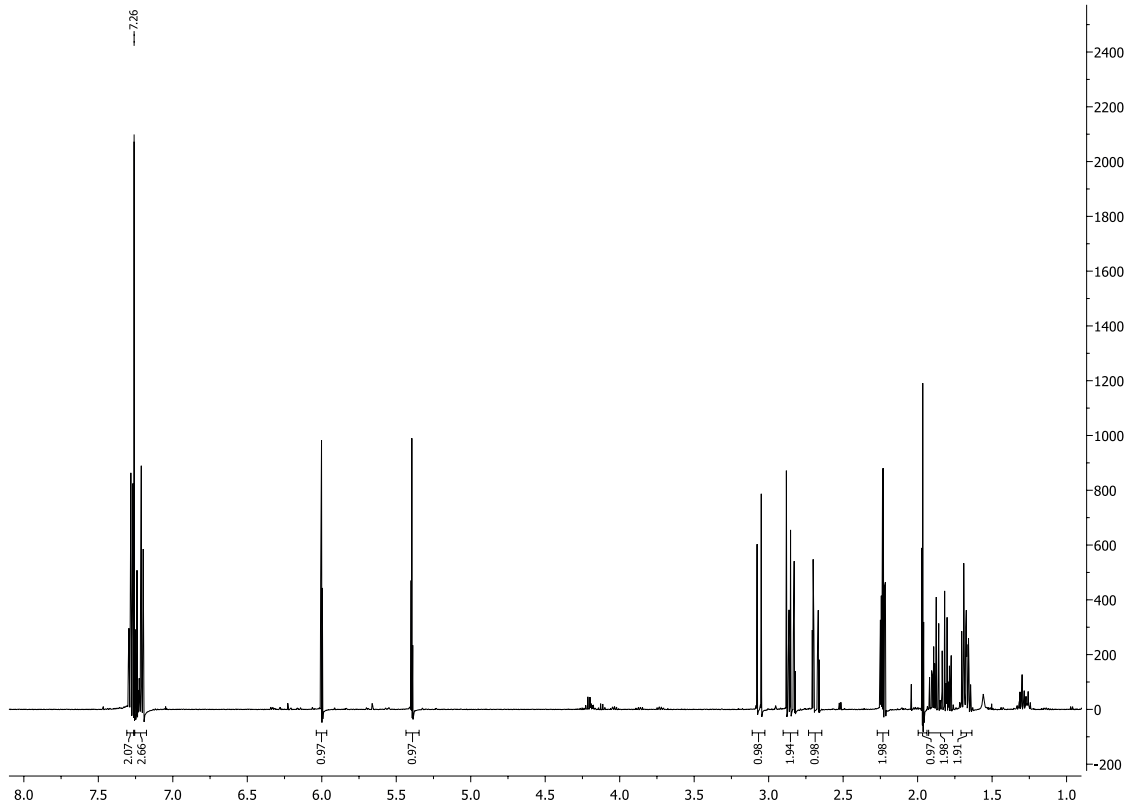
^1H - und ^{13}C -NMR of 1



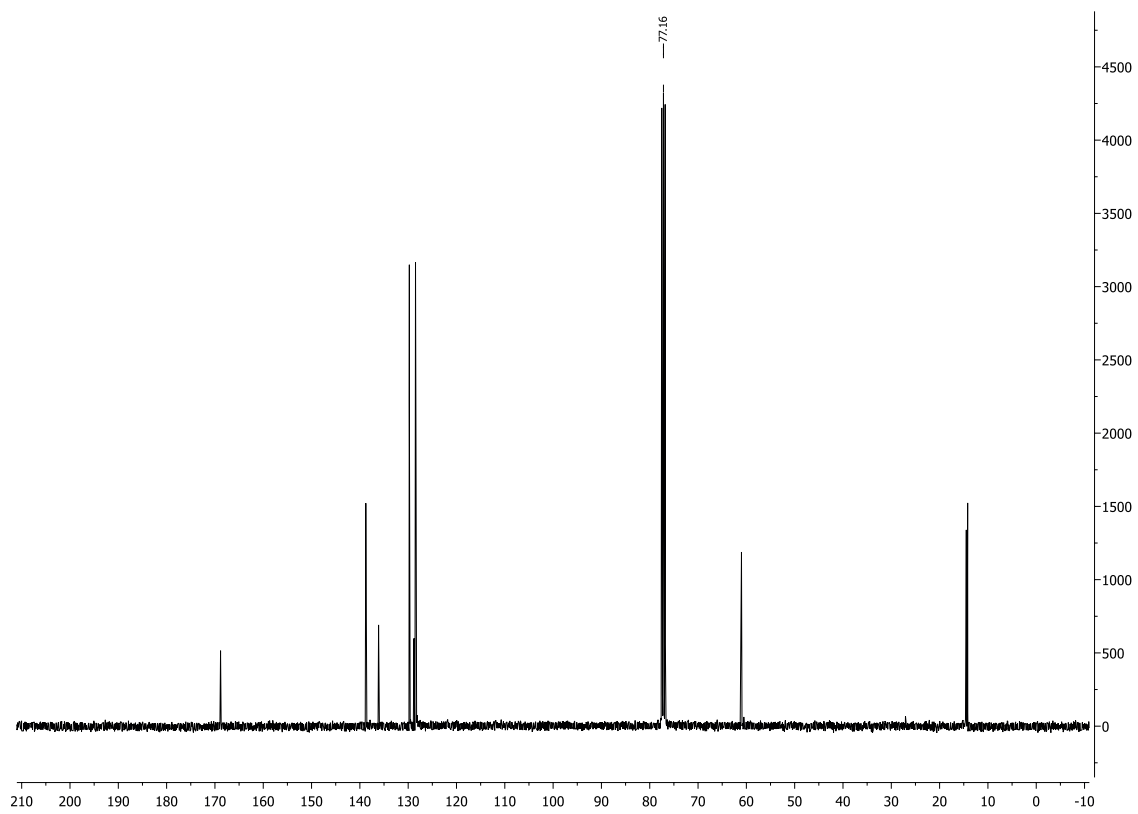
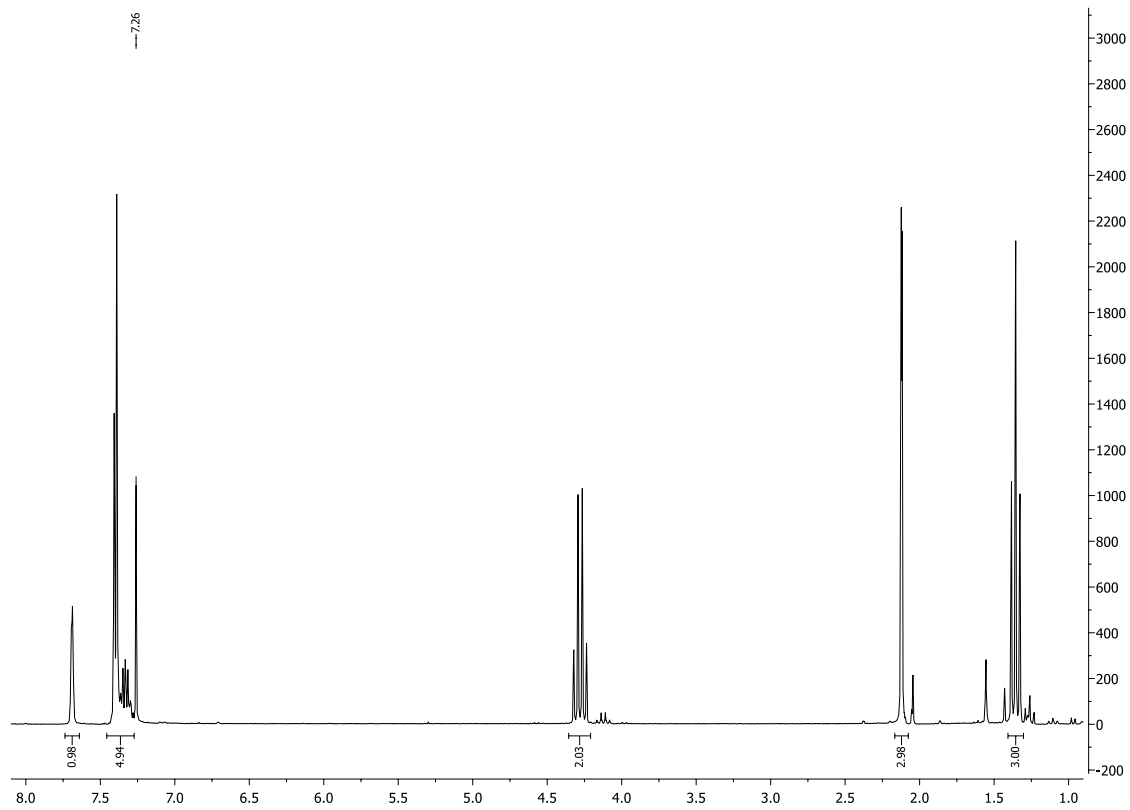
^1H - und ^{13}C -NMR of 13



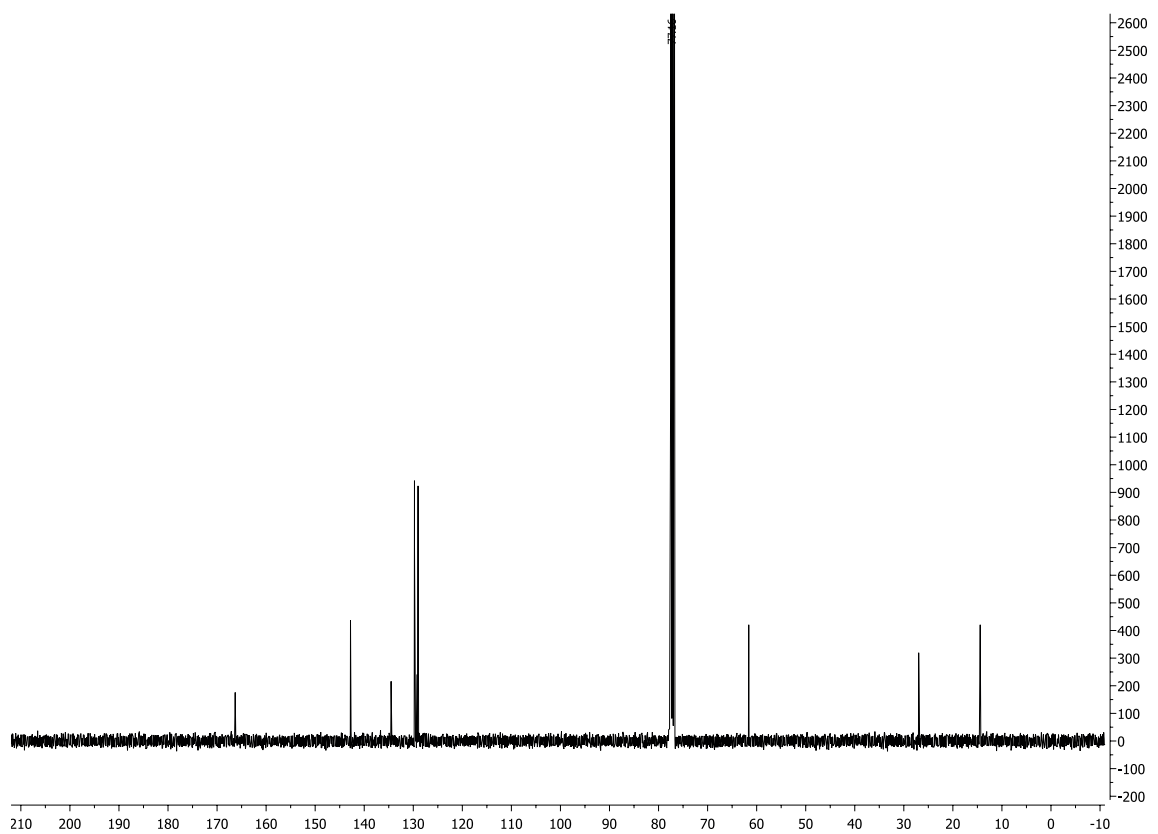
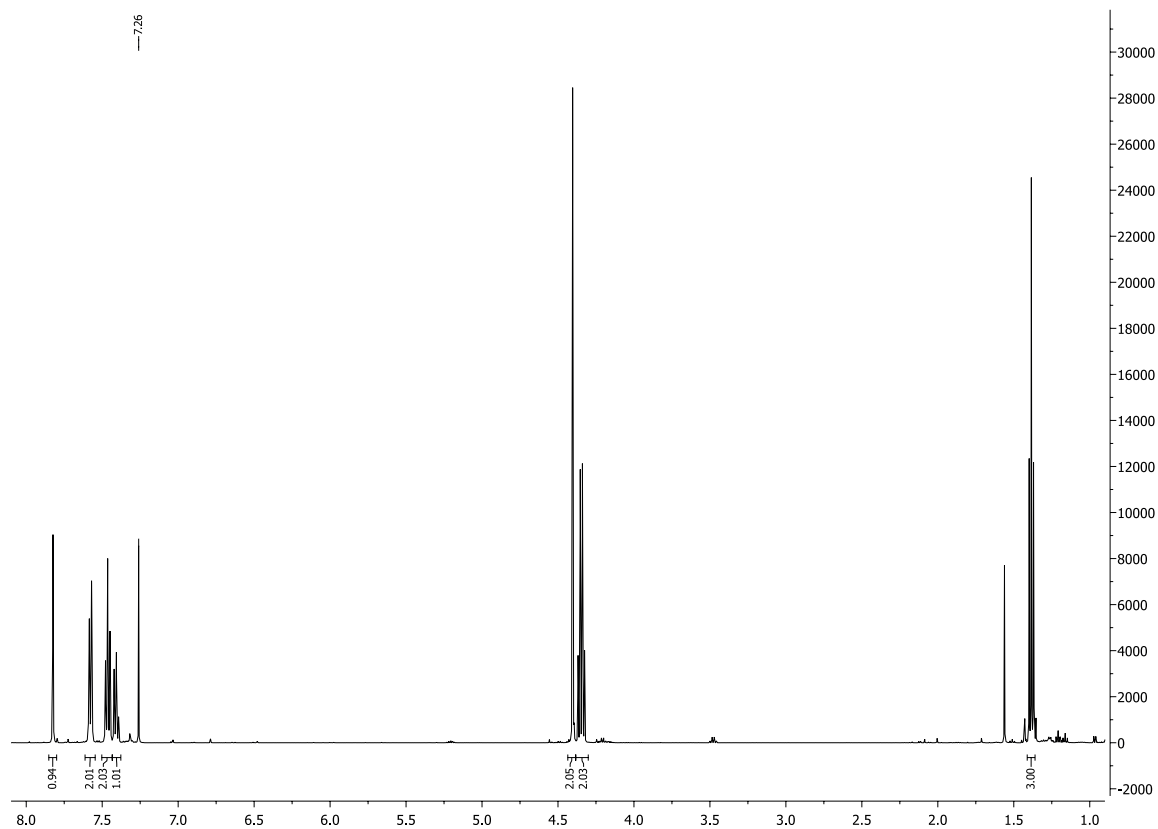
^1H - und ^{13}C -NMR of 2



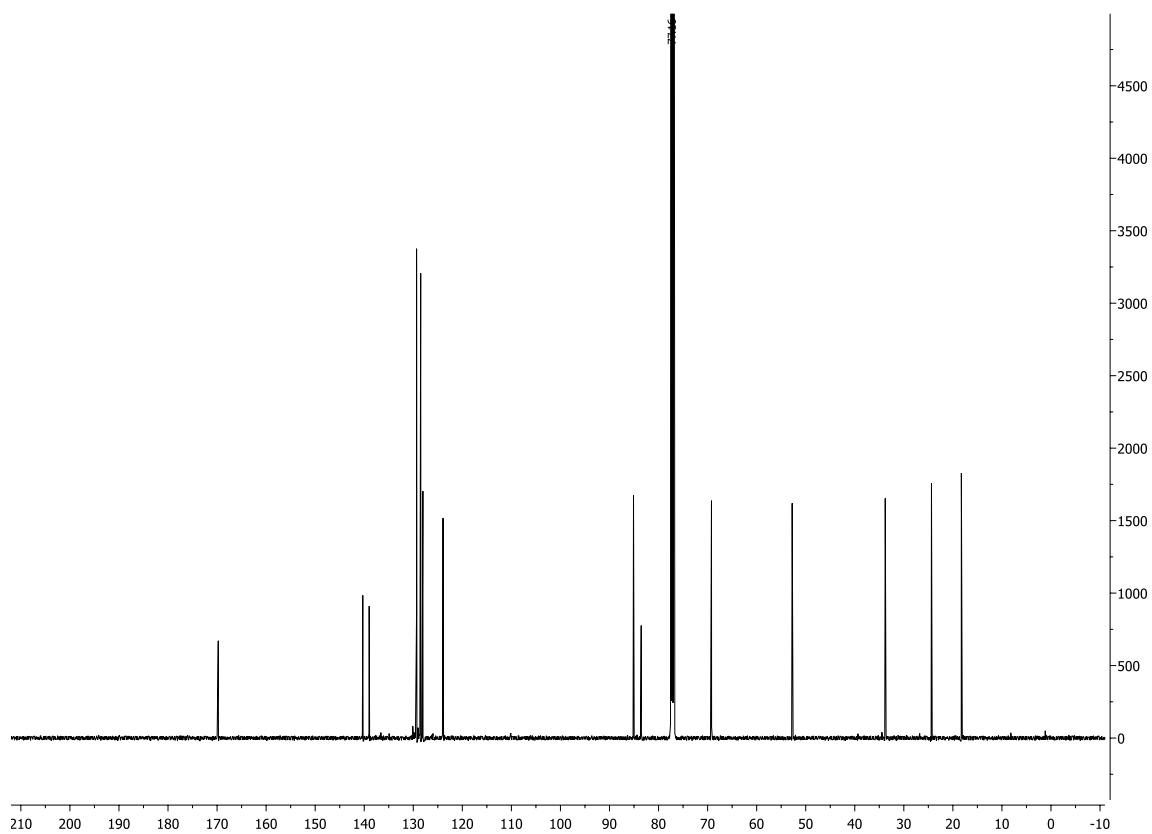
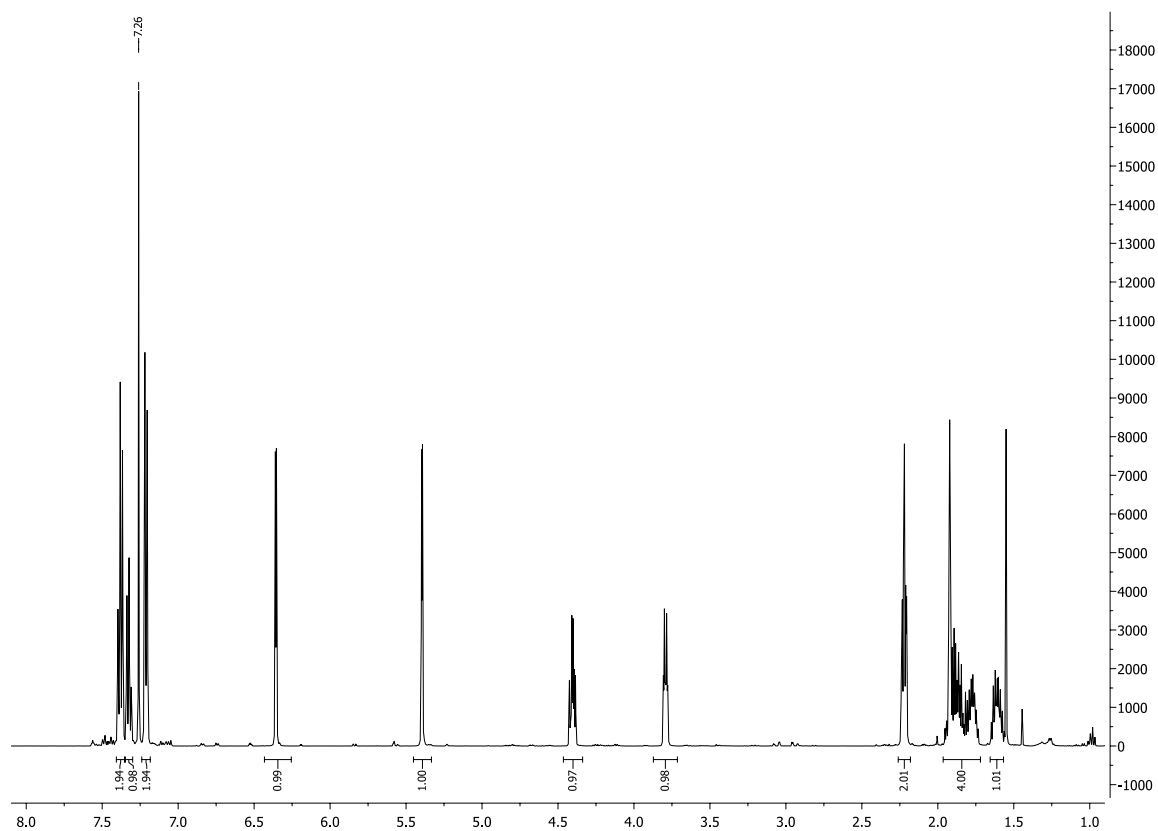
^1H - und ^{13}C -NMR of 14



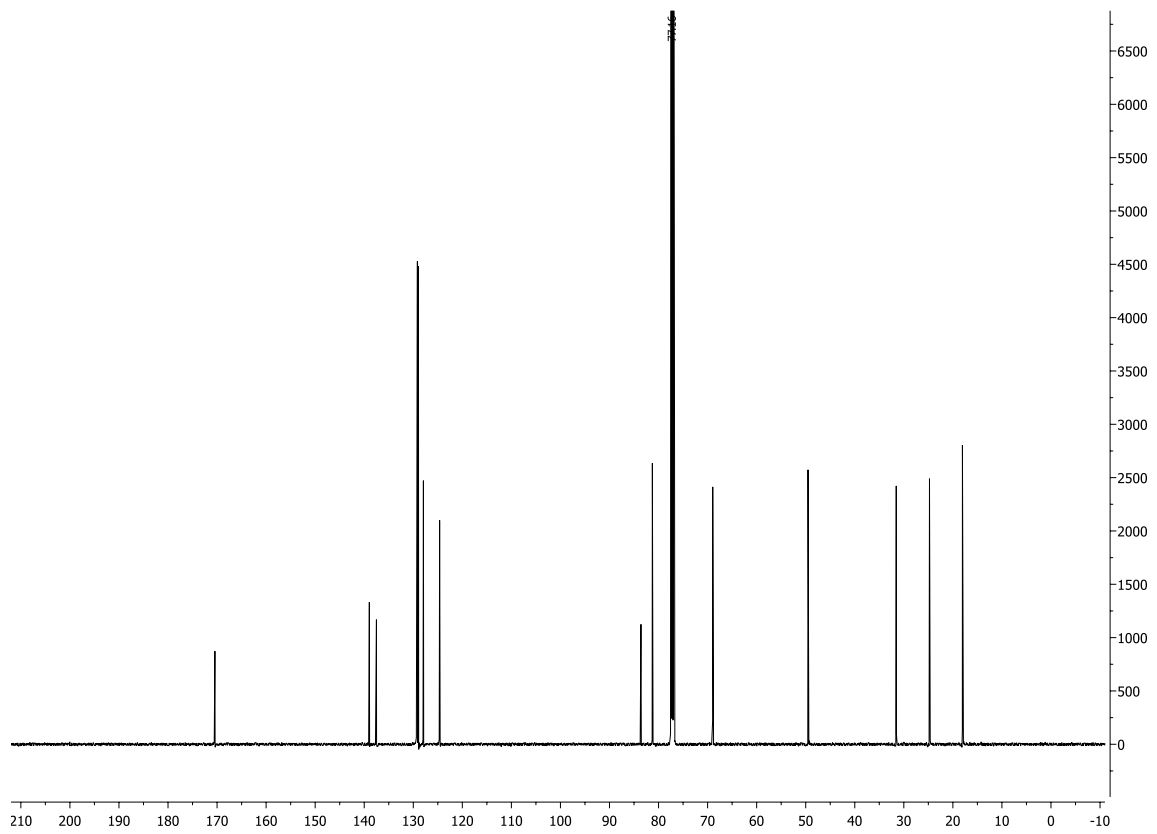
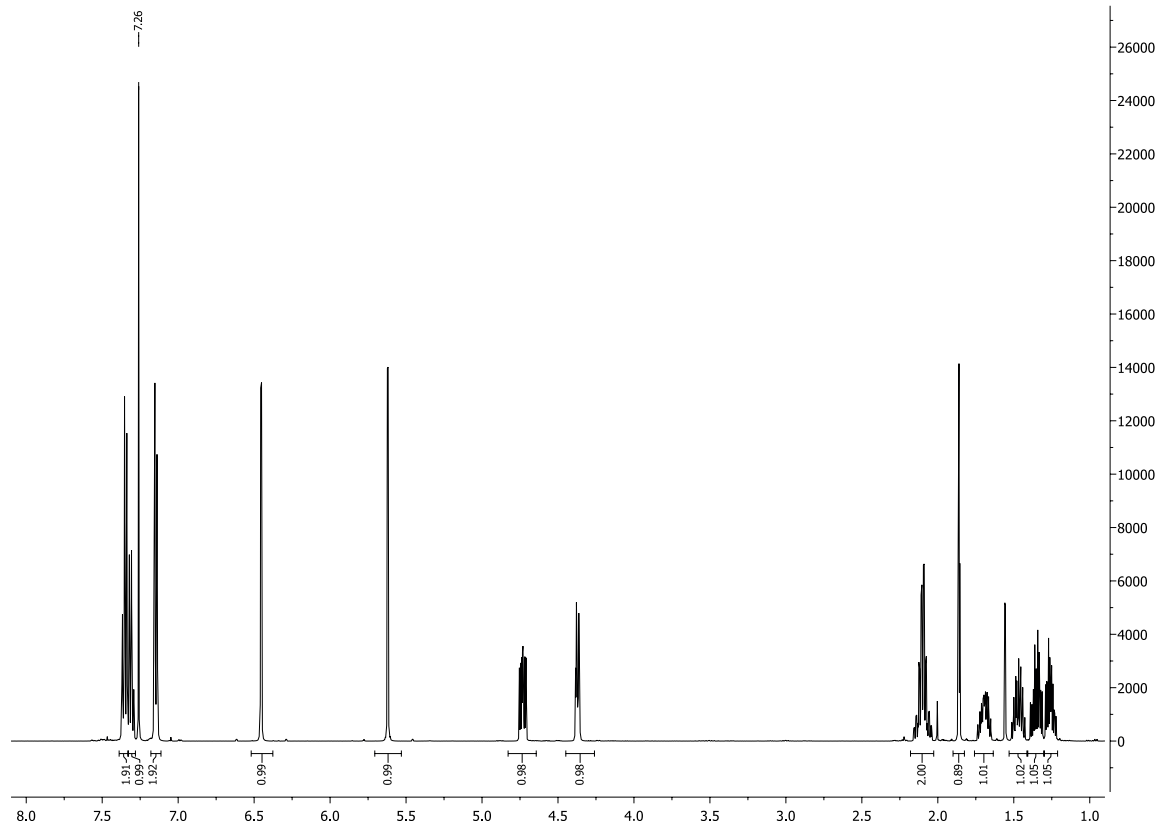
¹H- und ¹³C-NMR of 15



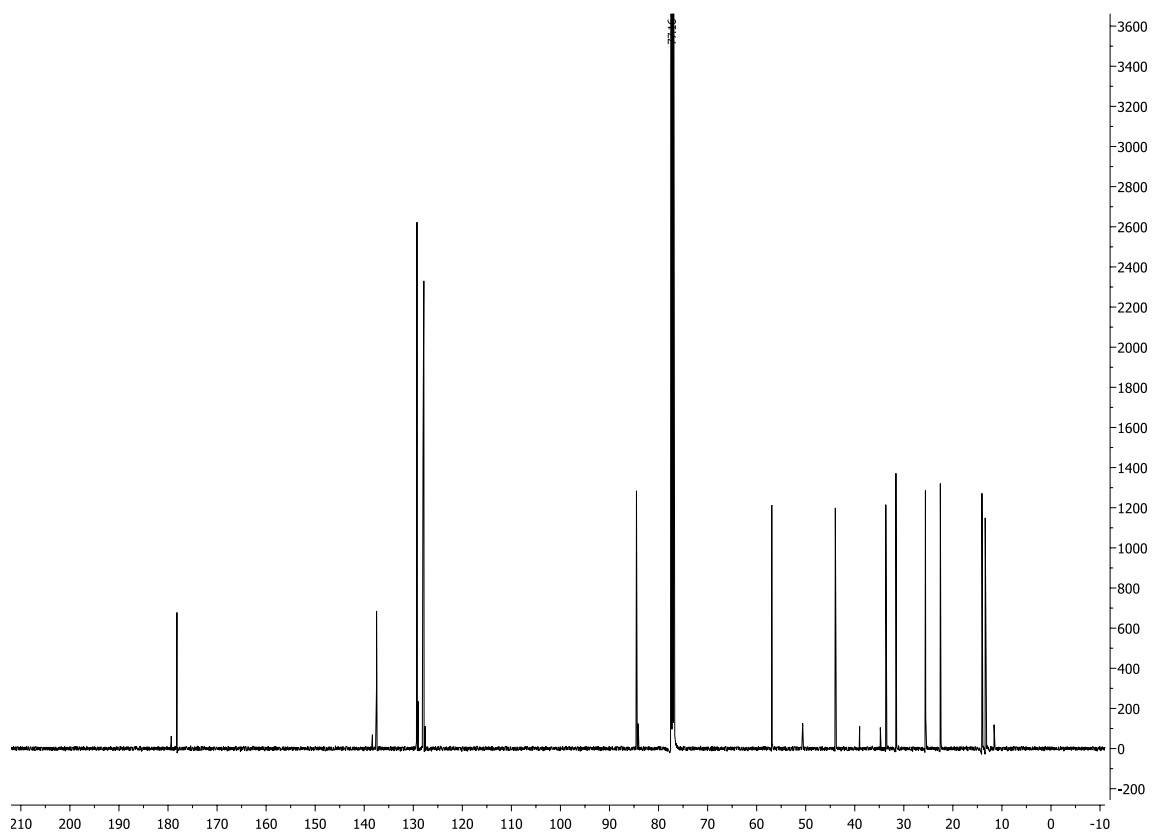
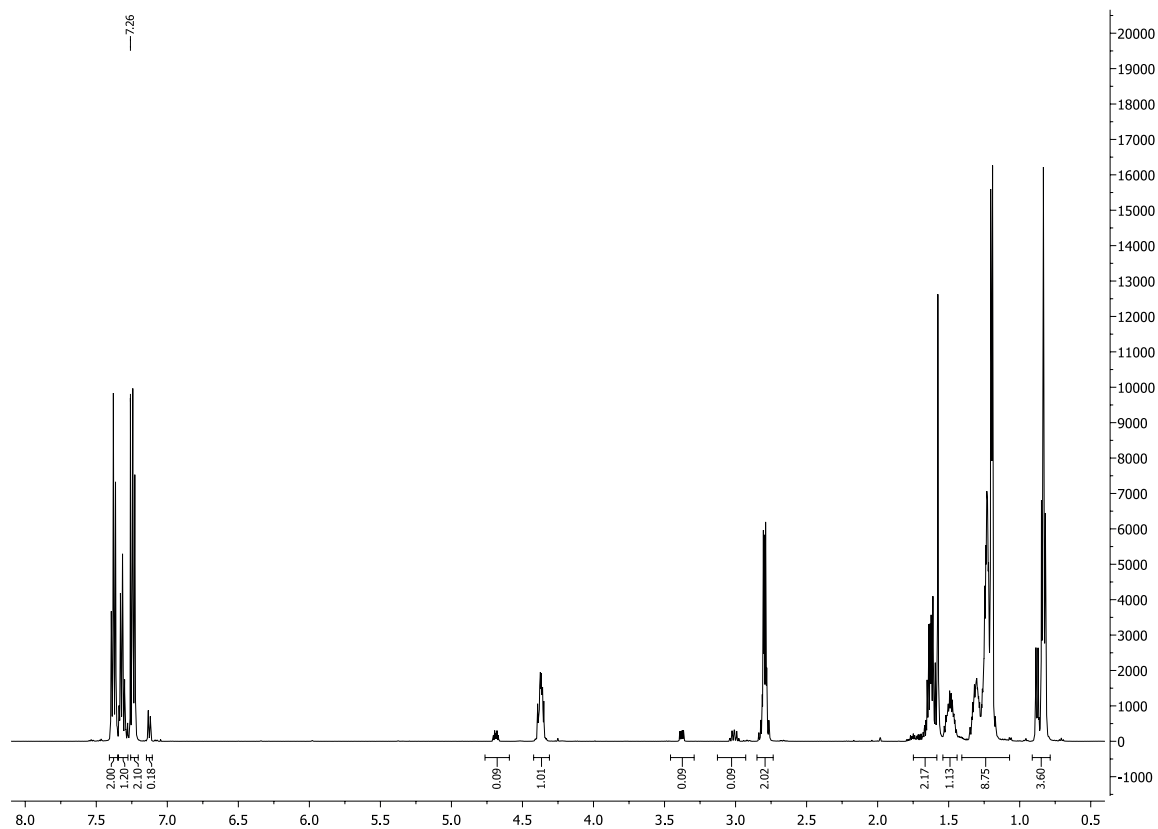
$^1\text{H-NMR}$ of 3^1H- und $^{13}\text{C-NMR}$ of 3



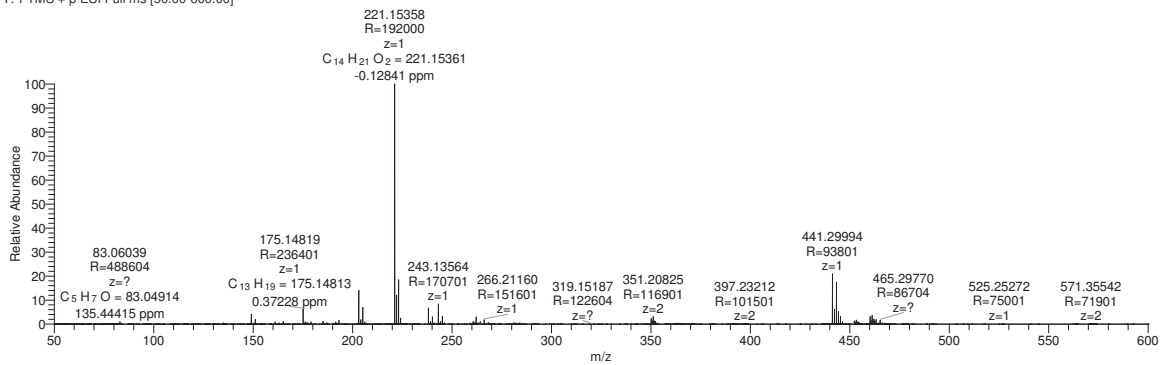
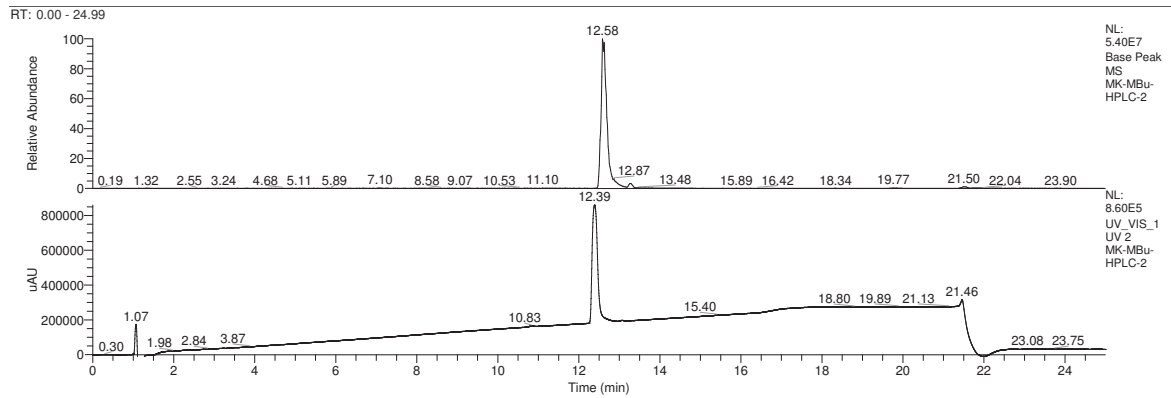
^1H - und ^{13}C -NMR of 4



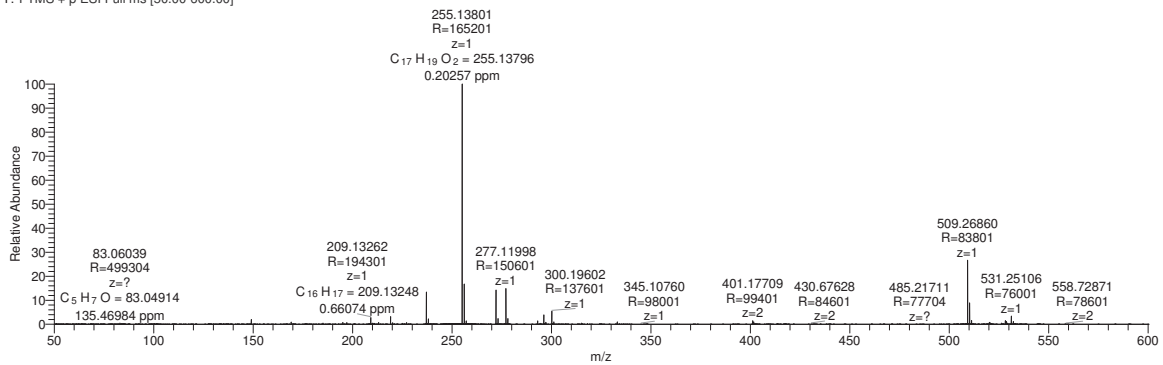
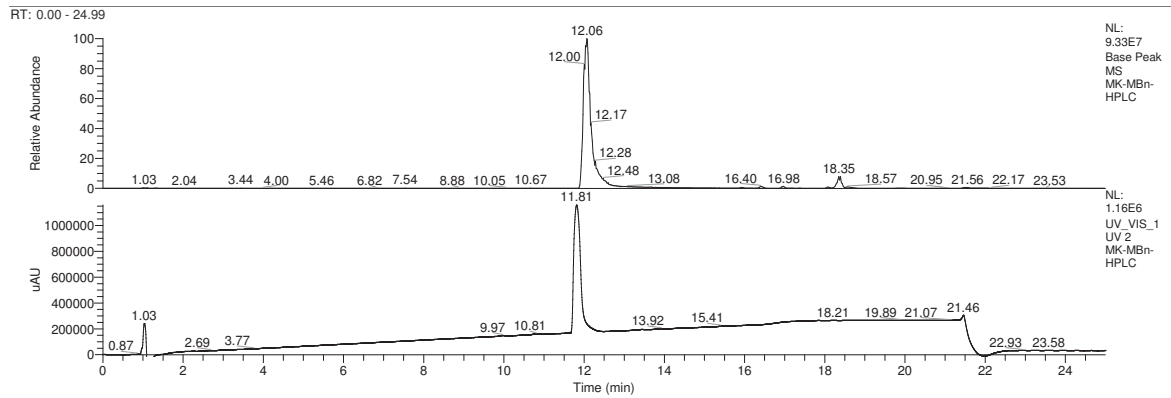
^1H - und ^{13}C -NMR of 10



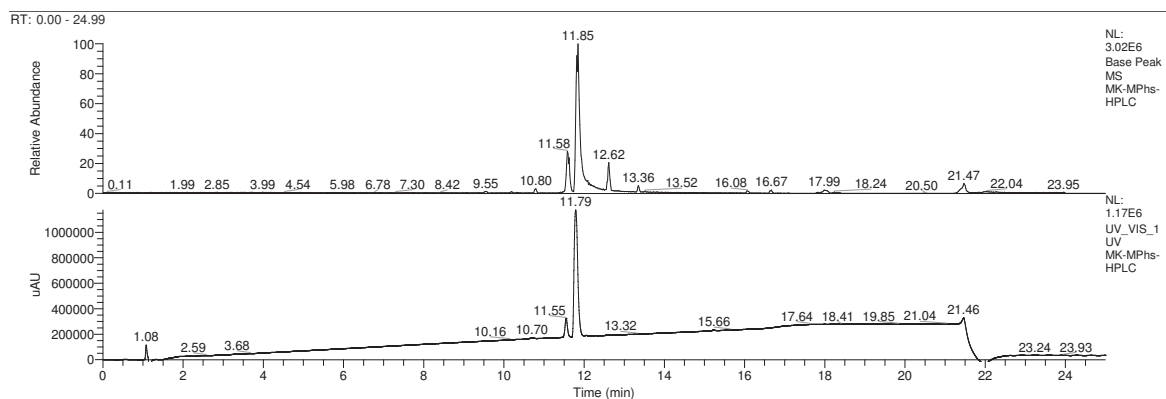
LC-HRMS-ESI of 1



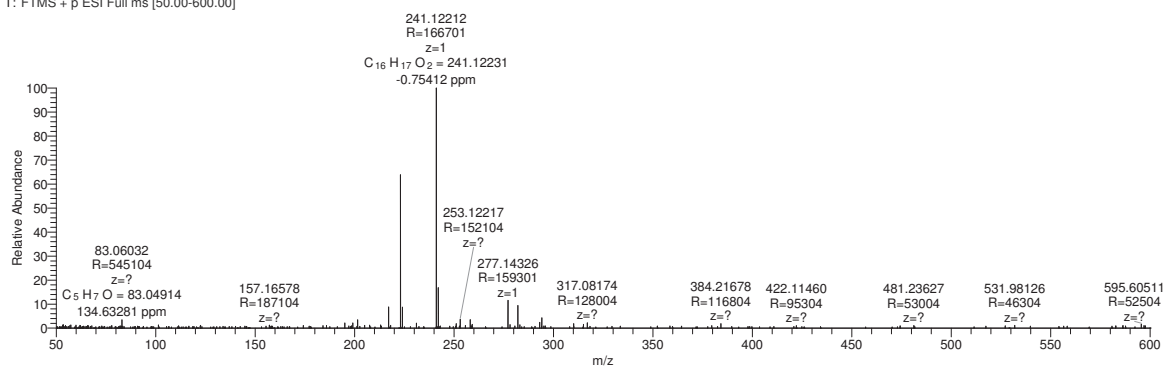
LC-HRMS-ESI of 2



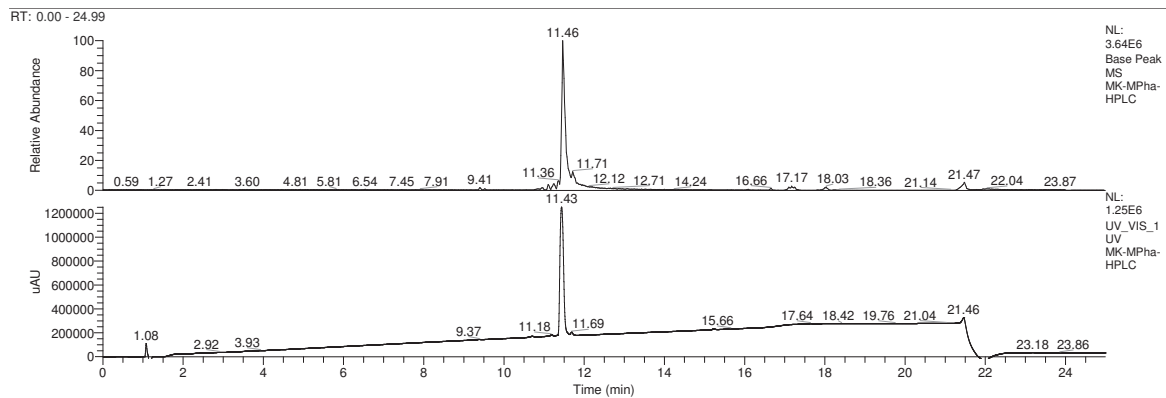
LC-HRMS-ESI of 3



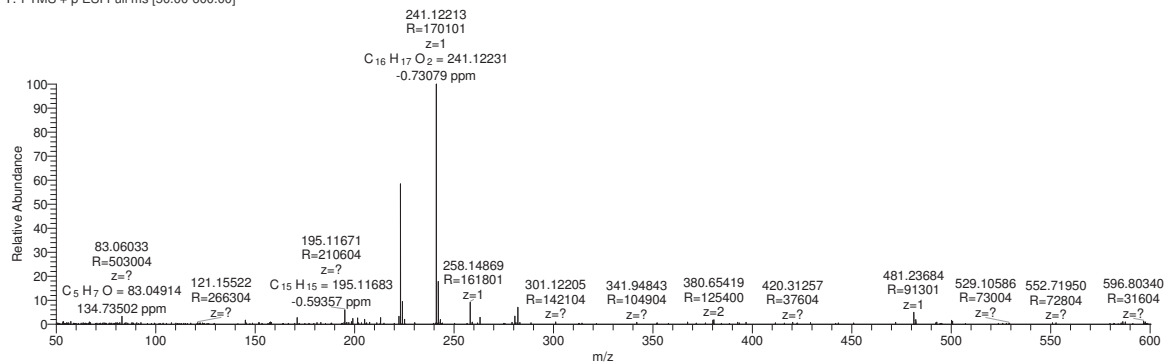
MK-MPhs-HPLC #769 RT: 12.09 AV: 1 NL: 2.53E5
T: FTMS + p ESI Full ms [50.00-600.00]



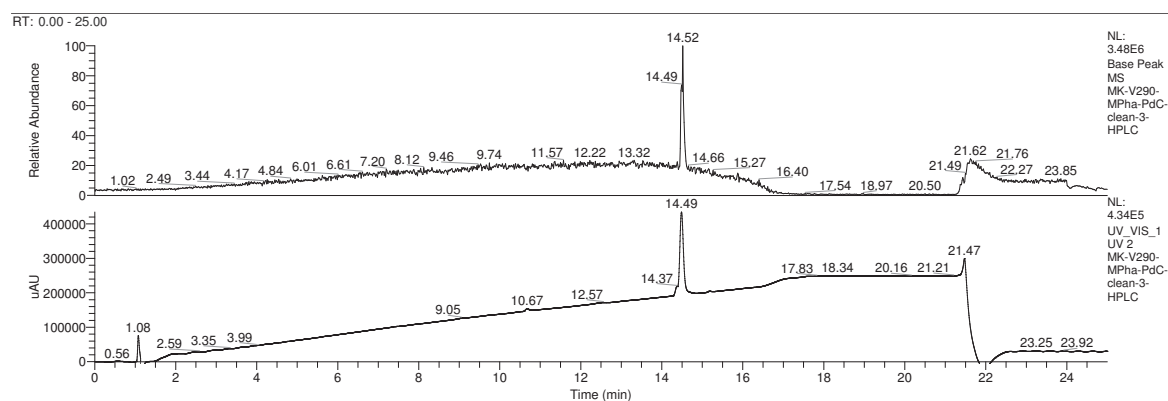
LC-HRMS-ESI of 4



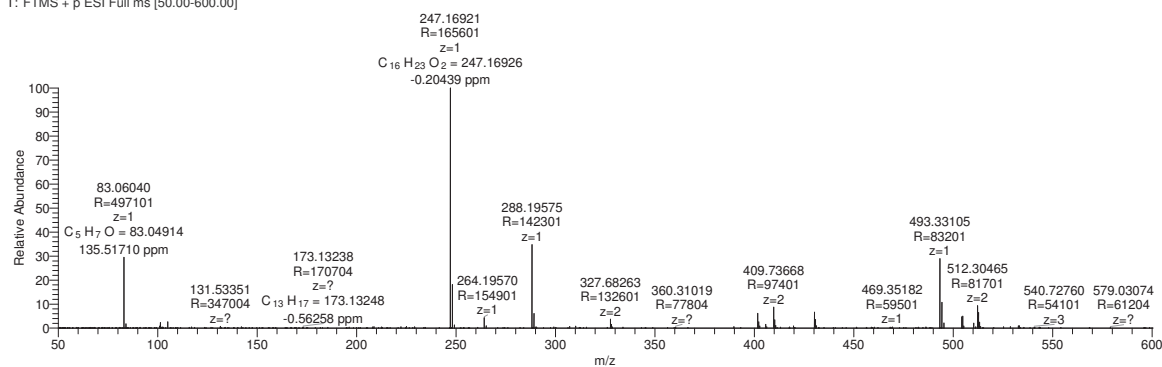
MK-MPha-HPLC #744 RT: 11.71 AV: 1 NL: 4.39E5
T: FTMS + p ESI Full ms [50.00-600.00]



LC-HRMS-ESI of 10



MK-V290-MPha-PdC-clean-3-HPLC #932 RT: 14.54 AV: 1 NL: 2.14E6
T: FTMS + p ESI Full ms [50.00-600.00]



ABBREVIATIONS

A	Adenine
ABPP	Activity-based protein profiling
BHB	Brain heart broth
bp	Base pairs
BSA	Bovine serum albumin
C	Cytosine
CFU	Colony forming units
d	Doublet
Da	Dalton
DC	Thin layer chromatography
DCM	Dichloromethane
DMSO	Dimethyl sulfoxide
DNA	Deoxyribonucleic acid
dNTP	Deoxynucleoside triphosphate

dsDNA	double-stranded DNA
DTT	Dithiothreitol
EC ₅₀	Half maximal effective concentration
ED ₅₀	Half maximal effective dose
EMSA	Electrophoretic mobility shift assay
ESI	Electrospray ionization
EtBr	Ethidium bromide
EtOAc	Ethyl acetate
G	Guanine
HEPES	4-(2-Hydroxyethyl)piperazine-1-ethanesulfonic acid
HPLC	High pressure liquid chromatography
Hz	Hertz
IC ₅₀	Half maximal inhibitory concentration
IGFS	in-gel fluorescence scanning
LB	Lysogeny broth
LC	Liquid chromatography
M	Molecular weight
M	Molar concentration
m/z	Mass to charge ration
MHz	Megahertz
MIC	Minimum inhibitory concentration
min	Minutes
MRSA	Methicillin resistant <i>Staphylococcus aureus</i>
MS	Mass spectrometry
NMR	Nuclear magnetic resonance
OD ₆₀₀	Optical density measured as absorption at 600 nm wavelength
PBS	Phosphate buffered saline
PCR	Polymerase chain reaction
PEP	Phosphoenolpyruvate
P _i	Inorganic phosphate
ppm	Parts per million
q	Quartet
quint.	Quintet
R _f	Retention factor
RNA	Ribonucleic acid

rpm	Revolutions per minute
RT	Room temperature
s	Singlet
SDS	Sodium dodecyl sulfate
SDS-PAGE	Sodium dodecyl sulfate polyacrylamide gel electrophoresis
sec	Seconds
sept.	Septet
ssDNA	Single-stranded DNA
t	Triplet
T	Thymine
T _m	Melting temperature
TCEP	Tris(2-carboxyethyl)phosphine
TEMED	1,2-Bis(dimethylamino)ethane
TFA	Trifluoroacetic acid
THF	Tetrahydrofuran
UV	Ultraviolet
V	Volt
v/v	Volume per volume
w/v	Weight per volume

BIBLIOGRAPHY

1. A. Signore, *EJNMMI research*, 2013, **3**, 8.
2. L. F. Barker, M. J. Brennan, P. K. Rosenstein and J. C. Sadoff, *Current opinion in immunology*, 2009, **21**, 331-338.
3. A. M. Cole, S. Tahk, A. Oren, D. Yoshioka, Y. H. Kim, A. Park and T. Ganz, *Clinical and diagnostic laboratory immunology*, 2001, **8**, 1064-1069.
4. F. D. Lowy, *The New England journal of medicine*, 1998, **339**, 520-532.
5. W. R. Jarvis, R. P. Gaynes, T. C. Horan, J. Alonso-Echanove, T. G. Emori, S. K. Fridkin, R. M. Lawton, M. J. Richards, G. C. Wright, D. H. Culver, J. P. Abshire, J. R. Edwards, T. S. Henderson, G. E. Peavy, J. S. Tolson, J. T. Wages and N. Syst, *Am J Infect Control*, 1998, **26**, 522-533.
6. E. Klein, D. L. Smith and R. Laxminarayan, *Emerging infectious diseases*, 2007, **13**, 1840-1846.
7. V. D. Rosenthal, D. G. Maki, A. Mehta, C. Alvarez-Moreno, H. Leblebicioglu, F. Higuera, L. E. Cuellar, N. Madani, Z. Mitrev, L. Duenas, J. A. Navoa-Ng, H. G. Garcell, L. Raka, R. F. Hidalgo, E. A. Medeiros, S. S. Kanj, S. Abubakar, P. Nercelles, R. D. Pratesi and M. International Nosocomial Infection Control Consortium, *Am J Infect Control*, 2008, **36**, 627-637.

8. V. D. Rosenthal, H. Bijie, D. G. Maki, Y. Mehta, A. Apisarnthanarak, E. A. Medeiros, H. Leblebicioglu, D. Fisher, C. Alvarez-Moreno, I. A. Khader, M. Del Rocio Gonzalez Martinez, L. E. Cuellar, J. A. Navoa-Ng, R. Abouqal, H. Guananche Garcell, Z. Mitrev, M. C. Pirez Garcia, A. Hamdi, L. Duenas, E. Cancel, V. Gurskis, O. Rasslan, A. Ahmed, S. S. Kanj, O. C. Ugalde, T. Mapp, L. Raka, C. Yuet Meng, T. A. Thu le, S. Ghazal, A. Gikas, L. P. Narvaez, N. Mejia, N. Hadjieva, M. O. Gamar Elanbya, M. E. Guzman Siritt, K. Jayatilleke and I. members, *Am J Infect Control*, 2012, **40**, 396-407.
9. A. N. Neely and M. P. Maley, *J Clin Microbiol*, 2000, **38**, 724-726.
10. R. W. Finberg, R. C. Moellering, F. P. Tally, W. A. Craig, G. A. Pankey, E. P. Dellinger, M. A. West, M. Joshi, P. K. Linden, K. V. Rolston, J. C. Rotschafer and M. J. Rybak, *Clinical infectious diseases : an official publication of the Infectious Diseases Society of America*, 2004, **39**, 1314-1320.
11. G. A. Pankey and L. D. Sabath, *Clinical infectious diseases : an official publication of the Infectious Diseases Society of America*, 2004, **38**, 864-870.
12. F. von Nussbaum, M. Brands, B. Hinzen, S. Weigand and D. Habich, *Angew Chem Int Ed Engl*, 2006, **45**, 5072-5129.
13. J. Clardy, M. A. Fischbach and C. T. Walsh, *Nature biotechnology*, 2006, **24**, 1541-1550.
14. A. E. Clatworthy, E. Pierson and D. T. Hung, *Nature chemical biology*, 2007, **3**, 541-548.
15. J. C. Pechere, D. Hughes, P. Kardas and G. Cornaglia, *Int J Antimicrob Agents*, 2007, **29**, 245-253.
16. L. A. Hicks, T. H. Taylor, Jr. and R. J. Hunkler, *The New England journal of medicine*, 2013, **368**, 1461-1462.
17. F. Aarestrup, *Nature*, 2012, **486**, 465-466.
18. E. Larson, *Annual Review of Public Health*, 2007, **28**, 435-447.
19. G. D. Wright, *BMC biology*, 2010, **8**, 123.
20. H. C. Neu, *Science*, 1992, **257**, 1064-1073.
21. C. Walsh, *Nature*, 2000, **406**, 775-781.
22. A. Giedraitiene, A. Vitkauskiene, R. Naginiene and A. Pavilionis, *Med Lith*, 2011, **47**, 137-146.
23. G. D. Wright, *Chemical communications*, 2011, **47**, 4055-4061.
24. X. Z. Li and H. Nikaido, *Drugs*, 2009, **69**, 1555-1623.
25. P. M. Hawkey and A. M. Jones, *The Journal of antimicrobial chemotherapy*, 2009, **64 Suppl 1**, i3-10.
26. E. V. Koonin, K. S. Makarova and L. Aravind, *Annual review of microbiology*, 2001, **55**, 709-742.
27. C. Walsh, *Nat Rev Microbiol*, 2003, **1**, 65-70.
28. T. Böttcher and S. A. Sieber, *Journal of the American Chemical Society*, 2008, **130**, 14400-14401.
29. T. Böttcher and S. A. Sieber, *ChemMedChem*, 2009, **4**, 1260-1263.
30. T. Böttcher and S. A. Sieber, *Chembiochem : a European journal of chemical biology*, 2009, **10**, 663-666.
31. *Nature*, 2004, **431**, 931-945.
32. Y. Taniguchi, P. J. Choi, G. W. Li, H. Chen, M. Babu, J. Hearn, A. Emili and X. S. Xie, *Science*, 2010, **329**, 533-538.
33. D. L. Black, *Annual review of biochemistry*, 2003, **72**, 291-336.
34. Y. Nakamura and A. Karamyshev, in *Encyclopedia of Molecular Biology*, John Wiley & Sons, Inc., 2002.
35. M. Mann and O. N. Jensen, *Nature biotechnology*, 2003, **21**, 255-261.
36. J. Reinders and A. Sickmann, *Biomol Eng*, 2007, **24**, 169-177.
37. H. Ryslava, V. Doubnerova, D. Kavan and O. Vanek, *Journal of proteomics*, 2013.
38. M. Tyers and M. Mann, *Nature*, 2003, **422**, 193-197.
39. M. J. Evans and B. F. Cravatt, *Chemical reviews*, 2006, **106**, 3279-3301.

40. B. F. Cravatt, A. T. Wright and J. W. Kozarich, *Annual review of biochemistry*, 2008, **77**, 383-414.
41. J. A. Joyce, A. Baruch, K. Chehade, N. Meyer-Morse, E. Giraud, F. Y. Tsai, D. C. Greenbaum, J. H. Hager, M. Bogyo and D. Hanahan, *Cancer Cell*, 2004, **5**, 443-453.
42. M. Fonovic and M. Bogyo, *Current pharmaceutical design*, 2007, **13**, 253-261.
43. M. B. Nodwell and S. A. Sieber, *Topics in current chemistry*, 2012, **324**, 1-41.
44. M. Kohn and R. Breinbauer, *Angew Chem Int Ed Engl*, 2004, **43**, 3106-3116.
45. V. V. Rostovtsev, L. G. Green, V. V. Fokin and K. B. Sharpless, *Angew Chem Int Ed Engl*, 2002, **41**, 2596-2599.
46. C. W. Tornøe, C. Christensen and M. Meldal, *J Org Chem*, 2002, **67**, 3057-3064.
47. J. E. Hein and V. V. Fokin, *Chemical Society reviews*, 2010, **39**, 1302-1315.
48. C. D. Hein, X. M. Liu and D. Wang, *Pharmaceutical research*, 2008, **25**, 2216-2230.
49. M. Ahlquist and V. V. Fokin, *Organometallics*, 2007, **26**, 4389-4391.
50. B. F. Straub, *Chemical communications*, 2007, 3868-3870.
51. N. J. Agard, J. A. Prescher and C. R. Bertozzi, *Journal of the American Chemical Society*, 2004, **126**, 15046-15047.
52. K. E. Beatty, J. D. Fisk, B. P. Smart, Y. Y. Lu, J. Szychowski, M. J. Hangauer, J. M. Baskin, C. R. Bertozzi and D. A. Tirrell, *Chembiochem : a European journal of chemical biology*, 2010, **11**, 2092-2095.
53. N. E. Mbuja, J. Guo, M. A. Wolfert, R. Steet and G. J. Boons, *Chembiochem : a European journal of chemical biology*, 2011, **12**, 1912-1921.
54. J. Li and P. R. Chen, *Chembiochem : a European journal of chemical biology*, 2012, **13**, 1728-1731.
55. I. Staub and S. A. Sieber, *Journal of the American Chemical Society*, 2008, **130**, 13400-13409.
56. M. H. Kunzmann, I. Staub, T. Böttcher and S. A. Sieber, *Biochemistry*, 2011, **50**, 910-916.
57. T. Böttcher and S. A. Sieber, *Angew Chem Int Ed Engl*, 2008, **47**, 4600-4603.
58. J. K. Eng, B. Fischer, J. Grossmann and M. J. Maccoss, *Journal of proteome research*, 2008, **7**, 4598-4602.
59. T. Koenig, B. H. Menze, M. Kirchner, F. Monigatti, K. C. Parker, T. Patterson, J. J. Steen, F. A. Hamprecht and H. Steen, *Journal of proteome research*, 2008, **7**, 3708-3717.
60. G. M. Cragg, D. J. Newman and K. M. Snader, *Journal of natural products*, 1997, **60**, 52-60.
61. H. T. Chan, D. Hughes, R. R. French, A. L. Tutt, C. A. Walshe, J. L. Teeling, M. J. Glennie and M. S. Cragg, *Cancer research*, 2003, **63**, 5480-5489.
62. G. M. Cragg and D. J. Newman, *Expert opinion on investigational drugs*, 2000, **9**, 2783-2797.
63. M. Gersch, J. Kreuzer and S. A. Sieber, *Nat Prod Rep*, 2012.
64. C. M. Cabello, W. B. Bair, 3rd, S. D. Lamore, S. Ley, A. S. Bause, S. Azimian and G. T. Wondrak, *Free radical biology & medicine*, 2009, **46**, 220-231.
65. E. H. Chew, A. A. Nagle, Y. Zhang, S. Scarmagnani, P. Palaniappan, T. D. Bradshaw, A. Holmgren and A. D. Westwell, *Free radical biology & medicine*, 2010, **48**, 98-111.
66. H. Fu, J. Park and D. Pei, *Biochemistry*, 2002, **41**, 10700-10709.
67. E. L. Smith, M. Landon, D. Piszkiwicz, W. J. Brattin, T. J. Langley and M. D. Melamed, *Proceedings of the National Academy of Sciences of the United States of America*, 1970, **67**, 724-730.
68. M. Pitscheider and S. A. Sieber, *Chemical communications*, 2009, 3741-3743.
69. H. Nishimura, M. Mayama, Y. Komatsu, H. Kato, N. Shimaoka and Y. Tanaka, *The Journal of antibiotics*, 1964, **17**, 148-155.
70. S. Roy-Burman, P. Roy-Burman and D. W. Visser, *Cancer research*, 1968, **28**, 1605-1610.
71. T. Böttcher and S. A. Sieber, *Journal of the American Chemical Society*, 2010, **132**, 6964-6972.
72. R. R. Kitson, A. Millemaggi and R. J. Taylor, *Angew Chem Int Ed Engl*, 2009, **48**, 9426-9451.
73. H. Yokoe, M. Yoshida and K. Shishido, *Tetrahedron Lett*, 2008, **49**, 3504-3506.

74. S. Takeda, K. Matsuo, K. Yaji, S. Okajima-Miyazaki, M. Harada, H. Miyoshi, Y. Okamoto, T. Amamoto, M. Shindo, C. J. Omiecinski and H. Aramaki, *Chemical research in toxicology*, 2011, **24**, 855-865.
75. Y. F. Xia, B. Q. Ye, Y. D. Li, J. G. Wang, X. J. He, X. Lin, X. Yao, D. Ma, A. Slungaard, R. P. Hebbel, N. S. Key and J. G. Geng, *Journal of immunology*, 2004, **173**, 4207-4217.
76. B. H. Kwok, B. Koh, M. I. Ndubuisi, M. Elofsson and C. M. Crews, *Chemistry & biology*, 2001, **8**, 759-766.
77. M. Ichimura, T. Ogawa, K. Takahashi, E. Kobayashi, I. Kawamoto, T. Yasuzawa, I. Takahashi and H. Nakano, *The Journal of antibiotics*, 1990, **43**, 1037-1038.
78. D. L. Boger and D. S. Johnson, *Proceedings of the National Academy of Sciences of the United States of America*, 1995, **92**, 3642-3649.
79. L. F. Tietze and K. Schmuck, *Current pharmaceutical design*, 2011, **17**, 3527-3547.
80. T. Wirth, K. Schmuck, L. F. Tietze and S. A. Sieber, *Angew Chem Int Ed Engl*, 2012, **51**, 2874-2877.
81. D. Hendlin, E. O. Stapley, M. Jackson, H. Wallick, A. K. Miller, F. J. Wolf, T. W. Miller, L. Chaiet, F. M. Kahan, E. L. Foltz, H. B. Woodruff, J. M. Mata, S. Hernandez and S. Mochales, *Science*, 1969, **166**, 122-123.
82. F. M. Kahan, J. S. Kahan, P. J. Cassidy and H. Kropp, *Annals of the New York Academy of Sciences*, 1974, **235**, 364-386.
83. E. D. Brown, E. I. Vivas, C. T. Walsh and R. Kolter, *Journal of bacteriology*, 1995, **177**, 4194-4197.
84. T. Skarzynski, A. Mistry, A. Wonacott, S. E. Hutchinson, V. A. Kelly and K. Duncan, *Structure*, 1996, **4**, 1465-1474.
85. M. Popovic, D. Steinort, S. Pillai and C. Joukhadar, *European journal of clinical microbiology & infectious diseases : official publication of the European Society of Clinical Microbiology*, 2010, **29**, 127-142.
86. E. K. Weibel, P. Hadvary, E. Hochuli, E. Kupfer and H. Lengsfeld, *The Journal of antibiotics*, 1987, **40**, 1081-1085.
87. C. Drahl, B. F. Cravatt and E. J. Sorensen, *Angew Chem Int Ed Engl*, 2005, **44**, 5788-5809.
88. P. Hadvary, H. Lengsfeld and H. Wolfer, *The Biochemical journal*, 1988, **256**, 357-361.
89. S. Harada, S. Tsubotani, T. Hida, H. Ono and H. Okazaki, *Tetrahedron Lett*, 1986, **27**, 6229-6232.
90. Y. Nozaki, N. Katayama, S. Harada, H. Ono and H. Okazaki, *The Journal of antibiotics*, 1989, **42**, 84-93.
91. Y. Nozaki, N. Katayama, H. Ono, S. Tsubotani, S. Harada, H. Okazaki and Y. Nakao, *Nature*, 1987, **325**, 179-180.
92. T. Brown, Jr., P. Charlier, R. Herman, C. J. Schofield and E. Sauvage, *Journal of medicinal chemistry*, 2010, **53**, 5890-5894.
93. P. Macheboeuf, D. S. Fischer, T. Brown, Jr., A. Zervosen, A. Luxen, B. Joris, A. Dessen and C. J. Schofield, *Nature chemical biology*, 2007, **3**, 565-569.
94. P. P. Geurink, L. M. Prely, G. A. van der Marel, R. Bischoff and H. S. Overkleeft, *Topics in current chemistry*, 2012, **324**, 85-113.
95. S. A. Fleming, *Tetrahedron*, 1995, **51**, 12479-12520.
96. E. L. Vodovozova, *Biochemistry (Moscow)*, 2007, **72**, 1-20.
97. Y. Tanaka, M. R. Bond and J. J. Kohler, *Molecular bioSystems*, 2008, **4**, 473-480.
98. F. Kotzyba-Hibert, I. Kapfer and M. Goeldner, *Angewandte Chemie International Edition in English*, 1995, **34**, 1296-1312.
99. A. Borodovsky, H. Ovaa, W. J. Meester, E. S. Venanzi, M. S. Bogyo, B. G. Hekking, H. L. Ploegh, B. M. Kessler and H. S. Overkleeft, *Chembiochem : a European journal of chemical biology*, 2005, **6**, 287-291.
100. E. Zeiler, N. Braun, T. Bottcher, A. Kastenmuller, S. Weinkauff and S. A. Sieber, *Angew Chem Int Ed Engl*, 2011, **50**, 11001-11004.

101. E. Zeiler, V. S. Korotkov, K. Lorenz-Baath, T. Böttcher and S. A. Sieber, *Bioorganic & medicinal chemistry*, 2011, **20**, 583-591.
102. T. Böttcher, M. Pitscheider and S. A. Sieber, *Angew Chem Int Ed Engl*, 2010, **49**, 2680-2698.
103. P. Y. Yang, K. Liu, M. H. Ngai, M. J. Lear, M. R. Wenk and S. Q. Yao, *Journal of the American Chemical Society*, 2010, **132**, 656-666.
104. M. Fonovic and M. Bogyo, *Expert Rev Proteomics*, 2008, **5**, 721-730.
105. M. Seitz and O. Reiser, *Curr Opin Chem Biol*, 2005, **9**, 285-292.
106. C. A. Machutta, G. R. Bommineni, S. R. Luckner, K. Kapilashrami, B. Ruzsicska, C. Simmerling, C. Kisker and P. J. Tonge, *J Biol Chem*, 2010, **285**, 6161-6169.
107. A. E. Speers, G. C. Adam and B. F. Cravatt, *J. Amer. Chem. Soc.*, 2003, **125**, 4686-4687.
108. R. Huisgen, *1,3 Dipolar Cycloaddition Chemistry*, Wiley, New York, 1984.
109. V. V. Rostovtsev, J. G. Green, V. V. Fokin and K. B. Sharpless, *Angew. Chem. Int. Ed. Engl.*, 2002, **41**, 2596-2599.
110. W. W. Qiu, J. Xu, J. Y. Li, J. Li and F. J. Nana, *Chembiochem*, 2007, **8**, 1351-1358.
111. C. M. Salisbury and B. F. Cravatt, *Proceedings of the National Academy of Sciences of the United States of America*, 2007, **104**, 1171-1176.
112. S. A. Sieber, S. Niessen, H. S. Hoover and B. F. Cravatt, *Nature chemical biology*, 2006, **2**, 274-281.
113. E. W. Chan, S. Chattopadhyaya, R. C. Panicker, X. Huang and S. Q. Yao, *Journal of the American Chemical Society*, 2004, **126**, 14435-14446.
114. L. Dubinsky, L. M. Jarosz, N. Amara, P. Krief, V. V. Kravchenko, B. P. Krom and M. M. Meijler, *Chemical communications*, 2009, 7378-7380.
115. K. P. Lu, G. Finn, T. H. Lee and L. K. Nicholson, *Nature chemical biology*, 2007, **3**, 619-629.
116. G. Kramer, A. Rutkowska, R. D. Wegrzyn, H. Patzelt, T. A. Kurz, F. Merz, T. Rauch, S. Vorderwulbecke, E. Deuerling and B. Bukau, *Journal of bacteriology*, 2004, **186**, 3777-3784.
117. H. Patzelt, G. Kramer, T. Rauch, H. J. Schonfeld, B. Bukau and E. Deuerling, *Biol Chem*, 2002, **383**, 1611-1619.
118. H. Patzelt, S. Rudiger, D. Brehmer, G. Kramer, S. Vorderwulbecke, E. Schaffitzel, A. Waitz, T. Hestekamp, L. Dong, J. Schneider-Mergener, B. Bukau and E. Deuerling, *Proceedings of the National Academy of Sciences of the United States of America*, 2001, **98**, 14244-14249.
119. B. Janowski, S. Wollner, M. Schutkowski and G. Fischer, *Analytical biochemistry*, 1997, **252**, 299-307.
120. E. Deuerling, A. Schulze-Specking, T. Tomoyasu, A. Mogk and B. Bukau, *Nature*, 1999, **400**, 693-696.
121. E. Deuerling, H. Patzelt, S. Vorderwulbecke, T. Rauch, G. Kramer, E. Schaffitzel, A. Mogk, A. Schulze-Specking, H. Langen and B. Bukau, *Molecular microbiology*, 2003, **47**, 1317-1328.
122. P. H. Boyle, Davis, A.P., Dempsey, K.J., Hosken, G.D., *Tetrahedron*, 1995, **6**, 2819-2828.
123. S. P. Mirza, B. D. Halligan, A. S. Greene and M. Olivier, *Physiol Genomics*, 2007, **30**, 89-94.
124. R. Orth, T. Böttcher and S. A. Sieber, *Chem Commun (Camb)*, 2010, **46**, 8475-8477.
125. M. H. Ngai, P. Y. Yang, K. Liu, Y. Shen, M. R. Wenk, S. Q. Yao and M. J. Lear, *Chemical communications*, 2010, **46**, 8335-8337.
126. E. Nibret, M. Youns, R. L. Krauth-Siegel and M. Wink, *Phytother Res*, 2011, **25**, 1883-1890.
127. E. T. Tsankova, A. B. Trendafilova, A. I. Kujumgiev, A. S. Galabov and P. R. Robeva, *Z Naturforsch C*, 1994, **49**, 154-155.
128. C. Roussakis, I. Chinou, C. Vayas, C. Harvala and J. F. Verbist, *Planta Med*, 1994, **60**, 473-474.
129. L. S. Favier, G. Acosta, M. R. Gomez, A. O. Maria and C. E. Tonn, *Pharmazie*, 2006, **61**, 981-984.
130. I. Ramirez-Erosa, Y. Huang, R. A. Hickie, R. G. Sutherland and B. Barl, *Can J Physiol Pharmacol*, 2007, **85**, 1160-1172.

131. A. Kovacs, A. Vasas, P. Forgo, B. Rethy, I. Zupko and J. Hohmann, *Z Naturforsch C*, 2009, **64**, 343-349.
132. B. Pinel, A. Landreau, D. Seraphin, G. Larcher, J. P. Bouchara and P. Richomme, *J Enzyme Inhib Med Chem*, 2005, **20**, 575-579.
133. E. Ginesta-Peris, Garcia-Breijo, F.J., Primo-Yufera, E., *Lett Appl Microbiol*, 1994, **18**, 206-208.
134. S. Takeda, K. Matsuo, K. Yaji, S. Okajima-Miyazaki, M. Harada, H. Miyoshi, Y. Okamoto, T. Amamoto, M. Shindo, C. J. Omiecinski and H. Aramaki, *Chemical Research in Toxicology*, 2011, **24**, 855-865.
135. F. C. Chen, C. F. Peng, I. L. Tsai and I. S. Chen, *J Nat Prod*, 2005, **68**, 1318-1323.
136. S. Y. Kuo, T. J. Hsieh, Y. D. Wang, W. L. Lo, Y. R. Hsui and C. Y. Chen, *Chem Pharm Bull (Tokyo)*, 2008, **56**, 97-101.
137. R. Huisgen, *Proc. Chem. Soc.*, 1961, 357-396.
138. W. P. Heal and E. W. Tate, *Topics in current chemistry*, 2012, **324**, 115-135.
139. A. W. Puri, P. J. Lupardus, E. Deu, V. E. Albrow, K. C. Garcia, M. Bogyo and A. Shen, *Chem Biol*, 2010, **17**, 1201-1211.
140. T. J. Wiles, R. R. Kulesus and M. A. Mulvey, *Exp Mol Pathol*, 2008, **85**, 11-19.
141. O. Gal-Mor and B. B. Finlay, *Cell Microbiol*, 2006, **8**, 1707-1719.
142. J. Hacker and J. B. Kaper, *Annual review of microbiology*, 2000, **54**, 641-679.
143. G. Chen, R. Wilson, G. Cumming, J. J. Walker and J. H. Mckillop, *Eur J Obstet Gyn R B*, 1994, **53**, 21-25.
144. R. R. A. Kitson, R. J. K. Taylor and J. L. Wood, *Organic Letters*, 2009, **11**, 5338-5341.
145. A. J. Pearson, Y. S. Lai, W. Lu and A. A. Pinkerton, *The Journal of Organic Chemistry*, 1989, **54**, 3882-3893.
146. M. G. Edwards, M. N. Kenworthy, R. R. A. Kitson, A. Perry, M. S. Scott, A. C. Whitwood and R. J. K. Taylor, *European Journal of Organic Chemistry*, 2008, **2008**, 4769-4783.
147. A. F. Abdel-Magid, K. G. Carson, B. D. Harris, C. A. Maryanoff and R. D. Shah, *The Journal of Organic Chemistry*, 1996, **61**, 3849-3862.
148. H. N. Pati, U. Das, R. K. Sharma and J. R. Dimmock, *Mini Rev Med Chem*, 2007, **7**, 131-139.
149. Y. Higuchi, F. Shimoma and M. Ando, *J Nat Prod*, 2003, **66**, 810-817.
150. E. G. Mueller, P. M. Palenchar and C. J. Buck, *Journal of Biological Chemistry*, 2001, **276**, 33588-33595.
151. L. B. Poole, *Archives of Biochemistry and Biophysics*, 2005, **433**, 240-254.
152. P. J. Hillas, F. S. del Alba, J. Oyarzabal, A. Wilks and P. R. Ortiz de Montellano, *Journal of Biological Chemistry*, 2000, **275**, 18801-18809.
153. J. Putze, C. Hennequin, J. P. Nougayrede, W. Zhang, S. Homburg, H. Karch, M. A. Bringer, C. Fayolle, E. Carniel, W. Rabsch, T. A. Oelschlaeger, E. Oswald, C. Forestier, J. Hacker and U. Dobrindt, *Infect Immun*, 2009, **77**, 4696-4703.
154. S. Homburg, E. Oswald, J. Hacker and U. Dobrindt, *FEMS Microbiol Lett*, 2007, **275**, 255-262.
155. J.-P. Nougayrède, S. Homburg, F. Taieb, M. Boury, E. Brzuszkiewicz, G. Gottschalk, C. Buchrieser, J. Hacker, U. Dobrindt and E. Oswald, *Science*, 2006, **313**, 848-851.
156. J. M. Hoover and S. S. Stahl, *Journal of the American Chemical Society*, 2011, **133**, 16901-16910.
157. J. Eirich, J. L. Burkhart, A. Ullrich, G. C. Rudolf, A. Vollmar, S. Zahler, U. Kazmaier and S. A. Sieber, *Molecular BioSystems*, 2012, **8**, 2067-2075.
158. W. W. Navarre and O. Schneewind, *Microbiology and molecular biology reviews : MMBR*, 1999, **63**, 174-229.
159. L. Cegelski, G. R. Marshall, G. R. Eldridge and S. J. Hultgren, *Nat Rev Microbiol*, 2008, **6**, 17-27.
160. D. T. Hung, E. A. Shakhnovich, E. Pierson and J. J. Mekalanos, *Science*, 2005, **310**, 670-674.
161. A. L. Cheung, A. S. Bayer, G. Zhang, H. Gresham and Y. Q. Xiong, *FEMS immunology and medical microbiology*, 2004, **40**, 1-9.

162. R. P. Novick, *Molecular microbiology*, 2003, **48**, 1429-1449.
163. E. A. George and T. W. Muir, *Chembiochem : a European journal of chemical biology*, 2007, **8**, 847-855.
164. A. L. Cheung, K. A. Nishina, M. P. Trotonda and S. Tamber, *The international journal of biochemistry & cell biology*, 2008, **40**, 355-361.
165. P. M. Dunman, E. Murphy, S. Haney, D. Palacios, G. Tucker-Kellogg, S. Wu, E. L. Brown, R. J. Zagursky, D. Shlaes and S. J. Projan, *Journal of bacteriology*, 2001, **183**, 7341-7353.
166. Y. Chien, A. C. Manna, S. J. Projan and A. L. Cheung, *The Journal of biological chemistry*, 1999, **274**, 37169-37176.
167. P. F. Chan and S. J. Foster, *Journal of bacteriology*, 1998, **180**, 6232-6241.
168. A. C. Manna, M. G. Bayer and A. L. Cheung, *Journal of bacteriology*, 1998, **180**, 3828-3836.
169. T. T. Luong, P. M. Dunman, E. Murphy, S. J. Projan and C. Y. Lee, *Journal of bacteriology*, 2006, **188**, 1899-1910.
170. T. T. Luong, S. W. Newell and C. Y. Lee, *Journal of bacteriology*, 2003, **185**, 3703-3710.
171. Y. Liu, A. C. Manna, C. H. Pan, I. A. Kriksunov, D. J. Thiel, A. L. Cheung and G. Zhang, *Proceedings of the National Academy of Sciences of the United States of America*, 2006, **103**, 2392-2397.
172. P. R. Chen, T. Bae, W. A. Williams, E. M. Duguid, P. A. Rice, O. Schneewind and C. He, *Nature chemical biology*, 2006, **2**, 591-595.
173. F. Sun, Y. Ding, Q. Ji, Z. Liang, X. Deng, C. C. Wong, C. Yi, L. Zhang, S. Xie, S. Alvarez, L. M. Hicks, C. Luo, H. Jiang, L. Lan and C. He, *Proceedings of the National Academy of Sciences of the United States of America*, 2012, **109**, 15461-15466.
174. I.-M. Jonsson, C. Lindholm, T. T. Luong, C. Y. Lee and A. Tarkowski, *Microbes and Infection*, 2008, **10**, 1229-1235.
175. A. K. Zielinska, K. E. Beenken, L. N. Mrak, H. J. Spencer, G. R. Post, R. A. Skinner, A. J. Tackett, A. R. Horswill and M. S. Smeltzer, *Molecular Microbiology*, 2012, **86**, 1183-1196.
176. R. Babai, B. E. Stern, J. Hacker and E. Z. Ron, *Infection and immunity*, 2000, **68**, 5901-5907.
177. J. Oscarsson, A. Kanth, K. Tegmark-Wisell and S. Arvidson, *Journal of bacteriology*, 2006, **188**, 8526-8533.
178. J. Morschhauser, G. Kohler, W. Ziebuhr, G. Blum-Oehler, U. Dobrindt and J. Hacker, *Philosophical transactions of the Royal Society of London. Series B, Biological sciences*, 2000, **355**, 695-704.
179. D. Frees, J. H. Andersen, L. Hemmingsen, K. Koskeniemi, K. T. Baek, M. K. Muhammed, D. D. Gudeta, T. A. Nyman, A. Sukura, P. Varmanen and K. Savijoki, *Journal of proteome research*, 2012, **11**, 95-108.
180. D. Frees, K. Sorensen and H. Ingmer, *Infection and immunity*, 2005, **73**, 8100-8108.
181. F. Sun, L. Zhou, B. C. Zhao, X. Deng, H. Cho, C. Yi, X. Jian, C. X. Song, C. H. Luan, T. Bae, Z. Li and C. He, *Chemistry & biology*, 2011, **18**, 1032-1041.
182. M. H. Kunzmann and S. A. Sieber, *Molecular bioSystems*, 2012, **8**, 3061-3067.
183. Q. C. Truong-Bolduc, Y. Ding and D. C. Hooper, *Journal of bacteriology*, 2008, **190**, 7375-7381.
184. J. Oscarsson, K. Tegmark-Wisell and S. Arvidson, *International journal of medical microbiology : IJMM*, 2006, **296**, 365-380.
185. E. Gustafsson and J. Oscarsson, *FEMS microbiology letters*, 2008, **284**, 158-164.
186. J. Krysiak and R. Breinbauer, *Topics in current chemistry*, 2012, **324**, 43-84.
187. S. Kamijo and G. B. Dudley, *Journal of the American Chemical Society*, 2006, **128**, 6499-6507.
188. M. S. Sawant, R. Katoch, G. K. Trivedi and U. R. Desai, *Journal of the Chemical Society, Perkin Transactions 1*, 1998, **0**, 843-846.
189. L.-W. Ye, X. Han, X.-L. Sun and Y. Tang, *Tetrahedron*, 2008, **64**, 1487-1493.
190. J. Eirich, J. L. Burkhart, A. Ullrich, G. C. Rudolf, A. Vollmar, S. Zahler, U. Kazmaier and S. A. Sieber, *Molecular bioSystems*, 2012, **8**, 2067-2075.

191. S. Ingavale, W. van Wamel, T. T. Luong, C. Y. Lee and A. L. Cheung, *Infection and immunity*, 2005, **73**, 1423-1431.
192. A. K. Zielinska, K. E. Beenken, H. S. Joo, L. N. Mrak, L. M. Griffin, T. T. Luong, C. Y. Lee, M. Otto, L. N. Shaw and M. S. Smeltzer, *Journal of bacteriology*, 2011, **193**, 2948-2958.
193. D. D. Boehr, W. S. Lane and G. D. Wright, *Chemistry & biology*, 2001, **8**, 791-800.
194. W. Du, J. R. Brown, D. R. Sylvester, J. Huang, A. F. Chalker, C. Y. So, D. J. Holmes, D. J. Payne and N. G. Wallis, *Journal of bacteriology*, 2000, **182**, 4146-4152.
195. M. B. Nodwell, H. Menz, S. F. Kirsch and S. A. Sieber, *Chembiochem : a European journal of chemical biology*, 2012, **13**, 1439-1446.
196. Y. Liu, A. Manna, R. Li, W. E. Martin, R. C. Murphy, A. L. Cheung and G. Zhang, *Proceedings of the National Academy of Sciences of the United States of America*, 2001, **98**, 6877-6882.
197. G. A. Somerville and R. A. Proctor, *Microbiology and molecular biology reviews : MMBR*, 2009, **73**, 233-248.
198. D. F. Fujimoto, R. H. Higginbotham, K. M. Sterba, S. J. Maleki, A. M. Segall, M. S. Smeltzer and B. K. Hurlburt, *Molecular microbiology*, 2009, **74**, 1445-1458.
199. A. Ballal and A. C. Manna, *Journal of bacteriology*, 2010, **192**, 336-345.
200. O. Uziel, I. Borovok, R. Schreiber, G. Cohen and Y. Aharonowitz, *Journal of bacteriology*, 2004, **186**, 326-334.
201. J. Messens, I. Van Molle, P. Vanhaesebrouck, M. Limbourg, K. Van Belle, K. Wahni, J. C. Martins, R. Loris and L. Wyns, *Journal of molecular biology*, 2004, **339**, 527-537.
202. A. Holmgren, *The Journal of biological chemistry*, 1979, **254**, 9627-9632.
203. E. Bjur, S. Eriksson-Ygberg, F. Aslund and M. Rhen, *Infection and immunity*, 2006, **74**, 5140-5151.
204. A. C. Manna and A. L. Cheung, *Molecular Microbiology*, 2006, **60**, 1289-1301.
205. A. S. Khan, I. Muhldorfer, V. Demuth, U. Wallner, T. K. Korhonen and J. Hacker, *Molecular & general genetics : MGG*, 2000, **263**, 96-105.
206. M. Steinert, U. Hentschel and J. Hacker, *Die Naturwissenschaften*, 2000, **87**, 1-11.
207. Y. Q. Xiong, A. S. Bayer, M. R. Yeaman, W. Van Wamel, A. C. Manna and A. L. Cheung, *Infection and immunity*, 2004, **72**, 1832-1836.
208. A. Karlsson, P. Saravia-Otten, K. Tegmark, E. Morfeldt and S. Arvidson, *Infection and immunity*, 2001, **69**, 4742-4748.
209. M. P. Horn, S. M. Knecht, F. L. Rushing, J. Birdsong, C. P. Siddall, C. M. Johnson, T. N. Abraham, A. Brown, C. B. Volk, K. Gammon, D. L. Bishop, J. L. McKillip and S. A. McDowell, *The Journal of pharmacology and experimental therapeutics*, 2008, **326**, 135-143.
210. S. Kamijo and G. B. Dudley, *Journal of the American Chemical Society*, 2006, **128**, 6499-6507.
211. M. S. Sawant, R. Katoch, G. K. Trivedi and U. R. Desai, *J Chem Soc Perk T 1*, 1998, 843-846.
212. L. W. Ye, X. Han, X. L. Sun and Y. Tang, *Tetrahedron*, 2008, **64**, 1487-1493.
213. J. W. Amoroso, L. S. Borketey, G. Prasad and N. A. Schnarr, *Organic Letters*, 2010, **12**, 2330-2333.
214. F. Lambert, B. Kirschleger and J. Villieras, *J Organomet Chem*, 1991, **406**, 71-86.
215. R. P. Novick, *Methods in enzymology*, 1991, **204**, 587-636.
216. B. N. Kreiswirth, S. Lofdahl, M. J. Betley, M. O'Reilly, P. M. Schlievert, M. S. Bergdoll and R. P. Novick, *Nature*, 1983, **305**, 709-712.
217. R. P. Novick, H. F. Ross, S. J. Projan, J. Kornblum, B. Kreiswirth and S. Moghazeh, *The EMBO journal*, 1993, **12**, 3967-3975.
218. R. Novick, *Virology*, 1967, **33**, 155-166.
219. K. Hiramatsu, H. Hanaki, T. Ino, K. Yabuta, T. Oguri and F. C. Tenover, *The Journal of antimicrobial chemotherapy*, 1997, **40**, 135-136.

CURRICULUM VITAE

Name, Vorname	Kunzmann, Martin Herbert
Geburtsdatum, -ort	19. November 1982, München
Staatsangehörigkeit	deutsch
Schulbildung	
09/1989 – 07/1993	Grundschule Vaterstetten
09/1993 – 07/1995	Hauptschule Vaterstetten
09/1995 – 07/1999	Staatliche Realschule Vaterstetten Abschluss Juli 1999: Mittlere Reife
09/1999 – 02/2000	Fachoberschule Wasserburg
03/2000 – 09/2000	verschiedene Praktika
09/2000 – 07/2003	Ausbildung zum Mikrotechnologen, Infineon Technologies AG
09/2003 – 07/2005	technische Berufsoberschule München Abschluss Juli 2004: Fachhochschulreife (1,6) Abschluss Juli 2005: Allgemeine Hochschulreife (1,7)
10/2005 – 10/2008	Studium der Chemie und Biochemie an der LMU München Abschluss Oktober 2008: B.Sc. Chemie und Biochemie (Note 1,5)
10/2008 – 08/2010	Studium der Chemie an der LMU München Abschluss August 2010: M.Sc. Chemie (Note 1,2)
Seit 10/2010	Promotion in organischer Chemie TU München, Forschungsgruppe Prof. Dr. S. A. Sieber
Berufserfahrung	
04/2006 – 03/2009	Studentischer Mitarbeiter, SÜSS MicroTec Litography GmbH
10/2009 – 12/2009	Tutor im chemischen Grundpraktikum, LMU München